Loughborough University

EFFECT OF SOME PROCESSING AND SERVICE CONDITIONS ON THE MECHANICAL PROPERTIES OF AN ENGINE MOUNT COMPOUND.

By

Frederick EDIAGE NGOLEMASANGO,
(BSc., MSc. (Applied Chemistry)

A Doctoral Thesis submitted in partial fulfilment of the requirements for the award of the degree of Doctor of Philosophy of Loughborough University, UK.

Supervisor: Jane Clarke, PhD, MRSC, CCHEM

Institute of Polymer Technology and Materials Engineering

September 2007

IPME

DEDICATION

To my wife Florence Zou, my lovely boys,
Mpacko Olaf, Hoigen Edimasango and Blessed Bame
and my late father Richard Ngolemasango (se Mbappe)

ACKNOWLEDGEMENT

I am indebted to the Almighty God for His loving Kindness, and to the following persons and institutions who were very instrumental towards the realisation of this research:

- The Commonwealth Scholarship and Fellowship Plan (CSFP) through the Association of Commonwealth Universities (ACU) for awarding me the scholarship for research towards the attainment of a higher degree, and those of the British Council who took great care of my financial needs
- To my Supervisor Dr. Jane Clarke for her constructive criticism, advice and for giving me a sense of direction in the pursuit of my research goals
- Professor Marianne Gilbert for being my research director,
- Mr. Martyn Bennett, Bob Ellis and all the staff of AVON MDC for their contribution towards the restructuring of the research,
- Joseph Hallett of Columbian Chemicals Company Bristol for assisting in carrying out the crack growth measurements
- Avon MDC for financial, material and other logistic support
- The authorities of the University of Buea Cameroon and the Cameroon government for granting me a study leave
- The authorities of IPTME, the technicians especially Ray Owens, Andy Woolley and the workshop staff for all their support.
- My family back in Cameroon and elsewhere for their Moral support and constant prayers.
- Members of the All Saints Church Thorpe Acre for their constant prayers and support especially those of the TIC – TAC cell
- To all those whose names cannot be mentioned I say thank you.

ABSTRACT.

Natural rubber is used for a variety of applications and especially in tyres and anti - vibration mounts, because of its superior mechanical properties. The useful (service) life of the rubber can be affected by the presence of flaws introduced during fabrication and by conditions experienced during service. In order to assess and predict the functional life of a natural rubber (NR) engine mount compound, the effect of ageing and the presence of deliberately introduced flaws on the physical and failure properties were determined.

Accelerated ageing was carried out at temperatures ranging from 70°C to 110°C at times of between one hour and five weeks. Static and dynamic measurements were used to quantify the effects of ageing on properties and assess ageing mechanisms.
Stiffness of the compound increased with ageing time while tensile strength and elongation at break decreased. Aerobic degradation mechanism of Ahagon Type I and III were predominant. The activation energy of ageing, in terms of its effect on tensile strength was found to be 93 kJ/mol for a cure temperature of 140°C and 86 kJ/mol for a cure temperature of 150°C when the Time Temperature Superposition method was applied. The tensile strength after ageing for 13 weeks at 50°C was predicted to be 18.7 MPa, which was very close to the experimental value of 19.0(± 2.25SD) MPa.

The presence of weld lines introduced before scorch did not significantly affect the tensile properties if sufficient time was allowed for healing, with the healing time reducing with increase in cure temperature. The activation energy for healing was found to be 31 kJ/mol for rubber cured between 110°C to 150°C. The presence of flaws, such as pinholes of varying sizes had a significant effect on both tensile strength and fatigue life, with the pin hole equivalent intrinsic flaw size estimated to be about 200μm.

Key Words: Rubber, degradation, kinetics, activation energy, healing, intrinsic flaw size, life prediction

TABLE OF CONTENT

TITLE PAGE i

DEDICATION ii

ACKNOWLEDGEMENT iii

CERTIFICATE OF ORIGINALITY iv

ABSTRACT. v

TABLE OF CONTENT vi

LIST OF FIGURES xii

LIST OF TABLES xvii

CHAPTER 1: GENERAL INTRODUCTION 1

1.0Background 1

1.1. Reasons for and Scope of the Study 3

1.2. Overall Project Objective 4

1.3. Specific Objectives 4

1.4. Structure of the Thesis 5

1.5 References 7

CHAPTER 2 **8**

2 Review of Composition, Properties and Structure of Natural Rubber and its Compounds8

2.1 Additives for Natural Rubber Compounds 9

2.1.1 Curatives 9

2.1.1.1 Accelerators 9

2.1.1.2 Activators 11

2.1.1.3 Fillers 11

2.1.1.4 Antioxidants 12

2.1.1.5 Plasticisers 12

2.2 Characterisation of Mechanical Properties of Elastomers 13

2.2.1 Tensile Strength, Modulus and Elongation at Break 13

2.2.2 Creep 14

2.2.3 Compression Set 14

2.2.4 Hardness 15

2.2.5 Dynamic Mechanical Properties of Rubber 15
2.3 Structure of the Rubber Network 17
2.3.1 Theory of Rubber Elasticity and the Entanglement Concept 17
2.3.2 Crosslink Density 18
2.4 References 22
CHAPTER 3 24
3 Review of Ageing of Rubber Compounds 24
3.1 Introduction 24
3.2 Ozone Ageing 26
3.3 Thermo-oxidative Ageing. 27
3.3.1 Mechanisms of Thermo-oxidative Ageing 27
3.3.2 The Role of Oxygen Diffusion in Thermo-oxidative Ageing 32
3.3.3 Role of Anti oxidants in Reducing Thermo-oxidative Ageing 33
3.4 Effect of Thermal Ageing on the Sulphur Crosslink Network of Rubber Compounds 37
3.5 Effect of Ageing on Properties of Rubber Compounds 39
3.6 Kinetics of Rubber Ageing in Terms of its Effect on Properties 41
3.7 Kinetics of High Temperature Degradation by Gravimetric Analysis 42
3.8 References 48

CHAPTER 4 51
4 Review of fatigue failure and fracture of rubber compounds 51
4.1 Introduction 51
4.2 Theoretical Treatment of Fatigue and Fracture Behaviour 52
4.2.1 Crack Nucleation and the Continuum Mechanics Approach 52
4.2.2 Crack Growth and the Fracture Mechanics Approach 53
4.3 Measurement of Crack Growth in Elastomeric Materials 57
4.3.1 Single-Edged Notch Specimen 57
4.3.2 Shear and Trouser Tear Test Specimens 57
4.4 Some Factors Affecting Strength and Fatigue Failure of Natural Rubber 58
4.4.1 Effect of Fillers 58
4.4.2 Effect of Crosslink Type 60
4.4.3 Effect of Temperature 61

4.4.3.1 Environmental Temperature 61
4.4.3.2 Temperature at Crack Tip 62
4.5 Life Prediction. 63
4.5 References 64

CHAPTER 5 67
5 Experimental 67
5.1 Materials 67
5.2 Mixing 67
5.3 Cure Measurements and Vulcanisation 69
5.4 Compression Set 69
5.5 Accelerated Thermal/Thermo – oxidative Ageing 69
5.5.1 Static Ageing 69
5.6 Thermogravimetric Analysis 70
5.7 Tensile Testing 70
5.8 Dynamic Mechanical Analysis of Aged Rubber 71
5.9 Crosslink Density Measurements 71
5.9.1 Swelling: 71
5.10 Crack Nucleation and Growth Measurements 72
5.10.1 Fatigue Testing 72
5.11 Investigation of Flaws Introduced During Moulding 76
5.11.1 Introduction of a Memory Interface 76
5.12 Introduction of particulate contamination 77
5.13 Pinhole Flaws 78
5.14 Microscopy 78
5.15 References 79

CHAPTER 6 80
6 Effect of Ageing on Static Mechanical Properties 80
6.1 Introduction 80
6.2 Effect of Cure Temperature on Properties 80
6.3 Effect of Cure Time on Modulus and Tensile Strength 82
6.4 Effect of Ageing on Tensile Strength and Elongation at Break. 86

6.4.1 Thermal Ageing: 86
6.4.2 Thermo-oxidative Ageing 88
6.4.3 Activation energy calculations for thermo-oxidative ageing 93
6.5 Effect of Ageing on Tensile Modulus 102
6.5.1 Compound Cured at 150°C - Kinetics of Ageing in Terms of its Effect on Modulus 104
6.6 Effect of Cure Temperature and Data Treatment Methods on the Activation Energy of Ageing 113
6.7 Crosslink Density 115
6.8 Mechanisms of Ageing as Deduced from Tensile Measurements 116
6.9 Kinetics of Ageing from Thermogravimetric analysis 120
6.9 Life predictions 125
6.10 Conclusion 130
6.11 References 131

CHAPTER 7 133
7 Effect of Ageing on Dynamic and Fracture Properties. 133
7.1 Introduction 133
7.2 Effect of Ageing on Dynamic Mechanical Properties 133
7.3 Effect of Temperature Variation on the Dynamic Mechanical Properties of the Aged Natural Rubber Compound 138
7.4 Effect of Ageing on Crack Growth 141
7.4.1 Effect of Ageing on Tearing Energy 141
7.4.2 . Effect of Ageing on Dynamic Crack Growth 145
7.4.3 Effect of Ageing on Fatigue Life 147
7.4.4 : Effect of Dynamic Ageing on Fatigue Life 150
7.5 Conclusion: 152
7.6 References 154

CHAPTER 8: Effect of Nature of Flaws on Failure Properties 156
8 Introduction 156
8.1 Effect of Memory Interfaces on Failure Properties of an Engine Mount Compound 156
8.1.1 Effect of Memory Interface and Cure Temperature on Failure Properties 157

8.1.2 Fatigue Measurements 160
8.1.3 Effect of Pre-curing to Scorch on the Tensile Properties of a Memory Interface 161
8.1.3.1 Effect of Pre-curing to Scorch on Modulus 161
8.1.3.2 Effect of Pre-curing to Scorch on the Tensile Strength and Elongation at Break of a Memory Interface 163
8.1.4 Healing of Memory Interfaces During Curing 164
8.1.4.1 Kinetics of Healing 168
8.2 Effect of Particulate Contamination on Failure Properties 170
8.2.1 Tensile Properties 170
8.2.2 Fatigue Measurements 176
8.3 Effect of Pinhole Flaws on the Mechanical Properties of the Natural Rubber Compound 176
8.3.1 Tensile Properties 177
8.3.2 Fatigue Life 181
8.4 Conclusions 181
8.5 References 183

CHAPTER 9: Conclusions and Recommendations 184
9.1 Conclusions 184
9.1.1 Effect of Ageing on Mechanical Properties 184
9.1.2 Activation Energy of Ageing 185
9.1.3 Mechanisms of Ageing 186
9.1.4 Effect of Ageing on Failure Properties 186
9.1.5 Dynamic Ageing 187
9.1.6 Effect of Flaws on Failure Properties 187
9.2 Recommendations for Further work 188
9.3 References 189
APPENDIX I 190
Figure A1.1: Normalised data to show the effect of thermal ageing on Tensile strength 190
Figure A1.3: Second order plot for the effect of ageing on elongation at break of the natural rubber compound cured at 140°C 191
Figure A1.4: Arrhenius plot for the rate constants for ageing determined from the effect of ageing on tensile strength for rubber cured at 140°C 191

Figure A1.5: Arrhenius plot for the rate constants for ageing determined from the effect of ageing on Elongation at break for rubber cured at 140°C 192
APPENDIX II 193
Publications from this Thesis 193

LIST OF FIGURES

Figure 1.1: Temperature rise with time in a car engine mount during service .[5] 2

Figure 2.1: Natural rubber tree with latex collected in a cup (courtesy CIRAD – CP) 12

Figure 2.2 : Effect of cross link density on physical properties.(Reprinted from "Engineering with Rubber" A.N. Gent Ed., 1992,[21]) 23

Figure 3.1: Scheme showing ozonolysis of a double bond compound 26

Figure 3.2: Mechanism for thermo – oxidative ageing of polymers 28

Figure 4.1: Regions of crack propagation[17] 56

Figure 4.2: The three modes of crack surface displacement (a) Mode I, opening or tensile mode, (b) mode II, sliding mode and (c) mode III, tearing mode 63

Figure 5.1: Scheme for the mixing sequence 68

Figure 5.2: Diagram of the test machine measuring crack growth characteristics adopted from[8] . (1) Motor, (2) High – Speed CCD camera, (3) Clamps, (4) Main shaft, (5) Cylinder, (6) stop ring, (7) crosshead, (8) load cell, (9) Chamber, (10) cylinder handle, (11) Cam. 74

Figure 5.3: Diagram of the SEN rubber sample to measure crack growth 75

Figure 5.4: Diagram of (a) trouser tear test piece and (b) different tear that may be observed. 76

Figure 5.5: Types of flaws introduced after pre - curing 78

Figure 6-1: Relationship between cure time and modulus cured at 150°C 82

Figure 6-2: Evolution of curemeter torque and 300% modulus with cure time for rubber cured at 150°C 83

Figure 6-3: Relationship between cure time and (a) % elongation at break, (b) tensile strength NR Compound 84

Figure 6-4: Effect of thermal ageing on the tensile strength of the compound (cured at 140°C) 86

Figure 6-5: Effect of thermal ageing on the elongation at break of the natural rubber compound (cured at 140°C) 87

Figure 6-6: Effect of thermal ageing on the Modulus of the natural rubber compound (cured at 140°C) 88

Figure 6-7: Effect of ageing on tensile strength for rubber cured at 140°C 89

Figure 6-8: Effect of ageing on tensile strength for rubber cured at 150°C 90
Figure 6-9: Effect of ageing on elongation at break for rubber cured at 140°C 90
Figure 6-10: Effect of ageing on elongation at break for rubber cured at 150°C 91
Figure 6-11: Light microscopic image showing crack surface of an aged rubber sample after tensile testing (Each minor division is 10μm) 92
Figure 6-12: Second order plot for the effect of ageing on tensile strength of the compound cured at 150°C 94
Figure 6-13: Second order plot for the effect of ageing on Elongation at break of the compound cured at 150°C 95
Figure 6-14: Temperature dependency of rate law on the tensile strength of natural rubber compound 96
Figure 6-15: Temperature dependency on rate law on elongation at break of a natural rubber compound 97
Figure 6-16: Time – temperature superposition plot for tensile strength for ageing of natural rubber at 70°C reference temperature for rubber cured at 140°C. 98
Figure 6-17: Time – temperature superposition plot for elongation at break for ageing of natural rubber compound cured at 140°C (70°C reference temperature) 99
Figure 6-18: Arrhenius plot for log of shift factor for tensile strength 100
Figure 6-19: Arrhenius plot for log of shift factor for elongation at break 101
Figure 6-20: Arrhenius plot for critical life of thermally aged rubber compound 102
Figure 6-21: Effect of ageing on stress at 100% strain (100% modulus) for rubber cured at 140°C 103
Figure 6-22: Effect of ageing temperature on the modulus at 100% strain for compound cured at 150°C 104
Figure 6-23: Relationship between ageing time and reduced modulus at the different ageing temperatures (cured at 150°C) 105
Figure 6-24: Fractional rate law plot for ageing reactions as they affect modulus for rubber cured at 150°C 106
Figure 6-25: Arrhenius plot for ageing in terms of its effect on modulus 108
Figure 6-26: Effect of ageing on reduced Modulus at 100% strain 109
Figure 6-27: Time – temperature superposition plot for reduced modulus at 100% strain for ageing of natural rubber at 70°C reference temperature 110
Figure 6-28: fractional rate law plots for aged NR samples in terms its effect on modulus. 112
Figure 6-29: Arrhenius plot for reduced modulus at 100% strain from fractional rate law 112

Figure 6-30: Effect of ageing on crosslink density for rubber cured at 140°C 115
Figure 6-31: Typical autoxidation reaction of natural rubber 117
Figure 6-32: Ahagon plot for the ageing mechanisms of natural rubber compound cured at 140°C 117
Figure 6-33: Ahagon plot for the ageing mechanisms of natural rubber compound cured at 150°C 118
Figure 6-34: Ahagon plot for the thermal ageing mechanisms of natural rubber compound cured at 140°C 119
Figure 6-35: TG and DTG curves in air atmosphere for engine mount compound aged at 80°C 122
Figure 6-36: TG and DTG curves in nitrogen atmosphere for engine mount compound aged at 80°C 122
Figure 6-37: Plot of logβ versus 1/Tmax (Doyle – Ozawa method) for the first decomposition step of the natural rubber compound 125
Figure 6-38: TG and DTG curves (a) in air and (b) in nitrogen atmosphere for engine mount compound aged at 110°C 127
Figure 6-39: TG and DTG curves (a) in air and (b) in nitrogen atmosphere for engine mount compound aged at 100°C 128
Figure 6-40: TG and DTG curves (a) in air and (b) in nitrogen atmosphere for engine mount compound aged at 90°C 129

Figure 7.1: Effect of strain amplitude on the storage modulus of the natural rubber compound aged at 70°C 134
Figure 7.2: Effect of strain amplitude on the loss tangent of the natural rubber compound aged at 70°C 135
Figure 7.3: Effect of strain amplitude on the loss modulus of the natural rubber compound aged at 70°C 135
Figure 7.4: Effect of strain amplitude on the storage modulus of natural rubber compound aged at 90°C 136
Figure 7.5: Effect of strain amplitude on the loss tangent of the natural rubber compound aged at 90°C 137
Figure 7.6: Effect of strain amplitude on the loss modulus of the natural rubber compound aged at 90°C 137

Figure 7.7: Effect of ageing at 90°C on the storage modulus 138
Figure 7.8: Effect of ageing at 90°C on the loss tangent 139
Figure 7.9: Effect of ageing at 90°C on the loss modulus 139
Figure 7.10: Effect of ageing at 110°C on the loss modulus 140
Figure 7.11: Effect of ageing at 110°C on the loss tangent 140
Figure 7.12: Effect of ageing at 110°C on the storage modulus 141
Figure 7.13: Effect of ageing on tearing energy of NR compound cured at 140°C. 143
Figure 7.14: Ageing time /ageing temperature superposition plot of the fracture energy 144
Figure 7.15: Arrhenius type plot of shift time with ageing temperature for tearing energy 144
Figure 7.16: Arrhenius plots of the log of critical life 145
Figure 7.17: Effect of ageing time on crack growth resistance of a NR engine mount compound 147
Figure 7.18: Fatigue life for aged natural rubber samples 148
Figure 7.19: Time temperature superposition graph for fatigue measurements after static ageing 149
Figure 7.20: Arrhenius type plot for the shift factors against inverse absolute temperature 150
Figure 7.21: Effect of dynamic ageing on fatigue life of NR compound. 151
Figure 7.22: Temperature rise with time during fatigue of natural rubber samples (A and B) monitored by thermal imaging camera 152
Figure 8.1: Effect of cure temperature and memory interfaces on the modulus of the NR compound 158
Figure 8.2: Effect of cure temperature and treatment on the tensile strength of a natural rubber compound 159
Figure 8.3: Effect of pre – curing at 140°C on memory interface 159
Figure 8.4: Effect of memory interface on the fatigue life of rubber compound. 160
Figure 8.5: Effect of pre-curing to scorch on the Modulus of natural rubber compound 162
Figure 8.6: Effect of pre-curing to scorch on the tensile strength of N.R compound 163
Figure 8.7: Effect of pre-curing to scorch on the elongation at break of natural rubber compound 164
Figure 8.8: Cure curve showing the parameters used to determine the healing time of the natural rubber compound (tc is time at which cut is introduced) 165
Figure 8.9 : Arrhenius relationship for scorch times 167
Figure 8.10: Effect of pre – cure time (tc) at different temperatures on the tensile strength of the NR sheet containing a memory interface 168

Figure 8.11: Effect of pre – cure time at different temperatures on the elongation at break of the NR sheet containing a memory interface 168
Figure 8.12: Effect of cure temperature on the Arrhenius relationship for healing 170
Figure 8.13: Effect of particulate contamination on the modulus of natural rubber compound (CBSappl – carbon black on surface application, CB cut – carbon black in cut) 171
Figure 8.14: Effect of particulate application on the elongation at break of NR compound 172
Figure 8.15: Effect of particulate contamination on the elongation at break of the natural rubber compound 173
Figure 8.16: SEM micrograph of tensile fractured surface of cut with carbon black application *(Agglomerates may have acted as stoppers to the advancement of the crack which propagates perpendicularly to the applied force)* 173
Figure 8.17: SEM micrograph showing carbon black agglomerate in the tensile fracture surface on sample with surface application of particulate. *(carbon black agglomerate that penetrated the rubber could be seen)* 174
Figure 8.18: SEM micrograph of tensile fractured sample showing carbon black agglomerate embedded in cut 175
Figure 8.19: SEM micrograph showing carbon black agglomerates on surface of rubber 175
Figure 8.20: Effect of particulate filler application on the fatigue life of N.R. compound. 176
Figure 8.21: Effect of pinhole flaw size on Tensile Modulus 177
Figure 8.22: Effect of pinhole flaw size on Elongation at break 178
Figure 8.23: Effect of pinhole flaw size on Tensile strength 178
Figure 8.24: A log – log plot to estimate the intrinsic flaw size of the rubber compound 179
Figure 8.25: Effect of pinhole flaw on fatigue life 181

LIST OF TABLES

Table 5.1: Typical engine mount formulation 67

Table 6.1: Cure behaviour of compounded natural rubber at different cure temperatures 80

Table 6.2: Properties of the engine mount compound cured at 140°C and 150°C 81

Table 6.3: Constants, errors and coefficients of correlation describing the relationship between cure time and modulus for rubber cured at 150°C 83

Table 6.4: Constants from equation 6.4 describing the master curves for tensile strength and elongation at break 99

Table 6.5: Order and rate constants for ageing of NR, in terms of effect on modulus for rubber cured at 150°C 107

Table 6.6: Rate constants and order of reaction from fractional rate law for modulus for rubber cured at 140°C 111

Table 6.7: Effect of data treatment method on the activation energies 113

Table 6.8 : Data comparing the modulus and elongation at break data for thermally aged and thermo – oxidatively aged rubber compound 120

Table 6.9 : Effect of ageing time on the temperature at weight loss regions 123

Table 6.10: Activation energies and service life prediction 126

Table 7.1: Critical life with respect to tearing energy for the aged N.R. compound..... 143

Table 8.1: Effect of temperature on cure characteristics and healing time..... 166

Table 8.2 : Flaw size, average tensile strength, stress - flaw constant and estimated tensile strength of rubber compound 180

CHAPTER 1: GENERAL INTRODUCTION

1.0 Background

Engine mounts are a set of rubber engineering components with related anti – vibration functions. Material properties and other important factors in the engine mount application are listed below:

- Each rubber component will normally be required to have a specified force / deflection behaviour in more than one direction.
- Compression of the rubber layers in the component may be combined with shear and / or torsion and/or rotation.
- Creep resistance is important for load bearing components such as the engine mount.[1]
- The component must have suitable vibration isolation characteristics. It should be stiff and highly damped to control the idle shake and engine mounting resonance from 5 to 30Hz.,
- It must be able to control, like a shock absorber, the motion resulting from quasi – static load conditions such as travel on bumpy roads, abrupt vehicle acceleration or deceleration, and braking and cornering.
- For small amplitude excitation over a higher frequency range, an acquiescent but lightly damped mount is required for vibration isolation and acoustic comfort[2].

Engine mounts, like all components, are susceptible to failure and deterioration throughout their service life. It is important to understand and where possible quantify, the processes leading to failure or decline in performance, in order to both avoid premature failure and to be able to predict accurately the useful life of the component. The main processes leading to failure of the rubber in the engine mount are ageing and fatigue fracture. Both of these processes occur simultaneously and each can have an effect on the other.

Natural rubber has a mechanical property envelope which makes it an important material in dynamically loaded applications such as engine mounts.[3] However, a

disadvantage of natural rubber is that it is susceptible to thermal and oxidative ageing. The problem of ageing is increasingly becoming important in recent years because the reduction in engine compartment volume, due to aerodynamic design of vehicles, has resulted in increased under-hood (under-bonnet) temperatures. The temperature rise experienced by an engine mount compound simulated for a car in service, shows a massive rise in temperature of about 35°C to 40°C after 25 minutes of running the engine (Figure 1.1). A levelling off of the temperature was recorded after 75 to 80 minutes of the start of the engine.[5] Temperatures of almost 120°C have also been recorded. The simulation therefore indicates the temperature range of interest for ageing studies of engine mount compounds.

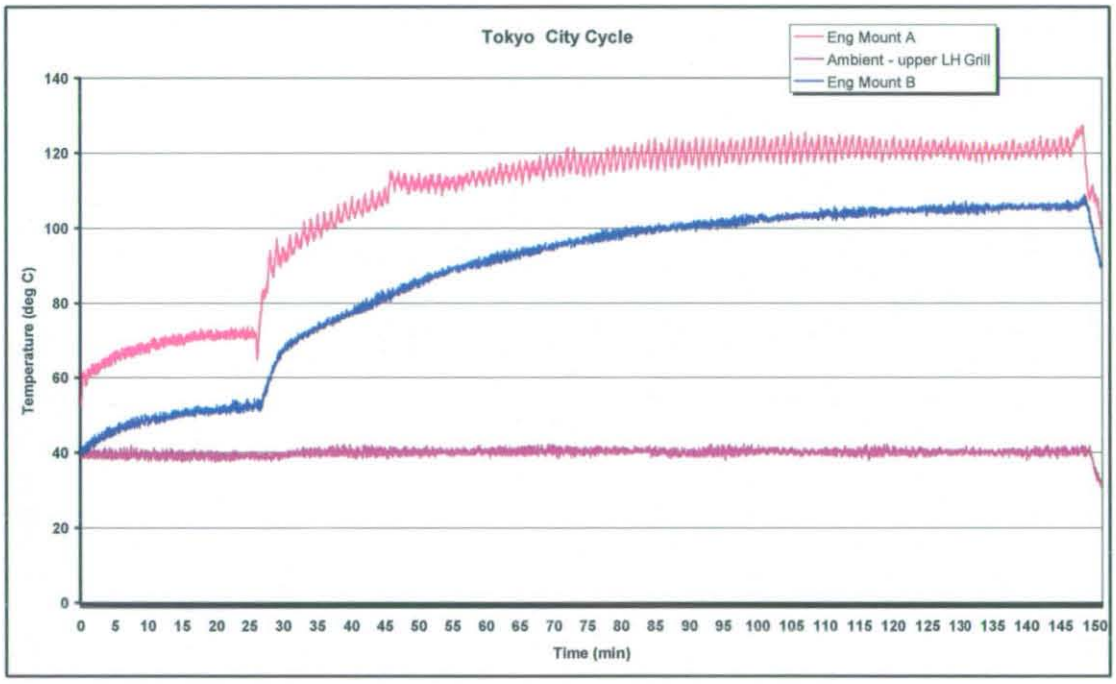

Figure 1.1: Temperature rise with time in a car engine mount during service .[5]

During the service life of an engine mount, it is exposed to both static and dynamic ageing, as well as other harsh environmental conditions. Static ageing results in changes in structure due to chain cleavage, crosslink formation and breakage, filler – filler network development, changes in filler:elastomer interactions and molecular relaxation. These changes influence bulk properties such as stiffness and hysteresis, but also failure properties such as tensile strength and fatigue life as a result of crack

initiation and crack propagation. Ageing under dynamic deformation conditions will result in somewhat similar effects. However, the fluctuating stress field will influence microstructural changes, such as molecular rearrangement of the network structure and distribution and alignment of filler particles. The dynamic movement may also result in significant local temperature rise, augmenting thermal effects. Diffusion of gases, such as oxygen, may also be enhanced, making oxidative ageing worse. The engine mounts and other automotive components also experience the combined effect of static and dynamic ageing, as vehicles are used intermittently rather than continuously. Ageing under these conditions may be different from ageing under the completely static or completely dynamic conditions that are normally used for testing. Periods of static ageing allow the structure to relax and randomise. Hence, the first cycles of deformation following static periods will result in higher stresses than would be experienced with continuous dynamic ageing once a steady state had been reached. If these peak values of stress were above some critical value, then the network structure could be damaged, which may lead to failure at an earlier point than would be expected from a purely dynamic ageing test[4].

Apart from the effects of ageing described above, flaws in the rubber, which might be as a result of processing or as a result of damage sustained during service can have a profound effect on the service life of the component. Flaws introduced during processing include weld lines and particles resulting from poor mixing or contamination. The flaws can raise the stress intensity factor then propagate under certain loading conditions into more permanent cracks resulting in failure. An understanding of the conditions under which such flaws give rise to crack initiation and the conditions under which cracks propagate is critical if the life of a rubber component is to be predicted. .

1.1. Reasons for and Scope of the Study

Although there is a large amount of published research on ageing of natural rubber, it has mostly been carried out under static conditions. However, rubber compounds are mostly used in dynamic applications and hence, a study into the differences between static and dynamic ageing is deemed essential. Furthermore, much work carried out on the ageing of rubber was carried out at high temperatures with extrapolations to predict behaviour at lower temperatures. In this study, a wide range of temperatures

will be used to investigate the validity of this type of extrapolation.

Fracture mechanics have been applied to crack propagation in rubber components; however, there is very little published work on the process of crack initiation. Crack initiation is arguably more important than crack propagation and an understanding of the factors controlling the process would be a very useful for component designers and manufacturers. In this study the effects of intrinsic flaws, such as particles and weld lines, on crack initiation and failure properties will be investigated. There is little published on the ability of weld lines in rubber to heal during processing and since this has a potentially important effect on failure properties, a study into the healing of weld-lines is included in the current study.

1.2. Overall Project Objective

The overall aim of the project is to contribute to the development of improved methods of predicting service life of rubber components. The scope of the study covers the effect of some process and service conditions on the mechanical and failure properties of a natural rubber engine mount compound. Process conditions include cure temperature, and flaws introduced during processing, such as weld lines and particulate contamination. Service conditions include static and dynamic ageing and flaws, such as cuts and holes. The application of various kinetic methods to model many of these effects is proposed. The objective will be achieved by studying the effects of static and dynamic ageing on properties, crack initiation and crack propagation processes.

1.3. Specific Objectives

For a typical NR based engine mount compound the project has the following specific objectives :-

- To study the effect of heat and oxygen ageing (static and dynamic conditions) on the properties of the natural rubber compound,
- To study the effect of cure temperature on ageing kinetics,
- To study the effects of dynamic ageing and its associated kinetics on the natural rubber engine mount compound,
- To study the effects of inherent flaws on the mechanical and failure properties

of the NR compound,

- Investigate the kinetics associated with the healing of a weld line (memory interface),
- Determine the critical flaw size of the natural rubber engine mount compound.

1.4. Structure of the Thesis

The use of kinetic methods to explain simple processes that take place during processing and during the functional life of an engine mount compound has been explored in this thesis which is presented in nine chapters.

Chapter 2 gives a general overview of natural rubber additives and their roles. Some of the mechanical properties of interest in determining the useful life of the material, as well as the network structure are presented.

In Chapter 3, thermal and thermo - oxidative ageing of rubber is reviewed. The mechanisms of thermo – oxidative ageing and the role of oxygen and some of the additives in determining the ageing behaviour is examined. The effect of ageing on the properties of natural rubber compounds, and the kinetics associated with ageing both at low and high temperature are reviewed.

In Chapter 4, fatigue failure and other fracture mechanics techniques, as applied to elastomers, are examined in terms of continuum mechanics as well as fracture mechanics. Mechanisms and modelling of crack nucleation and growth, as experienced by rubber compounds are reviewed.

Chapter 5 describes the detailed methods that have been used in this thesis in order to realise the objectives. The results are presented and discussed in Chapters 6 to 8.

In Chapter 6 the effect of static ageing on the mechanical properties of a natural rubber engine mount compound are discussed. Different methods are applied to calculate activation energies of aging, including; rate law, time temperature superposition and critical life methods. There is a discussion of the mechanisms associated with the ageing of the rubber, as deduced from the changes in mechanical properties and the kinetics of ageing. Kinetics associated with high temperature ageing using thermogravimetric analysis (TGA/DTG), is presented. A life prediction

using the Arrhenius model is attempted.

In Chapter 7, the effect of ageing on the dynamic and fracture properties of the natural rubber compound is presented. The effect of ageing on dynamic crack growth and tearing energy is determined, and the activation energy of ageing based on these measurements is calculated and compared to values determined from the effect of ageing on bulk properties. The effect of dynamic ageing on the fatigue life of the compound is also examined and discussed in relation to static ageing.

Chapter 8 deals with the way in which flaws that can arise as a result of processing can affect properties of the compound. The flaws studied include small cuts, interfaces introduced during processing and particulate contaminants. The healing of interfaces in the compound is investigated, and the kinetics of the healing process is presented. The effect of the nature of the flaw on the mechanical and fracture properties of the rubber compound and the equivalent pinhole intrinsic flaw size is discussed.

Finally in Chapter 9, conclusions and recommendations for further work are presented.

1.5 References

(1) Stevenson, A. *natuurrubber* , **2003** *5*.

(2) Singh, R. *Sdhan : Academy proceedings in engineering sciences.* **2000**, *25*, 319-330.

(3) Liauw, C. M.; Allen, N. S.; Edge, M.; Lucchese, L. *Polym. Degrad. Stab.* **2001**, *74*, 159-166.

(4) Clarke J. *Private Communication*, **2004**, .

(5) Ellis, R. L. *Private Communication* **2006**, .

CHAPTER 2

2 Review of Composition, Properties and Structure of Natural Rubber and its Compounds

Natural Rubber (NR) is obtained from the tree Hevea brasiliensis, commonly found in South America, Asia; notably Malaysia, Indonesia, Sri Lanka, Thailand and in Africa (Liberia, Nigeria, Cameroon, Cote d'ivoire, Ghana, Gabon). The latex is tapped and collected in cups by incision of the bark of the Hevea tree. It is either collected after coagulation in cups as cuplumps, or preserved with some ammonia and collected as field latex. The coagulum obtained by treatment of the latex with acid, followed by washing and drying, contains a high proportion of a hydrocarbon, mixed with proteins, resins and other constituents, typically it has a hydrocarbon content of 94.5%; acetone solubles 2.8%; nitrogen 0.4%; ash 0.2% [1].

Figure 2.1: Natural rubber tree with latex collected in a cup (courtesy CIRAD – CP)

Raw rubbers have few uses in their natural state because they are plastic and tacky. To achieve the desired range of properties, the raw rubber must be combined with a range of additives. The selection of appropriate additives and their skilful and consistent mixing is known as compounding. After compounding, the compounded stock is cured to the desired level at an appropriate temperature through a process known as vulcanization. Vulcanization, as defined in ASTM D1556, is a chemical process in which long chains of the rubber molecules become crosslinked by reactions with vulcanizing agents to form three dimensional structures. It can also be defined as "the process of treating elastomers with a chemical to decrease its plasticity, tackiness and sensitivity to heat and cold, and to give it useful properties such as elasticity, strength and stability"[2].

2.1 Additives for Natural Rubber Compounds

The additives in a rubber compound may vary from 2 - 3% by weight in some rubber compounds to over 60% in others, and will include some of the following:[3]

2.1.1 Curatives

These are active chemicals which bring about the crosslinking of the long chain rubber molecules. The introduction of the crosslinks improves the rubber – like elasticity of the natural rubber. Sulphur is one of the most widely used crosslinking agents.

2.1.1.1 Accelerators

Accelerators generally act by reducing the cure time of the compounded rubber. Inorganic compounds were the first accelerators in use, and this included basic salts and metal oxides. Litharge, lime magnesium oxide and zinc oxides are some of the most important. Organic vulcanization accelerators were first utilized around the 20th century and organic bases such as aniline and thiocarbanilide were introduced in 1906 as accelerators in rubber compounds to improve the quality of low grade rubber and to accelerate the rate of vulcanization.[4] Accelerators not only control the cure rate, but also the state of cure and the time to onset of cure[2] . Premature crosslinking (scorch) of the rubber must be prevented because it raises the viscosity of the rubber compound rendering it unfit to process[5]. Some accelerators are particularly good at preventing this from happening and are said to possess good scorch safety. Accelerators can be classified according to their chemical structure, which determines

their mode of action and effect on cure behaviour [6]. A few of the more common classes of accelerator, some of which are used in the current study, are described below.

(a) Sulphenamides (eg N – tert – butyl – 2 – benzothiazolesulphenamide, TBBS) These are medium fast curing primary accelerators with moderate scorch safety, used in all sulphur curable elastomers. They are generally used with a secondary accelerator to adjust curing characteristics. TBBS can be used with a high level of a secondary accelerator such as TMTD to obtain faster vulcanization cycles and improved ageing resistance.

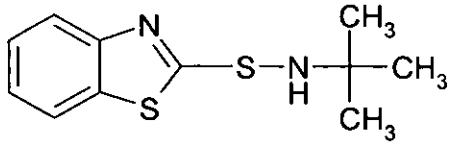

N - tert - butyl - 2 - benzothiazolesulphenamide

(b) Guanidines (e.g. diphenylguanidine, DPG): These are secondary accelerators for thiazole and sulphenamides, improving the vulcanization rate and crosslink density of the primary accelerator. DPG, exhibits better storage stability compared to thiurams and dithiocarbamates.

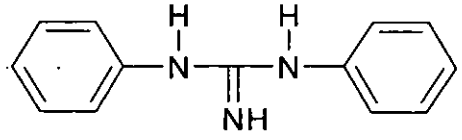

N,N' - Diphenylguanidine

(c) Thiazole and their derivatives (e.g. mercaptobenzothiazole, MBT), These are medium fast curing primary accelerators for natural rubber and synthetic rubber, with moderate scorch safety. They are generally used with a secondary accelerator to adjust curing characteristics.

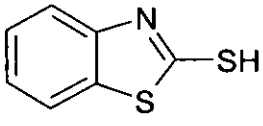

2 - mecaptobenzothiazole

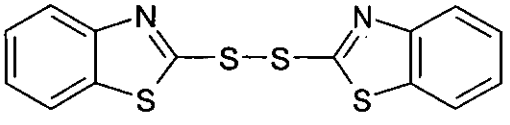

2,2' - Dimethiobis(benzothiazole)

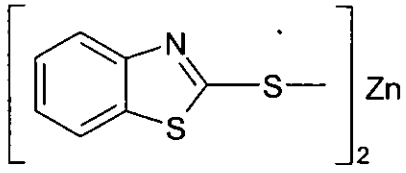

zinc - 2 - mercaptobenzothiazole

(d) Thiurams and dithiocarbamates (e.g. tetramethylthiuram disulphide and zinc dimethylthiocarbamate) Thiurams are scorchy, fast curing accelerators that provide high modulus. 'Thiurams and dithiocarbamates are secondary accelerators for thiazoles and sulphenamides.

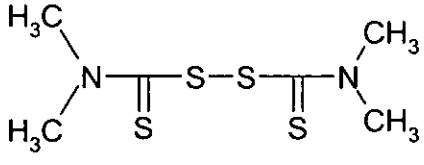

Tetramethylthiuram disulphide

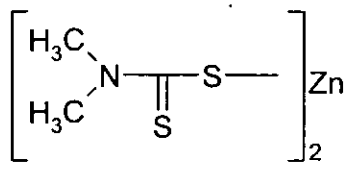

zinc dimethyldithiocarbamate

2.1.1.2 Activators

The function of activators is similar to accelerators, being mainly to reduce the time and temperature necessary to cure a rubber possessing the desired physical properties. An activator comprises ZnO and a fatty acid such as stearic acid. The activators should always be added at the beginning of the compounding process because of the difficulty in dispersing them evenly throughout the rubber mix.

2.1.1.3 Fillers

Fillers are materials that act to increase the stiffness of the polymer matrix to varying degrees. They affect properties such as strength, abrasion resistance and final compound cost. There are two types of filler; reinforcing and non-reinforcing.

Reinforcing fillers increase the stiffness and strength of the material. Carbon black and silica are the most commonly used. Others include, magnesium carbonate, china clay, hard clay. The way in which fillers reinforce compounds is described in more detail in section 4.4.1

Non-reinforcing fillers impart little or no improvement to the physical properties of a rubber but act as diluents. However, they may improve properties such as hardness and chemical resistance. Examples of non-reinforcing fillers include whiting, barites, talc, kieselguhr and slate dust.

2.1.1.4 Antioxidants

Antioxidants reduce oxidation and hence, maintain the physical properties of the rubbers while in service. Aromatic amines and certain phenols e.g. phenyl - β - naphthylamine are usually used. 2,2,4-Trimethyl -1,2-Dihydroquinoline, polymerized (TMQ) for example acts as a radical scavenger in vulcanized rubbers to protect against oxidative ageing. While N – (1,3 – dimethylbutyl) – N' – phenyl – p – phenylenediamine (6 – PPD), functions both as an antioxidant and antiozonant for natural and synthetic rubbers. They provide protection against fatigue degradation in both static and dynamic operating conditions.

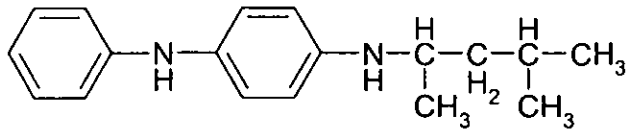

N - (1,3 - Dimethylbutyl) - N' - phenyl - p - phenylenediamine

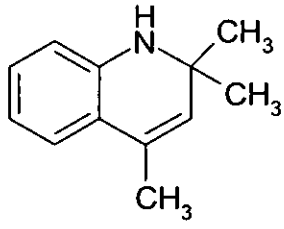

2,2,4 - trimethyl - 2 - dihydroquinoline

A more detailed discussion of oxidation and the role of antioxidants is given in Section 3.3.3

2.1.1.5 Plasticisers

Plasticisers are ingredients that lower a polymer's viscosity and the final rubber hardness. Plasticsers often also improve the low temperature tolerance of the rubber. Examples include

oils and liquid esters, resins and waxy materials. Plasticizers are used to increase flexibility of the rubber. A decrease in the plasticizer concentration in a polymer because the plasticizer has migrated out in service reduces ductility.

2.2 Characterisation of Mechanical Properties of Elastomers

Elastomers are polymers that are used well above their glass transition temperature, (Tg) and are characterised by low elastic modulus, high elongation at break and good recovery behaviour. The material properties most commonly used to differentiate between elastomeric materials are described in the following sections.

2.2.1 Tensile Strength, Modulus and Elongation at Break

Tensile tests measure the stress required to deform and break a specimen and the extent to which the specimen stretches or elongates up to that breaking point. The data is often used to specify a material, to design parts to withstand application of forces and as a quality control check of materials. Elongation at break, also known as ultimate elongation, is the maximum percent increase in length of a rubber specimen stretched until rupture occurs. Standard dumbbell test pieces are usually used for this test at a strain rate of 500mm min^{-1}..

Strain can be defined in several ways depending on the material.[7] For rubber, it is usually defined using the Cauchy or engineering strain as,

$$\varepsilon = \frac{L - L_o}{L_o} = \frac{\Delta L}{L_o} \qquad [2.1]$$

where L is the extended length and L_o is the original length of the rubber test sample.

The modulus of an elastomer is not a true modulus, as used for other materials, but it

is measured as the force per unit original cross-sectional area required to extend a sample to a specified percentage of its original length. Values most commonly quoted are 100% and 300% modulus, often written as M100 and M300 respectively. Hence, M100 = 3.0 MPa

means that the stress at 100% extension is 3.0MPa.

2.2.2 Creep

Under steady load the deformation of vulcanised rubbers increases continuously with time. This phenomenon is known as creep and follows a characteristic law, the deflection increasing proportionally with the logarithm of the time under load from a fraction of a second to many months.[8]

$$\alpha = d + b \log t \qquad [2.2]$$

where α = extension ratio,

t = time

d and b are constants.

2.2.3 Compression Set

Compression set can be used to indicate the ratio of viscous to elastic components of an elastomer's response to a given deformation. It is the deformation which remains in rubber after it has been subjected to and released from a specific compressive strain for a definite period of time at a prescribed temperature. It is considered an indicator of resistance to stress relaxation [5]. Longer polymer chains tend to give better set resistance because of the improved ability to store energy (elasticity). In a compression set test cylindrical test pieces of known diameter and thickness are compressed to say 25% of their original height and conditioned in an oven at a predetermined temperature for say 22 hours or more. The samples are then allowed to cool at room temperature for about 30 minutes, after which the applied load is removed and the compressed height recorded.

Compression set is expressed as:

$$\% \text{ compression set} = \frac{t_o - t_r}{t_o - t_s} x100 \qquad [2.3]$$

where t_o is the initial thickness, t_r is the recovered thickness and t_s is the compressed thickness

The use of compression set measurements is most beneficial for production quality control, indicating the state of cure. It is also important for sealing applications[9]

2.2.4 Hardness

This measurement is widely used in industry for specification of their material, because it is quick and easy to conduct. It can however, not be used for design purposes because it measures only the response of the material to small surface stress and not the entire elastomeric part. [10] Hardness is essentially a measurement of the reversible, elastic deformation produced by a specially shaped indentor under a specified load and is therefore related to the low strain modulus of the rubber. The hardness as measured by, for instance a Shore A Durometer is closely related to modulus of elasticity (Young's modulus). Shore A Durometer measures the penetration of a conically shaped indentor into the rubber. The result is expressed as a value between 0 and 100 Shore A (Sh. A). Engineering rubbers usually have hardness between 55 and 75 Shore A.

2.2.5 Dynamic Mechanical Properties of Rubber

Dynamic mechanical properties are particularly important where the rubber compound is exposed to repeated deformation and vibration, such as in a tyre or engine mount. Dynamic mechanical properties can be measured at a relatively large scale using servo-hydraulic test machines. Alternatively, small-scale tests with sample dimensions of a few millimetres can be carried out in a Dynamic Mechanical Analyser (DMA). If temperature can be varied as well then the technique is referred to as Dynamic Mechanical Thermal Analysis (DMTA). DMTA is particularly useful for measuring the Tg of polymers that are difficult to detect by other techniques.

Dynamic mechanical tests measure the response of the material to sinusoidal or other periodic stress or deformation. When the material responds perfectly elastically to the applied wave, an in-phase response is seen, but when the response is viscous, an out – of – phase response is recorded. Viscoelastic materials such as natural rubber show behaviour between

the in-phase and out-of-phase response. From the response recorded, the dynamic modulus and the phase angle can be determined[7]. Dynamic tests over a wide temperature and frequency range are especially sensitive to the chemical and physical structure of the elastomer. Results from dynamic mechanical testing are usually given in terms of the elastic modulus (or storage modulus, G'), viscous modulus (or loss modulus G'') and damping coefficient, tanδ., as a function of temperature, frequency or time. tanδ is a measure of the ratio of the energy dissipated as heat to the maximum energy stored in the material during one cycle of oscillation[7]

$$\tan\delta = \frac{G''}{G'} = \text{(loss modulus/ storage modulus)} \qquad [2.4]$$

The dynamic properties of natural rubber compounds used in tyres and other components such as engine mounts, have been widely investigated [11, 12] The addition of carbon black to rubber vulcanizates increases the stiffness, strength and abrasion resistance of the rubber but also increases the creep and a large part of heat build – up, especially in tyres. One of the reasons for the increase in stiffness with addition of carbon black is the hydrodynamic effect, which is a function of the volume concentration of carbon black[13, 14].

Earlier studies as quoted by Payne and Whittaker[13], on carbon black filled natural rubber indicate that there is a large decrease in the modulus with increasing amplitude compared to the unfilled rubber which showed little effect of amplitude on modulus or hysteresis. When carbon black filled natural rubber is cyclically strained, the modulus falls as the strain amplitude increases[13]. This non – linearity of modulus with strain amplitude increases with increase in carbon black loading. Gent et al suggested that this was due to a bond breaking mechanism. Payne [13] suggested that the decrease in the modulus of filled rubbers with amplitude was due to the breakdown of the three dimensional aggregates and the agglomerates of carbon black.

Hexiang Yan et. al.[12] in their experiment on the effect of nitrile rubber on properties of silica – filled natural rubber compounds for tyre, explained that larger values of tanδ obtained at 0°C, indicated a better wet traction property of the vulcanizate, while small tanδ values obtained at 60°C indicated a better rolling resistance of the vulcanizate. The tanδ values at

0°C and 60°C increased with an increase in the NBR content for silica filled vulcanizates. Molnár and Huba[15] carried out DMA studies on various silicone rubbers. They found that the storage modulus decreased two orders of magnitude from 10^9 Pa to 10^7 Pa in glass transition, and that the silicone rubbers show a frequency dependent behaviour near to the glass transition temperature. Also, Geethamma et.al.[16] used the DMTA technique to study the behaviour of short coir fibre reinforced natural rubber composites. Using the definition of a dynamic glass transition temperature as the temperature at which (i) the maximum of tanδ occurs or (ii) the maximum of G'' occurs or (iii) the middle point of G' versus temperature curve or (iv) the region where G' increases with increasing frequency at constant temperature. They found that the maxima of the loss tangent or damping factor (tanδ), and the loss modulus, G'' coincided for the unfilled rubber compound but not for the coir reinforced rubber compound. Also, little variation was observed in the elastic and loss modulus of the unfilled compound with frequency as was observed for the composite. At high frequency the viscous modulus and loss tangent decreased while the elastic modulus increased. This is due to the fact that the materials at high frequency have no time to undergo irreversible flow (permanent deformation) and so behave more elastically.. At low frequencies however, the molecules slip past each other and flow occurs with a resultant increase in the damping and loss modulus, as well as a decrease in the elastic modulus. It was further observed that the heat dissipation increases with coir fibre loading in the NR compound [16]

2.3 Structure of the Rubber Network

2.3.1 Theory of Rubber Elasticity and the Entanglement Concept

The accepted theory of rubber elasticity was first advanced by Meyer et.al. Their theory was based on the notion that thermal energy of atoms of a long chain molecule will lead to a greater amplitude of vibration in the direction perpendicular to the chain, since the forces between the chains are weaker than the primary valence forces within the chain. The repulsive pressure produced between parallel or extended chains draws the end of the chains together and are thus regarded as equivalent to longitudinal tension. A stretched rubber thus takes up an irregular statistically determined form by virtue of interchange of energy between constituent elements and the surrounding atoms.[17] It is frequently useful to think of entanglements as defined contact points between chains acting like pseudo-crosslinks in

order to apply the kinetic theory of elasticity, however, it is more correct to represent entanglements by a rather delocalised picture. If entanglements are thought of as localised points they have to be considered at least instantaneously, as fixed points like crosslinks.[18]

Rubber is composed of long chains of randomly oriented molecules, which are subject to entanglement and cross-linking. Entanglement is the mutual wrapping of polymer chains around each other. When the polymer chains are longer, there is more entanglement. Highly entangled polymers will resist deformation and so a relatively large amount of energy must be put into the system to cause the molecules to move relative to each other and disentangle.[19] The entanglement has a significant impact on the viscoelastic properties such as stress relaxation. When a rubber is exposed to stress or strain energy, internal rearrangements such as rotation and extension of the polymer chains occur. These changes occur as a function of the applied strain, the duration and rate of application, and the temperature at which the energy is applied.

2.3.2 Crosslink Density

Rubber products are typically cured at high temperature and pressure. The addition of curatives and accelerators forms cross-links between the polymer chains. It is this network of cross-links that largely determines the physical properties of tensile modulus, tensile strength, elongation at break and compression set. As explained by Zhao and Ghebremeskel[20] the mechanical behaviour of an elastomer depends strongly on cross link density as shown in Figure 2.2.

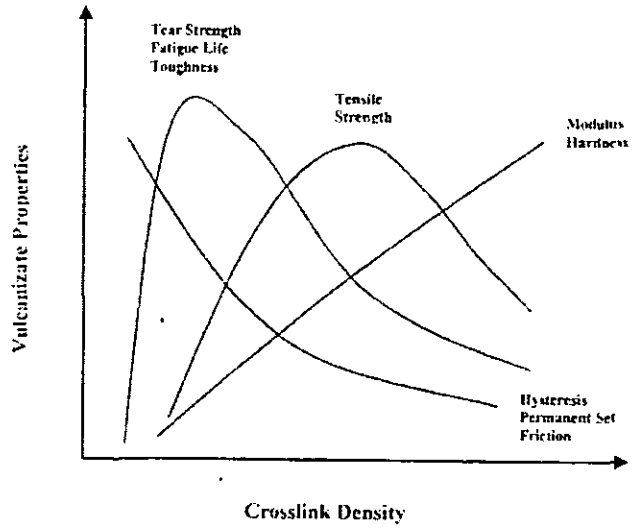

Figure 2.2 : Effect of cross link density on physical properties.(Reprinted from "Engineering with Rubber" A.N. Gent Ed., 1992,[21])

They showed that hardness and modulus increase monotonically with increasing cross link density, while fracture properties (tear strength, fatigue resistance, and tensile strength) pass through a maximum. They explained that the decrease in strength properties at high crosslink densities was due to chain motion becoming restricted and the "tight" network not being capable of dissipating much energy. The maximum in tear strength and fatigue life occurs at a lower cross link density than does the maximum for tensile strength.

The statistical theory of rubber-like elasticity provides relationships which describe both the stress - strain properties of crosslinked rubber and the extent to which it is swollen in suitable liquids.

In simple extension the force f required to extend a sample of rubber to an extension ratio λ is given by

$$f = \rho RTA_0^{-1}M_c^{-1}(\lambda - \lambda^{-2}) \qquad [2.5]$$

where M_c is the number - average molecular weight of rubber molecules between cross links, and is the basic variable characterising the network structure, ρ is the density, R is the gas constant, T the absolute temperature, and A_o the unstrained area of cross section. The

relationship between the equilibrium degree of swelling in a liquid and the network structure is given by the Flory - Huggins equation:

$$-\ln(1-v_r)-v_r-\mu v_r^2=\rho V_0 M_c^{-1} v_r^{1/3} \qquad 2.6$$

Where v_r is the volume fraction of rubber in the swollen material, μ an interaction constant characteristic of the rubber and the swelling liquid, and V_0 the molar volume of the swelling liquid.

The modified equation by Flory gives

$$-\ln(1-v_r)-v_r-\mu v_r^2=\rho V_0 M_c^{-1}[v_r^{1/3}-(\frac{v_r}{2})] \qquad 2.7$$

Measurements of the stress - strain properties or the degree of swelling of vulcanised rubber in conjunction with equations 2.5, 2.6, and 2.7 can thus be used to determine the value of M_c [22]

The cross link density of natural rubber has been measured using the swelling method[23-27]. In this method samples of known thickness and weight are immersed in toluene in the dark for a specified period of time, after which the cross link density is calculated using the Flory - Rehner equation:

$$\rho_c=-\frac{1}{2V_s}\frac{\ln(1-V_r)+V_r+\chi_1(V_r)^2}{(V_r)^{\frac{1}{3}}-\frac{V_r}{2}} \qquad 2.8$$

where ρ_c is the cross link density (mol/m^3), V_s, the molar volume of toluene (106.9 cm^3/mol. at 25°C); and χ_1, the interaction parameter or polymer solvent parameter (0.42 for black - filled NR) sometimes it is referred to as the Huggins Solubility parameter, and V_r can be determined from the equation 2.9 for black filled natural rubber:

$$\frac{V_r^o}{V_r}=1-[3c(1-V_r^{o\,1/3})+V_r^o-1]\frac{\phi}{1-\phi} \qquad 2.9$$

Where V_r^o is the rubber fraction in the swollen gel; c, the parameter for carbon - rubber

interaction(1.17); and ϕ, the volume fraction of carbon black.

For carbon black filled natural rubber, V_{ro} was determined from the equation 2.10 [23, 24, 26]

$$\frac{V_{ro}}{V_r} = 0.56e^{-z} + 0.44 \qquad [2.10]$$

where

V_r, is the measured volume fraction of rubber in the swollen network and is calculated from the equation 2.11.

z is the weight fraction of carbon black in the vulcanizate

$$\frac{1}{V_r} = 1 + \left(\frac{W_s \rho_r}{W_r \rho_s}\right) \qquad [2.11]$$

where W_r is the dry weight of the rubber specimen

W_s is the equilibrium swollen weight

ρ_r is the density of the rubber compound

ρ_s, the density of the solvent (toluene)

2.4 References

(1) Bateman, L. In *The chemistry and physics of rubber-like substances : studies of the Natural Rubber Producers' Research Association;* 1963: MacLaren, .

(2) FLEXSYS , Compounders pocket book; Chemicals for the rubber industry.

(3) Anonymous Harboro Handbook. *http://www.harboro.co.uk/html/harboro*2003).

(4) Aprem, A. S.; Joseph, K. Thomas, S. *Rubb. Chem. Technol.* **2005**, *78*, 458-488.

(5) Del Vecchio, R. J., Ed.; In *Fundamentals of Rubber Technology;* Rubber Division, American Chemical Society: Akron, 2003; , pp 321.

(6) Miles, D. C. In *Polymer Technology;* Templeton Press: London, 1965; , pp 282-295.

(7) Nielsen, L. E. In *Mechanical Properties of Polymers and Composites;* Marcel Dekker: New York, 1974; Vol. 1, pp 580.

(8) Davey, A. B. In *Rubber in engineering practice;* 1964: Maclaren, .

(9) Indian Rubber Institute In *Rubber engineering;* McGraw-Hill professional engineering; McGraw-Hill: New York, 2000; , pp 61.

(10) Mathew, N. In *Physical and technological Properties of Natural Rubber;* .

(11) Fan, R. L.; Zhang, Y.; Li, F.; Zhang, Y. X.; Sun, K.; Fan, Y. Z. *Polym. Test.* **2001**, *20*, 925-936.

(12) Yan, H.; Sun, K.; Zhang, Y.; Zhang, Y. *Polym. test.* **2005**, *24*, 32-38.

(13) Payne, A. R. *Rubb. Chem. Technol.* **1963**, *36*, 432-442.

(14) Payne, A. R.; Whittaker, R. E. *Rubb. Chem. Technol.* **1971**, *44*, 440-478.

(15) Molnár, L.; Huba, A. *Periodica Polytechnica Mechanical Engineering series* **2001**, *45*, 87-94.

(16) Geethamma, V. G.; Kalaprasad, G.; Groeninckx, G.; Thomas, S. *Composites Part A* **2005**, *36*, 1499-1506.

(17) Treloar, L. R. G. In *The physics of rubber elasticity;* Clarendon: Oxford, 2005; , pp 12.

(18) Paolo, L. *Polymer* **1992**, *33*, 1255-1260.

(19) Strong, A. B. In *Plastics, Materials and Processing;* Prentice hall,: Ohio, 2006; pp 102.

(20) Zhao J; Ghebremeskel GN *Rubber Chemistry and Technology* **2001**, *74*, 409.

(21) Gent, A. N. In Engineering with rubber, How to design rubber compounds; Hanser Verlag: Munich, 2001; pp 88.

(22) Mullins, L. *Rubb. Chem. Technol.* **1957**, *xxx*, 1-10.

(23) Porter, M. *Rubb. Chem. Technol.* **1967**, *40*, 866-882.

(24) Kim, S. G.; Lee, Suck - Hyun. *Rubb. Chem. Technol.* **1994**, *67*, 649-661.

(25) Sobhy, M. S.; El – Nashar, D.E.; Maziad, N. A. *Egypt. J. Sol.* **2003**, *26*, 241-257.

(26) Mathew, M. N.; Bhowmick, A. K.; De, S. K. *Rubber Chem. Technol.* **1982**, *55*, 51-61.

(27) Gent, A. N.; Hartwell, J. A.; Lee, G. *Rubber Chem. Technol.* **2003**, *76*, 517-532.

CHAPTER 3

3 Review of Ageing of Rubber Compounds

3.1 Introduction

Rubbery materials are usually subjected to physical and chemical property changes due to ageing, whether they are in service or during storage.[1-3] In the rubber industry, it is usually necessary to evaluate the ageing resistance of an automobile component such as the engine mount, tyres, seals etc. but this might take several years for a complete process to be observed in real service. Moreover, because of considerable variation in conditions in terms of location and seasonal variations, it is very difficult to evaluate changes due to degradation in a natural rubber compound in absolute terms. In real service conditions, engine mounts are exposed to a combination of factors including oxygen, heat, various liquids, dynamic motions etc. Ageing therefore is a composite of all these factors[4].

In recent years, studies on the mechanisms and types of degradation in natural rubber. has attracted wider attention because of the changing environment in which it is used, especially in the automobile industry.[1, 5, 6] This has necessitated new approaches in describing the mechanisms and service life predictions of engineering parts such as tyres, engine mounts, seals just to mention a few, since some standard models do not consider all the service environment of these components. Long term heat and weather resistance and high performance are key requirements for many rubber applications[7]. Recent technology in car manufacturing has resulted in very sophisticated and compact designs. The compactness has lead to an increase in under-bonnet temperatures and consequently, greater degradation resistance is required of rubber components such as the engine mounts.

Degradation of a polymer is generally taken to mean the irreversible change of chemical or physical properties which is caused by the chemical and/or physical action of agents. Degradation comprises the deterioration of macromolecules caused by bond scissions in the polymer backbone, chemical reactions in the side – chains and intermolecular crosslinking with formation of new chemical bonds between

different molecules.[8]

Degradation may occur during every phase in a polymer's engineering service life, which includes synthesis, processing and use. During processing of natural rubber and products from it for example, the material is subjected to very high thermal and mechanical stresses as a result of mastication, curing etc. that may initiate a whole series of degradation processes with the resultant deterioration of properties[9]. However, the degradation which is of greatest concern is that which occurs in service-life.

One of the factors usually associated with failure of polymers in-service, especially natural rubber products, is ageing. Ageing has been extensively studied for both synthetic and natural rubber, but much still needs to be done, especially in trying to understand the underlying mechanisms that influence the mechanical properties and their contributions to failure of the material in service. Ageing can be defined as the long term chemical changes occurring during service which lead to physical changes and that may result in component failure.[10] An elastomer undergoing deterioration due to ageing may undergo three types of change, which include[7]

1. Additional crosslinking resulting in higher crosslink density and embrittlement.
2. Chain scission leading to a reduction in the chain length and average molecular weight, and also leading to softening of the material.
3. Chemical alteration of the polymer chain by the formation of polar or other groups.

Most of the work that has been carried out on the ageing of NR has been centred on the chemistry involved, elucidating the structures of the scission or crosslink products. The most widely studied form of degradation for natural rubber is thermo-oxidative ageing. Others include ozone ageing (degradation) and environmental stress cracking. The mechanism of ozone ageing is discussed in the following section, while the remainder of the chapter is mostly concerned with thermo-oxidative ageing.

3.2 Ozone Ageing

Ozone is emitted as a product of combustion engines. Ozone attack on rubber causes chain scission and the formation of various decomposition products such as ozonides, polymeric peroxides, hydro peroxides, lactones, esters.

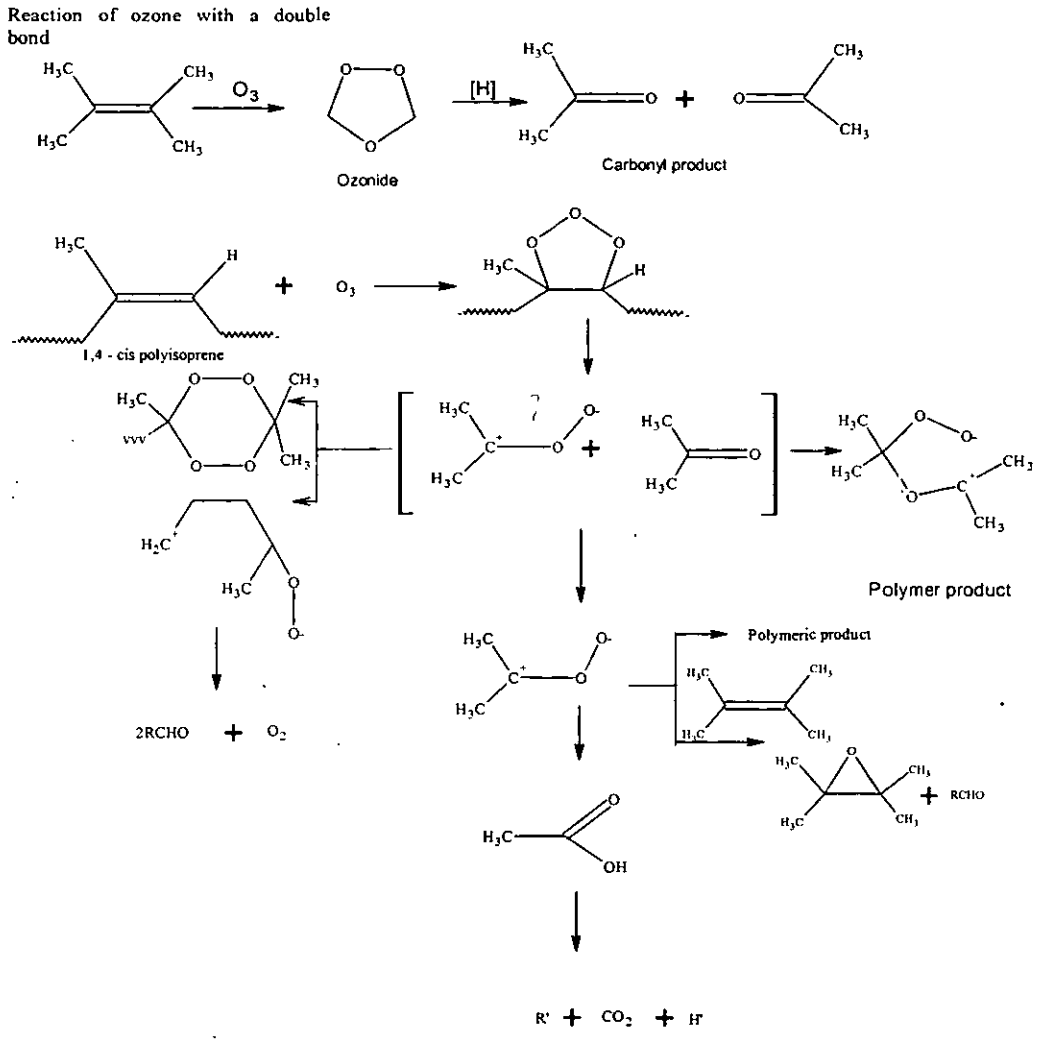

Figure 3.1: Scheme showing ozonolysis of a double bond compound

The reaction scheme shown in Figure 3.1 is known as ozonolysis. Ozone is concluded to be the active cause of cracking of rubber compounds but studies on soft vulcanized rubber indicated that ozone attacks and affects the rubber only under stress [11]. Carbon black however, was found to improve the ozone resistance both in natural rubber and blend vulcanizates, with black filled blends having a lower crack density than the

black - filled natural rubber, but the cracks were longer. [11]

3.3 Thermo-oxidative Ageing.

For thermo – oxidative ageing to take place, both heat and oxygen must be present. Heat resistance of an elastomer is said to be the maximum temperature at which the said elastomer is capable of operating for an extended period of time, while still retaining functionality[7].

Most organic compounds are oxidized by atmospheric oxygen and at moderate temperatures. Exposure of a natural rubber compound to elevated temperatures results in the cleavage of covalent bonds and subsequent degradation. The natural rubber compound has an unsaturated backbone which renders it very susceptible to heat because the energy required to break the second bond of the double carbon-carbon bonds (C = C) to form active radicals is relatively low. The NR can undergo a free radical chain reaction described as autoxidation, which involves transient alkyl peroxy radicals or photo – oxidation, a non radical process which involves electronically excited singlet oxygen.[6, 12, 13]

3.3.1 Mechanisms of Thermo-oxidative Ageing

Several mechanisms have been proposed for the thermo - oxidative degradation of natural rubber. A simple cyclic scheme to depict the general mechanisms of thermo – oxidation[8, 12, 14, 15] is that of Zhenghong Tao et. al.[7] and is as shown in figure 3.2

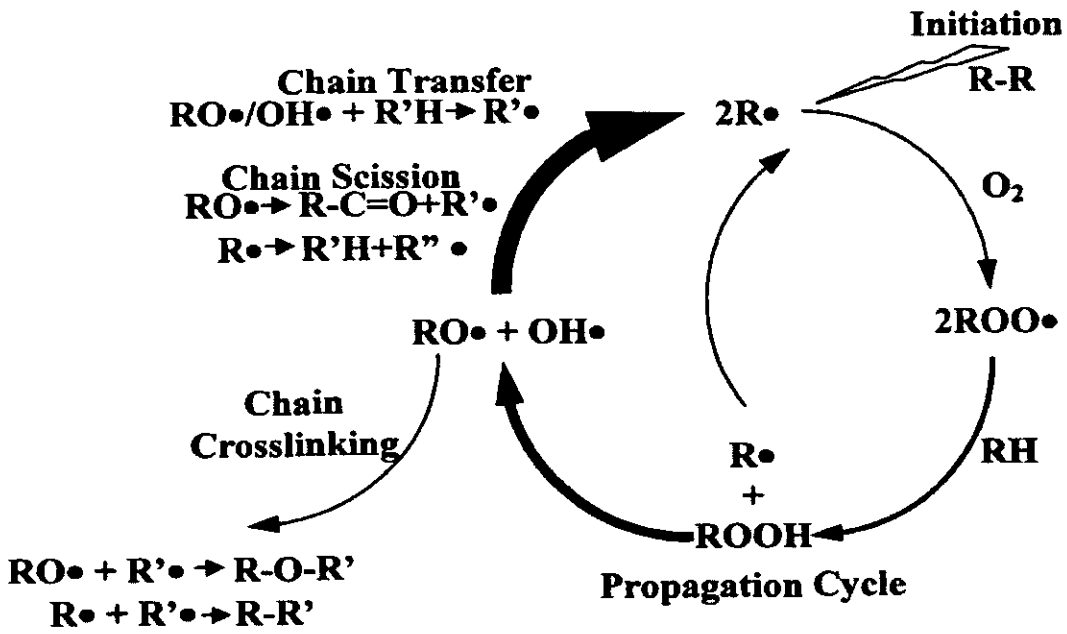

Figure 3.2: Mechanism for thermo – oxidative ageing of polymers

The above reaction takes place when there is a sufficient supply of oxygen. The hydroperoxide (ROOH) generated can itself break down to form two radicals (RO* + OH*) and so the reaction, once started is regarded as being autocatalytic. The decomposition of hydroperoxide (ROOH) occurs at a lower rate compared to the reaction of a peroxy radical with the polymer. Temperature influences the rate of the reaction and so is an important factor for thermo – oxidative ageing[9].

Metal catalysed oxidation can have an important effect on the lifetime of certain rubbers, e.g. natural rubber. Traces of certain transition metals, notably copper, manganese, cobalt and iron, are able to break down hydroperoxides in a redox reaction to give reactive peroxy radicals which then propagate oxidation and so ageing occurs at lower temperatures. They therefore have the opposite effect to a hydroperoxide deactivating antioxidant. The usual mechanism is:.[8, 15]

$$ROOH + M^{2+} \longrightarrow ROO^* + M^+ + H^+$$

$$ROOH + M^+ \longrightarrow RO^* + M^{2+} + OH^-$$

Where: M is the transition metal

In the absence of oxygen, the general mechanism for the thermal degradation of

natural rubber is thus;

Initiation (Initiator)I $\xrightarrow{\Delta}$ I*

I* + RH $\longrightarrow$ IH + R*

Chain Reaction R* + RH $\longrightarrow$ RRH

(containing a double bond) (a form of crosslinking)

Chain Transfer Reaction R* +R'H $\longrightarrow$ R'* + RH

Beta Scission Reaction R* $\longrightarrow$ $R_1 + R_2$*

Termination Reaction 2R* $\longrightarrow$ deactivated material (crosslinking reaction)

Hook Cleavage has been proposed by Boon [6] as a mechanism for scission in sulphur vulcanised natural rubber oxidation and he proposed the following scheme (Figure 3.3). The reaction of the allylic hydroperoxide to form two carbonyl fragments is acid catalysed (Scheme I). The allylic hydroperoxides are formed during autoxidation of natural rubber in the presence of chain breaking antioxidants.

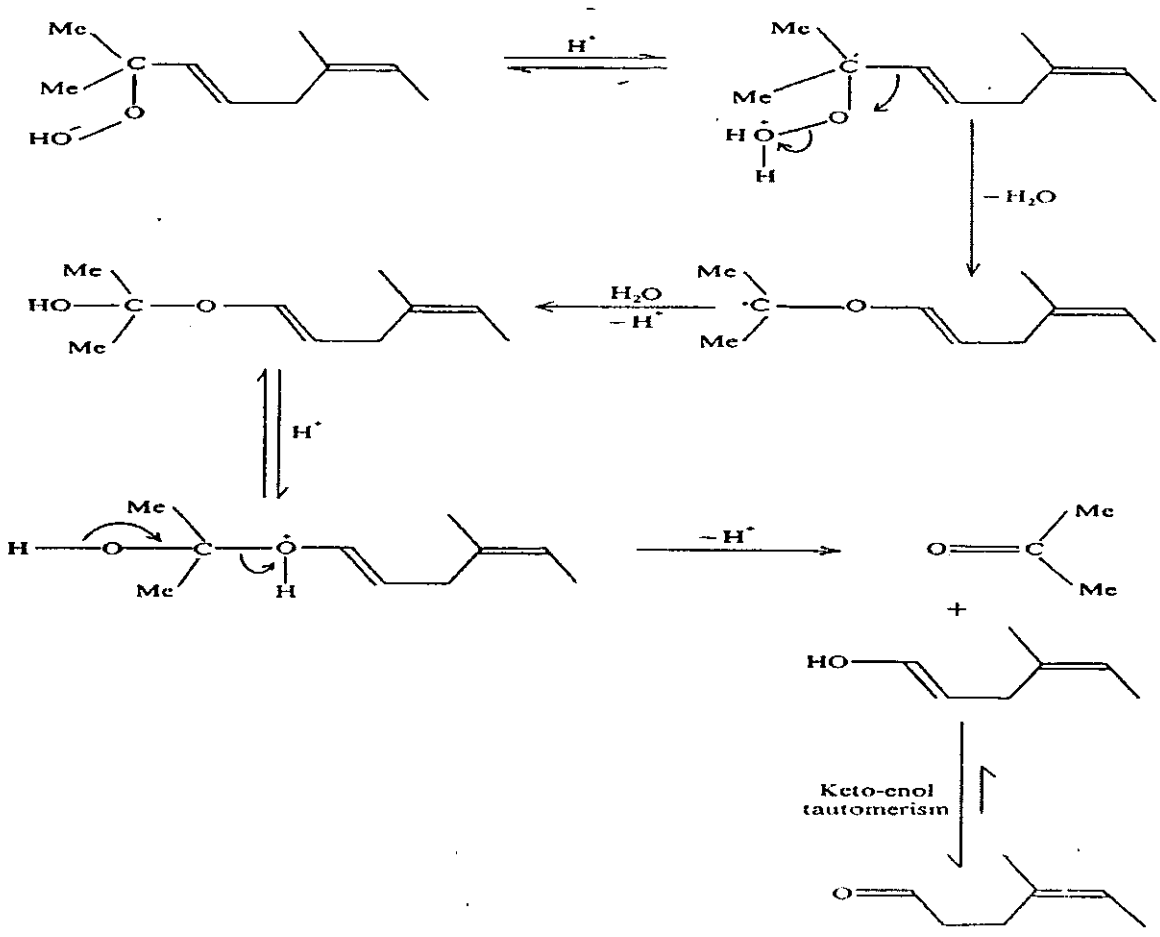

Scheme 1

Allylic abstraction of hydrogen in polyisoprene can occur either on site a or b to generate peroxy radicals which can then undergo 5 – exo or 6 – exo cyclisation (scheme 3). Tertiary hydroperoxide formation requires isomerisation of the double bond, generating a double allylic site. Abstraction of hydrogen at this site occurs readily, producing a pentadienyl radical. Addition of oxygen followed by abstraction of hydrogen generates the dihydroperoxide with conjugated double bonds (scheme 4). Hook cleavage of the tertiary allylic hydroperoxide produces a terminal methyl ketone and an aldehyde. Hook cleavage of the secondary allylic hydroperoxide produces 4 – oxopentanal (levulinaldehyde) (scheme 5).[6]

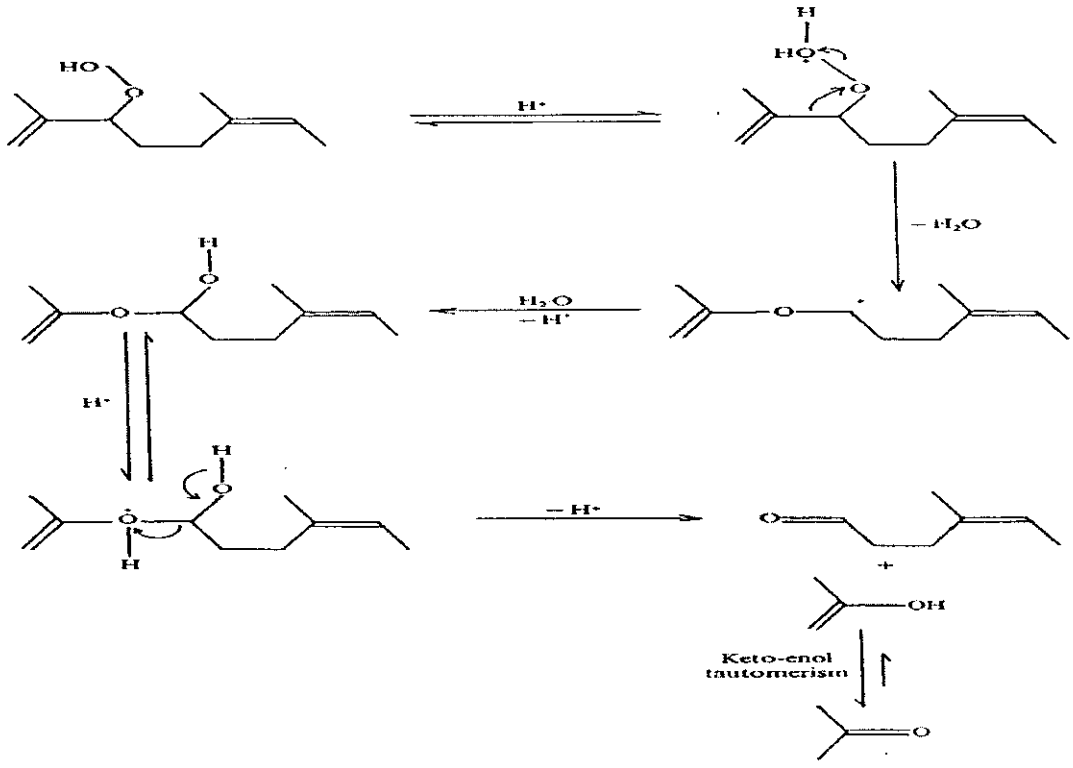

Scheme 2

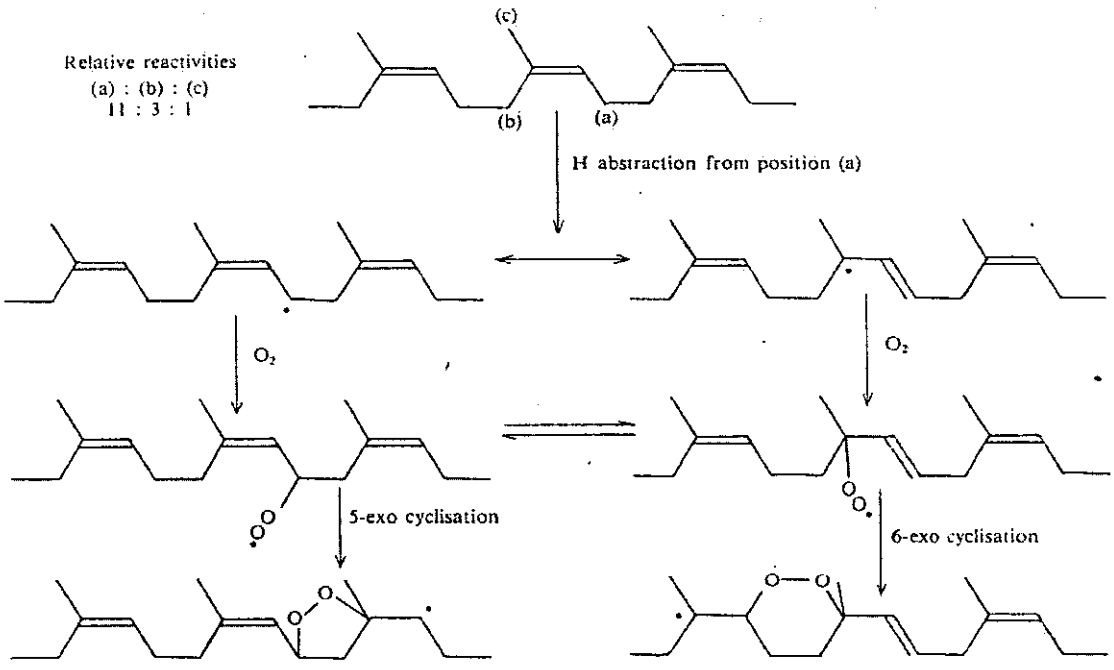

Scheme 3

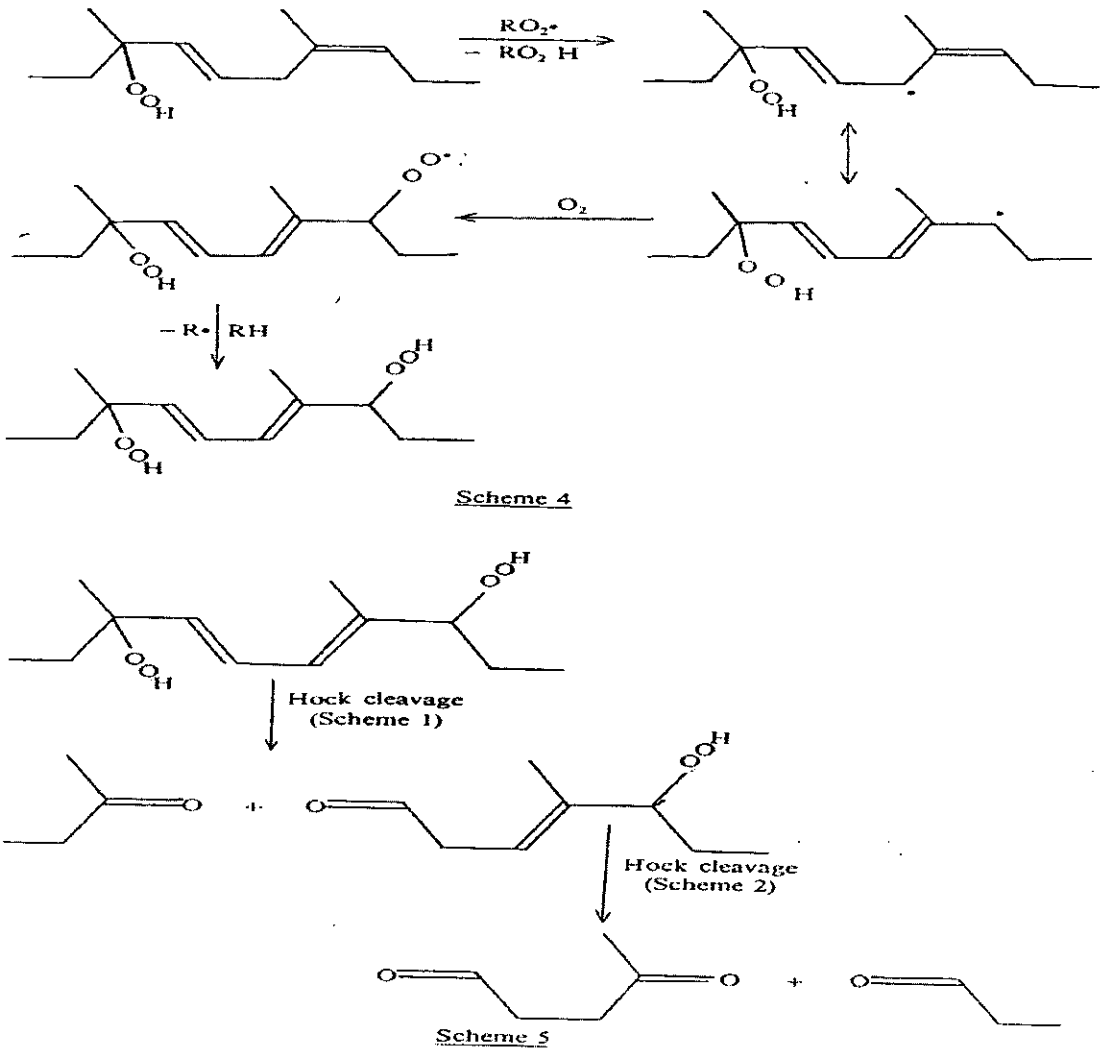

Figure 3.3: Schemes showing Hook Cleavage as the cause of chain scission in sulphur vulcanized NR

3.3.2 The Role of Oxygen Diffusion in Thermo-oxidative Ageing

The concentration and transport of oxygen in a polymer is critical to the ageing process. For example, the rate of oxidation has been linked to the rate of diffusion of oxygen through the polymer matrix.[16-18] The exposure of polymers in air during ageing often results in heterogeneously oxidized samples. This often leads to complications in understanding both the oxidation processes taking place in the polymer and in extrapolating accelerated exposures to long term conditions. One of these complications is diffusion limited oxidation, which can occur when the rate of oxygen consumption in the polymer is greater than the rate at which oxygen is being

supplied to the polymer through diffusion from the surrounding environment. An oxidation gradient is therefore established with oxidation occurring at the surfaces and only to a reduced or non – existent in the interior[9]. The oxygen diffusion rate can be dependent on the ageing conditions. Generally at moderate temperatures (30-40°C), permeability of oxygen is sufficient to reach almost the equilibrium solubility over the whole thickness of the sample (2mm thick). This means that most of the alkyl radicals initiated during ageing are transformed into peroxy radicals. [16, 17] . As explained by Williams and Neal,[19] the solubility of oxygen in rubber decreases with increasing temperature and that as long as the oxygen concentration remains above a certain minimum, the oxidation of the rubber will proceed at a uniform rate.[19]

3.3.3 Role of Anti oxidants in Reducing Thermo-oxidative Ageing

To improve on the resistance of natural rubber towards ageing, anti - oxidants and anti - ozonants are incorporated into the rubber during mixing. These antioxidants can be preventive or chain breaking. Antioxidants that retard the formation of free radicals in the initiation step are termed preventive antioxidants

Preventive antioxidants, also called primary antioxidants, act by slowing the oxidation without changing the mechanism. Secondary antioxidants, or chain breaking antioxidants[9] on the other hand, interrupt the propagation cycle by reacting with either R* or RO_2*. The Chain breaking antioxidants react by introducing competing reactions so that the mechanism of retarded autoxidation becomes more complex than the uninhibited reaction. The function of the antioxidant is to prevent or to retard, the deterioration of the physical properties of the rubber which results from oxidative attack.

Antioxidants react in more than one way which includes the prooxidant effect in addition to the desired antioxidant action. Four ways in which antioxidants take part in retarding oxidation include: [14]

- Prevention of peroxide initiation by decomposing hydroperoxides to form

stable products.

- Initiation by direct attack of oxygen on the antioxidant to produce chain – initiation radicals.
- Chain transfer with the antioxidant in which the radical derived from the antioxidant reacts in some way to reform a propagating free radical.
- Termination by hydrogen donation to RO_2* as in the chain transfer step followed by reactions of the antioxidant radical with a second RO_2*, thus terminating two kinetic chains per molecule of antioxidant consumed.

Peroxide destruction:

(Preventive antioxidant) $ROOH + AH \longrightarrow$ non radical products

Initiation: (Peroxide decomposition)

(O_2 attack on antioxidant) $nROOH \longrightarrow RO^*, RO_2^*, ---$

$AH + O_2 \longrightarrow A^* + HO_2.$

Propagation: (same as uninhibited) $RO_2^* + RH \longrightarrow ROOH + R^*$

$R^* + O_2 \longrightarrow RO_2^*$

Chain transfer: (with antioxidant) $RO_2^* + AH \longrightarrow ROOH + A^*$

Termination: (by antioxidant) $A^* + RH \longrightarrow AO_2H + RO_2^*$

$RO_2^* + AH \longrightarrow ROOH + A^*$

$RO_2^* + A^* \longrightarrow RO_2A$

$2A^* \longrightarrow A - A$

(as in uninhibited autoxidation) $2RO_2^* \longrightarrow$ Nonradical products $+ O_2$

$$RO_2^* + R^* \longrightarrow RO_2R$$

$$2R^* \longrightarrow R - R$$

Some examples of preventive antioxidants include: light absorbers such as carbon black, metal deactivators (eg FeS during sulphur vulcanization of rubber) and peroxide decomposers. Many alkyl and aryl sulphides and disulphides, the sulphoxides and thiolsulphinates are hydroperoxide decomposers.

Chain breaking antioxidants can be categorized as free radical traps, electron donors and hydrogen donors. Amine antioxidants such as 6 – PPD and phenyl – 2 – naphthylamine and hindered phenols such as 2,6 – di – t – butyl – 4 – methylphenol are hydrogen donors. The reactive N – H and O – H present in diarylamine and hindered phenol compete with the RO_2^* radical, by transferring hydrogen to form ROOH thereby terminating the kinetic chain. The antioxidant radical produced functions as a radical trap and terminates the second kinetic chain. [14] Hydro peroxide decomposers[9] act by countering the production of free radicals by reacting with the hydroperoxide - that is:

$$ROO^* + A_pH \longrightarrow ROOH + Ap$$

$$A_p + ROO^* \longrightarrow ROOA_p \text{ (stable)}$$

$$ROOH + A_sH \longrightarrow ROH + A_sOH \text{ (stable)}$$

Where: A_pH is the chain breaking antioxidant and A_sH is the hydroperoxide decomposer

The efficiency of the stabilisation of a polymer product by antioxidants against oxidation depends on the consumption and loss (evaporation) of the antioxidants from the material. Experiments have shown a direct relationship between the physical parameters, solubility and mobility of the antioxidant, and the service life of a polymer product. In order to obtain a good efficiency of the stabilizer against oxidation in the polymer, antioxidant molecules must be able to inactivate the radicals and /or decompose the hydro peroxide groups as soon as they are formed. The availability of the antioxidants at the oxidation site is determined by the solubility and mobility of the antioxidant in the polymer, and the availability of the oxygen by its permeability in the polymer. [16]

An engine mount compound will commonly contain a combination of antioxidants and anti-ozonants for example, TMQ, 6 – PPD and wax. TMQ and 6 – PPD are all anti – oxidants while wax is an anti – ozonant. Gui – Yang Li and Koenig[9] in their review of rubber oxidation explained the role of the various antioxidants and antiozonants which are incorporated in the rubber:

Wax protects the rubber by blooming to the surface of the material forming an impervious film of hydrocarbons. The wax protects the rubber from ozone attack if the film is thick enough. The thickness of the bloomed film depends on both the solubility and diffusion rate of the wax in the rubber. These parameters are temperature dependent. An increase in temperature results in the wax becoming very soluble and so it does not form a thick enough protective film. However, for microcrystalline waxes, their mobility is increased by increase in temperature and hence, their rate of migration to the surface is increased, with maximum film bloom thickness being formed at temperatures of between 50°C – 60°C.[9]

The anti – oxidant N – phenyl – N` - dimethyl – butyl – P – phenylenediamine (6 – PPD), used both in tyre and engine mount compositions has the advantage of long alkyl chains which result in low solubility in aqueous fluids, reducing leaching and high solubility in rubber, reducing blooming. The 6 – PPD has a higher rate of reaction with ozone than other antioxidants like TMQ. Once a concentration gradient has been established during oxidation, fresh antiozonants diffuse to the surface of the rubber, thereby forming a surface film. Another advantage of 6 – PPD compared to some antioxidants is that it inhibits thermal oxidation, reduces mechanical oxidative fatigue and raises the resistance of the rubber to ozone cracking under both static and dynamic strain conditions[9].

It is also well known that carbon blacks play a major role in the thermo – oxidative degradation of polymers. Carbon black can act as an antioxidant and on the other hand can accelerate oxidation depending on the concentration (loading) of the carbon black in the rubber and the active sites on the surface of the carbon black. Knowing whether carbon black acts as an inhibitor or an initiator in rubber degradation is very difficult.[20] However, the influence of carbon black on the kinetic parameters of inhibited oxidation has been studied, and it has been shown that there are three kinetic parameters that are important during the inhibited oxidation of a carbon black filled

polymer at high temperatures. These include:

- The effective rate constant of hydroperoxide composition;
- The effective rate constant of the reaction between a peroxide radical ROO* and an inhibitor molecule InH;
- The effective rate constant of the reaction between a peroxide radical ROO* and an inhibitor radical In*.

In studying the kinetics of the effect of carbon black in the thermo – oxidative degradation of linear low density polyethylene (LLDPE), Goldberg et. al [20]considered two aspects of carbon black which include:

(i) that carbon black has a conjugated double bond system and should show properties expected of free radicals and as such can function as an inhibitor or an initiator of oxidation depending on the reaction conditions

(ii) as carbon black is weakly efficient in affecting oxidation parameters at high temperatures, the action of carbon black can better be studied under conditions where the rate of oxidation is slow, in the presence of an oxidation inhibitor.

3.4 Effect of Thermal Ageing on the Sulphur Crosslink Network of Rubber Compounds

The type of vulcanization system applied to the rubber compound influences its resistance towards heat. The heat resistance of sulphur cured natural rubber is dependent on the length of the sulphur crosslinks. Sulphur vulcanization is the most widely used vulcanization system in the rubber industry especially for tyres and mountings. Sulphur vulcanization is of two categories, accelerated and unaccelerated sulphur vulcanization. Unaccelerated sulphur vulcanization is not commonly used because it is commercially unviable. Both polar and radical mechanisms have been advanced to operate during sulphur vulcanization of rubber in the presence of accelerators such as MBT and TMTD. The proposed radical mechanism for accelerated sulphur vulcanization is as shown in the Figure 3.4 below.[21]

$$XSSxZnSxSX \longrightarrow XSSx^* + XSxZn^*$$

$$XSSx^* + RH \longrightarrow XSSxH + R^*$$

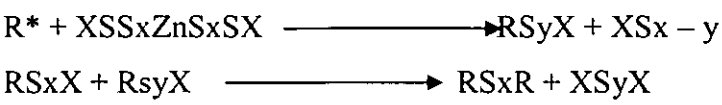

Figure 3.4: Radical mechanism of accelerated sulphur vulcanization

The intermediate which is formed as a result of the reaction between accelerator and sulphur, cleaves to form persulphuryl radicals, which then abstract protons. The rubber radical then reacts with another intermediate to form a rubber bound intermediate. The two rubber bound intermediates so formed then react with each other to form the actual crosslink. Maturity of the network then occurs through sulphur exchange reactions. Isomerisation which occurs through alkyl radical mechanism is widely observed in vulcanization. In the polar mechanism, isomerisation occurs by loss of the rubber bound intermediate as an ion.

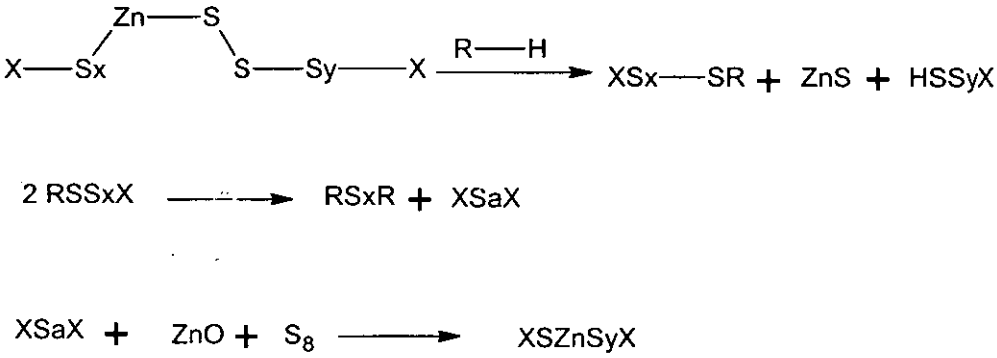

Where R – rubber chain, H – allylic hydrogen and X – accelerator residue.

Figure 3.5: Polar mechanism for accelerated sulphur vulcanization [22]

Various structures are formed in sulphur vulcanized natural rubber as shown in Figure 3.6.[21] Because the polysulphide bonds are much less thermally stable, vulcanizates with long sulphur crosslinks are more susceptible to deterioration under heat and oxygen. Sulphur crosslinks, initially formed during the accelerated sulphur vulcanization of rubber, can undergo any of a number of competing reactions under the action of heat, so that the net effect is dependent on vulcanization time and temperature. For example, at high temperatures, sulphur crosslinks are susceptible to breakage and can give rise to intramolecular sulphur cyclisation and in this state, the sulphur no longer contributes to the crosslinked network[23].

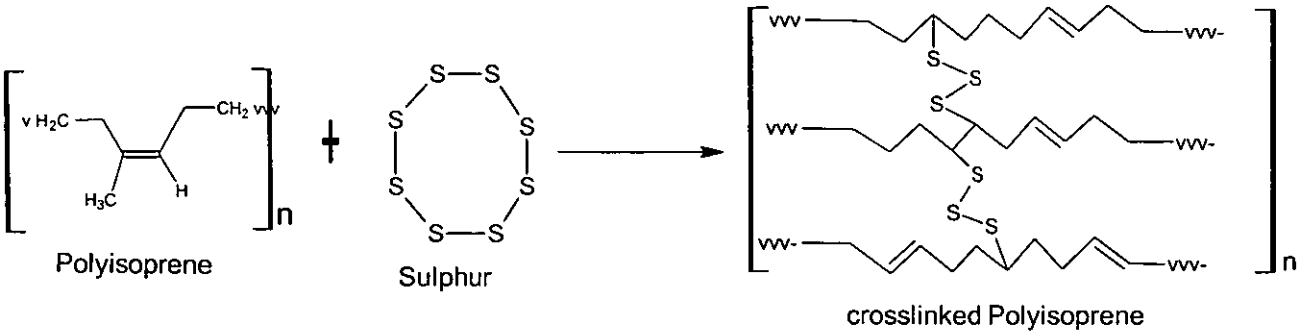

Figure 3.6: Reaction of sulphur with polyisoprene

Degradation behaviour caused by heat ageing of sulphur vulcanised diene – type rubbers has widely been described as a result of oxidation and / or desulphurisation reaction.[14, 15]. Decomposition and desulphurization of di and polysulphidic crosslinks are competitive. If desulphurisation is predominant, the final vulcanizate will contain a high proportion of monosulphidic crosslinks that are thermally stable. When desulphurisation is slow, the concentration of the polysulphides will be high and will thermally decompose causing a modulus reversion with low crosslinking efficiencies and extensive modification of the main rubber chains by conjugated double bonds and cyclic sulphide groupings[15]

3.5 Effect of Ageing on Properties of Rubber Compounds

The combined effect of oxygen and heat on rubber compounds used in components such as engine mounts brings about long term chemical changes which, in turn lead to physical changes. "Oxygen may be the breath of life to animate beings but for many inanimate objects it spells deterioration and loss of physical properties from which only alleviation, not escape, is possible"[12]. Natural rubber is no exception, and attack by atmospheric oxygen and ozone represents a significant threat to service life. [12, 24]. Changes may be in bulk properties which affect performance or may be local, such as surface cracks which may result in complete component failure [25-27]. To be able to determine the service life of a rubber component, subjected to a variety of environments, it is necessary to account for all modes of degradation. An obvious method of life prediction is to accelerate the ageing, so that deterioration of properties occurs over a feasible time scale (a few weeks)[28]. In their study of tensile behaviour after oxidative ageing of gum and black – filled vulcanisates of SBR and NR, Hamed and Zhao[27] observed that on air - oven aging of the vulcanized SBR samples at a

temperature of 100°C, an initial ageing period was observed in which stiffness and cross link density were unchanged. However, the tensile strength and strain - to - break were significantly reduced. As aging continued, the cross link density increased thereby stiffening and reducing extensibility. They suggested that the change in behaviour could be attributed to antioxidant depletion. For natural rubber, ageing (2-4 days) at temperatures of above 70°C, significantly reduced the tensile strength and the strains - to - break. The ageing in NR in its initial stages first softens before becoming stiff. The cross link density which was measured using the swelling method in toluene followed the same trend as the moduli upon ageing. [27]

Investigating the longitudinal cracking in a carbon black filled natural rubber vulcanizate during chemical stress relaxation, Hamed and Zhao[29] aged the rubber at 72°C while holding samples at fixed elongation. They found out that initially, the elongated specimen did not exhibit any cracking after ageing for one hour at 72°C. However, after sufficient oxidative attack, multiple strands could be seen as a result of longitudinal cracking which appeared to emanate from the regions of the dumbbell where its neck widens. Substantial tension set was also apparent. It was further observed that some of the strands in the catastrophically ruptured rubber initiated near the place where the neck widens and subsequently grew further into this region.

The changes in properties with ageing are not only important in themselves but can be used to indirectly indicate the mechanisms of ageing. According to Ahagon et. al.[1, 30] and Baldwin et.al.[2, 3] three types of ageing mechanisms are observed in NR. Type I ageing is characterized by crosslinking being the dominant event resulting in an increase in modulus and lowering of the elongation at break. Type II ageing, can be as a result of anaerobically aged rubber or high temperature ageing e.g above 90°C to 100°C. It is characterized by the breaking and rearranging of sulphur crosslinks. The modulus either changes a little or is reduced, with main – chain modifications reducing the number of extensible units. Type III ageing is characterised by both crosslinking and chain scission due to oxidation at high temperatures.

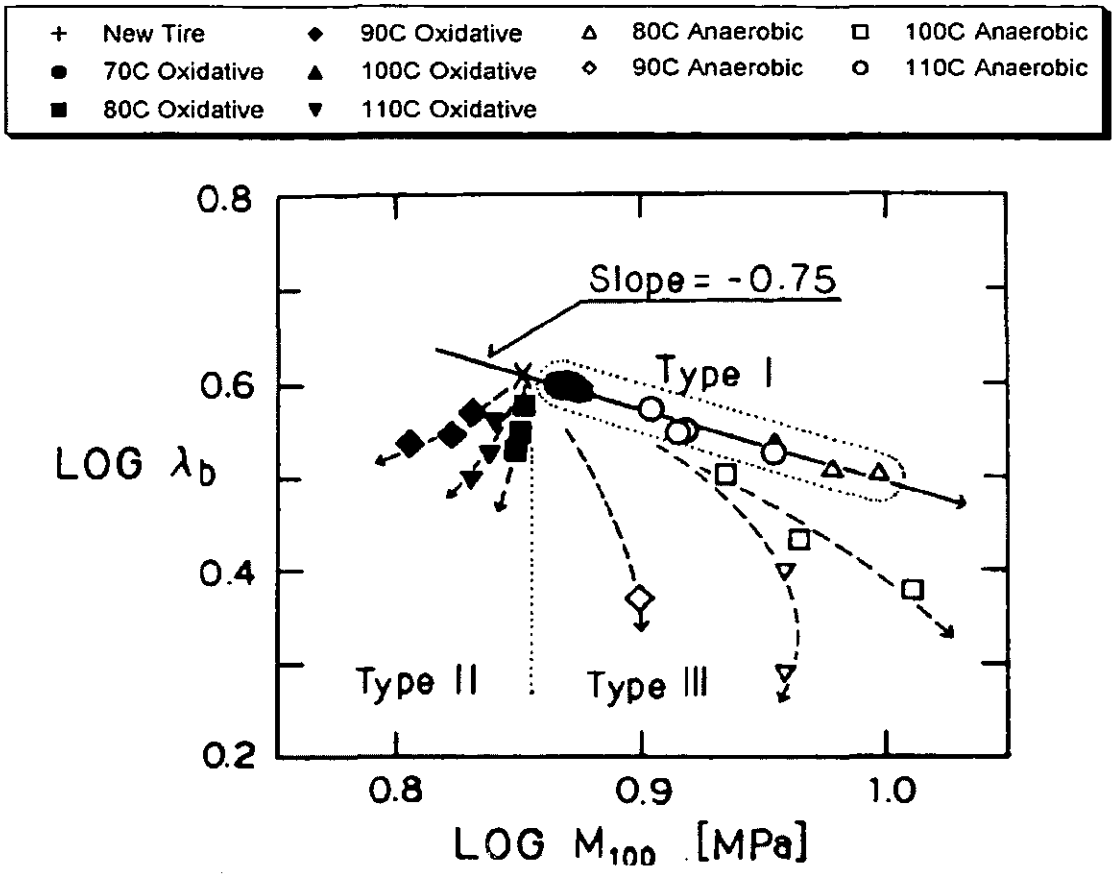

Figure 3.7: Ahagon plot of the log of the strain at break versus the log of the 100% Modulus used to understand the ageing mechanism[2]

The Ahagon plot has also been used to describe the type of ageing process taking place in rubber tyres [1, 30]. As explained by Gillen[31, 32], the whole concept of accelerated ageing is based on the fact that increasing the temperature will increase the degradation process by a constant factor that he refers to as a shift factor. He further stated that once the shift factors have been determined, they can be tested with various ageing models.

3.6 Kinetics of Rubber Ageing in Terms of its Effect on Properties

Life prediction of polymeric materials has been one of the most sort after objectives in the polymer industry. Reproducible methods and reliable predictive models must be obtained if premature failure is to be reduced to a minimum. The methods so derived can be useful for the development of new or modified compound formulations. The Arrhenius methodology is the most common and widely used for the calculation of

the activation energy for degradation at high temperatures, and functional life predictions. If the Arrhenius relationship holds, this is extrapolated to lower temperatures to make predictions. Many problems have been encountered when the Arrhenius model is used for prediction of the life of certain commercial polymers. Some of these problems, as explained by Gillen et. al.[31], are dependent on physical effects such as extrapolating across a polymer transition. Changes in the effective activation energy can also be brought about by such things as a switch in the dominant mechanism as the temperature is changed or a slow temperature dependent change due to the complex form of the effective activation energy. This has resulted in non – Arrhenius behaviour especially at low temperatures[33]. Gugumus[34] has attributed this non – Arrhenius behaviour in some polymers to the activity of transition metal impurities, like trace metal iron from processing equipment.

Despite these limitations Arrhenius methodology has been usefully applied to the study of rubber aging. Baldwin and others.[2] researching on tires and tire parts in different areas in the United States, found out that despite the difference in environmental conditions in the sampled states, the degradation mechanisms were almost the same no matter the make of the tires. Furthermore, Baldwin et. al [3] using the time temperature superposition approach developed by Gillen[31] studied the degradation kinetics of skim rubber, using swelling measurements and peel strength, when the rubber was subjected to degradation an air circulating oven. They found that when the tires were inflated with 100% air and a 50/50 blend of N_2/O_2, the apparent activation energies were the same (101 kJ/mol) for peel strength and swelling ratio (109 kJ/mol). However, Bauer et. al.[35] found that the rate of oxidation increases by a factor of 1.4 when a 50/50 blend of oxygen and nitrogen were used as the fill gases.

3.7 Kinetics of High Temperature Degradation by Gravimetric Analysis

Thermogravimetric (TG) analysis is a continuous process that examines the mass change of a sample as a function of temperature in the scanning mode or as a function of time in the isothermal mode. TG is used to characterize the decomposition and the thermal stability of materials under a variety of conditions and to examine the kinetics of the physicochemical processes occurring in the sample[36]. The thermogravimetric

analysis method has been widely used to study the degradation of polymeric materials. TG is used for quantitative compositional analysis of polymers, life time prediction and kinetic studies[37]. One disadvantage of natural rubber is its low value of high temperature stability; however, the additives used for compounding do affect the thermal stability of the natural rubber compound. Information on the thermal and thermo-oxidative stability of the rubber compound is obtained from thermal analysis methods such as thermogravimetry, TGA, differential Scanning Calorimetry, DSC, as well as differential thermal analysis, DTA. The temperature in a TG curve at which 50% decomposition occurs is generally considered as an index of thermal stability. Menon et. al. in their studies on the thermal degradation characteristics of natural rubber vulcanizates modified with phosphorylated cashew nut shell liquid, observed that the DTA of the unmodified NR samples in air showed a sharp endotherm peak The DTG for the decomposition of the samples in air showed two prominent peak in the regions 300 – 420°C and 460 – 560°C, with the major decomposition (~ 65- 70%) occurring between 300°C and 400°C. They advanced that the occurrence of the two peaks is an indication of the formation of thermally stable intermediate products. A shift of the DTG peak (Tmax) towards higher temperatures was an indication of the improved thermal stability of the PCNSL modified NR vulcanisate.

Resistance to thermo – oxidative decomposition is indicated by a reduction in the enthalpy of oxidation as measured from the DSC[38]. Thermal methods are important because these techniques can provide information about the thermal and oxidative stability of polymers, their life time or shelf – life under particular conditions. The life time or shelf life of a polymer can be estimated from kinetic data obtained from a TG plot. Flynn – Wall and Ozawa observed that the activation energy of a thermal event could be determined from a series of thermogravimetric runs performed at different heating rates, (non – isothermal methods). As the heating rate is increased, the thermogravimetric change occurred at higher temperatures. A linear correlation was obtained by plotting the logarithm of the heating rate or scan speed against the reciprocal of the absolute temperature at the same conversion or weight loss percentage. The slope was directly proportional to the activation energy and the known constants.

Chenyang Liu et al [39]explained in their studies on the thermal degradation of cyclic olefin copolymers, that if the thermogram of the DTG plots showing a maximum is used, the peak temperature can be obtained. The onset temperature of degradation can also be calculated from the TG curve by extrapolating from the curve at the peak of degradation to the initial weight of the polymer. The difference between the peak temperatures and the onset temperatures was described as the temperature range of thermal degradation. Yu et. al. carried out a study on the thermo - oxidative degradation process of chlorinated natural rubber from latex, using TG coupled with FTIR. They found that the TG/DTG curve is marked by two weight loss events characterised by two DTG peaks. The first weight loss event peak occurred between 160°C to 390°C with a weight loss of about 69 wt.%. The second weight loss peak occurred between 390°C and 585°C with a weight loss of about 31wt. %. Analysis of the evolved gases by FTIR indicated that for the first weight loss event, HCl with little amount of CO_2 was released indicating that HCl is eliminated from the molecular chains of CNR by scission of C – Cl and C – H bonds at 160°C – 390°C[40]

The application of dynamic TG methods hold great promise as a tool for unraveling the mechanisms of physical and chemical processes that occur during polymer degradation. At first a brief introduction of the kinetic methods is presented, and the reaction of conversion, α, is given by equation 3.1

$$\alpha = \frac{w_0 - w}{w - w_f} \qquad [3.1]$$

where w is the weight of sample and the subscripts, o and f , refer to values at the beginning and end of the weight loss event of interest.

The rate of conversion, $\frac{d\alpha}{dt}$ for TG experiment at constant rate of temperature change, $\beta = \frac{dT}{dt}$, may be expressed by

$$\frac{d\alpha}{dt} = \beta \frac{d\alpha}{dT} = K(T) f(\alpha) \qquad [3.2]$$

where $f(\alpha)$ and $K(T)$ are functions of conversions and temperature respectively.

$K(T)$, the temperature dependence of the rate of weight loss is often modelled successfully by Arrhenius equation

$$K(T) = Ae^{-E/RT} \qquad [3.3]$$

where E is the activation energy, A the pre – exponential factor and R the gas constant. And $f(\alpha)$ depends on the particular decomposition mechanism. The simplest and most frequently used model for $f(\alpha)$ in the analysis of TG data is

$$f(\alpha) = (1-\alpha)^n \qquad [3.4]$$

where n is the order of the reaction.

Insertion of equation (3.3) and (3.4) into equation (3.2) gives

$$\frac{d\alpha}{dt} = \beta\frac{d\alpha}{dT} = (1-\alpha)^n Ae^{-E/RT} \qquad [3.5]$$

Thermogravimetric curves are normally plotted with the mass change (Δm) expressed as a percentage on the vertical axis and temperature (T) or time (t) on the horizontal axis. For kinetic analysis of most compounds, the iso – conversional method is widely used because they give more reliable kinetic parameters. The Friedman – Ozawa method is mostly used for interpretation of non – isothermal data. Multiple runs are however needed in order to get reliable results. Ozawa has derived the reduced time (rts) TG approach to determine the activation energy of degradation of a polyimide. Other methods used for thermogravimetric degradation studies in either the isothermal runs or iso – conversional runs, include the Flynn – Wall – Ozawa and Kissinger – Akahira - Sunrose plots which are an all integral method. The Friedman – Ozawa plot which is used in iso – conversional kinetic analysis is a differential method.[41] The non – isothermal method involves both single heating rate and multiheating rates (iso – conversional method). At only one constant heating rate, the values of $\frac{d\alpha}{dt}$ and α can be determined from the equation $\frac{d\alpha}{dt} = k(1-\alpha)^n$. Xiong et.al using the single heating approach to study the kinetics of the curing of Bismaleimide modified with Diallylbisphenol A, considering the nth order kinetics found that, the kinetics of degradation can be described in two stages, a first stage with $\alpha < 30\%$ and another with $\alpha > 30\%$. The activation energy lies between 65 kJ/mol and 76 kJ/mol.[38, 42] Thermal degradation of fresh and aged chloroprene rubber has been studied by Elton et al [26] using thermogravimetric analysis (TGA); and Differential Thermogravimetric Analysis (DTG). Elton et al[26] observed that ageing induces a shift of the degradation

processes to lower temperatures, though the number of degradation processes in an air atmosphere was not the same as those obtained in inert nitrogen analysis. The degradation process was very efficient in air (100%) while in nitrogen, it was partial up to a temperature of 550°C. When the maximum temperature is elevated, the activation energies of the partial processes also increases [26]

Various kinetic models used for the computation and interpretation of thermogravimetric data, gives different activation energies as has been explained by Brown et. al.[43] Some kinetic model functions used for the calculation of the activation energy of polymers from thermogravimetric data are as shown on Table 3.1

Table 3.1: Kinetic model functions[44]

Model	Symbol	f(α)
Phase boundary controlled reaction (contracting area)	R2	$(1-\alpha)^{1/2}$
Phase boundary controlled reaction (contracting volume)	R3	$(1-\alpha)^{2/3}$
Random nucleation. Unimolecular decay law	F1	$(1-\alpha)$
n^{th} order reaction	Fn	$(1-\alpha)^{n}$
Johnson – Mehl – Avrami	JMA	$n(1-\alpha)[-\ln(1-\alpha)]^{1-1/n}$
Two dimensional growth of nuclei equation (Avrami equation)	A2	$2\left[-\ln(1-\alpha)^{1/2}\right](1-\alpha)$
Three dimensional growth of nuclei equation (Avrami equation)	A3	$3\left[-\ln(1-\alpha)^{2/3}\right](1-\alpha)$
One - dimensional diffusion	D1	$\frac{1}{2\alpha}$
Two - dimensional diffusion	D2	$1/[-\ln(1-\alpha)]$
Three - dimensional diffusion (Jander equation)	D3	$3(1-\alpha)^{2/3} / 2\left[1-(1-\alpha)^{1/3}\right]$
One dimensional diffusion (Ginstling – Brounshtein)	D4	$\frac{3}{2\left[(1-\alpha)^{-1/3}-1\right]}$
n – dimensional nucleation (Avrami – Erofeev equation)	An	$n\left[-\ln(1-\alpha)^{n}\right](1-\alpha)$

First order autocatalysis reaction	C1	$(1-\alpha)(1+K_{cat}\alpha)$
Nth order autocatalysis reaction	Cn	$(1-\alpha)^n(1+K_{cat}\alpha)$
Prout – Tompkins equation	Bna	$(1-\alpha)^n\alpha^a$

3.8 References

(1) Ahagon, A.; Kida, M.; Kaidou, H. *Rubber Chem Technol* **1990**, *63*, 683-697.

(2) Baldwin, J. M.; Bauer, D. R.; Ellwood, K. R. *Rubber Chem Technol* **2005**, *78*, 336-353.

(3) Baldwin, J. M.; Bauer, D. R.; Ellwood, K. R. *Rubber Chem Technol* **2005**, *78*, 767.

(4) Deng Huang, B.J. L.; Castro, J. M.; Ignatz – Hoover, F. *Polym. Degrad. Stab.* **2001**, *74*, 353-362.

(5) Bevilacqua E.M. In *Thermal and Oxidative Degradation of Natural Rubber and Allied Substances;* Robert T. Conley, Ed.; Thermal Stability of Polymers; Marcel Dekker: New York, 1970; Vol. 1, pp 189-222.

(6) Boon, A. J. *Journal of Natural Rubber Research* **1988**, *3*, 90.

(7) Tao, Z.; Viriyabanthorn, N.; Ghumman, B.; Barry, C.; Joey, M. *Rubb. Chem. Technol.* **2005**, *78*, 489-515.

(8) Brown RP **2001**, , vi,.

(9) Gui – Yang, L.; Koenig, J. L. *Rubb. Chem. Technol.* **2005**, *78*, 355-390.

(10) anonymous *http://merl.ltd.co.uk/index.shtml*2004).

(11) Shailendra, S.; Singh RP *Progress in Rubber and Plastic Technology* **2001**, *17*.

(12) Howard, J. *Rubb. Chem. Technol.* **1974**, *74*, 975-990.

(13) Bevilacqua, E. M.; English, E. S.; Gall, J. S.; Norling, P. M. *J. Appl. Polym sci.* **1964**, *8*, 1029.

(14) Shelton J.R. *Rubber Chemistry and Technology* **1972**, *45*, 359.

(15) Dunn J.R. *Rubb. Chem. Technol.* **1974**, *47*, 960-975.

(16) Arjen Boersma; Cangialosi, D.; Stephen, J. *Rubb. Chem. Technol.* **2003**, *47*, 960-438;975.

(17) White, J. R. *Plast. Rubber Compos. Process. Appl.* **1998**, *27*, 124-130.

(18) Audouin, L.; Langlois, V.; Verdu, J.; de Bruijn, J. C. M. *J. Mater. Sci.* **1994**, *29*, 569-583.

(19) Williams, I.; Neal, A. M. *Industrial and Engineering Chemistry* **1970**, *22*, 874.

(20) Goldberg A; Lesuer DR; Patt J; ACS, R. D. *Spring Meeting (133rd),1988* **1988**, *Dallas*, 25.

(21) Aprem, A. S.; Joseph, K. Thomas, S. *Rubb. Chem. Technol.* **2005**, *78*, 458-488.

(22) Nieuwenheuizen, P. J.; van Veen, J.; Haasnoot, J. G.; Reedijk, J. *Rubb. Chem. Technol.* **1999**, *72*, 43.

(23) da Costa, H. M.; Abrantes, T. A. S.; Nùnes, R. C. R.; Visconte, L. L. Y.; Furtada, C. R. G. *Polymer Testing* **2003**, *22*, 769-777.

(24) Malaysian Rubber Producers' Research Association In *Natural Rubber Science and Technology;* Oxford University Press: Oxford, 1988; .

(25) Anonymous Harboro Handbook. http://www.harboro.co.uk/html/harboro, 2003).

(26) Dernadin, E. L. G.; Dimitrios, S.; Paolo, R. J.; de Souza, P. G. *Rubb. Chem. Technol.* **2001**, *74*, 622.

(27) Hamed GR; Zhao J *Rubber Chemistry and Technology* **1999**, *72*, 721.

(28) Mott, P. H.; Roland, C. M. *Rubber Chem Technol* **2001**, *74;*, 79.

(29) Hamed, G. R.; Zhao, J. *Rubber Chem Technol* **1998**, *71;*, 157.

(30) Kaidou, H.; Ahagon, A. *Rubber Chem Technol* **1990**, *63*, 698-712.

(31) Gillen, K. T.; Celina, M.; Keenan, M. R. *Rubber Chem. Technol.* **2000**, *73*, 265-

283.

(32) Gillen, K. T.; Celina, M.; Bernstein, R. *Polym Degrad Stab* **2003**, *82*, 25-35.

(33) Gillen, K. T.; Bernstein, R.; Derzon, D. K. *Polym. Degrad. Stab.* **2005**, *87*, 57-67.

(34) Gugumus, F. *Polym. Degrad. Stab.* **1999**, *63*, 41-52.

(35) Bauer, R. D.; Baldwin, J. M.; Ellwood, R. K. *Rubber.Chem. Technol.* **2005**, *78*, 777-792.

(36) Williams, P. T.; Besler, S. *Fuel* **1995**, *74*, 1277-1283.

(37) Price, D. M.; Houston, D. J.; Dumont, F. In *Application of Intrumental methods;* Meyers, R. A., Ed.; Encyclopaedia of Analytical Chemistry; John Wiley and sons Ltd: Chichester, 2000; Vol. 9, pp 8094-8105.

(38) Menon, A. R. R.; Pillai, C. K. S.; Nando, G. B. *Polym. Degrad. Stab.* **1996**, *52*, 265-271.

(39) Chenyang, L.; Jian, Y.; Xinghua, S.; Zhang, J.; Jiasong, H. *Polym. Degrad. Stab.* **2003**, *81*, 197-205.

(40) He - ping, Y.; Si - dong, L.; Jie - ping, Z.; Kui, X. *Thermochim Acta* **2004**, *410*, 119-124.

(41) Ozawa, T. *Thermochim Acta* **2000**, *356*, 173-180.

(42) Xiong, Y.; Boey, F. Y. C.; Rath, S. K. *J. Appl. Polym. Sci.* **2003**, *90*, 2229-2240.

(43) Brown, M. E., et al *Thermochim Acta* **2000**, *355*, 125-143.

(44) Pielichowski, K.; Njuguna, J. In *Thermal Degradation of Polymeric Materials;* Rapra Technology: Shawbury, 2005; , pp 40.

CHAPTER 4

4 Review of fatigue failure and fracture of rubber compounds

4.1 Introduction

With the ever increasing trend in the utilisation of polymeric materials for structural purposes, it has become important to know under what loading and environmental conditions fracture may occur. Elastomeric components in service mostly operate under multiaxial stresses and strains. Multiaxial loading histories of components over the loading cycle may involve both variations in the stress/strain biaxiality or rotation in the principal stress/ strain directions, relative to the material. Loading conditions include not only the extent but the rate of loading, to which polymer materials are particularly sensitive, as well as factors such as ozone.[1].

In addition to external factors, the manufacture and construction of engineering components and structures necessarily involves the introduction of defects which include; holes, grooves, welds and joints. The materials from which they are made also have smaller imperfections, such as surface scratches, inclusions, voids etc. All these imperfections range in size from sub microns to many millimetres[2, 3]. The point of initiation of a fracture process is usually conditioned by these imperfections. In general, one or more tiny cracks start in the material, and then grow until complete failure occurs. In order to predict or avoid structural failure, engineers and designers of components and structures must be fully aware of the level and orientation of the applied loading and the density, size, shape and orientation of the defects[2]. In addition to crack initiation, crack growth is influenced by both the structure and inhomogeneities in the material.

To predict failure it is necessary to model the fracture initiation and propagation processes, including both internal factors, such as bulk properties and the presence of flaws, and the external factors such as loading regime and temperature. In the following sections theoretical methods of modelling the fracture processes will be

discussed and then factors affecting fracture and failure properties of rubber will be reviewed.

4.2 Theoretical Treatment of Fatigue and Fracture Behaviour

The term fatigue is most commonly used to refer to failure of materials under cyclic loading below their yield strengths, due to growth of one or more cracks. In order to ascertain the safety and reliability of the rubber component and so prevent sudden and unexpected failures during service, fatigue analysis and strength evaluation of the designed components are carried out. In this way, relationships are established that can be used for the prediction of the functional life of a component.

Two approaches have been used to study failure in natural rubber and other elastomers, one is based on the crack nucleation approach[4-6] and the other on the crack growth approach[7-11]. The two approaches are discussed in more detail in the following sections.

4.2.1 Crack Nucleation and the Continuum Mechanics Approach

The crack nucleation approach is based on the fact that the material is considered to have an intrinsic life determined by the history of stress or strain at a point. The number of cycles required to cause the appearance of a crack of a certain size is then termed the fatigue crack nucleation life. The appropriateness of this approach is in applications where the initial flaws that determine component life are smaller than a size critical for crack propagation. The fatigue life parameters used for the prediction of crack nucleation in rubber are the maximum principal strain and the strain energy density[5].

Energy is stored during the deformation of rubbers. This energy is termed strain energy. It has been observed that cracks in rubber initiate on the plane perpendicular to the direction of the maximum tensile strain. The initial stage for crack growth involves cracks that are present in the rubber but cannot be seen with the naked eye, and can only become apparent when a continuous load is applied along the direction

of stretch. The region where a crack will first appear during testing is not apparent but it has been proposed that crack initiation and propagation can be deduced from the energy release rate, assumed to be the driving force for crack growth. Mars and Fatemi [5]have determined the energy release rate for such small cracks; they proposed that the energy release rate can be calculated from:

- The cracking energy density, which is the stored elastic energy density that is available to a crack on a given material plane, and can be calculated for an arbitrarily complex strain history.
- Strain energy density
- Maximum principal strain.

From the strain energy density, W, which is the area under the stress strain curve, the energy release rate T_w can be calculated thus:

$$T_W = 2KWa \qquad [4.1]$$

Where a is the crack length

K is given by the equation

$$K = \frac{2.95 - 0.08\varepsilon}{(1-\varepsilon)^{\frac{1}{2}}} \sim = \frac{\pi}{(1+\varepsilon)^{\frac{1}{2}}} \qquad [4.2]$$

ϵ is the maximum strain

In simple tension, the cracking energy density is equal to the strain energy density with W_c replacing W in equation 4.1

The energy release rate, T_ε, based on the maximum principal strain is given by

$$T_\varepsilon = C\varepsilon^2 a \qquad [4.3]$$

Where C is a material constant and is related to the Young's modulus.

These equations (equations 4.1 – 4.3) cannot be applied for cracks larger than 6mm because cracks larger than 6mm are dominated by boundary effects[5].

4.2.2 Crack Growth and the Fracture Mechanics Approach

Rubber is used most commonly under dynamic stress conditions and under cyclic loading it fails by a crack growth mechanism. The quantity of crack growth is determined by the magnitude of the strain energy which can be released by creating

new surfaces[12]. As explained by Lake and Thomas, irreversible processes occur in the rubber at the vicinity of the moving crack tip leading to energy losses. These energy losses must be made up from the available elastic energy, whose magnitude is determined by the rubber properties, the strain in the crack tip region, and the rate of crack growth. The energy losses in the crack tip region are of prime importance for rubbery materials for which losses in the bulk are negligible[13]. Crack growth occurs only under the loading process, and the extent of growth is determined by the maximum tearing energy, T (which is the energy needed to propagate a crack) attained during the process. Thomas found that the crack growth behaviour of rubbers under cyclic stress conditions[10] obeyed the relationship.

$$R = BT^{\alpha} \qquad [4.4]$$

Where R is the crack growth per cycle, T is the maximum energy attained for each cycle, and B and α are constants, which can be experimentally determined.

This relationship has generally been represented in terms of the rate of crack growth (dC) per cycle (dN) for samples where the load is returned to zero for each cycle, using the Paris Power law relationship.

$$\frac{dC}{dN} = BT^{\alpha} \qquad [4.5]$$

The value of the exponent α, represents the behaviour of various vulcanisates over a useful range of T values. This exponent has been found to be about 2 for natural rubber and 4 or more for non crystallising rubbers such as SBR[10].

The fracture mechanics approach is based on the criterion for crack growth proposed by Griffith for brittle material and applied successfully by Rivlin and Thomas to the tearing of rubbery materials[14]. The approach assumes that the energy necessary to cause a crack to propagate at any given rate in a strained specimen is independent of the specimen type used. Using this approach therefore, the elastic energy, needed to propagate a crack can be written as

$$\mathrm{T} = \left(-\frac{1}{h}\right)\left[\frac{\partial E}{\partial c}\right]_{l} \qquad [4.6]$$

Where E is the total elastic energy stored in the test piece,

c is the crack length,

h is the specimen thickness, The partial differential indicates that the clamped length l, of the test piece is kept constant so that the external forces do no work. T is the strain energy release rate, tear energy or fracture energy[10, 15]. The tearing energy can

be evaluated for a wide variety of sample geometries. The tearing energy is equal to the strain energy density, W_o times a certain factor that depends on geometry. The energy release rate under certain conditions is said to be proportional to the product of the strain energy density and the crack size. If this is so then the strain energy density is the measure of the energy release rate of naturally occurring flaws. Various failure properties such as tensile strength and fatigue failure have been related to crack growth behaviour of rubbers using this approach[10]. To determine the fracture toughness and the tearing energy, using the fracture mechanics approach, small notches are usually made on the elastomer. In order to estimate the life of a polymeric material through fatigue measurements, crack growth is followed under fatigue and the number of cycles to a particular length of crack is measured and the rate of crack growth determined. Rubbers have a maximum tearing energy, T_c (critical energy) which the rubber can withstand without crack propagation. For crack propagation to occur, the tearing energy T must be greater than the critical energy T_c. That is the criterion for crack propagation and is given by:

$$T \geq T_c$$

When the tearing energy T is less than the critical tearing energy T_c, the crack growth rate is virtually zero. The only mechanism that produces crack growth in this situation is ozone attack. T_c can be related to the primary bond strength and molecular structure of a vulcanizate. The curve for the crack growth rate versus maximum energy release rate (both log scales) for a typical natural rubber and styrene butadiene rubber is as shown in Figure 4.1. The fatigue crack growth rate in the sub threshold region is much slower and remains almost constant when T is below a threshold T_o as earlier explained. The region which obeys the power law is termed the stick slip region and is particular to filled rubbers because of the presence of fillers which act like crack stoppers. In this region, which is also sometimes called the stable crack growth region, a linear relationship usually results which has a slope ranging from 1 to 4. At higher tearing energies, the slope becomes much steeper. This region has been called the catastrophic crack growth region (unstable crack growth region) since the rate approaches the velocity of elastic waves in rubber. This region usually results from a change in crack morphology from rough to smooth.[16, 17]

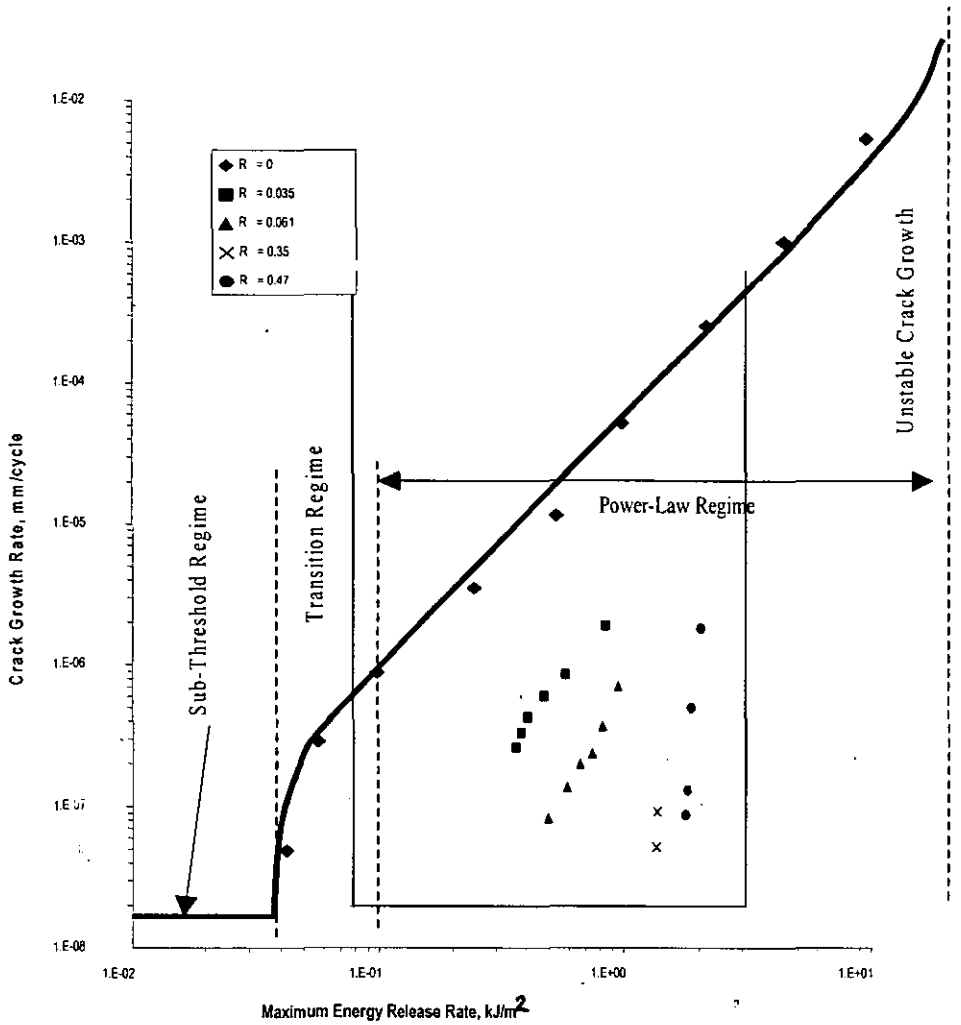

Figure 4.1: Regions of crack propagation[17]

The intrinsic flaw size is a parameter that must be taken into account when estimating the fatigue life of a rubber compound. The intrinsic flaws that can be as a result of processing and manufacturing processes distribute themselves randomly in the rubber. For rubber with a single cut and under cyclic tensile loading with an energy release rate in the power law region, the fatigue crack growth can be expressed thus:

$$\frac{dC}{dN} = B\left(2\pi\lambda^{-1/2}Wc\right)^{\alpha} \qquad [4.7]$$

Assuming that the intrinsic flaw size c_o is much smaller than the final failure size c_c, the expression for describing the fatigue life of rubber is thus[11]

$$N = \frac{1}{B(\alpha - 1)\lambda^{-\alpha/2}(2\pi W)^{\alpha} c_o^{\alpha-1}} \qquad [4.8]$$

The fatigue life of rubber thus increases with decreasing intrinsic flaw size as shown in equation 4.8

4.3 Measurement of Crack Growth in Elastomeric Materials

Crack growth in elastomers has been measured using various specimen types and shapes, from which various energy values are deduced.

4.3.1 Single-Edged Notch Specimen

To determine the characteristic fracture mechanics parameters which quantify the resistance of the material to unstable crack propagation, angled and split, single – edged – notched (SEN) test pieces, with a sharp crack have been used[4]. For an SEN test piece, the rubber is in a state of simple extension away from the clamp and the cut, but not extending across the test piece. It has been shown by Rivlin and Thomas[18] that the total elastic energy before (U_o) and after (U_c) the cut is introduced obey the relationship

$$U_o - U_c = Kc^2 t \qquad [4.9]$$

Where K is a proportionality constant dependent on strain. K which is a function of λ, is given as

$$K = kW \qquad [4.10]$$

With k and W as defined in section 4.2.1

4.3.2 Shear and Trouser Tear Test Specimens

Tearing energy of rubbers has been studied for different shapes and specimen geometry. Trouser and pure shear test pieces are widely used for crack growth studies of rubber. For a trouser test piece, the tear energy, T, is given by

$$T \cong \frac{2F}{t} \qquad [4.11]$$

Where F is the applied force, and t is the thickness.

$$N = \frac{1}{B(\alpha - 1)\lambda^{-\alpha/2}(2\pi W)^{\alpha} c_o^{\alpha-1}} \qquad [4.8]$$

The fatigue life of rubber thus increases with decreasing intrinsic flaw size as shown in equation 4.8

4.3 Measurement of Crack Growth in Elastomeric Materials

Crack growth in elastomers has been measured using various specimen types and shapes, from which various energy values are deduced.

4.3.1 Single-Edged Notch Specimen

To determine the characteristic fracture mechanics parameters which quantify the resistance of the material to unstable crack propagation, angled and split, single – edged – notched (SEN) test pieces, with a sharp crack have been used[4]. For an SEN test piece, the rubber is in a state of simple extension away from the clamp and the cut, but not extending across the test piece. It has been shown by Rivlin and Thomas[18] that the total elastic energy before (U_o) and after (U_c) the cut is introduced obey the relationship

$$U_o - U_c = Kc^2 t \qquad [4.9]$$

Where K is a proportionality constant dependent on strain. K which is a function of λ, is given as

$$K = kW \qquad [4.10]$$

With k and W as defined in section 4.2.1

4.3.2 Shear and Trouser Tear Test Specimens

Tearing energy of rubbers has been studied for different shapes and specimen geometry. Trouser and pure shear test pieces are widely used for crack growth studies of rubber. For a trouser test piece, the tear energy, T, is given by

$$T \cong \frac{2F}{t} \qquad [4.11]$$

Where F is the applied force, and t is the thickness.

For a pure shear test piece,

$$T = l_0 U \qquad [4.12]$$

Where l_0 is the unstrained value of height l of the pure shear test piece between grips, U is the strain energy density in the rubber in the pure shear region. U can be determined from stress strain behaviour of the rubber, and from the measured strain in the pure shear region[13].

Kadir and Thomas[15] investigated the tear behaviour of rubber using a pure shear test piece. For SBR, which is a non – crystallising rubber, three tear regions were identified. A fairly steady tearing was observed at low tearing rates of 0.1mm/s.

4.4 Some Factors Affecting Strength and Fatigue Failure of Natural Rubber

Several factors have been found to influence the strength and fatigue failure of natural rubber composites, including type of filler, the state of mix, and the types of crosslinks. These factors will be discussed in the following sections.

4.4.1 Effect of Fillers

Carbon black is one of the most traditionally used fillers for rubbers. Its use in the automobile industry is attributed to the strength it confers to the rubber matrix. Generally, tensile strength increases with increase in carbon black loading up to a certain level because of the reinforcement mechanisms, and then decreases at higher loading due to carbon black dispersion effects. As explained by Zhao and Ghebremeskel[19] at high loading, carbon black may agglomerate into large clusters which flourish flaws that can easily cause cracks to grow and then develop into a catastrophic failure.

The addition of particulate filler to an elastomer does not change the inherent strength of the backbone bonds in the network chains, it does, however, increase hysteresis (mechanical energy dissipation). Motions of filler particles, chain slippage or breakage, and dewetting at high strains heighten hysteretic behaviour. Higher tear strength in rubbers is therefore associated with high hysteresis[19, 20]. When a chain is

being pulled along a filler surface, if the molecular friction between the two is sufficiently high and the motion occurs over a sufficient distance, more energy may be expended than would be required to rupture the chains. Mullins[20] in his studies on reinforcement of rubber by fillers, reported that for unfilled styrene butadiene rubber (SBR), the tearing energy increases with increasing rate of tearing, but with black filled vulcanizates of the same rubber, the large increase in tearing energy observed at lower rates, is substantially reduced at higher rates of tearing because of the reinforcement effects. Bhowmick et.al.[21] demonstrated that with a black filled elastomer, the tear strength was 3 – 4 times stronger than the unreinforced vulcanisate of the same elastomer under threshold conditions. Under threshold conditions, dissipative effects are minimised and as such there is a substantial degree of reinforcement. The higher tear strength observed for the black filled elastomers was attributed to the detachment of adhering polymer molecules from the particles of carbon black at forces below those causing main chain fracture. The effective network chain segments are initially short, giving a stiff material but at high stresses, when detached from the filler particle, the effective chain segment would become larger, giving a less stiff but stronger and more tear resistant material.

In addition to providing for increased energy dissipation, dispersed particles serve to deflect or arrest growing cracks thereby delaying the onset of catastrophic failure[19].

Fujimoto et.al.[22] studying the three dimensional stress fatigue of carbon black filled natural rubber explained that the rubber molecules exist in 3 different phases having different levels of mobility. Far away from the filler particles there is excellent mobility (phase A), but adjacent to the carbon black surface there is a glassy phase (phase C) that is immobile. In the fatigue process, Phase A changes to a phase where the entropy of the rubber molecular chains increases and the interaction between the rubber molecule chains is reduced.[22, 23] this increases the internal energy and thus negatively affecting the fatigue life since this energy will be used for crack propagation. Phase C on the other hand, changes to a mobile phase with increased rubber molecular chain interaction and reduced internal energy. It therefore takes a longer time for the maximum energy for fatigue to be attained. They also observed that carbon black aggregates formed a dispersed structure of layers at intervals of 0.5μm in the principal compression stress direction and oriented in the direction of the

principal tensile stress.[22, 23] overall, the fatigue life will depend not only on the behaviour at the phases but also on the nature of the filler and the crosslink density.

4.4.2 Effect of Crosslink Type

The type of crosslink has been found to affect the fatigue life of a natural rubber compound. Thomas deduced that the nature of the crosslink in a natural rubber vulcanizate has a significant effect on the value of the threshold tear energy, T_o. He observed that vulcanizates containing polysulphidic crosslinks have T_o values 50% greater than those containing monosulphidic crosslinks.[10] Similar observations were made by Yanyo et.al.[12, 24] who noted that the bimodal networks have a 70% higher tear strength compared to a monomodal network for polydimethyl siloxane (PDMS). Thomas[10] also found out in his studies on the effect of crosslink type on the fracture of natural rubber vulcanisates that polysulphidic networks showed the slowest cut growth rate over a range of tearing energies followed by monosulphidic and carbon – carbon crosslinks in that order. The reason for this is based on the argument that, the chains in the longer polysulphidic crosslinks are able to move under stress, dissipating energy which would otherwise be used in crack propagation. This same observation has been made by Bhowmick et.al.[21] who reported that, at the same general level of crosslinking, and at similar values of the Young's modulus, the threshold tear strength of materials with polysulphidic crosslinks were approximately twice as high as those with monosulphidic or disulphidic crosslinks. The observed strengthening feature of the polysulphidic crosslinks was due apparently to crosslink rearrangements or scission before rupture of the main chains. Zhao et.al.[19] in their review on factors affecting the fatigue life of rubbers explained that at high crosslink levels, chain motions become restricted and the tight network is not capable of dissipating much energy. Maximum energy of tear strength and fatigue life occurs at lower crosslink densities than that required for the tensile strength. The broken S – S bonds may either reform again under load or link up with the carbon black to form either chemical carbon – gel bonds or physical carbon – gel linkages. The reformed bonds can continue to support stress and can generate more energy dissipation due to chain slippage as the deformation is increased. Another explanation of the strength of S – S crosslinked elastomers is that crosslinks interchange during vulcanization, and in this way relieve internal stresses generated as the network is formed. They further reported that the molecular weight of a polymer does affect the fatigue life of a

polymer[19]. They observed that low molecular weight SBR showed a higher fatigue life under constant strain conditions. This observation they said was due to the fact that low molecular weight SBR vulcanizates, have low equilibrium modulus, a sparse spatial network and large number of free chain ends which lead to the development of a large viscous flow portion. They explained that the molecular chains of fractions with high molecular weight possess lower mobility due to greater intermolecular interactions resulting in a large amount of combined sulphur. Because of the procession of more branched structures and a large number of free molecular chains, this leads to a considerable micro heterogeneity of the material, and the fatigue life is lowered. Zhao et.al.[19] further explained that high vinyl structure of rubber shows high viscoelastic dissipation and therefore delays fatigue failure by viscoelastic energy dissipation. High cis – structure introduces strain – induced crystallisation which acts as a reinforcing domain. Crystallisation not only dissipates energy associated with formation and melting of crystallites, but also provides plastic domains that will block or retard a growing micro – crack. Strain induced crystallisation not only improves ultimate properties, but also the threshold surface free energy for rupture, tear and fatigue life.

4.4.3 Effect of Temperature

High temperatures are generally used to assess the susceptibility of a rubber compound to oxidation or other chemical reactions, but it can also have a significant effect on physical fracture and failure.

4.4.3.1 Environmental Temperature

Young and Danik [16]have investigated the effect of temperature on the fatigue and fracture of different rubbers. They found out that natural rubber showed no deviations in the magnitude of the slope of the crack growth rate versus tearing energy graph, for temperatures from 0°C to 100°C and for tearing energies up to 6000J/m^2. For other rubbers such as BIIR compound, a catastrophic fatigue crack growth rate (FCG) with a steeper slope was obtained for tearing energies above 2500J/m^2. However, for natural rubber, at lower temperatures (0 to -25°C) and at low strains there was a deviation from the slope. This deviation at low strains and temperature for natural rubber was believed to as a result of the strain crystallising behaviour of natural

rubber. Strain crystallisation for natural rubber occurs at relatively low strains in the presence of carbon black filler[16] Bhowmick et.al.[21] investigated the tear strength of elastomers under threshold conditions. The elastomers studied included polychloroprene, SBR, polybutadiene, and ethylene propylene copolymer (EPDM). The polymers were either filled with carbon black or unfilled, swollen in suitable solvents or unswollen. They demonstrated that for polychloroprene alone, the tear strength for the unswollen samples were unexpectedly high (150 – 500J/m^2), but decreased significantly at over 120°C. This behaviour, which has also been observed in cis – polyisoprene.[21] was attributed to the occurrence of strain induced crystallinity at the tip of the propagating tear. Lake et al. [9]stated that under steady load, crystallisation is observed in natural rubber and these crystallites tend to prevent crack growth. The tear strength of the swollen samples was found to be lower and did not significantly vary with test temperature or with the nature of the swelling liquid.

Degradation is known to be increased by mechanical stress. If a chemical bond is put under sufficiently high stress, it will break[25]. It has also been found that oxygen can reduce the tearing energy, by a factor of two when compared with measurements in a vacuum. This is due to the fact that the presence of oxygen in unsaturated rubbers brings about chain cleavage resulting in more shorter chain segments between crosslinks, thereby reducing the tearing energy as explained in sections 3.3 and 4.4.2. High stress can also increase the rate of oxidation at elevated temperatures[10].

4.4.3.2 Temperature at Crack Tip

All the studies in the literature regarding temperature at the crack tip are for rigid thermoplastic materials; however, it is possible that somewhat similar effects may be observed for rubber.

Dynamic crack initiation is generally treated both theoretically and experimentally as an isothermal phenomenon. As observed by Rittel,[26] when specific phenomena such as shear band formation and propagation are involved, the analysis include thermo-mechanical conversion of strain and or fracture energy into heat. He observed that very significant temperature rises can develop which cause softening of the crack – tip material[26]. Research into dynamic impact fracture indicates very high temperature at crack tips, thus accelerating the failure process either by direct fracture or by shear band formation.[27]

Dynamic crack initiation in components can either be by mode I loading, which is a tensile mode cracking Mode II, which is the sliding mode of cracking and Mode III loadings, which is a tearing mode[28].

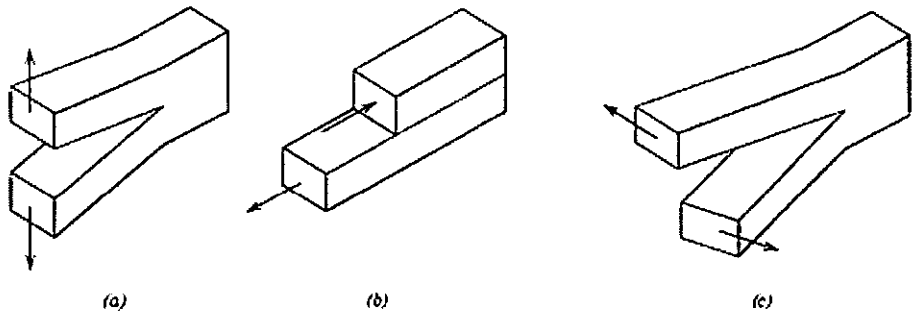

Figure 4.2: The three modes of crack surface displacement (a) Mode I, opening or tensile mode, (b) mode II, sliding mode and (c) mode III, tearing mode

Furthermore, in his work on the thermomechanical aspects of dynamic crack initiation, Rittel[26], observed that for a dynamic mode I loading, the crack tip temperature drops significantly prior to crack propagation, which is understood to be a moving heat source which contributes to the ensuing temperature rise. This same results had been observed by Weichert and Schonert who investigated the temperature rise during fracture of glass plates.[29] For mode II loading, there was a significant rise in temperature prior to or during a crack propagation, and therefore concluded that both the thermoplastic and thermoelastic deformations are relevant to dynamic crack initiation and must be considered as potent factors in the determination of the fracture toughness of the material at different loading rates.

Rittel and Maigre [30] observed that for PMMA using compact compression specimen(CCS), the fracture was due largely to transient effects in the sense that the specimens fracture shortly after the stress wave has loaded the crack, and that all specimens fractured by mode I. The Mode I mechanism increasing with increase in the stress intensity factor. They suggested that dynamic crack initiation in PMMA occurs by the nucleation of several micro cracks along the notch front

4.5 Life Prediction.

In the majority of elastomeric components, failure is not due to a large static load resulting in catastrophic failure but to much smaller cyclic fatigue loads. This mode of

failure should therefore be used as the failure criterion when designing a component. The fatigue crack propagation portion of the fatigue life is a predictable quantity if dC/dN as a function of Δk (where k is the stress concentration factor) has been empirically established[31]

For successful life prediction using a combination of Finite Element Analysis and a fracture mechanics approach, the elastomer properties should be accurately characterised. To do this, three aspects of elastomeric behaviour are required for modelling and must be measured. The three aspects are: the elastic response to deformation, the reduction in stress associated with repeated cyclic loading and the relationship between tearing energy and crack growth rate. Using the material information the tearing energies generated in the component under applied loads can be determined and then fracture mechanics used to determine the rate of crack propagation[32].

An alternative, stress-based fatigue life technique, commonly known as the S - N (stress - life) technique, is the conventional method used to investigate the fatigue behaviour of polymers[32]. For example, total life analysis has been used to predict the service life of an engine mounting lug in aircraft. [32] . The objective of the total life method is to ensure that the part survives its design life. Total life refers to the life to catastrophic failure and makes no distinction between initiation and propagation of cracks The S - N method does not model yielding and load redistribution. A modification of the method, the local strain approach (strain - life or ε - N) has been used to model design life, which is more appropriate for low - cycle fatigue problems. Unfortunately, there is no standard S – N curve for natural rubber or its compounds. Therefore, for each component and compound an S – N curve needs to be produced from a series of fatigue data, from which the service life of the component could be predicted.

4.5 References

(1) Sharma, M. G.; Lim, C. K. *Polymer Engineering and Science* **1965**, *5*, 254-262.

(2) Kanchanomai, C.; Mutoh, Y. *Materials Science and Engineering A* **2004**, *381*, 113-120.

(3) Kanchanomai, C.; Mutoh, Y. *Scripta Materalia* **2004**, *50*, 83-88.

(4) Thomas, A. G. *Rubb. Chem. Technol.* **1994**, *67*, G50-G60.

(5) Mars, W. V.; Fatemi, A. *International Journal of Fatigue* **2002**, *24*, 940-961.

(6) Mars, V. M.; Fatemi, A. *Rubb. Chem. Technol.* **2004**, *77*, 391.

(7) Lake GJ *Rubber Chemistry and Technology* **2003**, *76*, 567.

(8) Lake GJ *Rubber Chemistry and Technology* **2001**, *74*, 509.

(9) Lake, G. J. *Rubb. Chem. Technol.* **1995**, *68*, 435.

(10) Thomas, A. G. *Rubb. Chem. Technol.* **1975**, *48*, 902-912.

(11) Gent, A. N. In Engineering with rubber, How to design rubber compounds; Hanser Verlag: Munich, 2001; pp 88.

(12) Yanyo, L. C. *Int. J. Fract.* **1989**, *39*, 103-110.

(13) Lake, G. J.; Thomas, A. G. In Gent, A. N., Ed.; Engineering with Rubber, How to design rubber compounds; 2001; pp 100.

(14) Ellul, M. D. In Gent, A. N., Ed.; Engineering with Rubber: How to design rubber compounds; 2001; pp 140.

(15) Kadir, A.; Thomas, A. G. *Rubb. Chem. Technol.* **1981**, *54*, 15-23.

(16) Young, D. G. *Axel Physical testing services report* **July 2001**, *VI*, 1.

(17) Kallrath, J.; Altstadt, V.; Schloder, J. P.; Bock, H. G. *Polym. Test.* **1999**, *18*, 11-35.

(18) Rivlin, R. S.; Thomas, A. G. *J. Polym. Sci.* **1953**, *10*, 291-318.

(19) Zhao J; Ghebremeskel GN *Rubber Chemistry and Technology* **2001**, *74*, 409.

(20) Mullins, L. *Rubb. Chem. Technol.* **1960**, *33*, 315-325.

(21) Bhowmick, A. K.; Gent, A. N.; Pulford, C. T. R. *Rubb. Chem. Technol.* **1983**, *56*, 226-232.

(22) Fujimoto, K.; Kofuji, H.; Ueki, T.; Mifune, N. *International Polymer Science and Technology* **1987**, *14*, T65.

(23) Fujimoto, K.; Mifune, N. *Int. Polym. Sci. and Technol.* **1987**, *14*, T/29-T/33.

(24) Yanyo, L. C.; Kelley, F. N. *Rubb. Chem. Technol.* **1987**, *60*, 78-88.

(25) Kuleznev, V. N.; Shershnev, V. A., Eds.; In *Chemistry and Physics of Polymers;* Mir Publishers: Moscow, 1990; .

(26) RITTEL, D. *Int. J. Fract.* **1999**, *99;*, 199.

(27) Rittel, D. *Int. J. Solids Structures* **2000**, *37;*, 2901.

(28) Callister Jr, W.D. *Material Science and Engineering: An Introduction, student learning resources*, 6th edition. John Wiley and sons Inc, New York, 2003, Page W-12.

(29) Weichert, R.; Schonert, K. *Journal of the mechanics and physics of solids* **1978**, *26*, 151-161.

(30) Rittel, D.; Maigre, H. *Mech. Mater.* **1996**, *23*, 229.

(31) Singh, P. J.; Guha, B.; Achar, D. R. G. *Eng. Fail. Anal.* **2003**, *10*, 383-393.

(32) Mustafa, S.; Ahmet, A. In *Fatigue Behaviour of Discontinuous Glass Fiber Reinforced Polypropylene;* Moalli, J., Ed.; Plastic Failure - Analysis and Prevention; William Andrew Publishing: USA, 2001; pp 17-22.

CHAPTER 5

5 Experimental

5.1 Materials

Natural rubber (SMRCV60) was supplied by the Tun Abdul Razak Research Centre, UK. Carbon black (N772) was supplied by Columbian Chemicals UK. Accelerators Tetramethylthiuram disulphide, (TMTD), N – (1,3 – dimethylbutyl) – N" – phenyl – phenylenediamine, (6-PPD), 2,2,4 – Trimethyl – 1,2 – dihydroquinoline, (TMQ), N – tert- -butyl - 2 – benzothiazolesulphenamide, (TBBS), were supplied by FLEXSYS Belgium. Sulphur, Zinc oxide, antiozonant wax, stearic acid were used as supplied.

5.2 Mixing

A typical engine mount formulation as shown in Table 5.1 was used for the compounding.

Table 5.1: Typical engine mount formulation

Material	Composition in parts per hundred rubber (phr)
NRCV60	100
Carbon black (N772)	49
Zinc Oxide	5
Stearic acid	2
Anti ozonant wax	2
6 – PPD	1.5
TMQ	1
TBBS	0.7
TMTD	0.5
Sulphur	1.7

The sequence of mixing was as shown on Figure 5.1

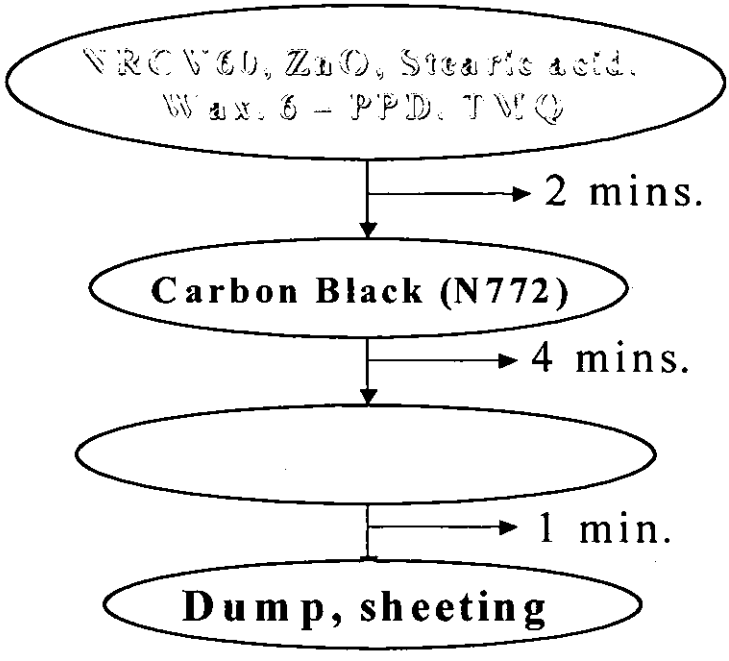

Figure 5.1: Scheme for the mixing sequence

The natural rubber compound was prepared in a water cooled Francis-Shaw K1 intermix having a volume of 5.5l. A fill factor of 0.55 was used and the mixing was done at a speed of 40 rpm, the rotors and mixing chambers were cooled with circulating water at 40°C. The rubber was first masticated in the internal mixer for 2 mins together with the activators (zinc oxide and stearic acid) and the anti-ozonant wax. Carbon black was then added and the compound was mixed for a further four minutes before introducing the anti oxidants (TMQ, and 6 – PPD), accelerators, (TMTD and TBBS) and the crosslinking agent (sulphur). The mixing was then carried out for a further 1minute before dumping. The compound was then sheeted out on a two roll mill.

5.3 Cure Measurements and Vulcanisation

Cure parameters were determined using a Monsanto R100S Rheometer operating at a strain amplitude of 3° and at a cure temperature of 140°C or 150°C. From the rheographs obtained, the scorch time, cure rate index, minimum and maximum torque were obtained. Test sheets were then compression moulded using a hydraulic press with electrically heated platens to 95% cure at 140°C for 24 minutes and at 150°C for 15 minutes.

5.4 Compression Set

Compression set measurements were conducted on type I cylindrical test pieces (13.0 ± 0.5mm diameter and 6.3 ± 0.3mm thickness) strained at 25% of their original thickness and aged in an oven of controlled ventilation at 70°C for 22 hours. The test pieces were then removed and allowed to cool for thirty minutes and the thickness measured using a micrometer to the nearest 0.01mm. The compression set was calculated using formula[1]

$$\text{Compression set} = \frac{h_0 - h_1}{h_0 - h_s} x100 \qquad [5.1]$$

Where h_o is the initial thickness of test piece in mm

h_1 the thickness, in millimeters, of the test piece after recovery

h_s is the height, in millimeters, of the spacer

5.5 Hardness test

The hardness test was determined on a cylindrical test piece of 25mm diameter using a Durometer type M (Shore instruments and MFG Co.). The hardness value was determined after penetration of the Durometer indenter into the sample, and the results recorded in shore A.

5.6 Accelerated Thermal/Thermo – oxidative Ageing

5.6.1 Static Ageing

Thermal ageing and Thermo- oxidative ageing was carried out in an air circulating oven at temperatures of 70°C, 80°C, 90°C 100°C and 110°C for times ranging from one hour to five weeks. At the end of each ageing time, samples were removed and kept at room temperature before testing within 48 hours of removal from the oven.

In order to carry out thermal ageing of the rubber samples, the vulcanised rubber sheets were placed between aluminium foil sheets. The sheets were compressed at 100°C for about five minutes in order to evacuate any entrapped oxygen that might affect the thermal ageing process. Another aluminium foil was then folded over the initial one to ensure that any crevices where oxygen can penetrate are closed. Owing to the fact that evacuation of oxygen was done before ageing was carried out, any volatile matter produced in the course of ageing was trapped between the sample and the foil. Sheets were then aged at temperatures of 70°C, 80°C, 90°C, and 100°C for times ranging from one hour to 4 weeks.

5.7 Thermogravimetric Analysis

Thermogravimetric measurements were conducted on both aged and unaged compound using a Texas instrument TA 2940 in alumina pans at heating rates of 10°C.min^{-1}, 15°C.min^{-1}, 20°C.min^{-1} and 25°C.min^{-1}over a temperature range from ambient to 700°C under a steady flow of air (60 ml.min^{-1}) in one instance and nitrogen in another. Data of sample temperature, weight of sample and the derivative weight loss were recorded by an analytical computer using the Texas instrument software. The initial weights of the samples were recorded before the heating process began.

5.8 Tensile Testing

Tensile properties were measured in accordance with the BS903 – A2 [2], using type II dumbbell test pieces which were die stamped from the 2 mm thick vulcanised sheets

along the milling direction. A Houndsfield tensile testing machine operating at a cross head speed of 500mm/min was used, with a Houndsfield 500L laser control apparatus attached to it to measure the extension. Reflective benchmarks were placed at a distance of 2 cm from each other. The tensile strength, elongation at break and modulus were acquired using the QMAT – Dongle: 2003 computer software. At least eight specimens were tested from each moulded sheet.

5.9 Dynamic Mechanical Analysis of Aged Rubber

The effect of ageing on the dynamic mechanical properties of an engine mount compound was investigated using a TA Instrument Thermal Analysis DMA 2980 operated at a strain sweep of 0μm - 2500μm (0 – 25% strain) and at a fixed frequency of 30Hz, operating in tensile mode. Aged natural rubber vulcanisate samples of rectangular geometry and dimensions of 23.52mm by 5.33mm and thickness of 2.33mm were clamped in the furnace at a temperature of 30°C.

Temperature sweep measurements (-100 to 120°C) for the storage modulus, loss modulus and the tandelta of the aged rubber compounds were measured on a Rheometric Scientific dynamic mechanical thermal analyser MKII (Surrey, UK) using rectangular samples of similar dimensions as above, but operating on a single cantilever bending mode. Tests were performed at a frequency of 30Hz with a deflection amplitude of 256μm

5.10 Crosslink Density Measurements

5.10.1 Swelling:

Samples with dimensions 10mm by 10mm by 2.4mm thick were cut from cured sheets of both unaged and compounds aged at 70°C, 80°C, 90°C, 100°C and 110°C for periods ranging from 1hr to 4weeks. Samples were swollen to equilibrium volume in toluene for five days. The excess solvent was then blotted from the sample with a filter paper and the swollen weight measured. The swelling ratio of the rubber compound was measured at equilibrium swelling. Solvent was then decanted and the samples allowed to dry in air and in vacuo at 80°C for 24hrs. The dry weight of the

sample was then recorded. The swelling ratio was calculated using the following relationship[3]

$$R = \frac{W_t - W_{ot}}{W_o} \qquad [5.2]$$

Where W_o is the weight of test piece before swelling

W_t is the swollen weight after time t of immersion

From the swelling measurements the crosslink density (V_e) of the cured and aged rubber was calculated using the Flory - Rehner equation[4-7]

$$V_e = \frac{[\chi V_{ro}^2 + \ln(1 - V_{ro}) + V_{ro}]}{V_o(0.5V_{ro} - Vo_r^{1/3})} \qquad [5.3]$$

Where

V_{ro} = corrected volume fraction of rubber network in swollen sample

V_o = molar volume of the solvent (toluene = 106.9 cm^3/mol)

X = is polymer – solvent interaction parameter which for toluene / black filled natural rubber is 0.42[7].

For carbon black filled natural rubber, V_{ro} was determined from the equation

$$\frac{V_{ro}}{V_r} = 0.56e^{-z} + 0.44 \qquad [5.4]$$

Where

V_r, is the measured volume fraction of rubber in the swollen network and is calculated from the equation 5.

z is the weight fraction of carbon black in the vulcanizate

$$\frac{1}{V_r} = 1 + (\frac{W_s \rho_r}{W_r \rho_s}) \qquad [5.5]$$

Where Wr is the dry weight of the rubber specimen

Ws is the equilibrium swollen weight

ρ_r is the density of the rubber compound

ρ_s, the density of the solvent (toluene)

5.11 Crack Nucleation and Growth Measurements

5.11.1 Fatigue Testing

Type II Dumbbell samples cut from the aged rubber sheets were fatigue tested in uniaxial tension using a Hampden dynamic testing machine to determine the fatigue life of the rubber compound. A frequency of 2Hz and a strain amplitude of 100%, with the strain on each test piece relaxed to zero after each fatigue cycle was applied. At least 14 test pieces were tested for each ageing time and temperature. The number of cycles to failure was then recorded. All the measurements were carried out at ambient temperature.

In order to follow the temperature rise in the samples during fatigue measurements, an FLIR ThermoVision A40M thermal imaging camera was used, with each thermal image built from 76,800 individual picture elements sampled 60 times per second by the camera's on – board electronics and soft ware to measure temperature.

5.11.1.1 Dynamic Ageing

Dynamic ageing was carried out on a modified fatigue machine. A combination of air and heat was supplied by a hot air gun operating at different set temperatures. The temperature of the chamber was kept constant through a thermocouple connected to an automated switch controlling the air gun. The temperature of the chamber was controlled to within ± 2°C of the set temperature. The fatigue cycle was started as soon as the sample temperature was at equilibrium. Test temperatures included 17°C, 30°C, 40°C, 50°C, 60°C, and 70°C. The number of cycles to failure at each test temperature was recorded.

5.11.1.2 Crack Growth Measurements

The experimental set up is as shown in Figure 5.3.6 The rubber with a nick of about 1mm was clamped in a temperature controlled chamber. The upper clamp was connected to a load cell fixed to a crosshead and the bottom clamp was connected to a disc – type drum cam driven by and electrical servo – motor. The testing was carried out at a temperature regulated electrically at 50°C to avoid discrepancies in crack growth as a result of temperature rises due to dynamic heat build - up. The rubber samples which were statically aged at 100°C for periods ranging from 0 hours to one

week, were subjected to a test frequency of 5Hz with displacement amplitude of up to 100%. The crack growth of the rubber specimen was monitored through an image process system with a high speed CCD camera. Measurements were made to track the tip of the crack, and the length of crack growth was recorded as a function of the strain cycles, providing the rate of fatigue growth[8].

The tearing energy (energy release rate), G, using the tensile strip shown in Figure 5.4, was calculated using the relation.

$$G = 2KUc \qquad [5.6]$$

Where c is the crack length, U is the elastic energy density in the simple extension region (taken as the area under the stress – strain curve), and K is a slowly varying function of the strain given by

$$K = \frac{3}{\sqrt{\lambda}} \qquad [5.7]$$

Where λ is the extension ratio in the simple extension region.

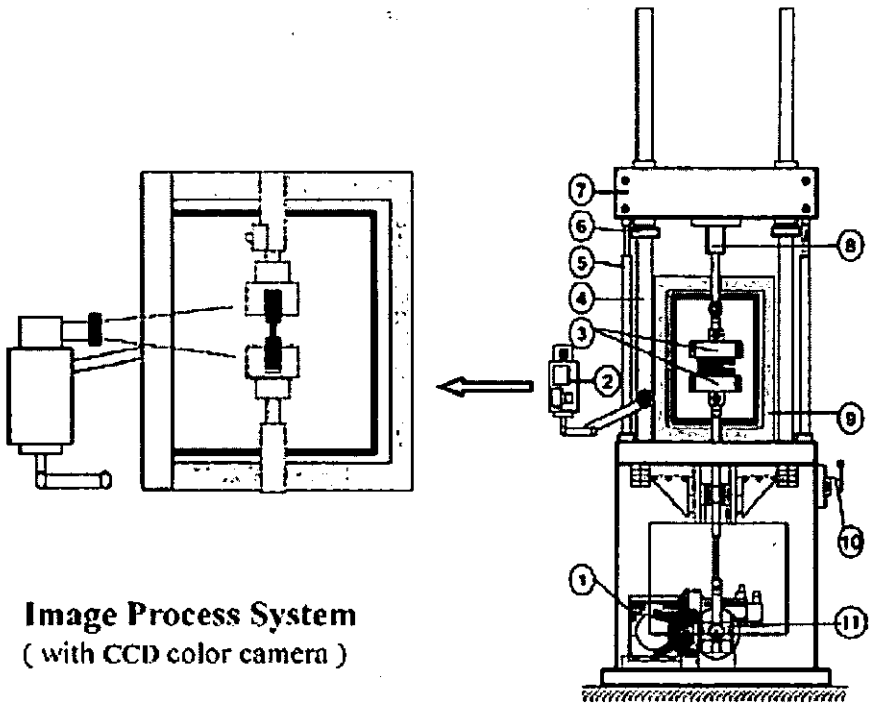

Figure 5.2: Diagram of the test machine measuring crack growth characteristics adopted from[8] . (1) Motor, (2) High – Speed CCD camera, (3) Clamps, (4) Main shaft, (5) Cylinder, (6) stop ring, (7) crosshead, (8) load cell, (9) Chamber, (10) cylinder handle, (11) Cam.

The crack growth measurements were carried out by Columbian chemicals Bristol – UK.

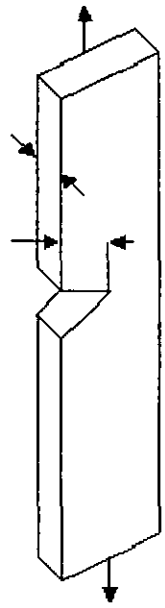

Figure 5.3: Diagram of the SEN rubber sample to measure crack growth

5.11.1.2.1 Trouser Tear

Rectangular test pieces of dimensions of 100mm long, 30mm wide and 2.2 mm thick were compression moulded at 140°C to full cure. The cured sheets were then aged as earlier described in an air circulating oven at temperatures of 70°C to 110°C. Using a sharp razor, a cut of about 30mm was made midway along the width of the test piece to form a trouser test piece as shown in Figure 5.5a. The tests were performed on a Houndsfield tensile testing machine operating at a cross head speed of 50mm.min^{-1} [9]. A minimum of five test pieces were used to for each ageing temperature. The tearing force from each test piece was recorded. The first and last peaks which represented the onset of crack growth and when the sample failed were discarded. The remaining peaks were used to calculate the average tearing force for the rubber The tearing energy was calculated using the relationship

$$T = \frac{2F}{t} \qquad [5.8]$$

Where F is the force and t is the thickness.

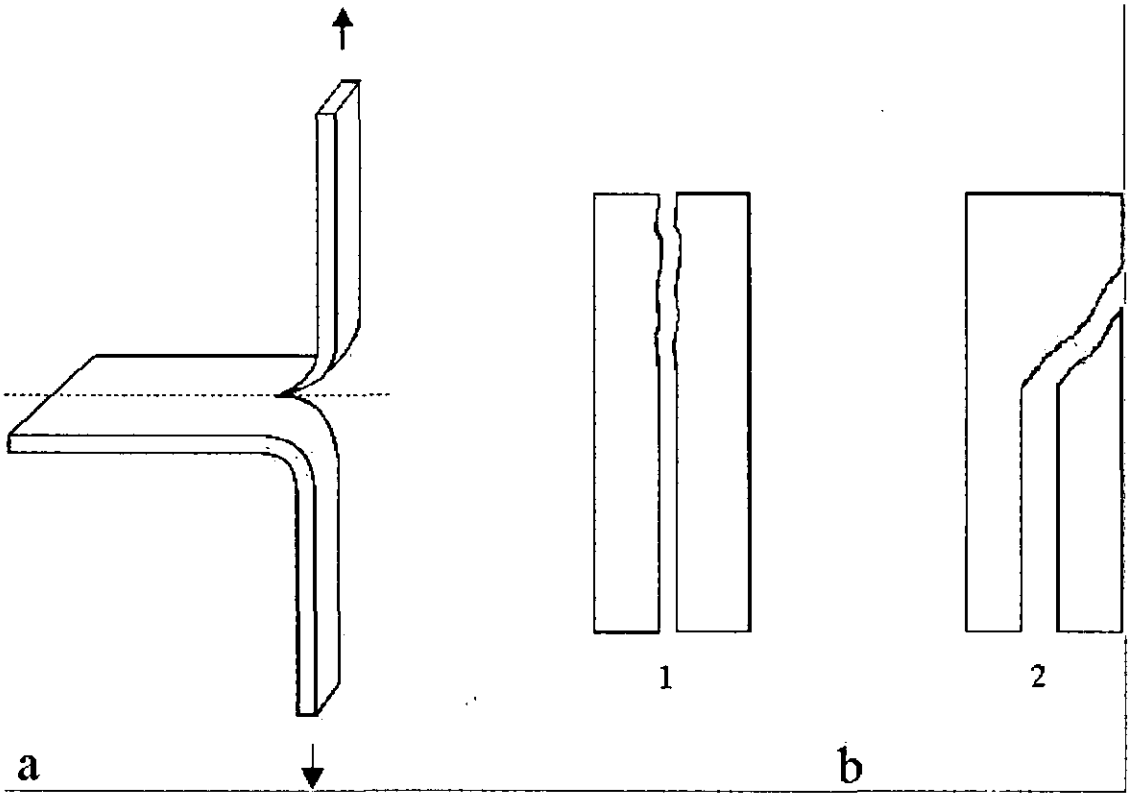

Figure 5.4: Diagram of (a) trouser tear test piece and (b) different tear that may be observed.

5.12 Investigation of Flaws Introduced During Moulding

To investigate the effect of flaws during processing of the rubber compound, various flaws were introduced to the rubber compound prior to curing. Flaws included memory interfaces and particulate contamination.

5.12.1 Introduction of a Memory Interface

Carbon black filled natural rubber sheets of dimensions 12 cm by 12 cm were pre - cured below scorch at 120 ^{o}C for five minutes. Using a new razor blade, pre-cured sheets were carefully cut across the centre of the sheet. Three treatments were made: The control which had no cut, the partially cut sample created by cutting partially through a pre-cured sheet (Figure 5.5d) and a third treatment made by entirely cutting

through a pre-moulded sheet (Figure 5.5a). These samples were compression moulded to their full cure at 150°C, 160°C and 180°C, thereby creating different types of memory interfaces (weld lines).

To assess the effect of cure temperature, the compound was pre – cured below scorch for 3 minutes at 120°C and to scorch for 13 minutes at 120°C. The various memory interfaces were introduced as earlier described, and the rubber compound cured completely at 150°C, 160°C, and 180°C.
The rubber compounds were then subjected to mechanical testing to assess the effect of pre-cure temperature and cure temperature on the tensile properties of a memory interface in natural rubber.

5.12.1.1 Healing Time

Rubber sheets were pre-moulded at various time intervals up to their various scorch times (ts_2) at temperatures of 100°C, 110°C, 120°C, 130°C, 140°C and 150°C. Using a new lubricated razor blade, the pre-moulded sheets were carefully cut through the centre and were compression moulded to their full cure at the cure temperatures indicated. The rubber compounds were then subjected to mechanical testing to assess the effect of cure temperature on the healing time of a flawed rubber compound.

5.13 Introduction of particulate contamination

Samples of the natural rubber compound pre –cured well below scorch at 100°C, and 140°C. Carbon black was applied carefully on the surface centrally of an uncut sample (Figure 5.5 b) and in the cut of a partially cut sample (Figure 5.5c). The samples were then completely cured at 140°C. The samples were tensile tested as described in section 5.5. For fatigue testing, samples were cured fully at 150°C and 180°C. This was to assess also cure temperature effects. Control samples had no cut.

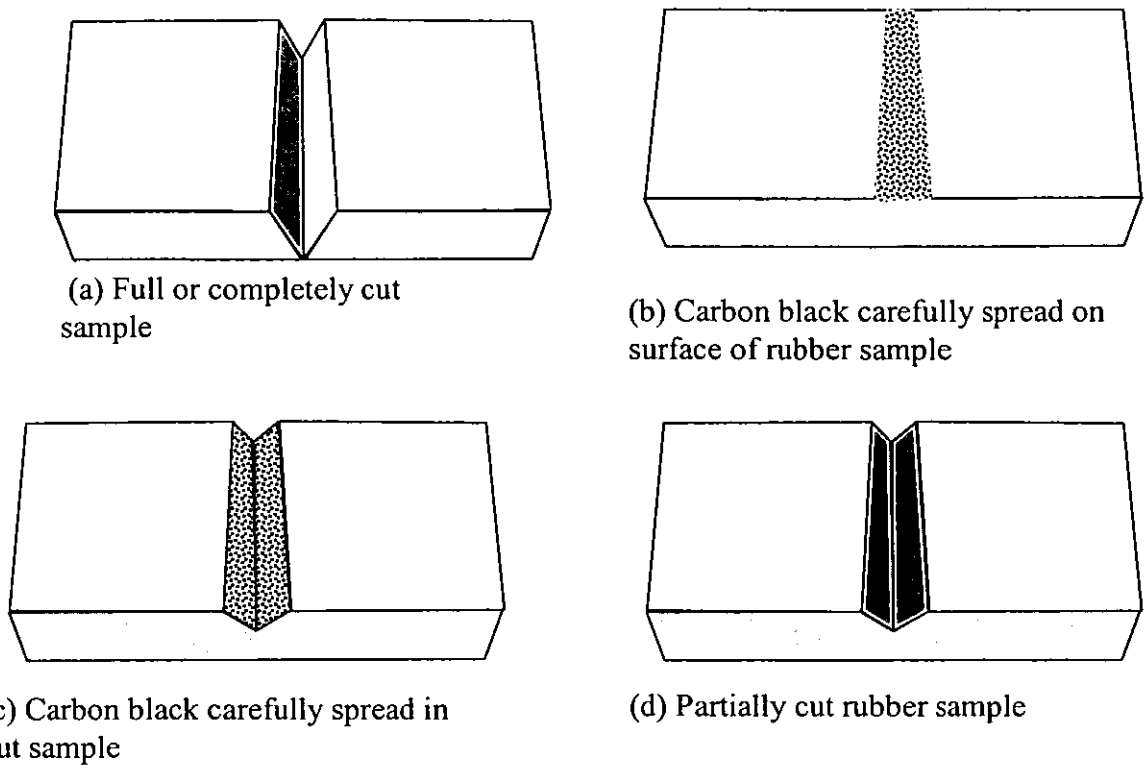

Figure 5.5: Types of flaws introduced after pre - curing

5.14 Pinhole Flaws

In order to estimate the intrinsic flaw size of the rubber engine mount compound, pinhole flaws with flaw size ranging from 0mm to 1.2mm, were made on dumbbell test pieces of a previously cured rubber sheet as described in section 5.3 by piercing the dumbbells centrally with pins of various sizes. Tensile and fatigue measurements were then carried out on these samples. An average of five samples for each pinhole flaw size was used.

5.15 Microscopy

The cut surfaces (healed and fractured) were examined by Scanning Electron Microscopy (SEM) after first sputter coating with gold to avoid electrostatic charging and poor image resolution.

5.16 References

(1) British Standard Institution *BS903 – A6* **1995.**

(2) British Standards In *Method for determination of tensile stress - strain properties;* Physical testing of rubber; British Standard Institution: 1995; Vol. A2

(3) Sobhy, M. S.; El – Nashar, D.E.; Maziad, N. A. *Egypt. J. Sol.* **2003**, *26*, 241-257.

(4) Porter, M. *Rubb. Chem. Technol.* **1967**, *40*, 866-882.

(5) Kim, S. G.; Lee, Suck - Hyun. *Rubb. Chem. Technol.* **1994**, *67*, 649-661.

(6) Mathew, M. N.; Bhowmick, A. K.; De, S. K. *Rubber Chem. Technol.* **1982**, *55*, 51-61.

(7) Gent, A. N.; Hartwell, J. A.; Lee, G. *Rubber Chem. Technol.* **2003**, *76*, 517-532.

(8) Kaang, S.; Woong Jin, Y.; Huh, J.; Lee, W.; Bin Im, W. *Polym. Test.* **2006**, *25*, 347-352.

(9) British Standard Institution *BS 903* **1995**, *Part A2.*

CHAPTER 6

6 Effect of Ageing on Static Mechanical Properties

6.1 Introduction

In order to assess and predict the functional life of a natural rubber (NR) engine mount compound, the physical property changes caused by ageing were determined using accelerated ageing conditions. The compound was thermally (anaerobically) and thermo - oxidatively aged in an oven at temperatures ranging from 70°C to 110°C, and at times of between one hour and five weeks. Static mechanical measurements, such as tensile properties, were used to characterise the effect of ageing and elucidate ageing mechanisms of the engine mount compound. Two cure temperatures, 140°C and 150°C, were used to determine whether the ageing process was affected by cure temperature. Before the effects of ageing are discussed, the effect of the cure process on properties is discussed in the following two sections (Section 6.2 and 6.3).

6.2 Effect of Cure Temperature on Properties

The cure properties of the compound cured at 140°C and 150°C are as shown in Table 6.1. Other properties of the compound are shown in Table 6.2.

Table 6.1: Cure behaviour of compounded natural rubber at different cure temperatures

Cure property	cured at 140°C	cured at 150°C
Maximum torgue (M_H) (dN.m)	95.41	92.09
Minimum torgue (M_L) (dN.m)	21.02	20.61
Scorch time (ts_2) (mins)	5.46	2.83
Cure rate index (CRI)	13.23	23.64
tc_{95} (min : secs)	23.56	14.42

The cure rate index (CRI) is a measure of the speed with which the cure reaction is taking place and is given by the equation

$$CRI = 100/(t_{90} - t_2) \quad \text{-- -- -- -- -- --} \quad [6.1]$$

It is not surprising that the formation of crosslinks is faster at 150°C than at 140°C. However, it is also possible that the types of crosslink formed will be affected by the cure temperature. Low temperature cure is expected to give more polysulphidic crosslinks than high temperature curing.[1]

Table 6.2: Properties of the engine mount compound cured at 140°C and 150°C

Property	Cure temperature	
	150°C	140°C
ML 1+4 @100°C	69	72
Mooney Scorch (minutes)	13.2	/
Hardness (Shore A)	56	57
Tensile Strength (MPa)	15	23.18
Elongation at break (%)	360	446
100% Modulus (MPa)	2.8	3.3
Compression set 22hrs @ 70°C (%)	50	56

6.3 Effect of Cure Time on Modulus and Tensile Strength

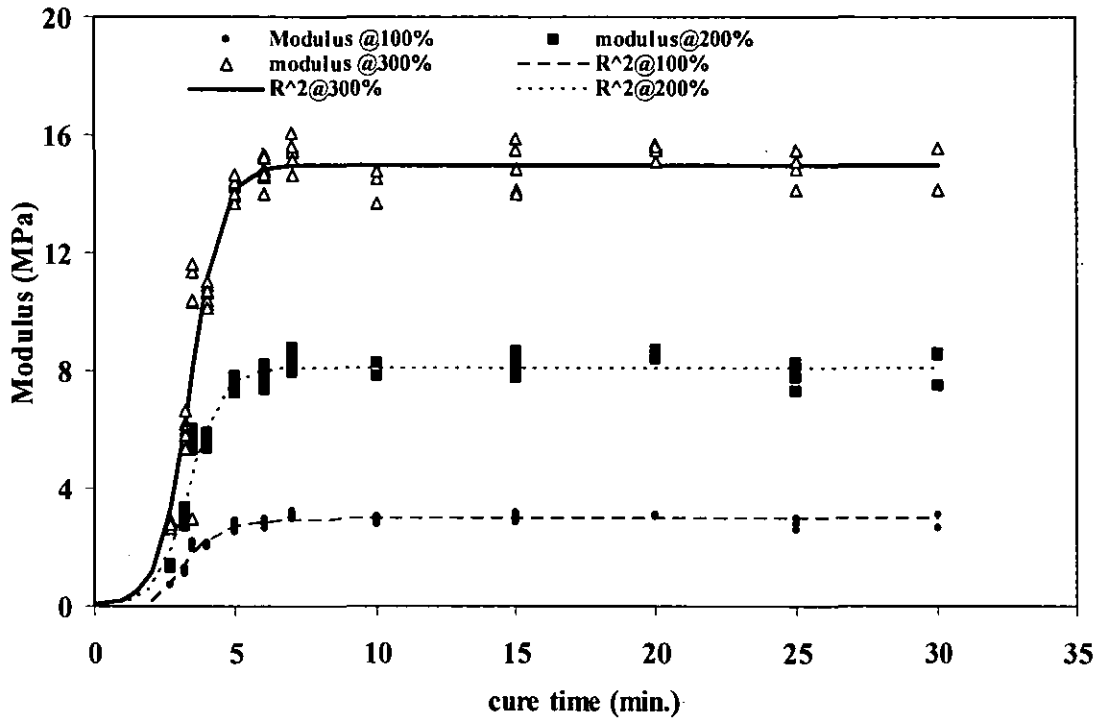

Figure 6-1: Relationship between cure time and modulus cured at 150°C

Natural rubber compounds were compression moulded at 150°C to various degrees of cure from 2.7 minutes to 30 minutes representing 50% cure to more than 100% cure. This was to select the appropriate cure time and to look at the effect of over curing on tensile properties. The effect of the cure time on the modulus at 100%, 200% and 300% are presented in Figure 6.1. The modulus tends to increase with cure time up to a maximum, after which it levels off.

The empirical relationships $M_{100} = \frac{ab + ct^d}{b + t^d}$, and $M_{200,300} = \frac{a}{1 + be^{-ct}}$ (where M is the modulus, t is the cure time in minutes, a, b, c, and d are constants) were used to describe the evolution of the modulus with cure time. The coefficient of correlation was found to be between $0.96 < R < 0.98$. as indicated in Table 6.3.

Table 6.3: Constants, errors and coefficients of correlation describing the relationship between cure time and modulus for rubber cured at 150°C

Modulus (MPa) at different %strain	Model							Coefficients	
	$M = (ab+cx^d)/(b+x^d)$				$M = a/(1 + be^{-cx})$			S	r
	a	b	c	d	a	b	c		
100	-0.0498	626.42	2.98	5.423				0.173	0.977
200					8.079	387.66	1.756	0.521	0.975
300					14.98	425.77	1.781	1.123	0.967

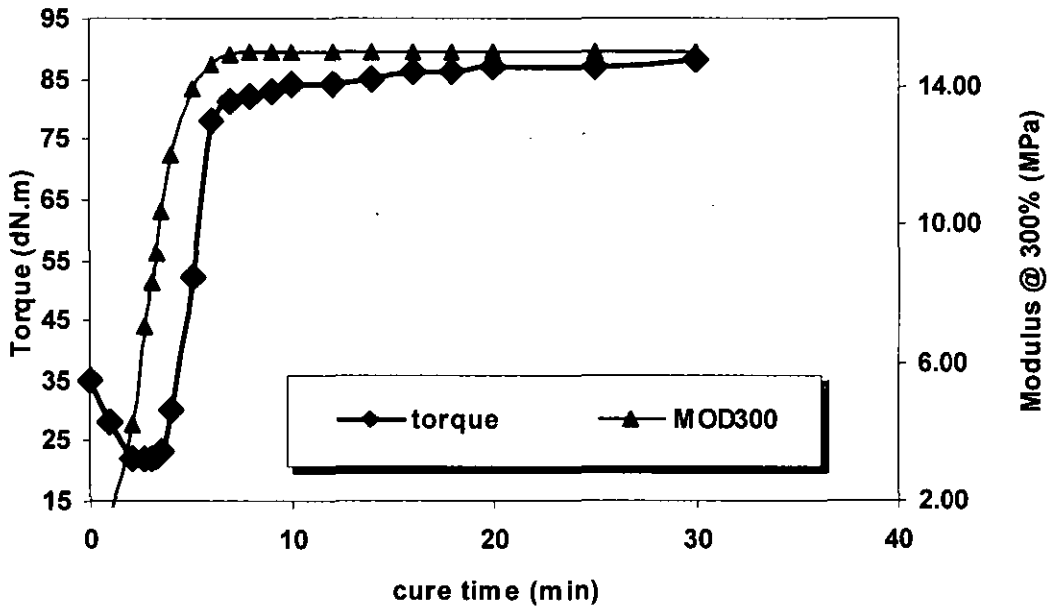

Figure 6-2: Evolution of curemeter torque and 300% modulus with cure time for rubber cured at 150°C

Figure 6.2 show that the evolution in curemeter torque with cure time followed a similar pattern to the 300% modulus. In this compound no reversion in the torque was observed, but rather a plateau which continued up to 30 minutes. When the rubber is placed in the rheometer, there is a heating up process and as the rubber is sheared,

there is a fall in the torque as a result of the heat transfer process. As the cure time increases, there is formation of crosslinks which makes the rubber increasingly stiff, resulting in an increase in the torque. Bartenev[3], have proposed that the formation of a three dimensional network occurs in a two stage process. In the first stage in natural rubber, the material is still plastic, but individual molecules are crosslinked into larger formations. Only after these molecular aggregates have reached a definite size does the subsequent crosslinking lead to formation of a continuous spatial network in the second stage.

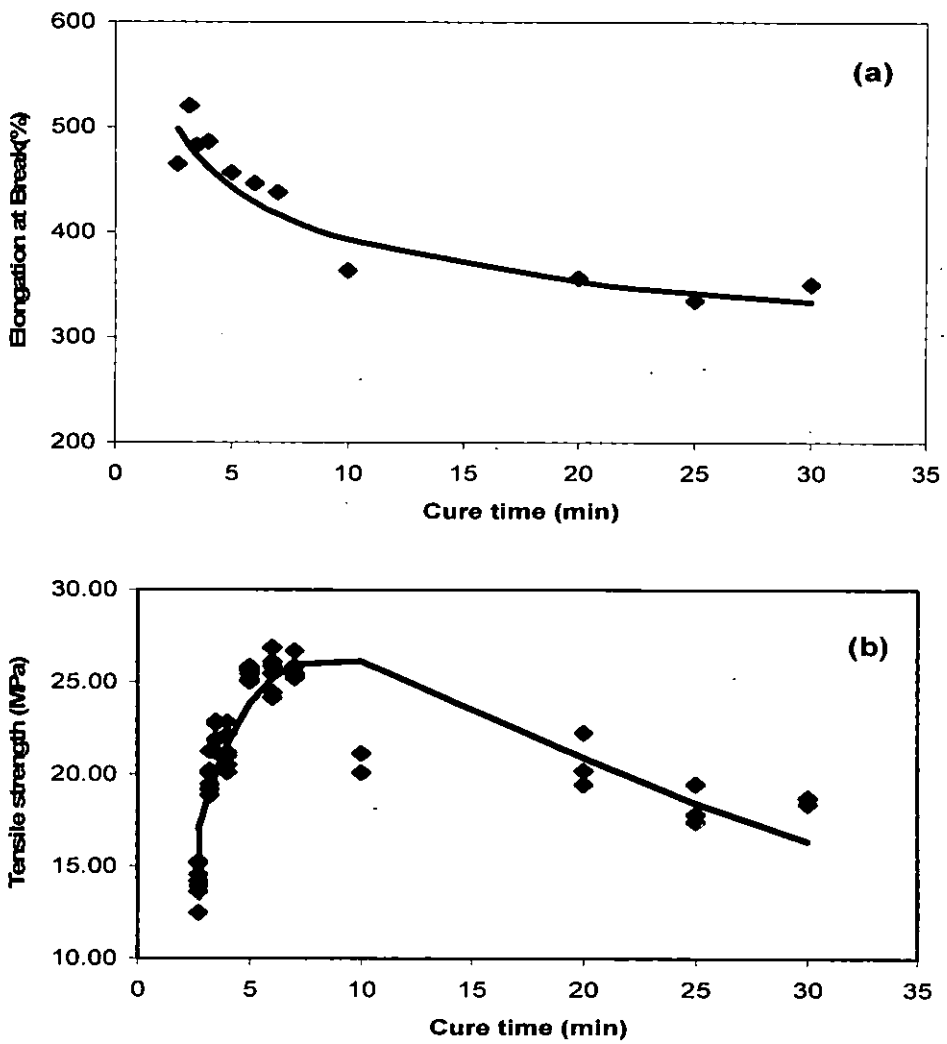

Figure 6-3: Relationship between cure time and (a) Elongation at break, (b) tensile strength NR Compound

Figure 6.3 shows how the elongation at break and tensile strength change with cure time. The expression $E_b = \frac{1}{a + bt^c}$ (where E_b is the elongation at break, and t is the cure time in minutes, with a, b, c being constants) was used to describe the relationship between the elongation at break and the cure time. (Fig. 6.3a). Also the relation between tensile strength, ξ and cure time, t was better described by the rational function $\xi = \frac{a + bx}{1 + cx + dx^2}$ (where a, b, c and d are constants with s = 1.96 and r = 0.914). These relationships were highly correlated.

Figure 6.3 shows that as the cure time increases, the elongation at break decreases and the tensile strength increases up to a maximum then drops with increasing cure time (Fig.6.3b). The initial increase in tensile strength and decrease in elongation at break occurs as the modulus increases steeply in the first five minutes of cure (Figure 6.2). All the changes are as a result of the formation of more crosslinks with curing time. The more highly crosslinked molecules are not easily stretched, resulting in increased stress and hence, stiffness and strength. However, the polysulphidic crosslinks that are formed early in curing are thermally unstable and are transformed into di - and mono – sulphidic bonds as curing progresses. This is sometimes called "maturation" of the crosslinks and is accompanied by an increase in modulus, because the shorter crosslinks are more rigid. As the curing time increases, a period is reached where almost all the crosslinks are di - and mono - sulphidic bonds and any further increase in curing time may only bring about chemical degradation of the rubber molecules and/or crosslinks resulting in the fall in the elongation at break and tensile strength of the rubber compound. It is worthwhile noting that the overall stiffness remains the same while the tensile strength decreases. This suggests that degradation of crosslinks or polymer chains that would be expected to reduce modulus, must be balanced by any increase in modulus, caused by the maturation of crosslinks.

6.4 Effect of Ageing on Tensile Strength and Elongation at Break.

The effect of ageing on tensile strength and elongation at break was used to assess and quantify the ageing process of the compound. Ageing of the compound, was carried out both in the absence and the presence of oxygen, at 70°C, 80°C, 90°C 100°C and 110°C. The results were used to assess mechanisms and kinetics of ageing.

6.4.1 Thermal Ageing:

In order to simulate what happens to a rubber engine mount compound when it is encapsulated and air is excluded, the rubber compound was anaerobically aged. The results of the anaerobically aged natural rubber vulcanizates are shown in Figures 6.4, 6.5 and 6.6 for tensile strength, elongation at break and modulus respectively.

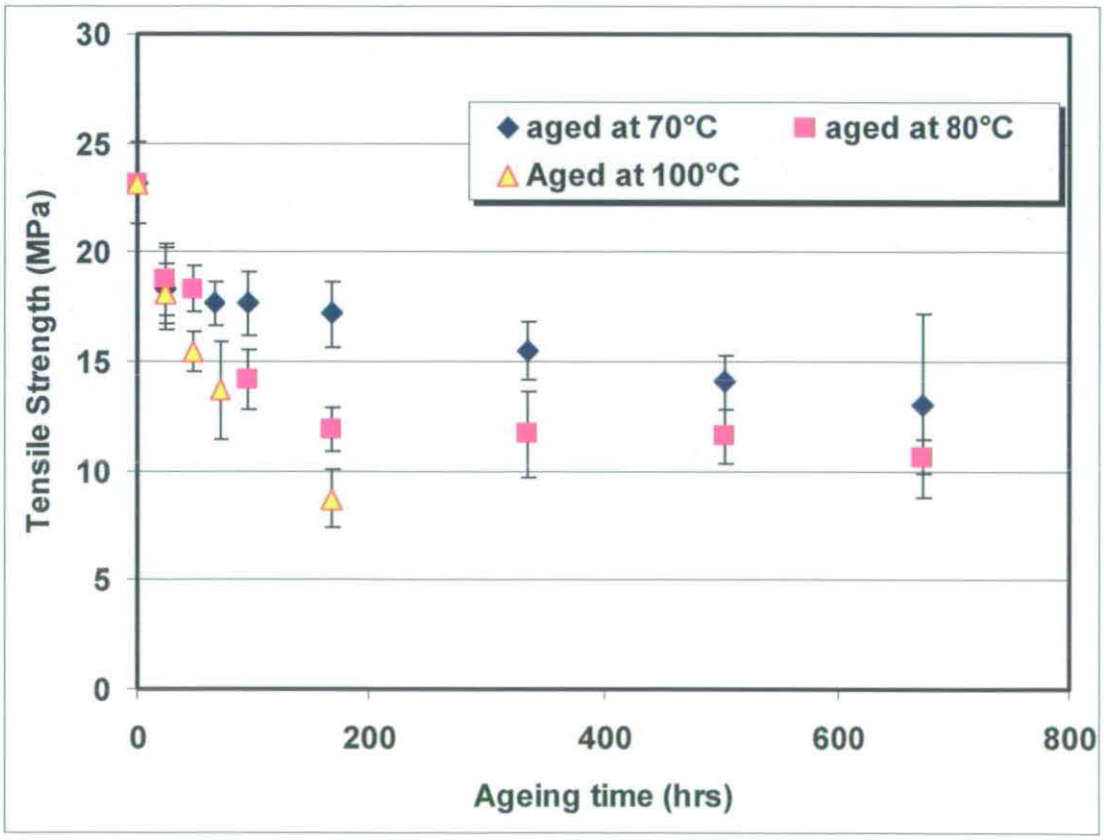

Figure 6-4: Effect of thermal ageing on the tensile strength of the compound (cured at 140°C)

The tensile strength and elongation at break reduce with increase in ageing time and the rate of reduction increases with increase in ageing temperature. Figure 6.6 shows the modulus data for the thermally aged rubber engine mount compound. The results show that the modulus generally increases with increase in ageing time, indicating that crosslinking reactions are occurring. However, ageing for long times at 100°C results in a decrease in modulus, indicating that scission reactions occur at high temperatures or at a late stage in aging.

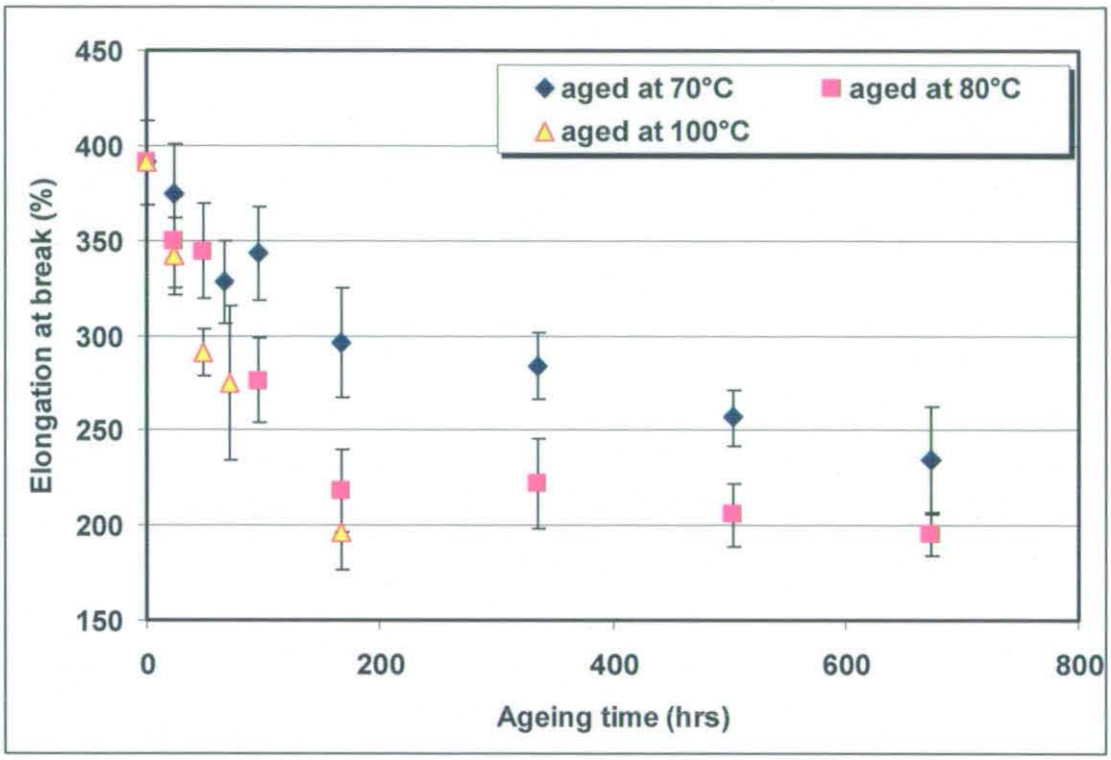

Figure 6-5: Effect of thermal ageing on the elongation at break of the natural rubber compound (cured at 140°C)

Thermal ageing in natural rubber is a stepwise process by which the polysulphidic crosslinks, convert to disulphidic crosslinks and then the disulphidic crosslinks transforms to monosulphic crosslinks resulting in increased stiffness. The fall in strength and elongation at break might be as a result of maturation of the crosslinks. Maturation as explained by Hamed and Zhao[5] causes a decrease in the number of polysulphidic crosslinks and an increase in the monosulphidic crosslinks, resulting in a reduction in the strength. This is so because the monosulphidic crosslinks, which are shorter and so more rigid, are less able to dissipate energy at a growing crack tip than

the polysulphidic crosslinks. More energy will hence be available for growth of the crack and hence, failure of the compound is more likely.

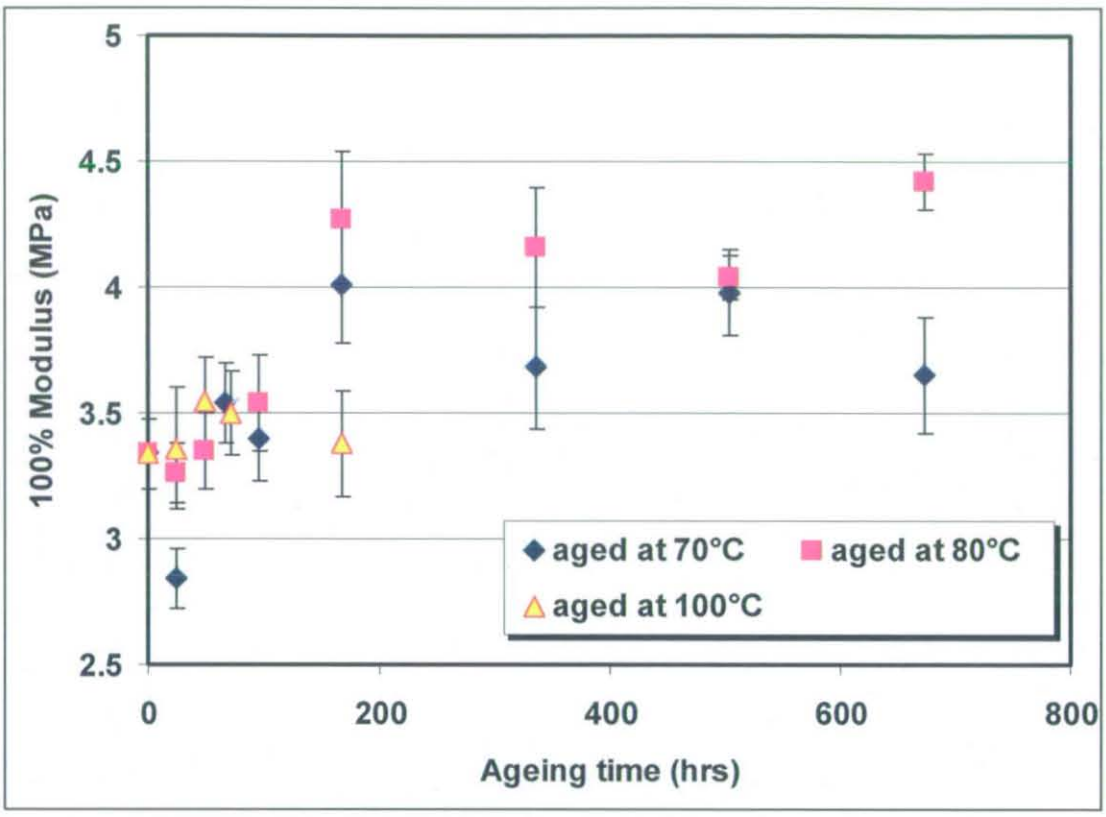

Figure 6-6: Effect of thermal ageing on the Modulus of the natural rubber compound (cured at 140°C)

6.4.2 Thermo-oxidative Ageing

To simulate what happens to an engine mount compound when exposed to air, the natural rubber engine mount compound was aerobically aged in an air circulating oven. The results for the tensile strength and elongation at break for rubber cured at 140°C and 150°C are presented in Figures 6.7 to 6.10. The tensile strength and elongation at break of the natural rubber compound generally decrease with ageing time, but the rate of decrease in these properties decreases with decrease in the ageing temperature.

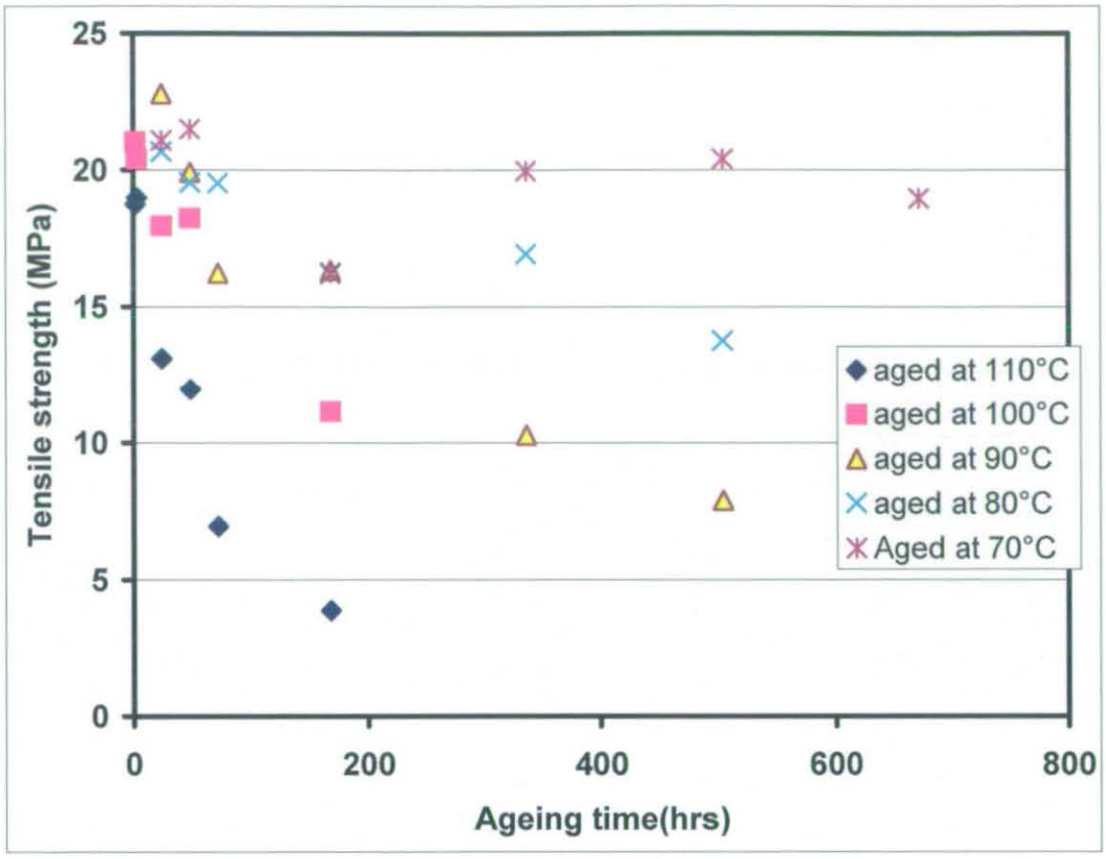

Figure 6-7: Effect of ageing on tensile strength for rubber cured at 140°C

Oxidatively induced crosslinks have been advanced as another reason for the reduction in tensile strength in aged natural rubber,[5] apart from the maturation of crosslinks as explained in section 6.4.1.

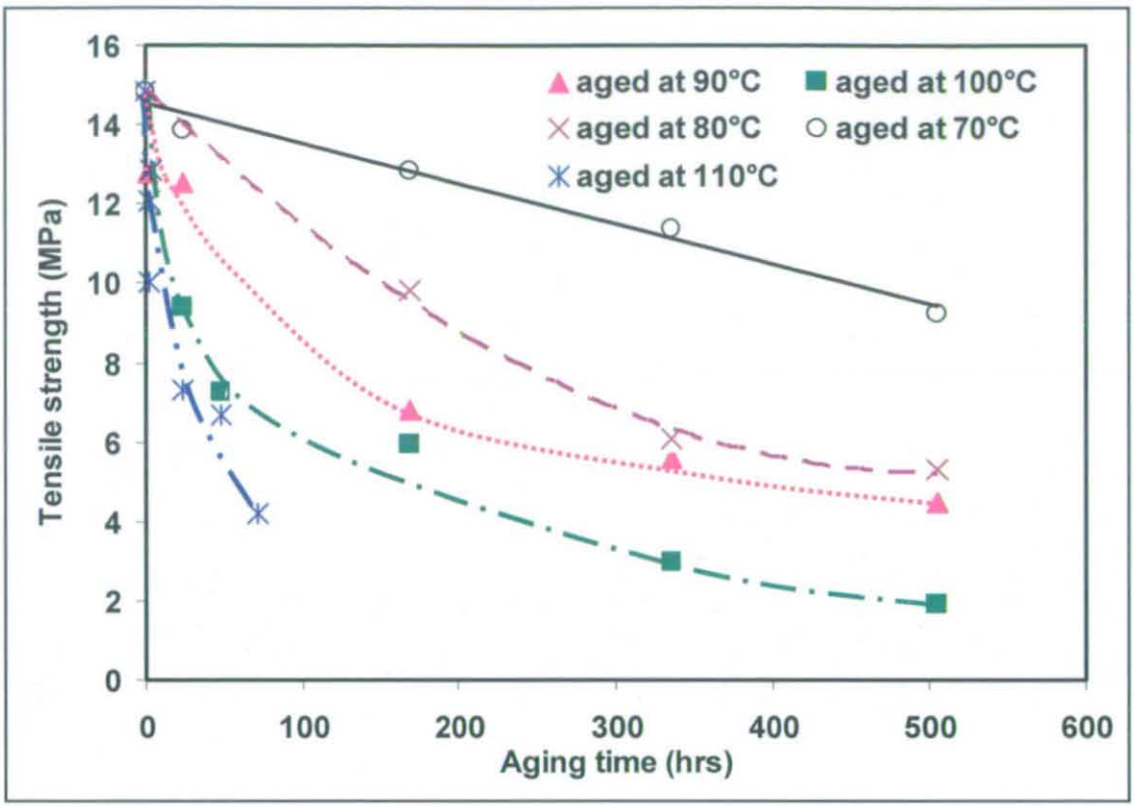

Figure 6-8: Effect of ageing on tensile strength for rubber cured at 150°C

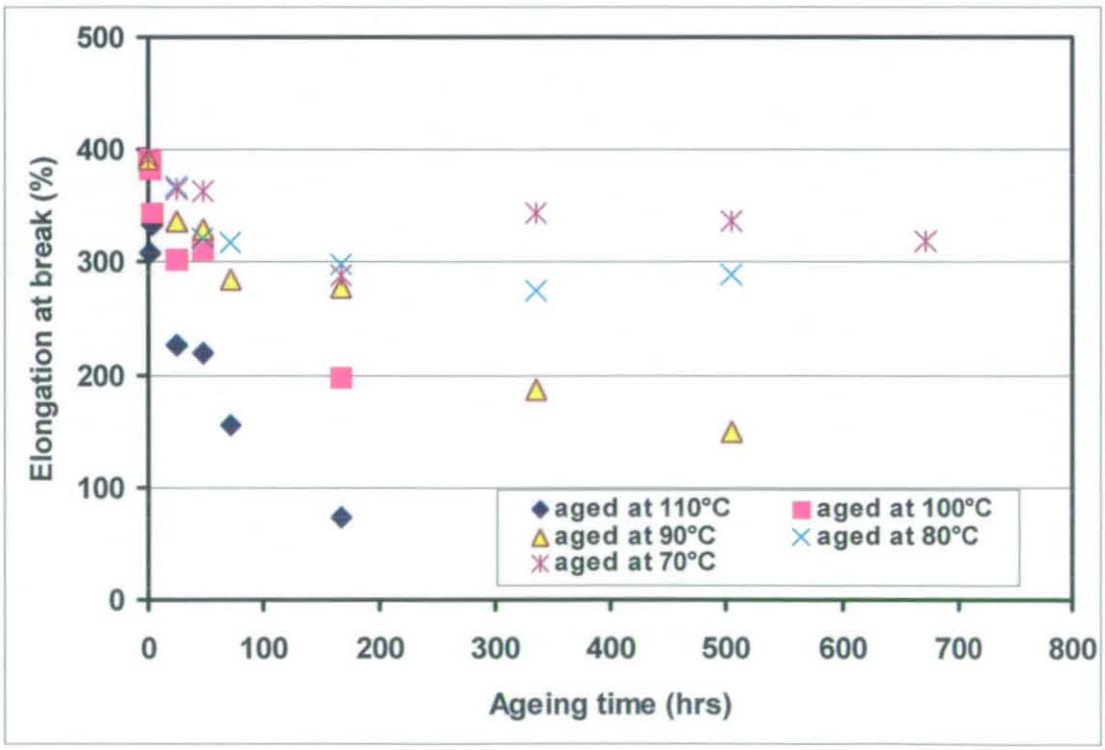

Figure 6-9: Effect of ageing on elongation at break for rubber cured at 140°C

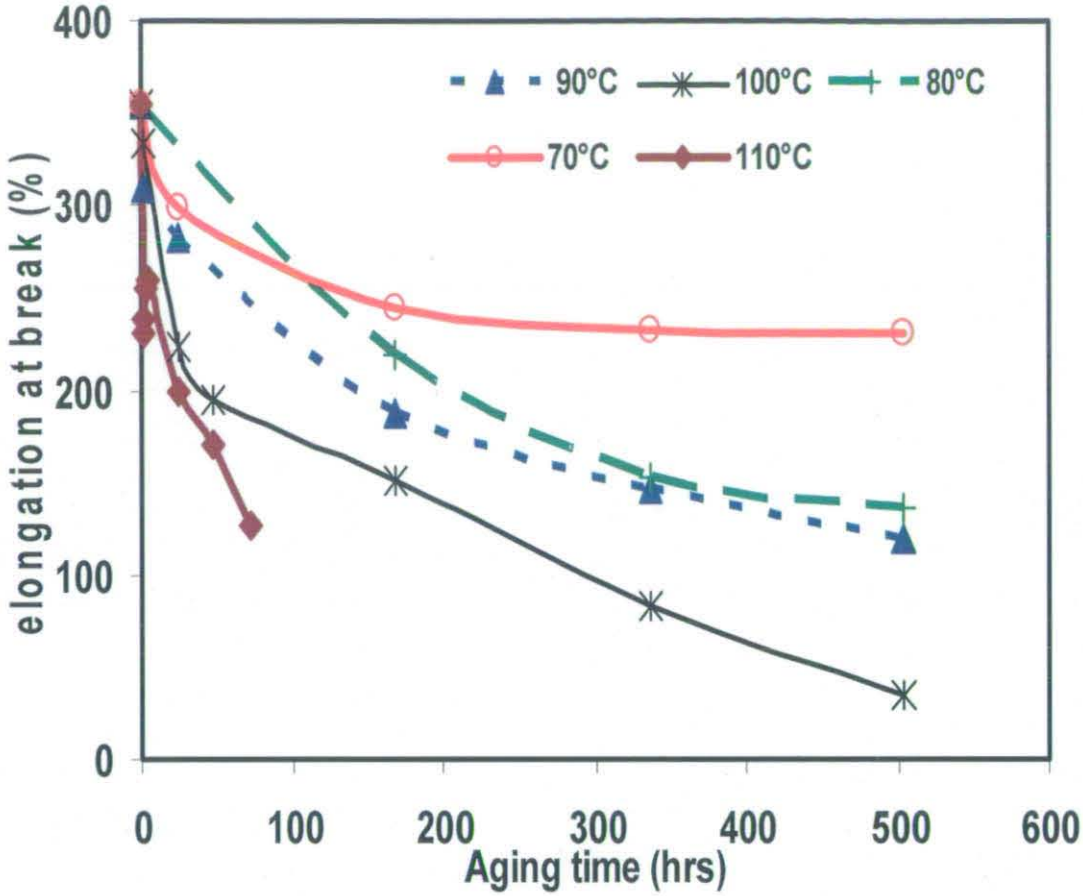

Figure 6-10: Effect of ageing on elongation at break for rubber cured at 150°C

Upon tensile testing of rubber samples which had been aged at 90°C for about 72 hours, cracks could be seen spreading across the surface in all directions

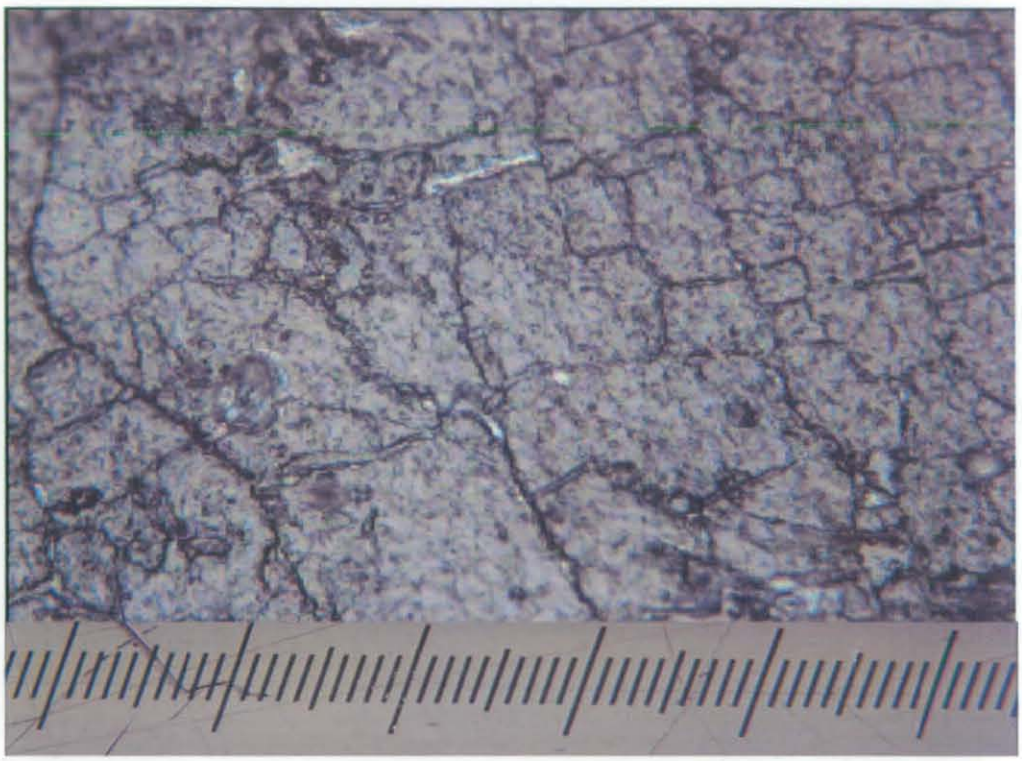

Figure 6-11: Light microscopic image showing crack surface of an aged rubber sample after tensile testing (Each minor division is 10μm)

(Figure 6.11). The presence of cracks indicates that surface hardening has taken place. The hard surface layer is probably due to greater oxidation at the surface because oxidation is occurring more rapidly than oxygen diffusion. Surface oxidation which results in a brittle surface layer causes cracks to form on the surface of the rubber as it is being stretched. These cracks act as stress concentrators thereby reducing both the tensile strength and elongation at break. As ageing time is increased, more and more antioxidants are being consumed resulting in an increase in oxygen diffusion into the rubber and an increase in thickness of the oxidised layer accompanied by a further decrease in tensile strength. According to Bell et. al.[6] as ageing increases, the thickness of the hard layer and hence, the size of the cracks increase. At a particular

level of ageing the cracks become greater than the critical value for crack propagation, and test pieces tear rather than fracture, resulting in low tensile strengths.

6.4.3 Activation energy calculations for thermo-oxidative ageing

Various kinetic models have been employed to study the degradation of polymers[7]. Using the Kissinger, Ozawa, Van Krevellen, Horowitz – Metzger, Coats – Redfern and MacCallum – Tanner methods, Regnier and Guibe[8] found that the activation energy for the multistage degradation of polyimide polymer was between 143 kJ/mole and 206 kJ/mole. It is worthwhile noting that all these methods apply high temperature weight loss thermal analysis techniques and not direct physical property measurements, as in our case. In the current study activation energies were calculated using the tensile measurements and applying various kinetic techniques, which include the rate law approach, the time temperature superposition approach and the critical life approach. Each of the techniques is discussed separately in the following sections.

6.4.3.1 Rate law approach

To demonstrate the use of the rate law approach, data for rubber cured at 150°C is presented. The effect of ageing on tensile strength and elongation at break was found to follow second order kinetics.

$$\frac{1}{\xi_t} = kt + \frac{1}{\xi_o} \qquad [6.2]$$

Where ξ_t is the property at time t of aging and ξ_o is the initial value before aging.

A plot of $\frac{1}{\xi_t}$ versus t using equation (6.2) gives straight lines (Figures 6.12 and 6.13), for rubber aged at 70°C, 80°C 90°C 100°C and 110°C. The significance of these plots are $0.878 \leq r^2 \leq 0.9767$, indicating a good correlation.

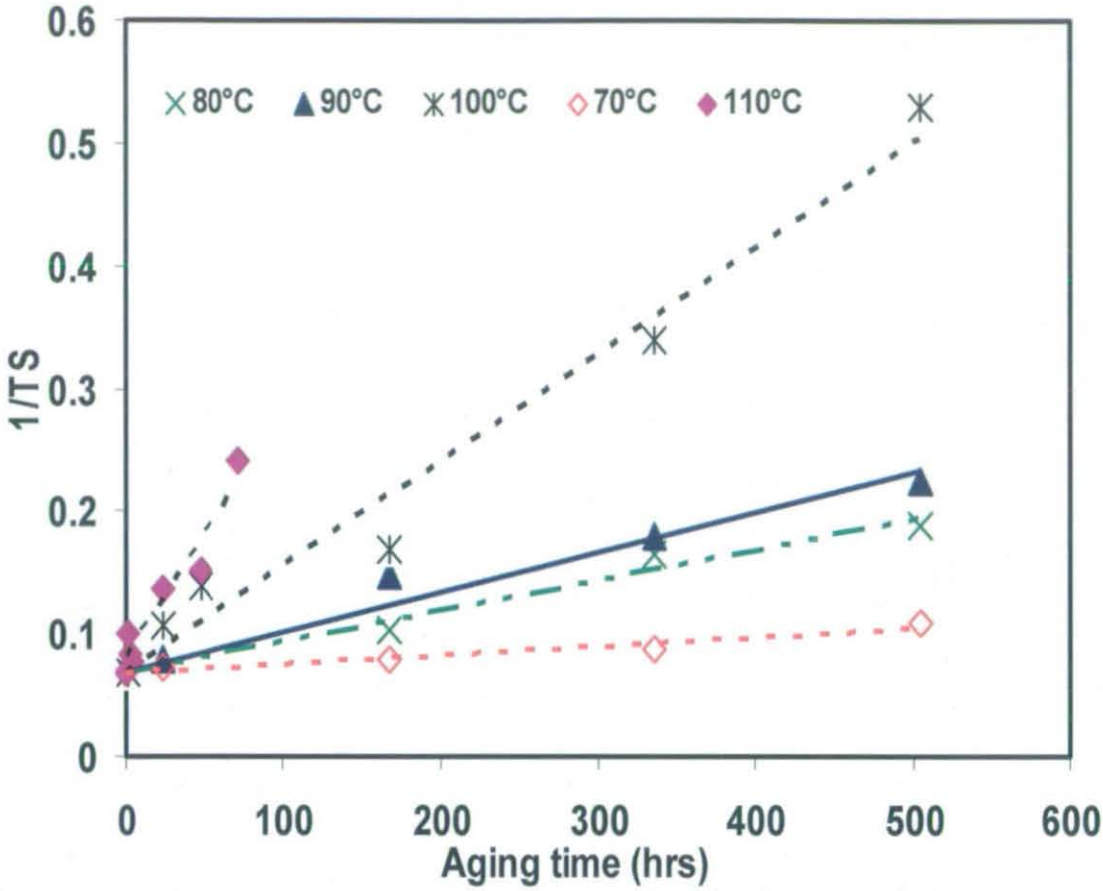

Figure 6-12: Second order plot for the effect of ageing on tensile strength of the compound cured at 150°C

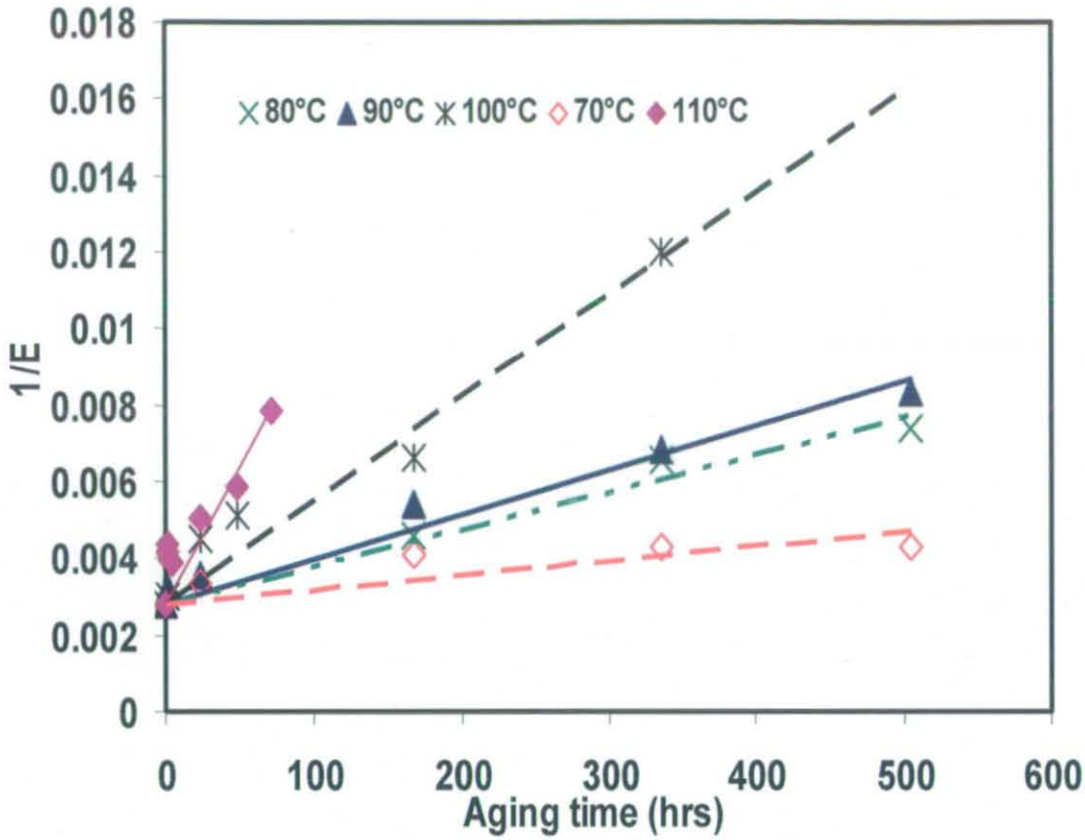

Figure 6-13: Second order plot for the effect of ageing on Elongation at break of the compound cured at 150°C

The rate constants, determined from the slopes of the lines, were then plotted on Arrhenius coordinates (Figures 6.14 and 6.15 for tensile strength and elongation at break respectively). The activation energy was calculated to be about 88 kJ/mol., for the tensile strength and 74 kJ/mol for the elongation at break.

Other investigators found that the activation energy for the oxidation of sulphur vulcanised natural rubber was 102 $kJmol^{-1}$ [9]. For accelerated ageing of tires, Baldwin and co-workers[10] inflated some tyres with air and a 50/50 blend of N_2/O_2, and oven aged at temperatures of between 40°C and 100°C, for periods of 2 weeks to 12 weeks. The tyres were then dissected at the end of the steel belts and tested for tensile strength and elongation at break. The wedge rubber that was obtained between the steel belts, had an ageing activation energy of 107 $kJmol^{-1}$. Using swelling and peel strength measurements and applying the same technique from their previous study[10],

Baldwin et.al.[11] found an activation energy for ageing of skim rubber in the tested tyres was 101 $kJmol^{-1}$ for the swelling ratio and 109 $kJmol^{-1}$ for the peel strength. Straus and Madorsky[12] studied the effect of various additives on the pyrolysis in vacuum of cured and uncured natural rubber. They found that pyrolysis was completed at 390°C and carried out all subsequent experiments at this pyrolysis temperature. They found the activation energy value for the thermal degradation of vulcanised natural rubber was between 234.42 $kJmol^{-1}$ and 272.09 $kJmol^{-1}$ for different formulations. Meanwhile Mott and Roland[13] found the activation energy for the aging of natural rubber in air and seawater at temperatures ranges of 60°C to 120°C in both cases, to be around 94 $kJmol^{-1}$ and 66 $kJmol^{-1}$ respectively. The results obtained for ageing at low temperatures by these authors are close to what we obtained in our study (temperature range 70°C – 110°C), for the effect of ageing on tensile strength and elongation at break.

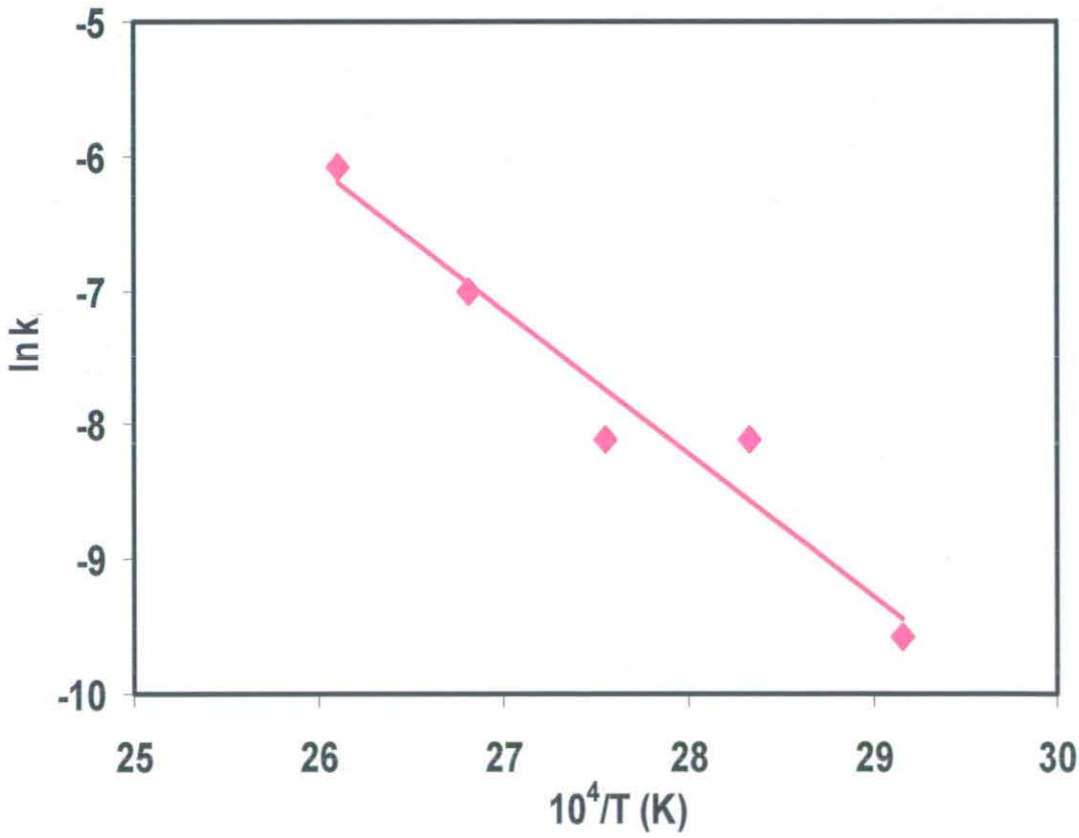

Figure 6-14: Temperature dependency of rate law on the tensile strength of natural rubber compound

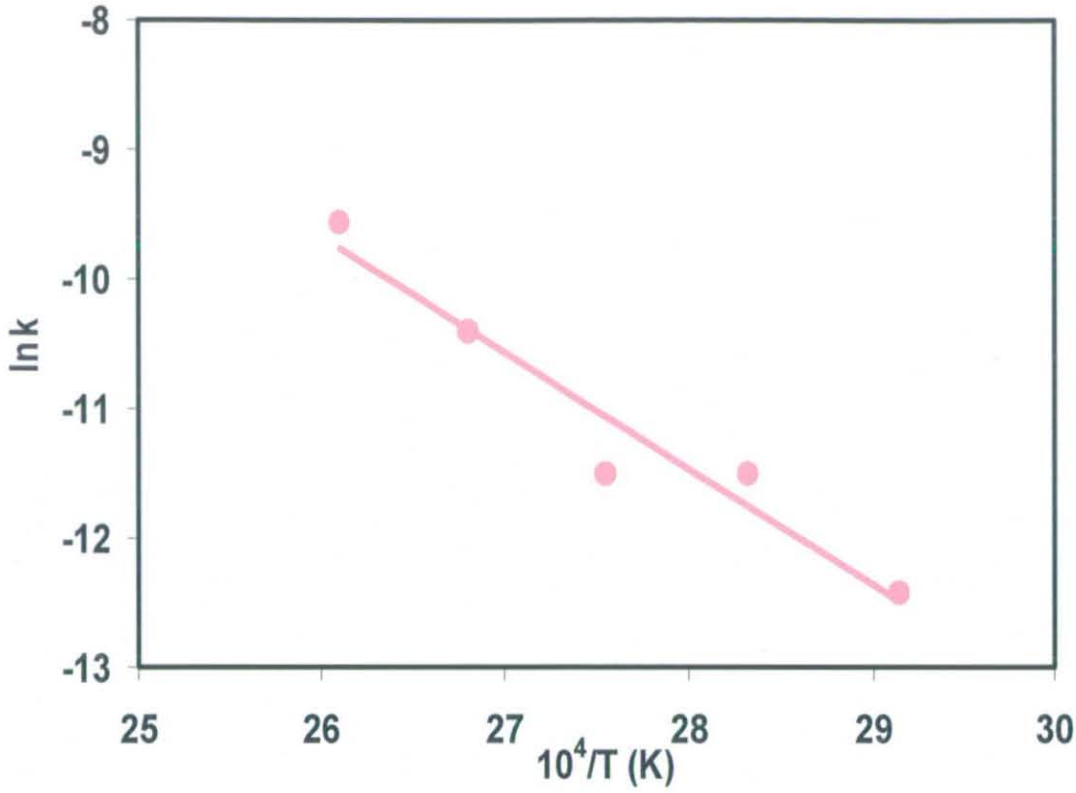

Figure 6-15: Temperature dependency on rate law on elongation at break of a natural rubber compound

6.4.3.2 Time temperature Superposition Approach

One of the shortcomings of the simple rate law method is that measurements from individual ageing temperatures are used to calculate the rate constants k which are then plotted on Arrhenius coordinates and the slopes of these lines are used to calculate the activation energy.[14] The amount of data manipulation may lead to inaccuracies in the results.

In the time – temperature superposition (TTS) method all the individual data at all the ageing temperatures (70°C – 110°C) are used to construct a master curve. The TTS method may therefore give more reliable results because this way of "averaging" results may be less prone to error since there are fewer stages in the manipulation of the data.

Gillen et. al.[15, 16] developed a TTS method which could conveniently be used to predict the service life of a material, which is subjected to ageing. In this method, the lowest ageing temperature is used as the reference temperature. Then for each set of data at a higher temperature T, the experimental times at this temperature are multiplied by a constant shift factor, a_T. The shift factor is empirically determined, such that the data at this temperature best superposes the reference temperature data. The Arrhenius type model is then used to explain the relationship between the empirically determined shift factors and the temperature.

$$a_T = \exp\frac{E_a}{R}\left(\frac{1}{T_{ref}} - \frac{1}{T}\right) \qquad [6.3]$$

If the Arrhenius expression is valid then, a plot of $\log a_T$ against 1/T (in Kelvin) should be linear.

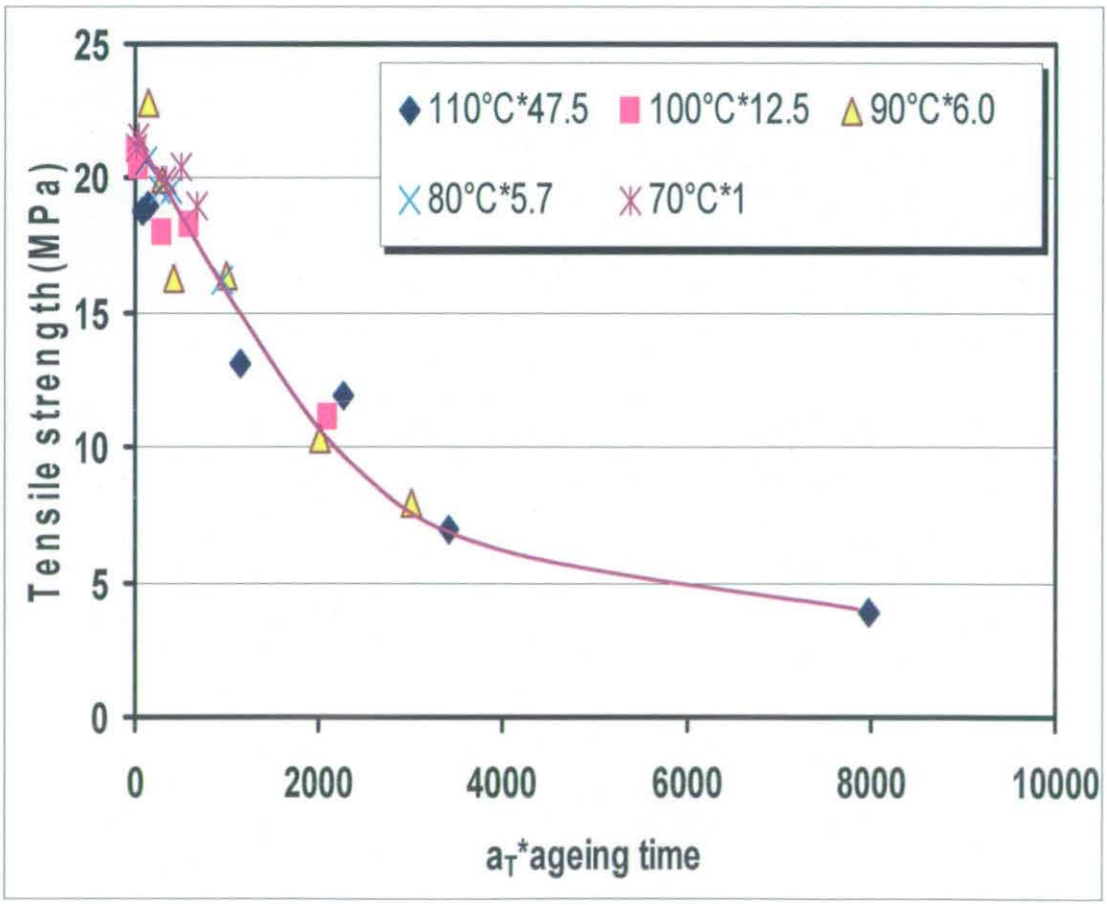

Figure 6-16: Time – temperature superposition plot for tensile strength for ageing of natural rubber at 70°C reference temperature for rubber cured at 140°C.

Data from the rubber cured at 140°C was used to validate the time temperature superposition approach. Figures 6.16 and 6.17 are shifted plots for tensile strength and elongation at break. The curve on the plot is the master curve for the shifted data. The equation for the master curve is:-

$$\zeta = \beta e^{-\varphi t} \qquad [6.4]$$

Where ζ , is the property, β and φ are constants and t is the shift time multiplied by the ageing time. The values of the constants are shown in Table 6.4

Table 6.4: Constants from equation 6.4 describing the master curves for tensile strength and elongation at break

Property	Constants		r^2
	β	φ	
Tensile strength (MPa)	22.38	- 0.0003	0.9195
Elongation at break (%)	344.31	- 0.0002	0.9439

Correlation coefficients (r^2), of 0.9195 and 0.9439 were obtained for tensile strength and elongation at break master curves respectively.

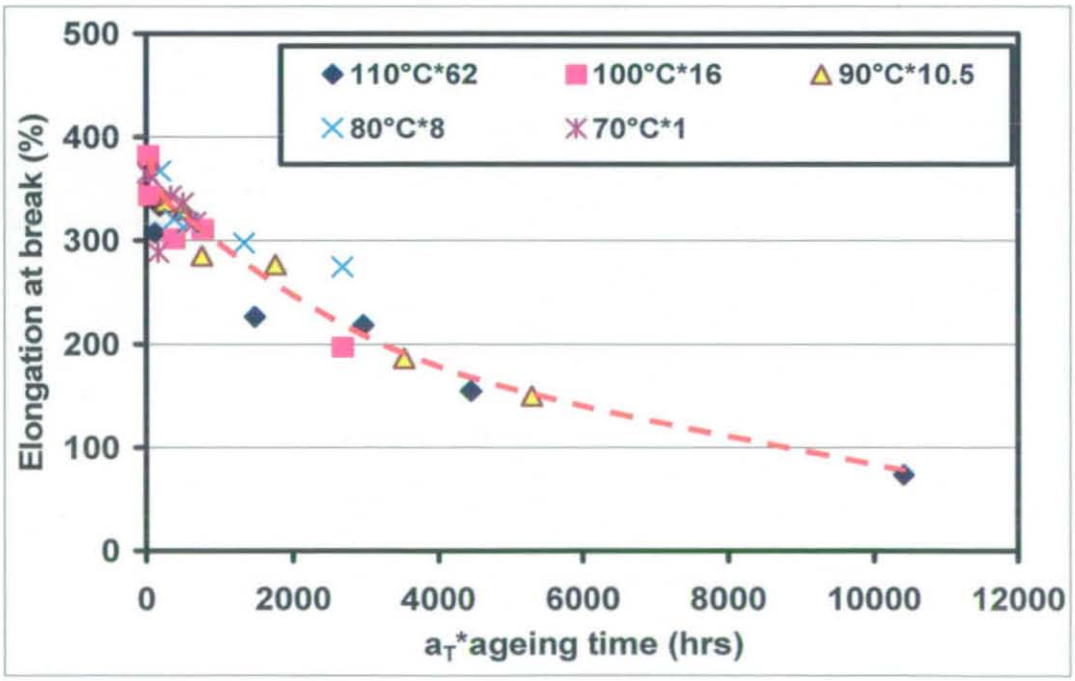

Figure 6-17: Time – temperature superposition plot for elongation at break for ageing of natural rubber compound cured at 140°C (70°C reference temperature)

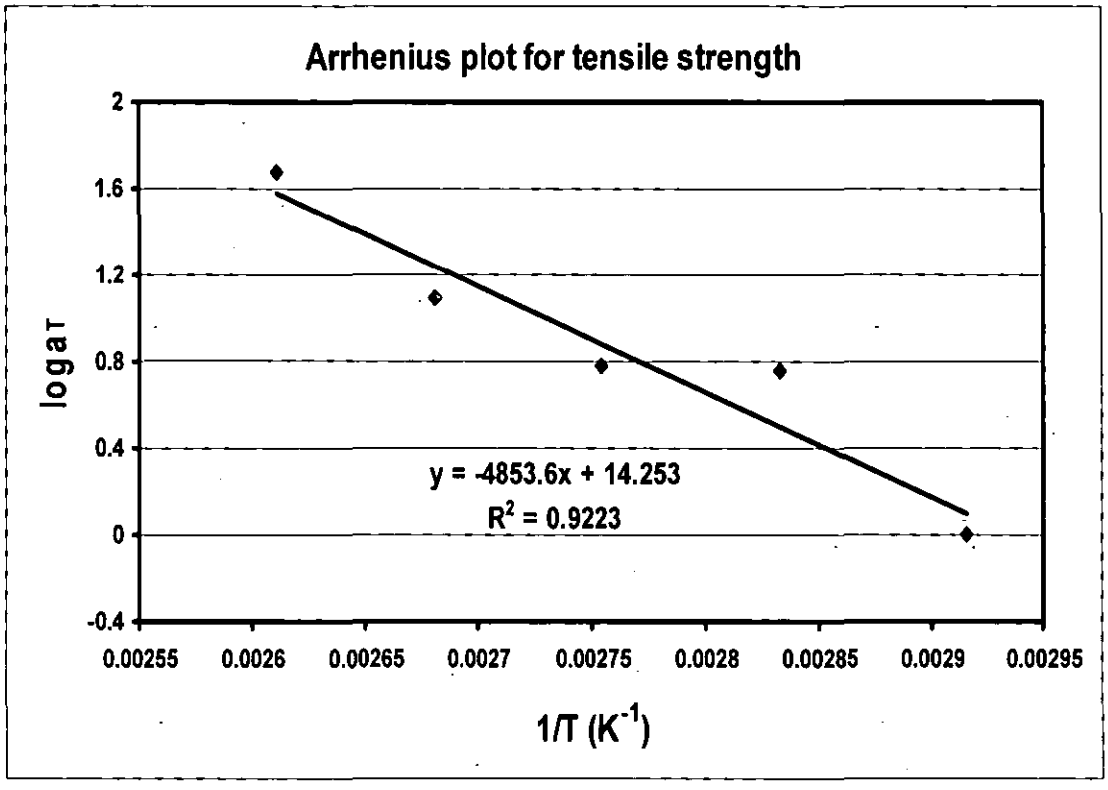

Figure 6-18: Arrhenius plot for log of shift factor for tensile strength

A plot of the logarithm of the shift factors against the inverse absolute temperature was constructed for both tensile strength and elongation at break, in order to determine the activation energy. Correlation coefficients of 0.9223 were obtained for tensile strength (Figure 6.18) and 0.9065 for elongation at break (Figure 6.19). From these plots the activation energy was calculated to be ~ 93 kJ/mol for tensile strength and ~ 98 kJ/mol for elongation at break. As explained by Gillen et. al.[16] the activation energy for oxidation processes is normally in the range of 80 – 120 kJ/mol.

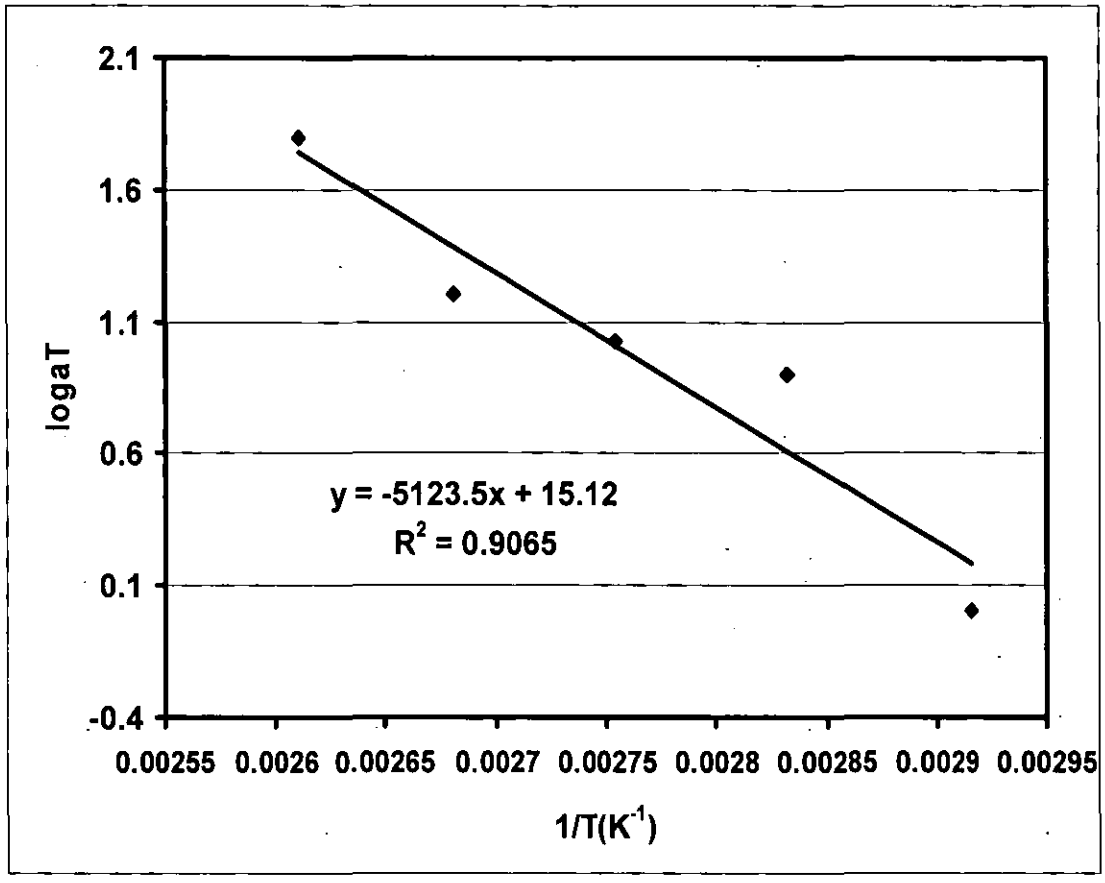

Figure 6-19: Arrhenius plot for log of shift factor for elongation at break

6.4.3.3 Critical Life Approach

The very simplest, but least precise approach to kinetic analysis of aging is the "critical life" approach. In this method, the critical life or time to "failure" is measured over a range of temperatures. The failure criterion could be the reduction of a particular property to a particular level. The critical life approach was applied to data for the thermal ageing of the compound (ageing in absence of oxygen). A failure criterion of a 50% reduction in tensile strength was used. A plot of the log of the critical time and the inverse of the absolute temperature gave a straight line graph with a positive slope. Figure 6.20 shows the critical life plot in terms of the tensile strength with respect to ageing temperature. The activation energy was determined to be approximately 79 kJ/mol (Figure 6.20)

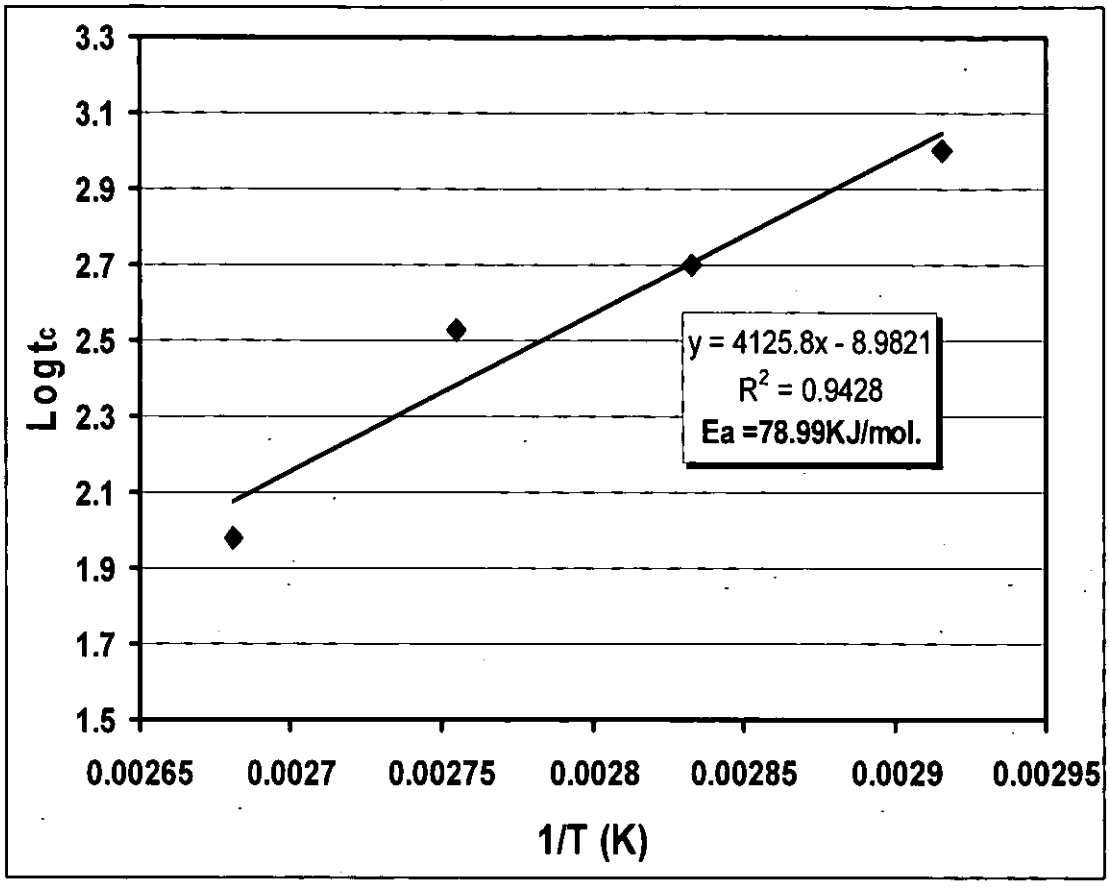

Figure 6-20: Arrhenius plot for critical life of thermally aged rubber compound

6.5 Effect of Ageing on Tensile Modulus

Figures 6.21 and 6.22 shows the effect of ageing temperature on the stress at 100% elongation (100% modulus) for the compound cured at 140°C and 150°C respectively. The modulus generally increases with increase in ageing time, the rate of increase generally increasing with ageing temperature. This was the same trend observed by Ahagon et. al[17] and Baldwin et. al.[10, 11] in their studies of accelerated ageing of tyre compounds.

For rubber cured at 140°C however, the change in modulus with ageing time is quite complex, for many temperatures a peak in modulus is observed at relatively short ageing times, less than 100 hours. This peak is generally higher and occurs at shorter times at the higher ageing temperatures. Hamed and Zhao[5],explained that in the early stages of ageing, additional network chains could result from crosslinking by either

residual curatives, rearrangement of crosslinked sulphur and/ or oxidative coupling. A reduction in the rank of sulphur and some additional crosslinking as a result of maturation of the sulphur crosslinks would result in an increase in modulus. With increasing ageing time, the modulus drops and then starts increasing again. The drop in modulus maybe due to scission of bonds taking place. The increase in the modulus after this slight decrease observed can be attributed to chain cleavage resulting in the formation of free radicals which then bond to form new crosslinks, hence leading to an overall increase in crosslink density. Overall, the reason for the general increase in modulus can be attributed to the crosslinking reactions outweighing the scission reactions during the thermo – oxidative ageing process.

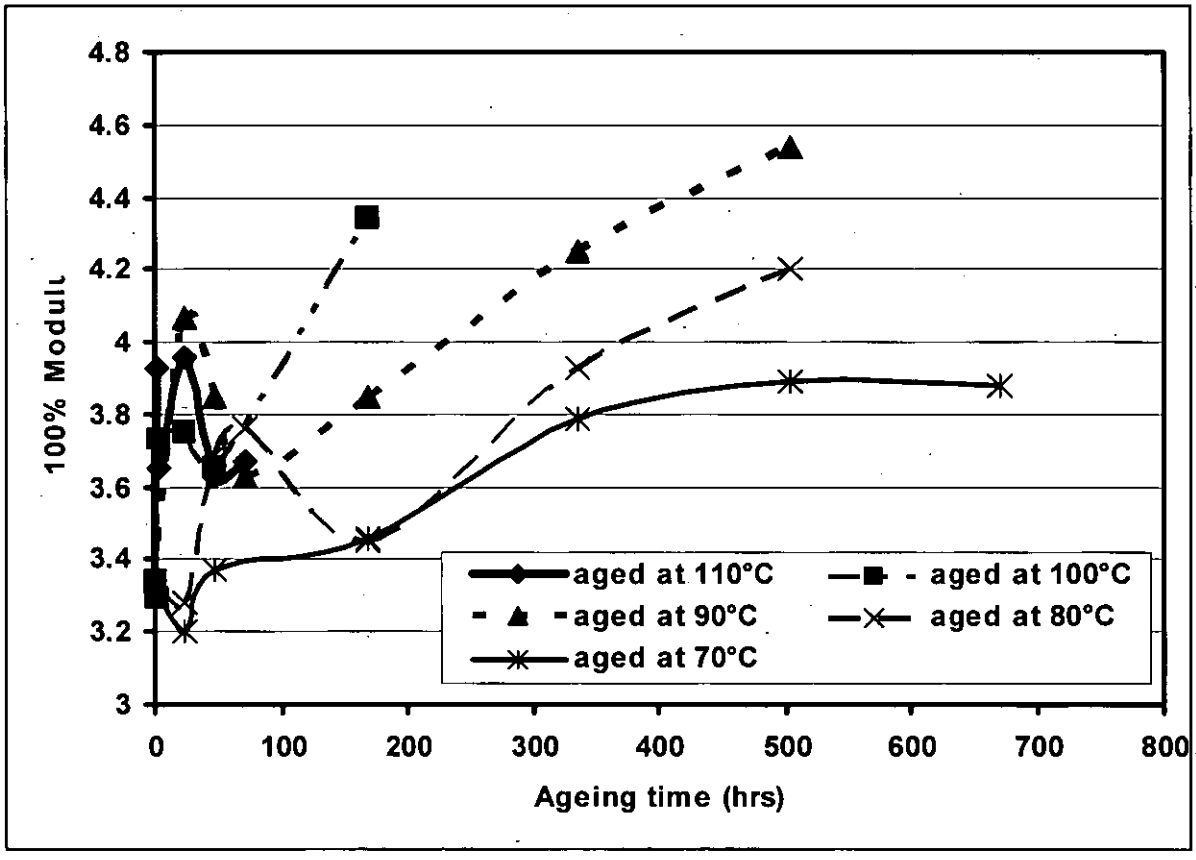

Figure 6-21: Effect of ageing on stress at 100% strain (100% modulus) for rubber cured at 140°C

For rubber cured at 150°C, the rate of modulus increase for rubber aged at 110°C to 90°C decreases with increasing temperature, as would be expected. The initial increase and decrease in the modulus that was observed for rubber cured at 140°C was not present for rubber cured at 150°C. This is probably because the maturation stage

of the sulphur crosslinks and any other processes that accounted for this peak had occurred during the curing process at this higher temperature. However, at ageing temperatures between 90°C and 70°C the rate of modulus increase increases with decrease in temperature. Particularly striking is the fact that ageing at 100°C and 70°C has a similar effect on modulus, at least up to 200 hrs. The apparently anomalous behaviour is likely to be due to the balance between cross-linking and scission reactions which changes with temperature.

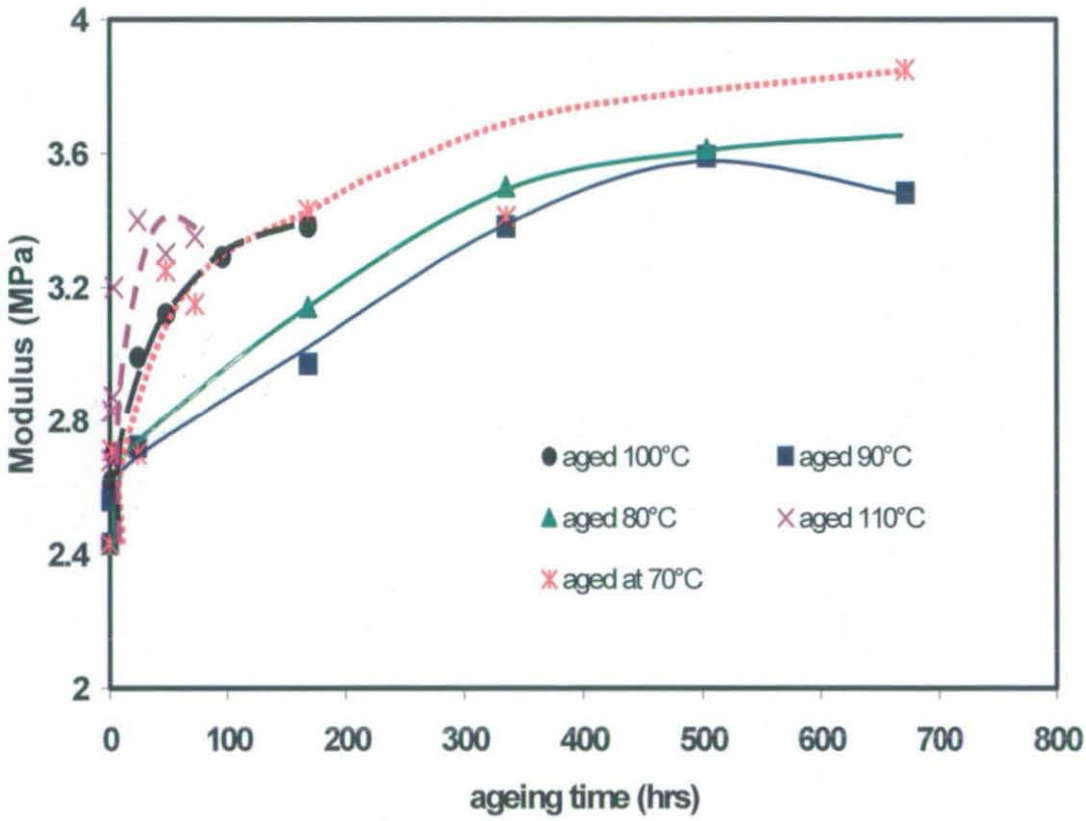

Figure 6-22: Effect of ageing temperature on the modulus at 100% strain for compound cured at 150°C

6.5.1 Compound Cured at 150°C - Kinetics of Ageing in Terms of its Effect on Modulus

The fractional life equation[19] was used (since simple rate laws show very large divergence) to describe the kinetics of ageing in terms of its effect on the 100%

modulus (M_{100}) of the natural rubber vulcanisate aged at 70°C, 80°C, 90°C, 100°C and 110°C. For $F = 80\%$.

$$t_F = \frac{(0.8)^{1-n} - 1}{k(n-1)}\left(M_{ref} - M_t\right)^{1-n} \qquad [6.5]$$

Where t_F is the time period over which the modulus at any point in the curve reduces to 80% of its value. In this method, a plot of the reduced modulus ($M_{ref} - M_t$) versus ageing time, t (Figure 6.23) is made and a smooth curve representing the data is drawn in order to determine t_{80} values.

n is the order of the reaction

k the rate constant

$M_{ref} - M_t$ is the reduced modulus, with M_{ref} being the reference modulus, the maximum or plateau modulus value that the compound tends towards with increased ageing.

Taking logarithms on both sides of equation 6.5, we have

$$\log t_F = \log\left(\frac{0.8^{1-n} - 1}{k(n-1)}\right) + (1-n)\log(M_{ref} - M_t) \qquad [6.6]$$

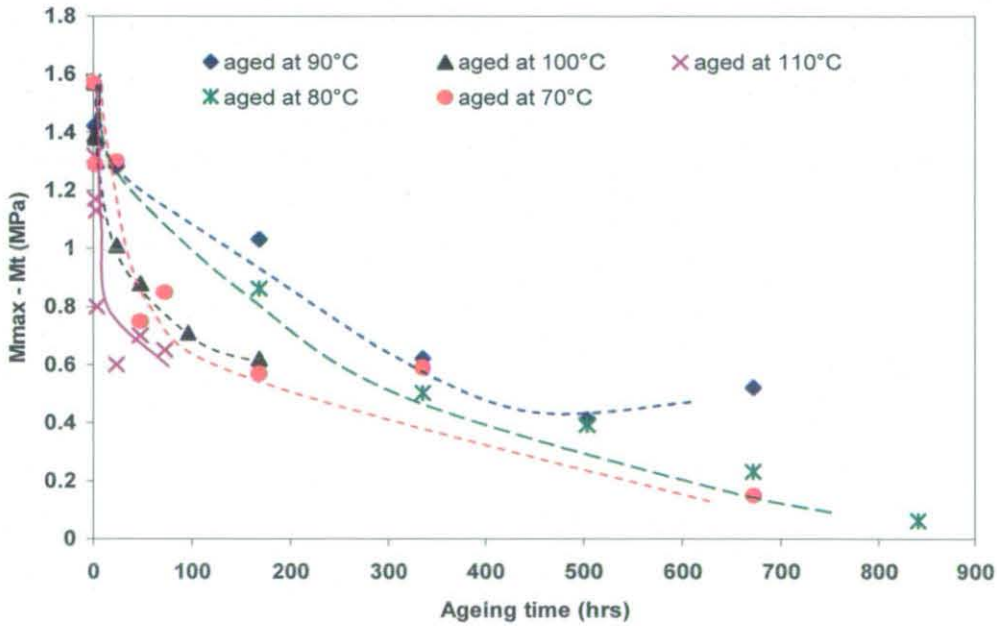

Figure 6-23: Relationship between ageing time and reduced modulus at the different ageing temperatures (cured at 150°C)

From equation 6.6, it can be seen that a plot of $\log t_F$ against $\log (M_{ref} - M_t)$ should give straight lines. Using this plot, the order of the reaction can be obtained from the slope and the rate constant from the intercept. Figure 6.24 shows the fractional rate law plots for the various ageing temperatures. The results were highly correlated with $0.9214 \leq r^2 \leq 0.9913$, supporting the validity of using this approach to describe the kinetics of ageing. It is notable that the slope and therefore, the order of the ageing reaction varies with ageing temperature. The orders of reaction and reaction rate constants were obtained from the plots and are shown in Table 6.5. There is a general increase in the order of reaction with increase in ageing temperature and this is perhaps a reflection of the increased complexity of the reactions affecting modulus at higher temperatures.

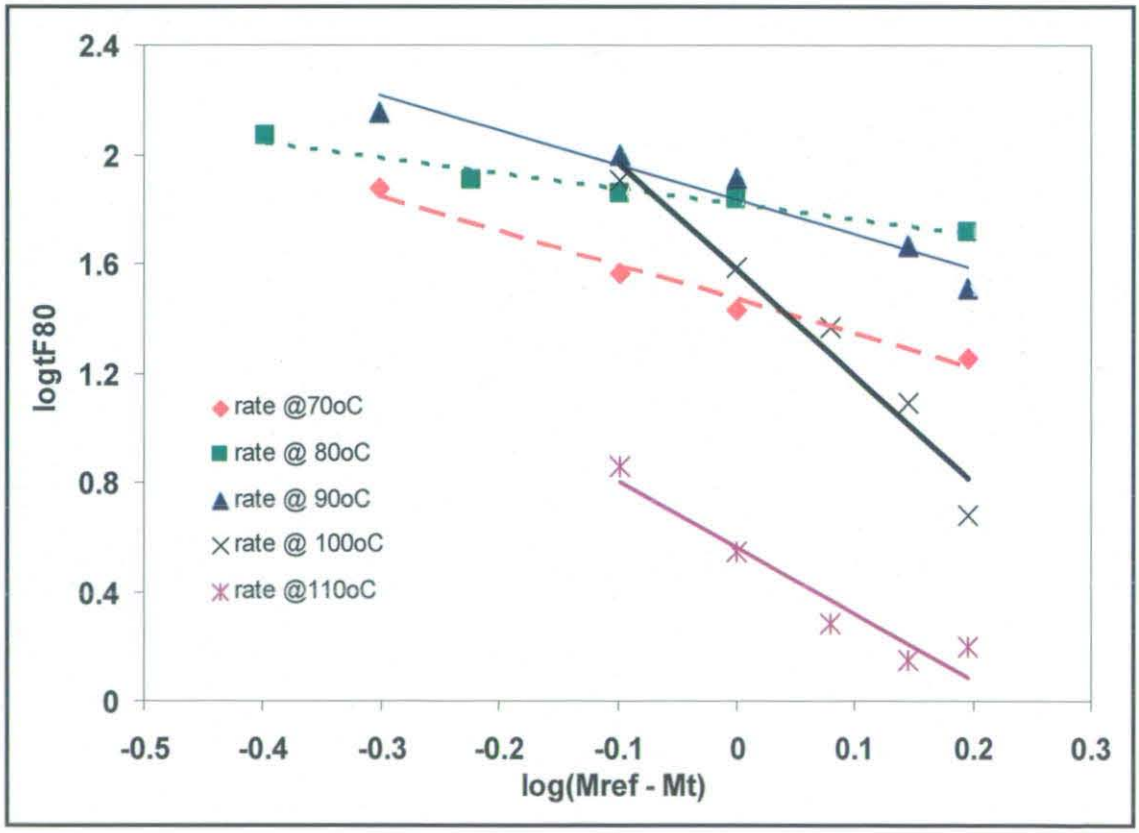

Figure 6-24: Fractional rate law plot for ageing reactions as they affect modulus for rubber cured at 150°C

Applying the Arrhenius relationship below, to obtain activation energies of reactions.

$$k = Ae^{(-Ea/RT)} \qquad [6.7]$$

Where A is the pre-exponential constant,

E_a, the activation energy

R, the gas constant

T, is the absolute temperature

k, is the rate constant at temperature T

From which one obtains

$$\ln k = \ln A - \frac{Ea}{RT} \qquad [6.8]$$

and plotting lnk against 1/T, the slope of the resulting straight line can be used to give the activation energy.

Table 6.5: Order and rate constants for ageing of NR, in terms of effect on modulus for rubber cured at 150°C

Ageing temperature.(°C)	n	K (x 10^{-3})	r^2	Ea (kJ/mol.)
70	2.26	8.1	0.9806	
80	1.55	3.56	0.9601	
90	2.26	4.5	0.9316	
100	4.91	12.8	0.9571	151.92
110	3.43	62.7	0.9214	

Figure 6.25 shows an Arrhenius plot for the ageing reaction in terms of modulus. The points clearly do not lie on a straight line but lie on a curve which passes through a minimum. Using only the higher ageing temperature results (90°C – 110°C) an activation energy of 151 kJ/mol can be obtained. However, if these high temperature data were extrapolated to lower temperatures, to predict the changes in modulus during the service life of the rubber material then completely incorrect values would be obtained.

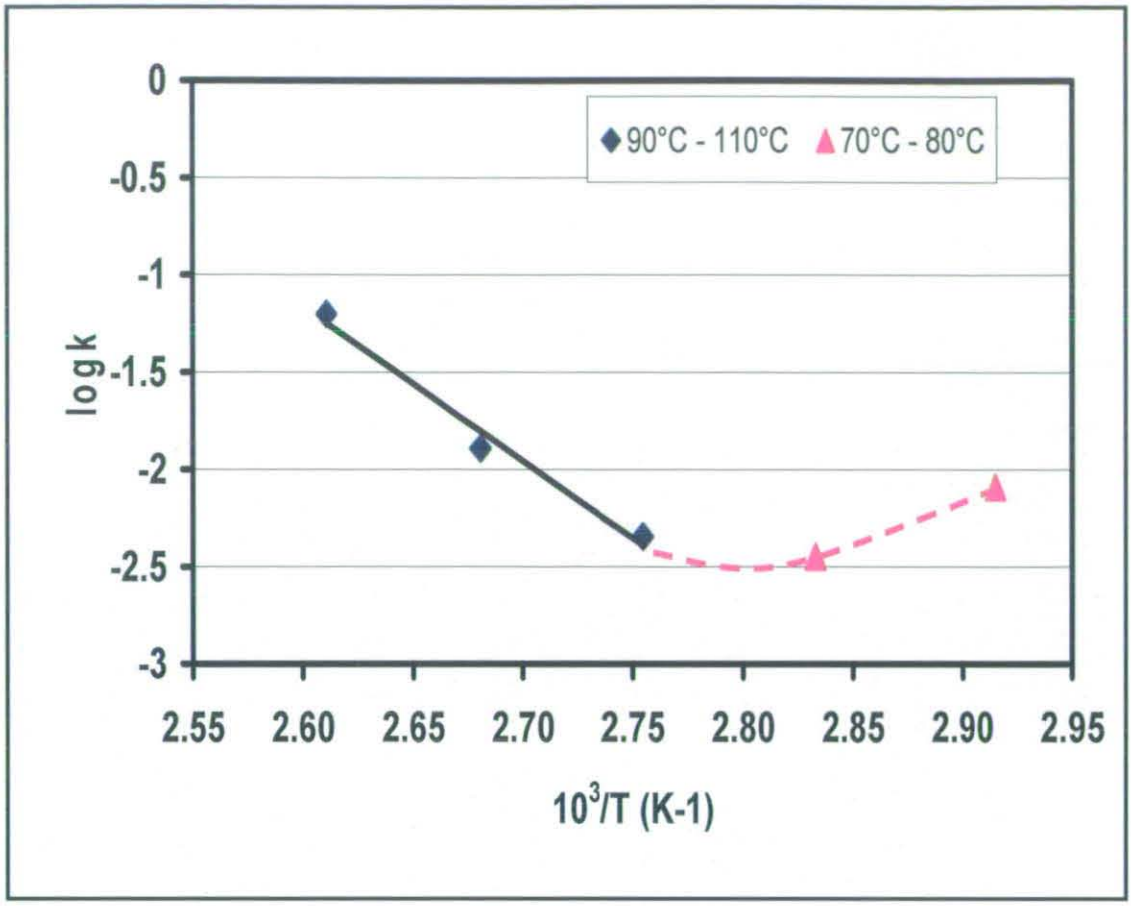

Figure 6-25: Arrhenius plot for ageing in terms of its effect on modulus

The results illustrate the dangers of using accelerated ageing data to build predictive models. The curved shape of the Arrhenius plot indicates that there are two processes which affect modulus in opposite ways and that each process has a different activation energy. It is known that ageing causes both cross-linking reactions, which result in an increase in modulus and scission reactions, which result in a decrease in modulus. Both of these reactions will increase in rate with increase in temperature. However, the results indicate that the scission reactions have a higher activation energy than the crosslinking reactions. Hence, with decrease in temperature the rate of scission reactions decrease more rapidly than the rate of crosslinking, giving the appearance, over a particular temperature range, (70 – 80°C) that rate of crosslinking actually increases as temperature decreases. Extrapolating this effect to lower temperatures, would suggest that the lower the temperature the more rapid the increase in modulus would become. Clearly, this will not happen and so, at lower ageing temperatures it is expected that a negative slope for the Arrhenius plot would be re-established. It is likely that the slope in the low temperature region will be lower than in the high

temperature region, corresponding to the lower activation energy required for crosslinking reactions.

6.5.2 Compound cured at 140°C - Kinetics of ageing in terms of its effect on modulus

In order to explain the kinetics of ageing in terms of the modulus for rubber cured at 140°C, the data was reduced with respect to a reference modulus. A reference modulus of 5 was chosen as the asymptotic value approached at long ageing times especially at low temperatures. Figures 6.26 and 6.27 shows the reduced modulus data and the TTS plot for the reduced modulus data for the aged natural rubber compound respectively.

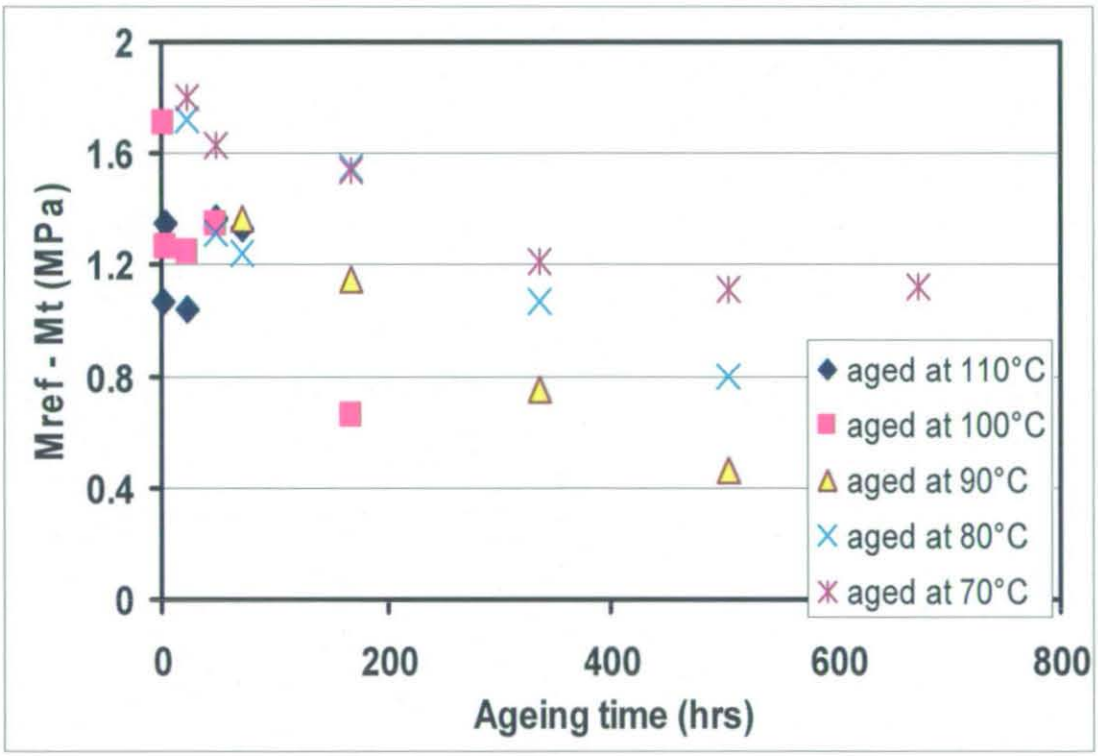

Figure 6-26: Effect of ageing on reduced Modulus at 100% strain

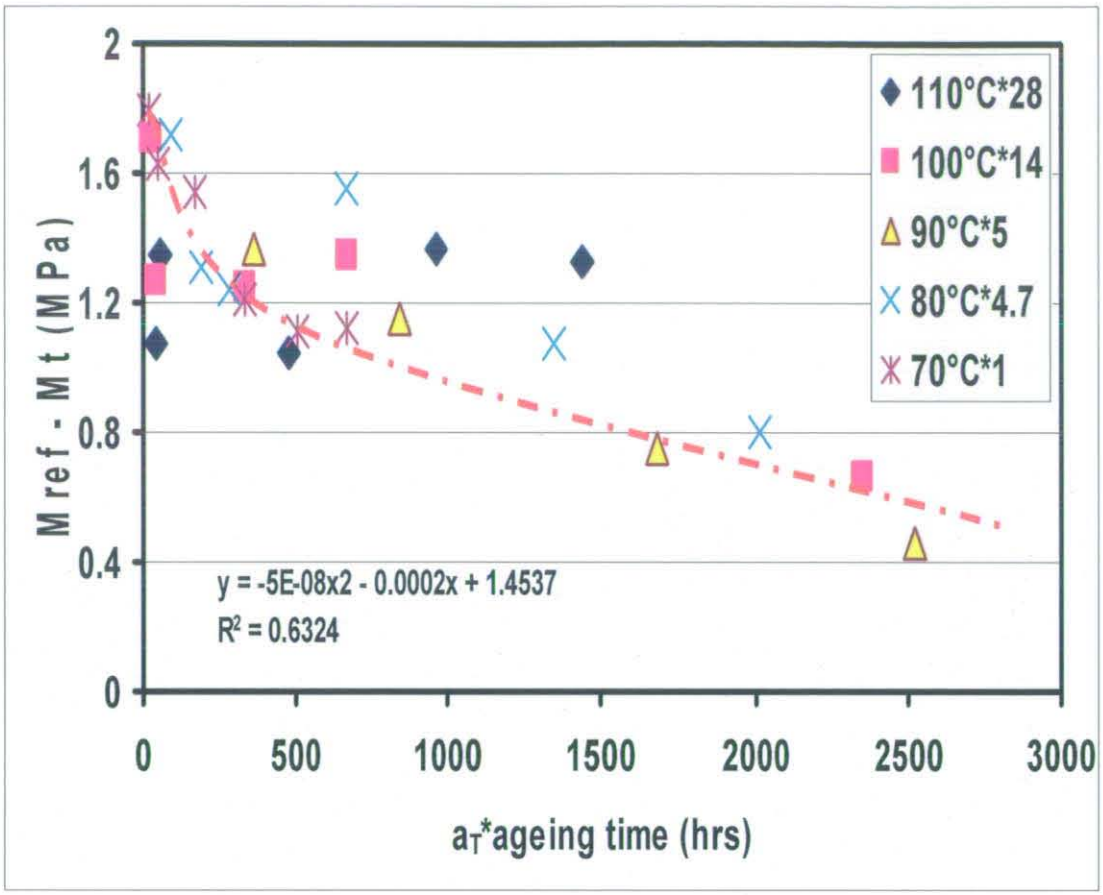

Figure 6-27: Time – temperature superposition plot for reduced modulus at 100% strain for ageing of natural rubber at 70°C reference temperature

The Time Temperature Superposition plot for the reduced modulus (Figure 6.27) shows a very large scatter (correlation coefficient = 0.6324) and as such could not be conveniently used to describe the kinetics of degradation for the aged natural rubber. The results are however, presented for comparison purposes.

Instead of the time-temperature superposition approach, the fractional life approach was therefore used to describe the degradation kinetics of the aged natural rubber in terms of its reduced modulus as has been explained elsewhere.[14] Figure 6.28 shows the fractional rate plots for the natural rubber engine mount compound aged at temperatures of 70°C – 110°C. The rate constant and the order of the reaction obtained from the fractional equation and plots are shown in Table 6.6. It can be observed that the rate of ageing in terms of its effect on modulus increases with ageing temperature. The order of the reaction obtained decreases with increasing ageing temperature up to 90°C and then increases sharply with increasing ageing

temperature. This shows how complex it could be to predict the mechanism of the degradation taking place in the rubber samples. The complexity lies on the fact that network chains break and reform depending on the temperature and rate of oxygen diffusion as such the way in which crosslinks are either going to form or break cannot be easily determined.

Table 6.6: Rate constants and order of reaction from fractional rate law for modulus for rubber cured at 140°C

Ageing temperature (K)	K (x 10^{-4})	n	r^2	Ea (kJ/mol)
343	1.22	6.95	0.8927	
353	5.34	6.86	0.9505	
363	8.99	3.49	0.9717	87.84
373	22.72	5.27	0.9333	
383	32.1	8.49	0.9775	

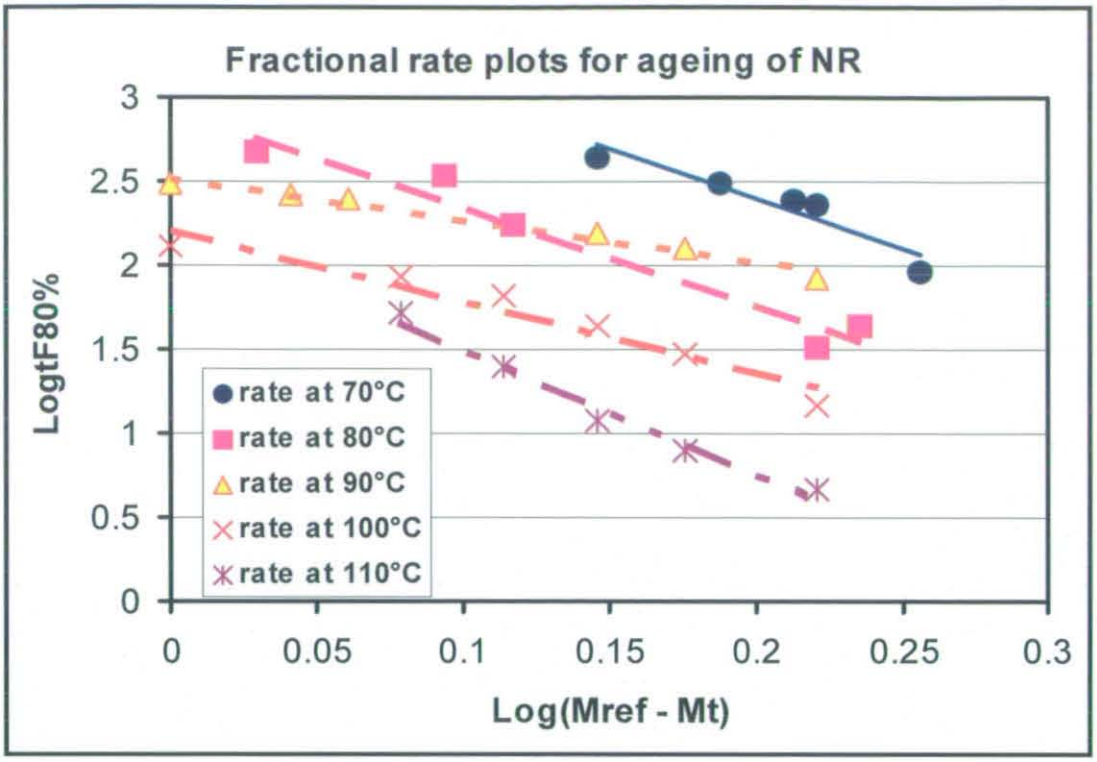

Figure 6-28: Fractional rate law plots for aged NR samples in terms its effect on modulus. (rubber cured at 140°C)

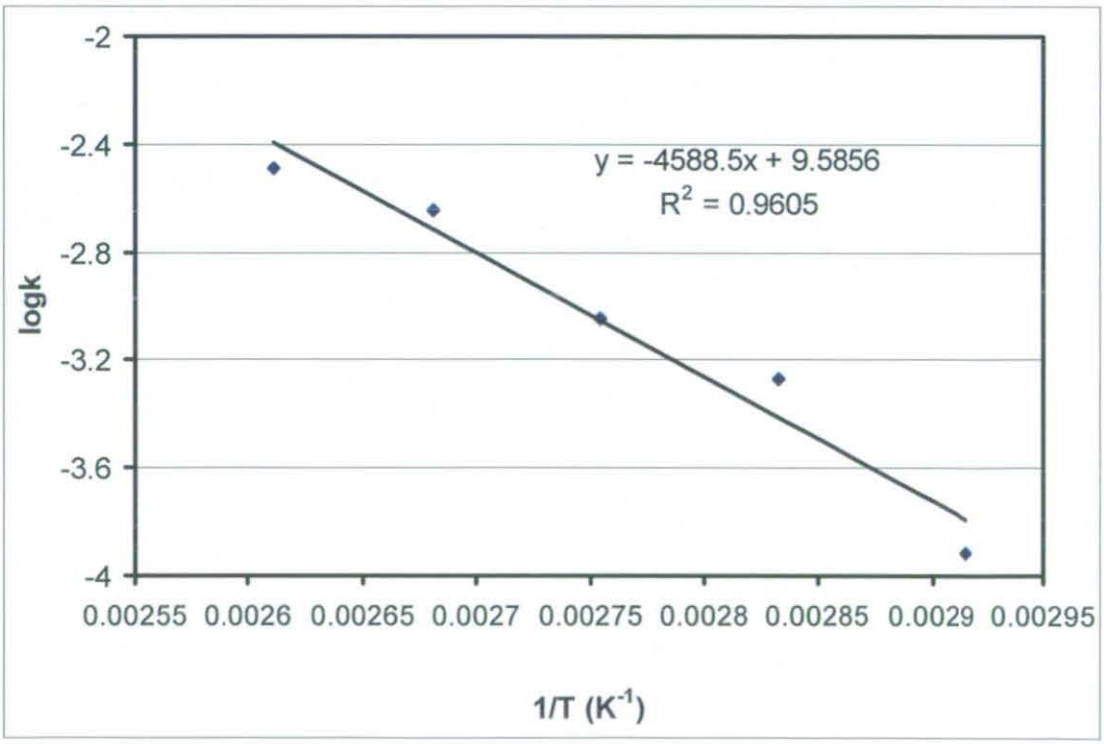

Figure 6-29: Arrhenius plot for reduced modulus at 100% strain from fractional rate law (rubber cured at 140°C).

From the Arrhenius plots of lnk against 1/T, (Figure 6.29) it could be seen that the plots lie on a straight line with a linear regression coefficient of $r^2 = 0.9605$. From this plot, the activation energy was calculated to be 87.84 kJ/mol. This value is quite similar to predictions for tensile strength and elongation at break.

6.6 Effect of Cure Temperature and Data Treatment Methods on the Activation Energy of Ageing

The effects of data treatment method on the values of activation energy for thermo – oxidatively aged natural rubber are shown in Table 6.7. Graphs for the rubber cured at 140°C are shown in the appendix 1 for tensile strength and elongation at break.

Table 6.7: Effect of data treatment method on the activation energies

Cure Temp.	140°C			150°C		
Property	Activation energy (kJ/mol)			Activation energy (kJ/mol)		
	Rate law	TTS	CL	Rate Law	TTS	CL
Tensile strength(MPa)	109	93	103	88	86	81
Elongation at break(%)	110	98	98	74	86	87
Modulus(MPa)	88	80		151	144♣	

TTS: Time-Temperature Superposition, CL : Critical life @ 60% ♣Ea considered between 90°C – 110°C

For rubber cured at 140°C, the activation energy determined by the rate law approach was found to be higher by about 15% than that determined by the time temperature superposition method. The lower activation energy encountered using the TTS approach might be as a result of the greater contribution of the low temperature measurements (70°C and 80°C) which may give low activation energies. Gillen et.al.[20] had explained that lower activation energies may be observed as the temperature of ageing is reduced. For the compound cured at 150°C, the activation energies using the rate law and the TTS approach were close, though the activation

energy using the TTS approach for elongation at break was about 10 kJ/mol higher than the rate law method. The effect of cure temperature on the activation energy of ageing can be clearly seen in Table 6.7, particularly if the rate law method is considered. The activation energy for the rubber compound cured at 140°C was about 19 % higher than that cured at 150°C when we consider tensile strength measurements, for example. The difference in activation energy may be due to the fact that the rubber cured at a lower temperature originally had more polysulphidic networks, which convert to disulphidic and monosulphidic networks during ageing. Thus ageing takes the form of maturation of the crosslink networks without excessive damage of the main network chains, resulting in a lesser reduction in the tensile strength.

The activation energy using the critical life approach (in this case the time for the rubber to degrade to 60% of its original property value was considered as the critical life) was generally close to the TTS or rate law approach. The tensile strength and elongation at break gave similar results, and either of them can be used practically to determine activation energies for ageing. The critical life method is therefore a quick and viable approach for the calculation of the activation energy of the natural rubber compound subjected to ageing.

Using the rate law and the time temperature superposition approach to determine the kinetics of ageing of the natural rubber in terms of modulus, it could be seen that the activation energy differ by about 8 kJ/mol for rubber cured at 140°C and 7 kJ/mol for rubber cured at 150°C (Table 6.7). An increase in cure temperature seems to increase the activation energy of ageing in terms of its effect on modulus, contrary to the effect observed for tensile strength and elongation at break. The reason for this is likely to be that only the higher ageing temperatures were used to calculate the activation energy for the 150°C cured compound and as was mentioned earlier, this will likely lead to an overestimation of the activation energy. However, it is also possible that the activation energy is affected by the nature of the crosslinks in the compounds in a converse way to tensile strength and elongation at break. The compound cured at the lower temperature, having more polysulphidic crosslinks, is more susceptible to hardening through crosslink maturation than the compound cured at the higher temperature.

6.7 Crosslink Density

The effect of ageing on the crosslink density determined from swelling experiments is as shown in Figure 6.30

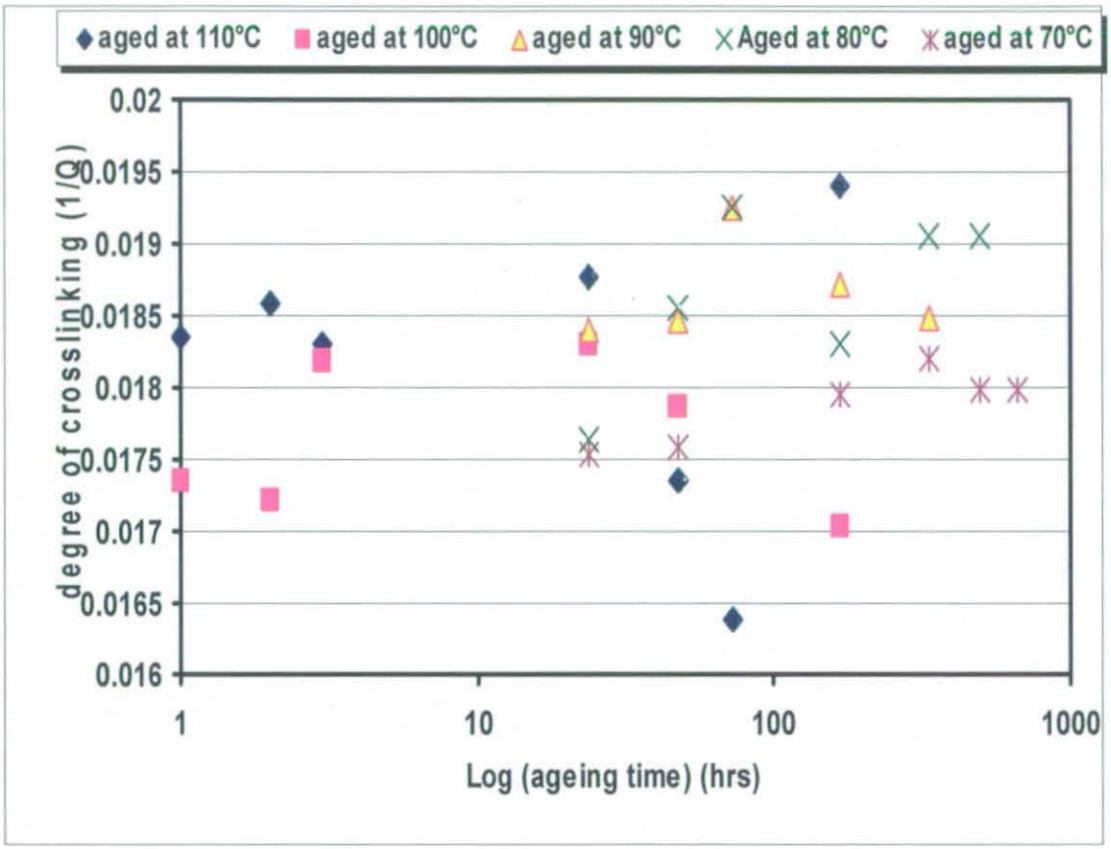

Figure 6-30: Effect of ageing on crosslink density for rubber cured at 140°C

Generally the crosslink density increases with an increase in the ageing time especially at low temperatures of ageing (70°C). At high temperature ageing, the crosslink density passes through a maximum and then falls to lower values. It is known that crosslink density as measured by solvent swelling reflects the modulus of most polymers. In this study however there is a slight difference between the crosslink density measurements and the modulus measurements, especially at longer ageing times for the high temperature measurements. Physical crosslinks which are present in the rubber, such as chain entanglements tend to increase the modulus but these entanglements are disentangled as solvent is being absorbed during solvent swelling.

Polar interactions between oxygen functional groups introduced during ageing could also add to stiffness in the compound but are broken by solvents. In this way, lower crosslink densities may be obtained from swelling measurements compared to those suggested by modulus measurements.

6.8 Mechanisms of Ageing as Deduced from Tensile Measurements

The mechanisms of thermo- oxidative ageing are discussed using tensile strength data from rubber cured at 140°C and 150°C. Various schemes have been proposed for the ageing of rubber and other polymers,[16, 23, 24] (Figure 6.31) but all of them point to the fact that crosslinking and scission takes place almost simultaneously. To follow the degradation mechanism during the thermo – oxidative ageing of the natural rubber engine mount compound, we used the method described by Ahagon et. al.[17] and Baldwin et.al.[10, 11]. Two types of ageing mechanisms were observed when a plot of the log of the elongation at break against the log of the modulus was made (Figure 6.32 and 6.33). Type I is predominantly a crosslinking mechanism with a characteristic slope of – 0.71 and -0.89 for rubber cured at 140°C (Figure 6.32) and 150°C (Figure 6.33) respectively. The points which are enclosed within the ellipse lie on lines with a slope close to -0.71. At the lowest ageing temperature of 70°C all the data lie on this line, indicating the predominance of crosslinking reactions. For the other ageing temperatures, apart from 110°C, data from the early stages of ageing fall within the Type I category, showing that crosslinking reactions were predominant at the early stages of ageing. The remaining data lie on lines with steeper slopes, corresponding to the Type III mechanism, characterised by mostly scission reactions. The results indicate that at high temperatures and at later stages in the ageing process, scission processes predominate.

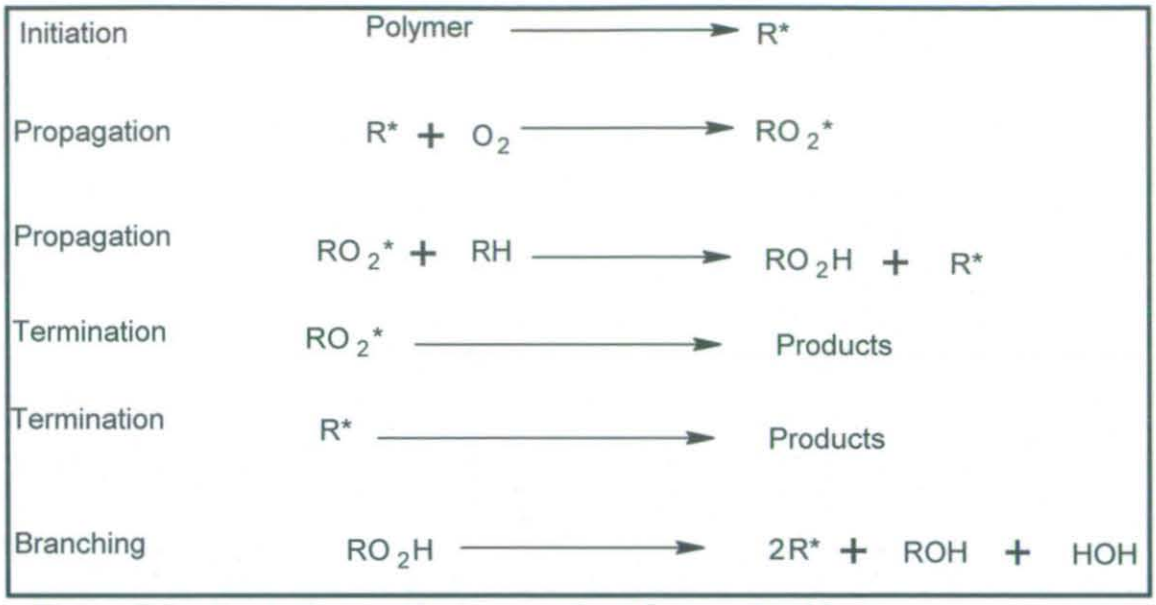

Figure 6-31: Typical autoxidation reaction of natural rubber

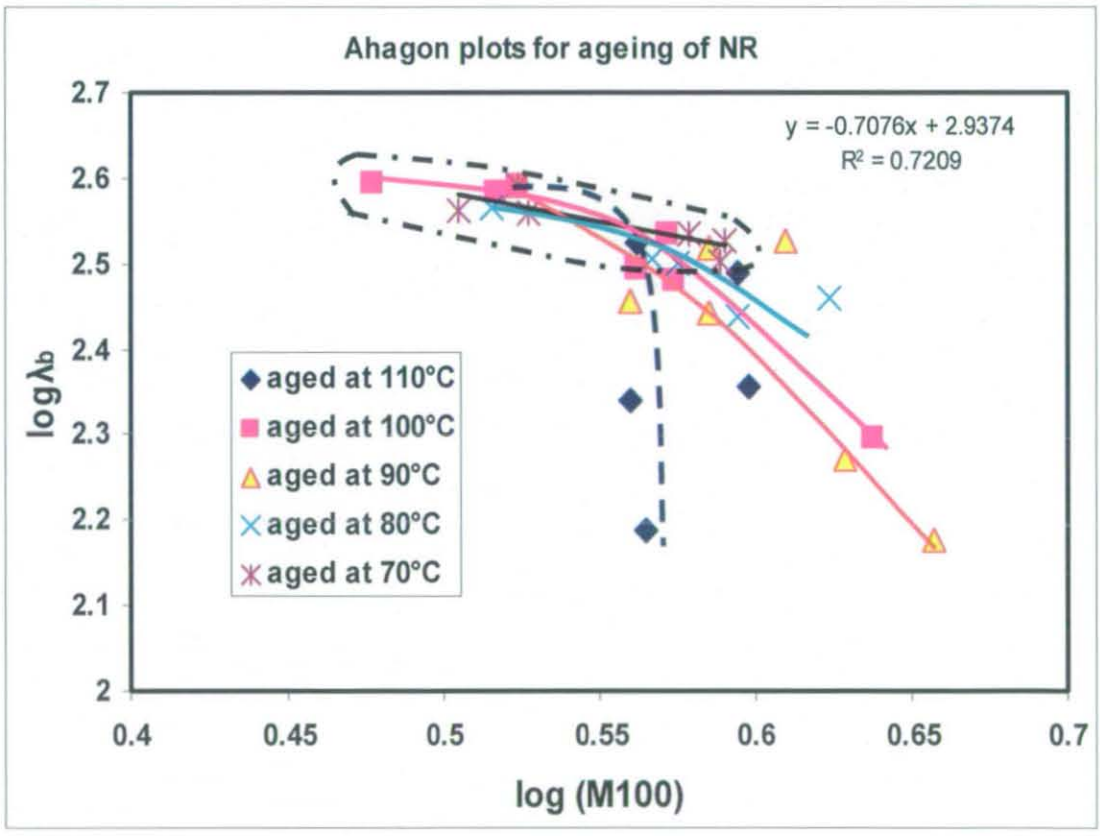

Figure 6-32: Ahagon plot for the ageing mechanisms of natural rubber compound cured at 140°C

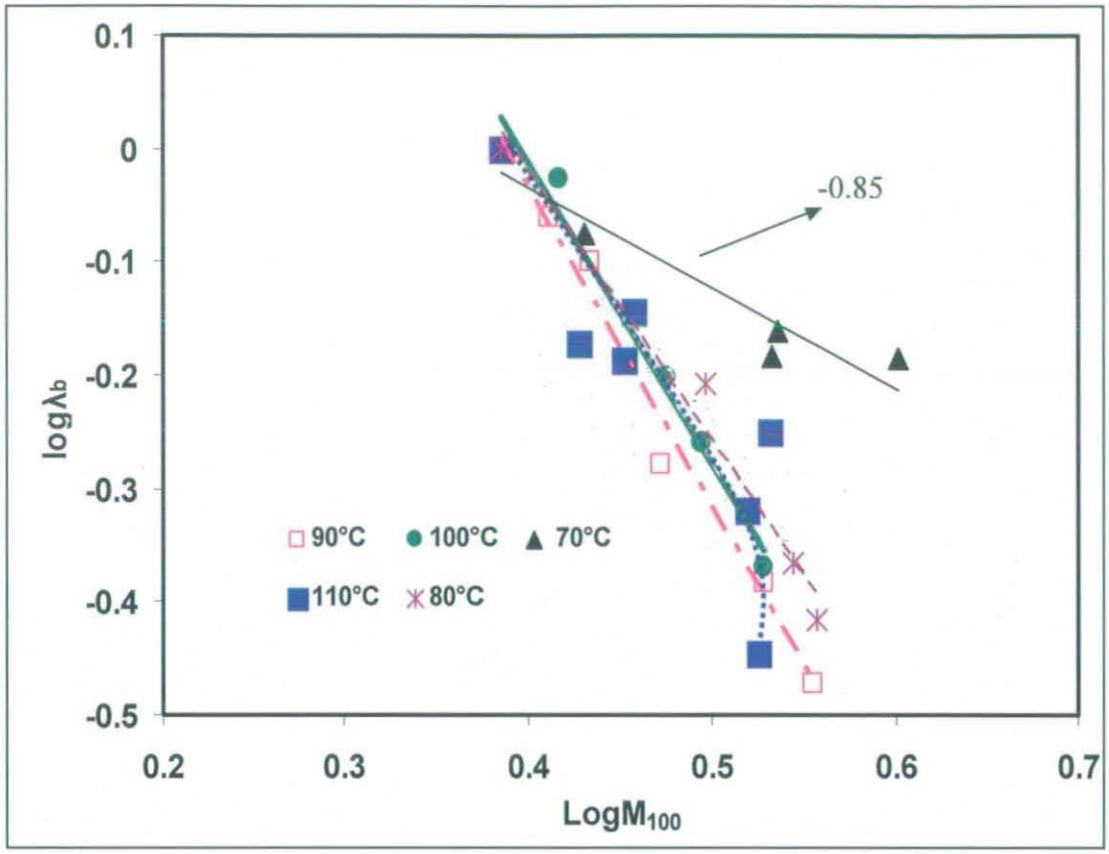

Figure 6-33: Ahagon plot for the ageing mechanisms of natural rubber compound cured at 150°C

The slopes for the rubbers cured at 140°C and 150°C are different because of the different mechanisms that have taken place in the vulcanizates during curing as earlier explained. For the rubber cured at 140°C, there are more crosslinking reactions taking place. Meanwhile when the rubber is cured at 150°C, there are more scission reactions taking place than crosslinking. The reason being that the compound cured at 140°C has more polysulphidic linkages when compared to that cured at 150°C.

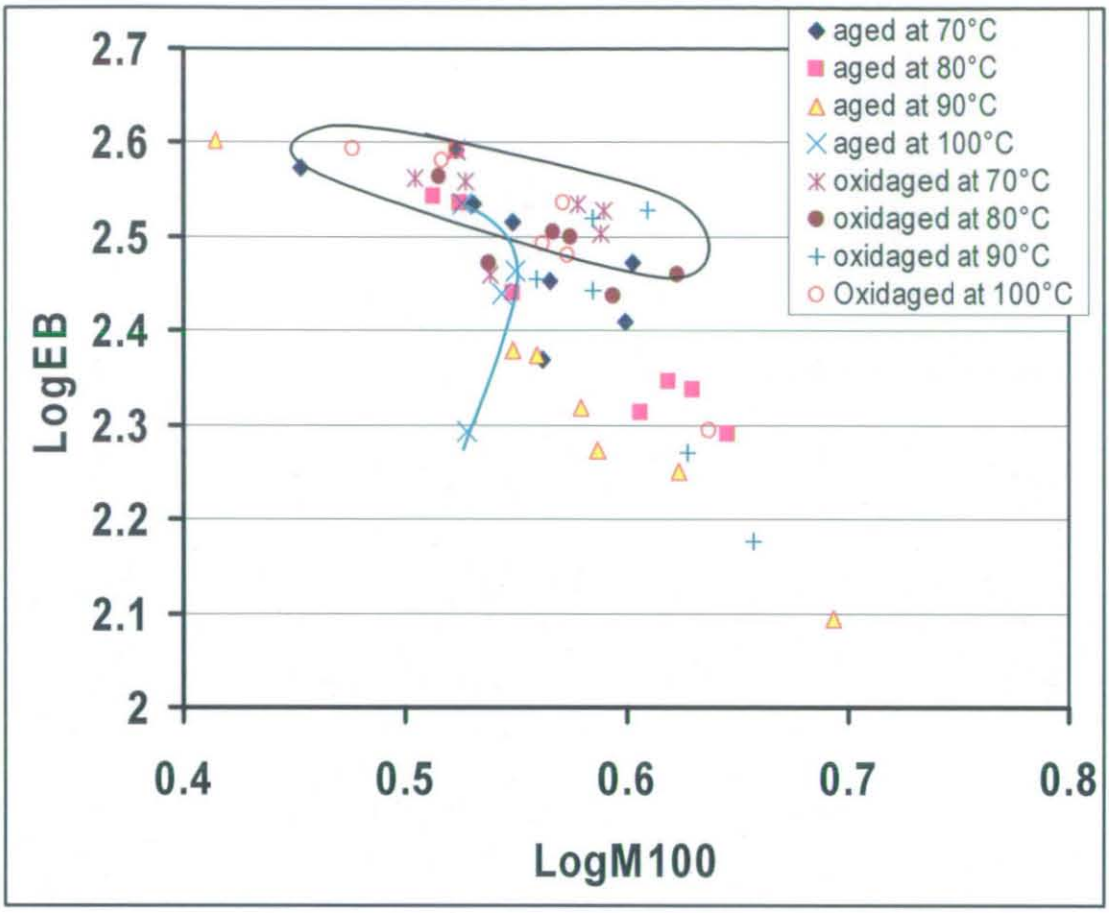

Figure 6-34: Ahagon plot for the thermal ageing mechanisms of natural rubber compound cured at 140°C

Figure 6.34 shows the Ahagon plot for thermally aged natural rubber cured at 140°C. This has been combined with data for thermo – oxidatively aged data. The data for the oxidatively aged rubber compound lie in the ellipse, meanwhile most of those thermally aged lie at the exterior of the ellipse. From this data we can say that thermal ageing is also characterised by three types of ageing mechanism which include Type I and Type II and Type III ageing mechanisms but more predominantly Types II and III.

Type II mechanism is typical of an anaerobic mechanism with the M_{100} values either changing a little or reduced compared to the original values. This is usually obtained at high temperatures (usually above 90°C – 100°C) and is characterised by the breaking and rearrangement of sulphur crosslinks.[10, 25] It could be observed from Figure 6.34 that the rubber anaerobically aged at 100°C experienced a type II ageing mechanism. Table 6.8 shows selected data comparing the modulus and elongation at break data for thermally aged and thermo – oxidatively aged rubber compound. The

modulus for the thermo – oxidative aged rubber compound was consistently higher than that which was thermally aged, confirming the fact that oxidative ageing was characterised more by crosslinking.

Table 6.8 : Data comparing the modulus and elongation at break data for thermally aged and thermo – oxidatively aged rubber compound

		Thermal Ageing		Oxidative ageing	
Ageing temp (°C)	Ageing time (hours)	M_{100}	λ_b	M_{100}	λ_b
80	0	3.34	390.9	3.34	390.9
	24	3.26	349.4	3.28	366.7
	48	3.35	344.5	3.69	320.5
	72	3.54	276.2	3.76	316
	168	4.27	217.9	3.45	297.1
	336	4.16	221.8	3.93	274.3
	504	4.04	205.5	4.20	228
100	24	3.36	341.9	3.75	302
	48	3.55	291.1	3.65	311.4
	72	3.50	274.8		
	168	3.38	196.4	4.34	197.3

6.9 Kinetics of Ageing from Thermogravimetric Analysis

Kinetics has been used as a means of studying the degradation patterns of polymers and subsequent prediction of service life of the material. Various kinetic equations have been developed for the interpretation of information obtained from thermogravimetric analysis in order to calculate the activation energies, order of a reaction and other degradation parameters. The techniques have been applied either for processes termed as isothermal or non isothermal (isoconversional) processes. Thermogravimetry has been used to study the degradation kinetics of several polymer systems as well as polymer additives.

Figures 6.35 and 6.36 shows the TG and DTG curves carried out in air and nitrogen atmosphere for rubber thermo – oxidatively aged at 80°C. Only a single weight loss was recorded for the DTG curves for samples decomposed under a nitrogen atmosphere. The degradation of the rubber compound at 20°C/min heating rate in air was characterised by three weight loss stages. The first weight loss stage occurs between 200°C and 435°C for the unaged sample, and between 200°C and 465°C for the aged samples. The second weight loss stage occurred between 470°C to 537°C, while the third weight loss stage occurred at around 537°C to 619°C. The second and third weight loss stages are believed to be thermo – oxidative in nature since they do not occur in the nitrogen atmosphere. The initial degradation step may correspond to the compounding ingredients such as the antioxidants and antiozonants (TMQ, 6 – PPD and wax) accelerators etc. These materials however undergo decomposition throughout the degradation temperatures. Degradation of the natural rubber as explained by Ramesan[26] starts at a temperature of about 296°C though this depends on the heating rate. The maximum of weight loss for the first degradation stage occurred at a temperature of about 400°C in air atmosphere and at about 396°C in nitrogen atmosphere.

As the ageing time increases, the $\frac{dm}{dT}$ values on the DTG curve decreases for the first weight loss stage, and then increases with ageing time for the second weight loss stage, though corresponding values are far less than the first stage.

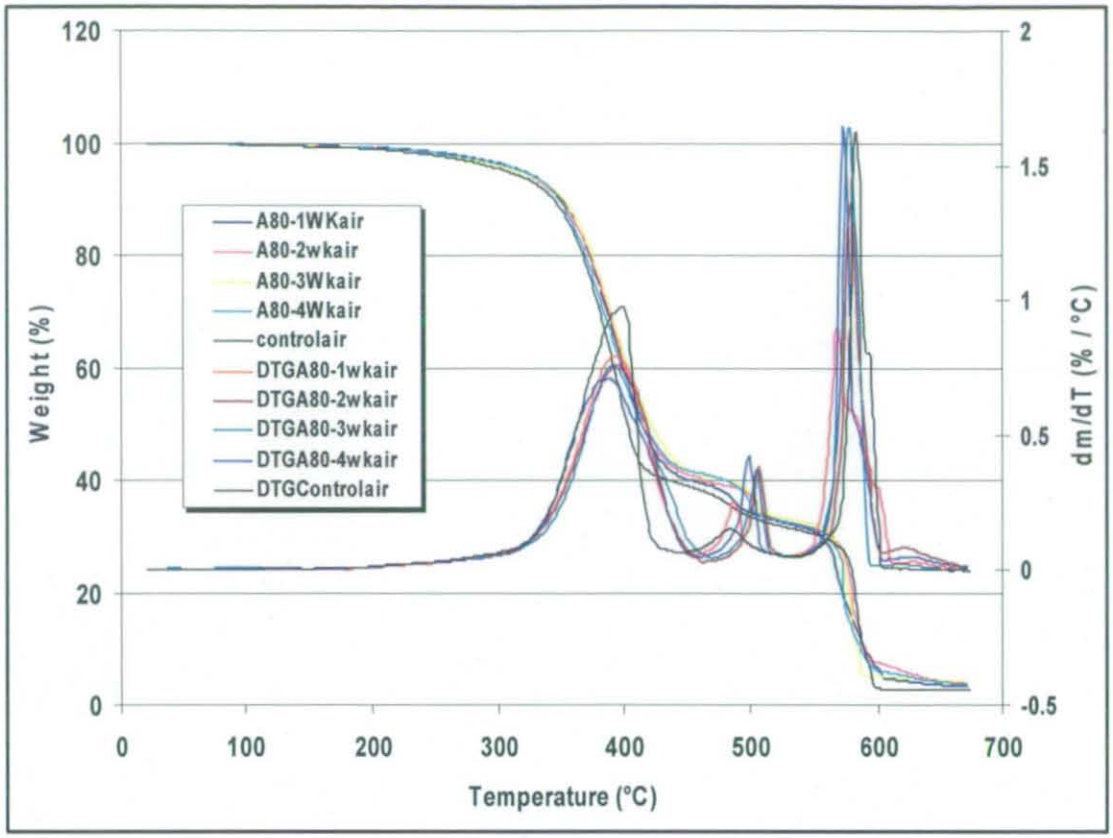

Figure 6-35: TG and DTG curves in air atmosphere for engine mount compound aged at 80°C

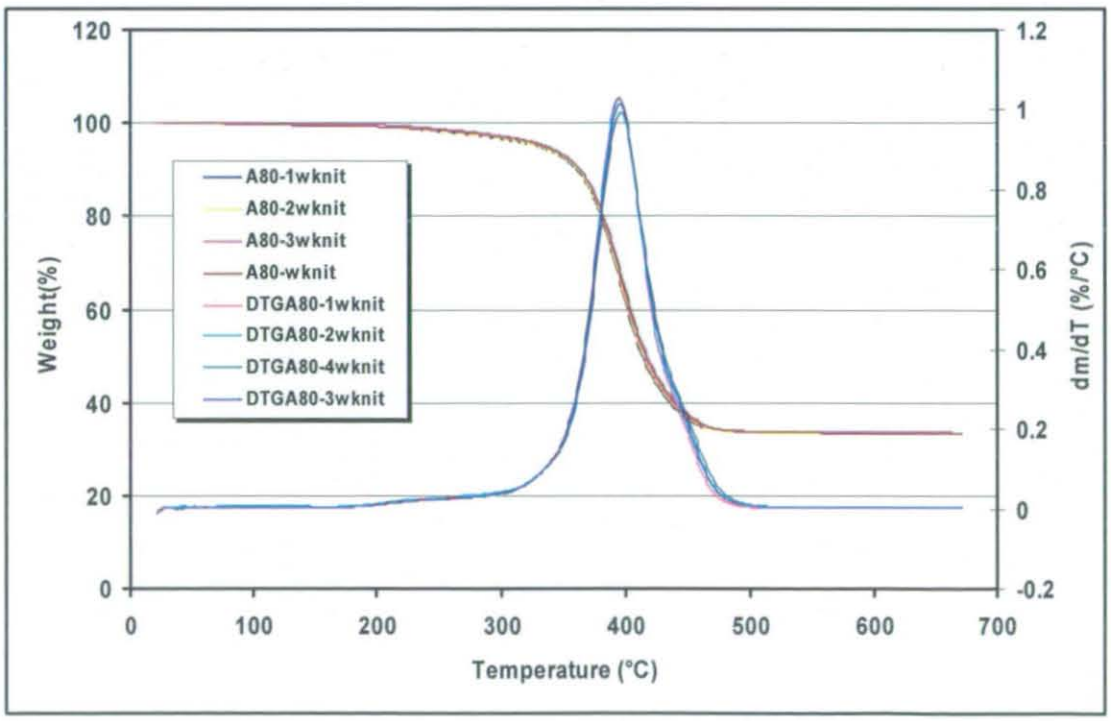

Figure 6-36: TG and DTG curves in nitrogen atmosphere for engine mount compound aged at 80°C

Chauhari et.al.[27] have suggested that the thermograms of polymers could be divided into four weight loss regions (0 – 5%, 5 – 10%, 10 – 80% and 80 – 100%). The 0 – 5% and 5 – 10% weight loss regions are said to be as a result of groups that causes the scission of rubber chains and this is associated to weight loss. The maximum decomposition of the natural rubber takes place in the 10 – 80% region, which Ramesan[26] says begins at a temperature of 298°C. The decomposition of all other compounds takes place in the 80 – 100% weight loss region. The 100% weight loss region corresponds to complete degradation of the rubber compound.

Considering the different aged compounds, the TGA curves show a shift in the temperature from the first weight loss region. This shift in temperature might be due to enhanced crosslinking which is usually associated with a shift in the degradation temperature at the 5% weight loss region to higher temperatures. In this study, if we agree that degradation of the rubber starts typically in the 10 – 80% region then for the natural rubber compound degradation begins typically between 345°C and 355°C depending on the ageing time and temperature (Table 6.9). While the 5% weight loss temperature for the control is recorded as 306°C, the aged samples had a 5% weight loss of 312°C and 322°C. This shift in weight loss region to a higher temperature for the aged samples compared to the control maybe as a result of some loss of labile material during ageing or an increase in stability due to crosslinking.

Table 6.9 : Effect of ageing time on the temperature at weight loss regions (derived from Figures 6.38 – 6.40)

		Temperature at Weight loss regions (°C)				
Ageing temp (°C)	Ageing time (hrs)	5%	10%	50%	80%	> 95%
Control	0	306	344	402	582	605
80	168	318	350	414	572	609
	336	316	349	417	579	600
	504	316	351	422	577	596
	668	319	348	416	574	599
90	168	312	347	414	588	605
	336	319	351	427	590	602

	504	317	345	437	587	607
	668	306	345	439	491	602
100	24	315	350	413	577	599
	48	318	351	416	572	612
	168	321	352	421	576	608
	336	315	350	435	583	616
110	4	311	355	405	567	613
	24	318	348	408	570	597
	48	316	350	415	575	601
	72	322	353	424	579	608

If we consider the temperature in a TG curve at which 50% decomposition occurs as an index of thermal stability as described by Menon et.al.[28], it could be observed that the stability temperature goes to higher temperatures with ageing time at the different ageing temperatures.

Using the Doyle – Ozawa method to calculate the activation energy for the degradation of natural rubber, we have

$$\frac{d\log\beta}{d\left(\frac{1}{T_{\max}}\right)} = \frac{-0.4567E}{R} \quad \text{------- ------- ------- ---} \qquad [6.9]$$

Rearranging gives

$$\log\beta = \frac{-0.4567E}{R} * \frac{1}{T_{\max}} + C \qquad [6.10]$$

Where β is the heating rate (°C/min), T_{max} is the highest peak temperature for the first weight loss peak, R is the universal gas constant, and c is a constant. When a plot of logβ against 1/Tmax is made, a straight line with slope $\frac{-0.4567E}{R}$ is obtained whose intercept is C. (Figure 6.36)

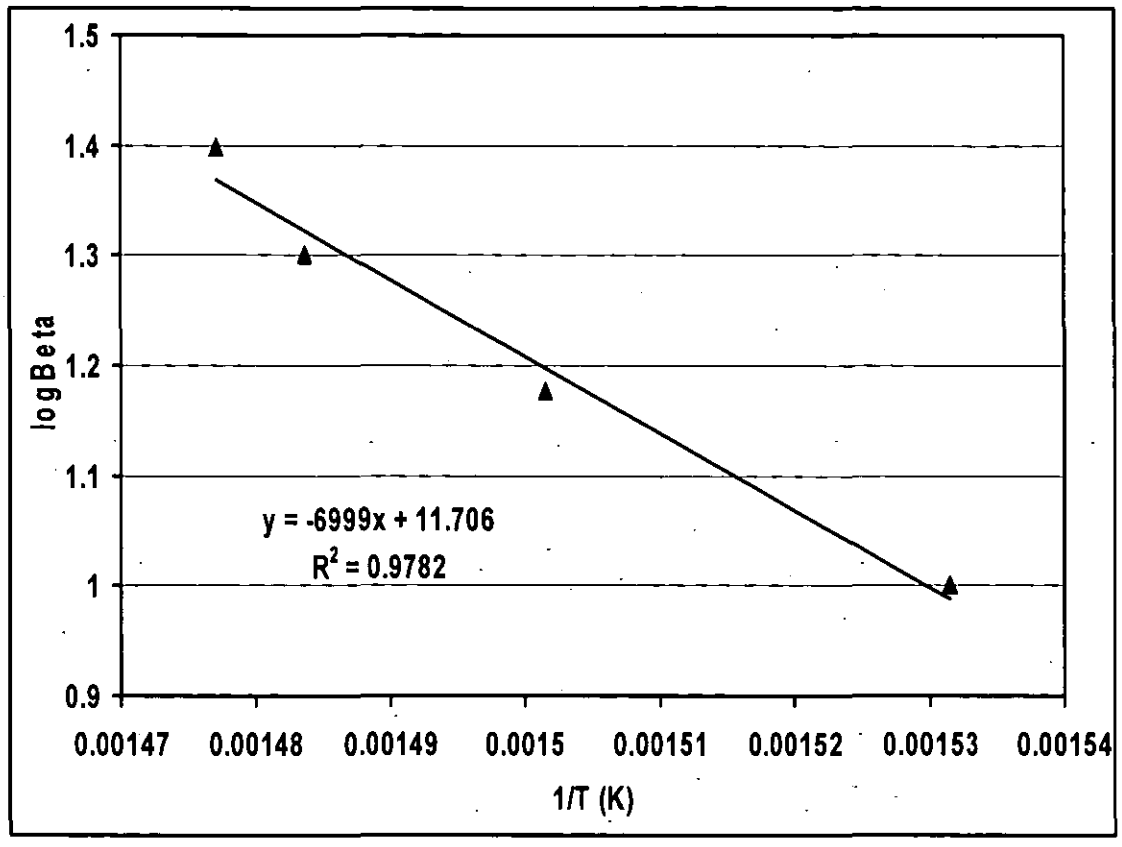

Figure 6-37: Plot of logβ versus 1/Tmax (Doyle – Ozawa method) for the first decomposition step of the natural rubber compound

From this plot, the activation energy of decomposition was calculated to be about 127.4 kJ/mol. The value obtained though higher than that proposed for the oxidative ageing of natural rubber, were consistent with activation energy for the thermogravimetric measurements from rubbers as obtained by Regnier and Guibe[8]. This is consistent with the idea that activation energies of ageing generally increase with increase in ageing temperature.

6.9 Life predictions

In order to validate the use of the time – temperature superposition model for the prediction of the functional life of our material, the rubber was aged at 50°C for more than three months. The tensile strength after ageing for 13 weeks at 50°C was measured as 19.0(±2.25) MPa, and the predicted value at 50 °C was 18.7 MPa. (Table 6.10). The percentage reduction in tensile strength after 13 weeks of ageing at 50°C

compared to the unaged sample was about 20%. The time-temperature superposition model thus predicts the ageing at this relatively low temperature, long time condition rather well. However, ideally longer times and lower temperatures should also be tested for full validation of the model. If a 50% reduction in tensile strength and elongation at break is selected as a failure criterion, it was predicted that the engine mount compound will take approximately 80 days for the tensile strength to reduce by fifty percent at a temperature of 70°C. At 23°C the samples would take approximately 140 times its lifetime at 70°C to deteriorate to the same level (Table 6.9).

Table 6.10: Activation energies and service life prediction

Property	Ea (kJ/mol)	Prediction using TTS model	
		Experimental value at 50°C	Predicted value at 50°C
Tensile strength (MPa)	93	19.04 (±2.3SD)	18.73
Elongation at break (%)	98	321.04 (±33.8SD)	327.12
Modulus (MPa)	80	4.17 ((±0.09 SD)	3.66

Service life Prediction (Failure criteria – 50% property reduction)

Property	Temperature			
	70°C	50°C	40°C	23°C
Tensile strength (MPa)	~80days	~ 1.3yrs	~ 4yrs	~ 31 yrs

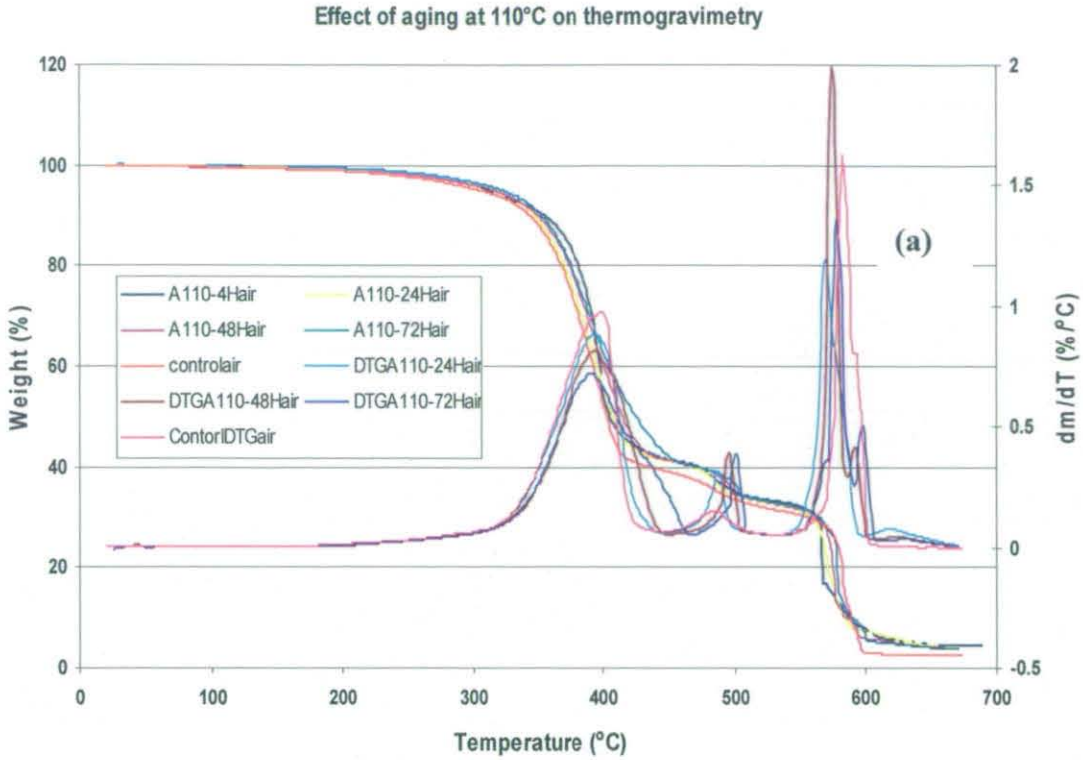

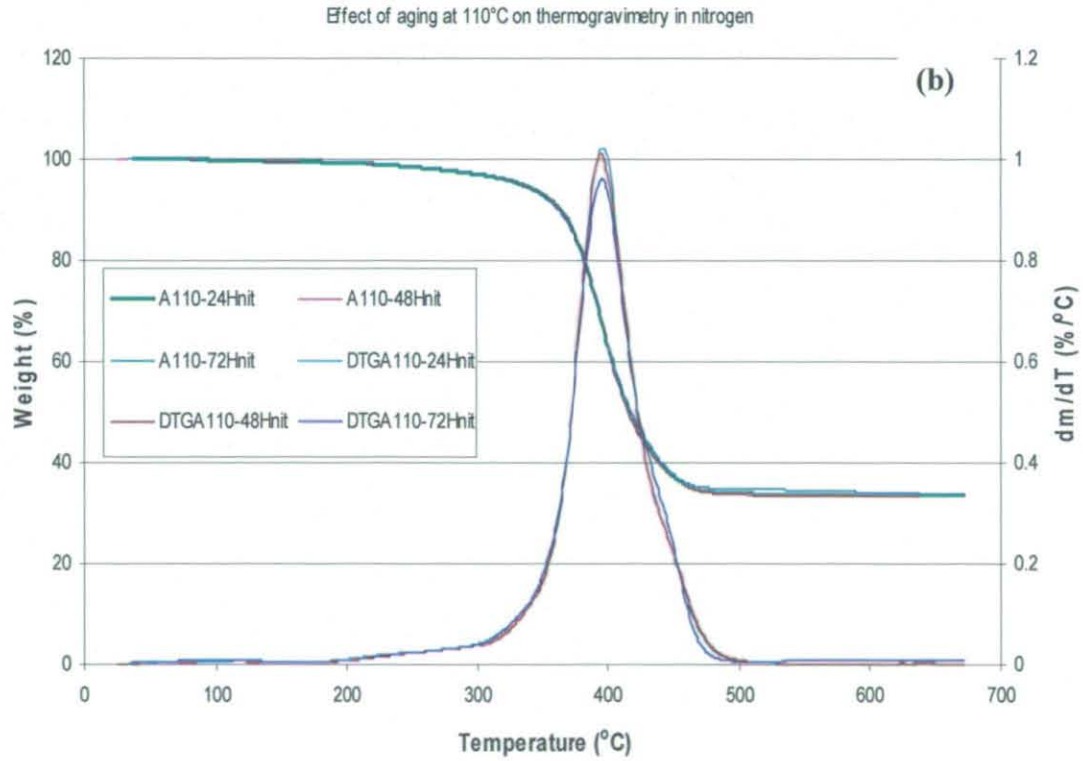

Figure 6-38: TG and DTG curves (a) in air and (b) in nitrogen atmosphere for engine mount compound aged at 110°C

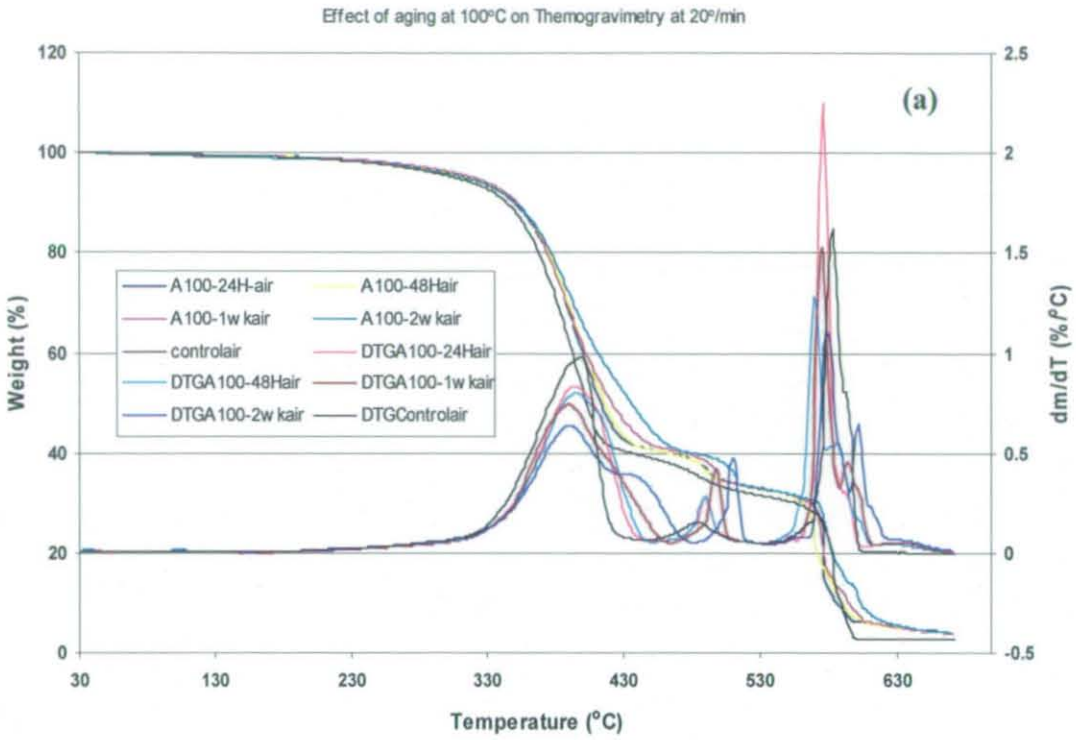

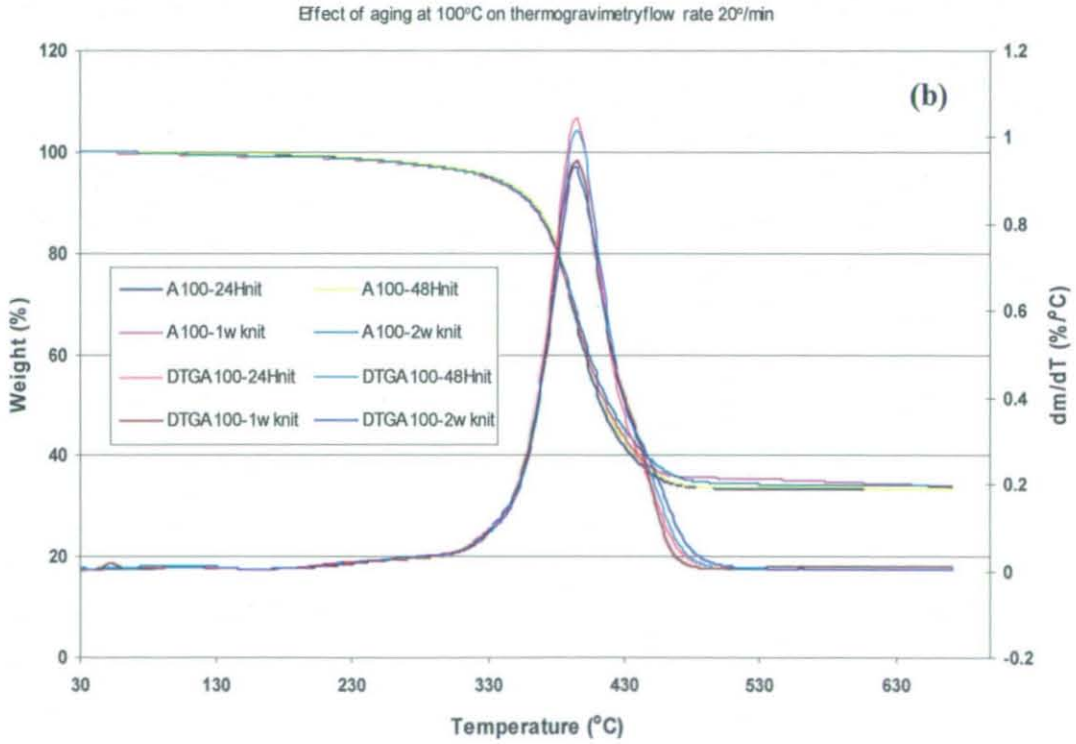

Figure 6-39: TG and DTG curves (a) in air and (b) in nitrogen atmosphere for engine mount compound aged at 100°C

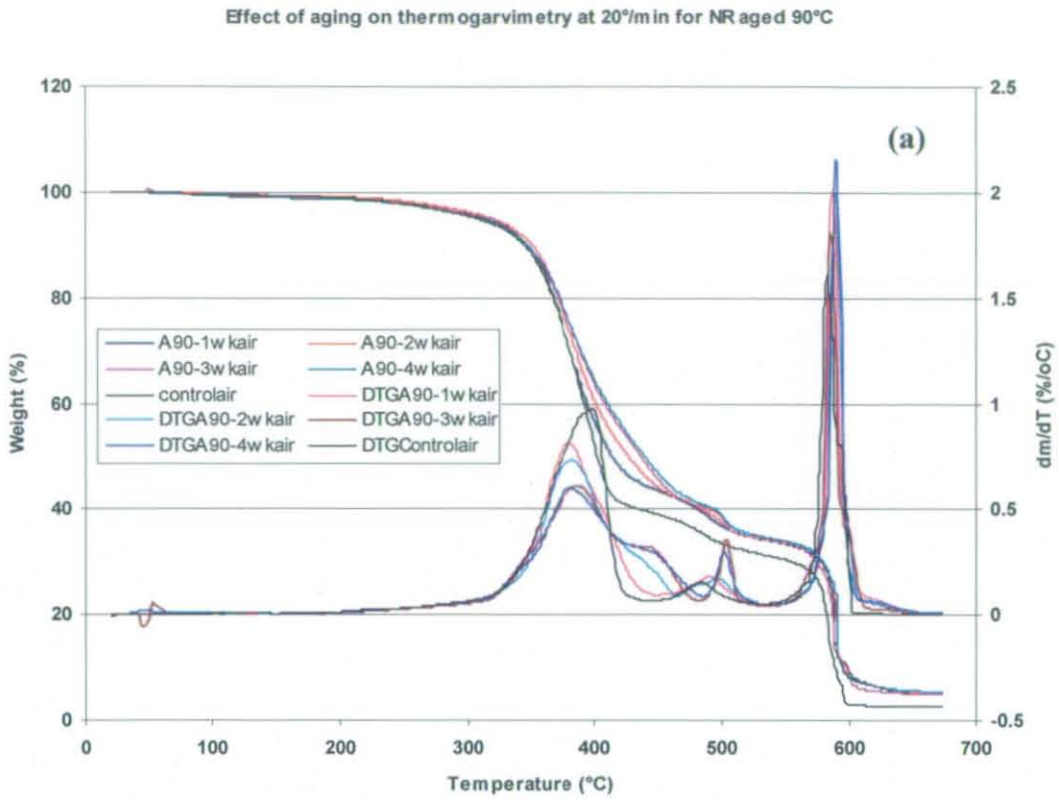

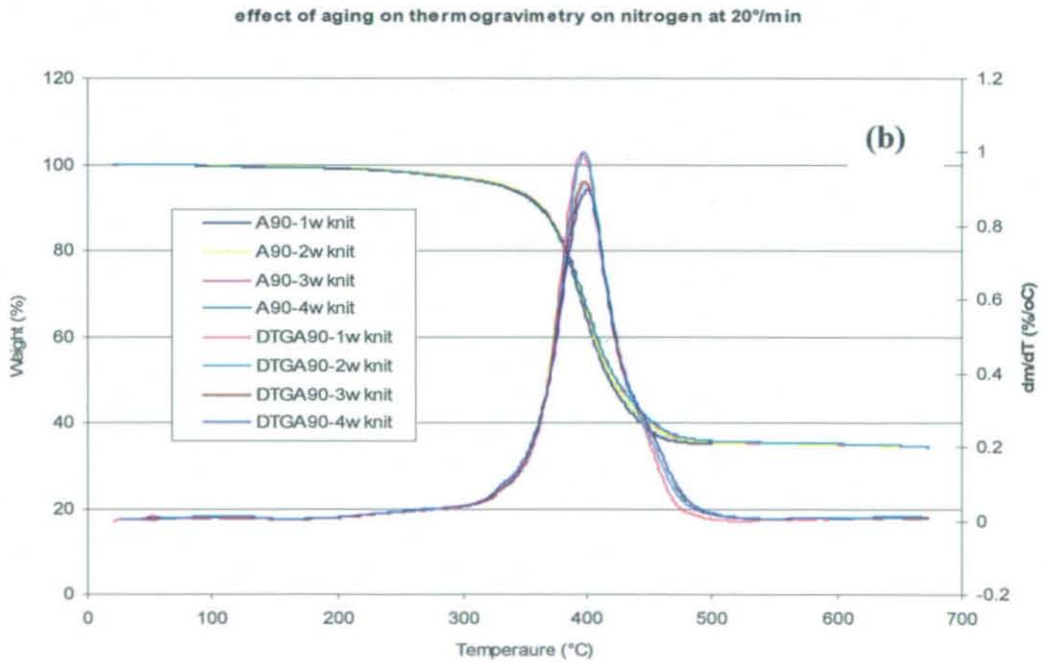

Figure 6-40: TG and DTG curves (a) in air and (b) in nitrogen atmosphere for engine mount compound aged at 90°C

6.10 Conclusions

- Modulus data for rubber cured at 140°C showed maxima at relatively short ageing times (less than 100 hours) which were absent for the rubber cured at 150°C. The peaks were attributed to maturation of the crosslinks (conversion of polysulphidic to di – and mono-sulphidic crosslinks).
- The activation energy of ageing in terms of its effect on strength, was generally higher when the rubber was cured at 140°C (109 kJ/mol) than when cured at 150°C (88 kJ/mol). The higher activation energy is attributed to ageing occurring predominantly through crosslink maturation in the 140°C cured sample, with relatively little main-chain damage or cross-link scission.
- There was some evidence that activation energies of aging were higher at higher ageing temperatures.
- The activation energy for the kinetics of ageing determined from tensile strength and elongation at break gave similar results, e.g. they were found to be about 93 kJ/mol and 98 kJ/mol respectively for the Time temperature Superposition approach.
- The activation energy using the thermogravimetric measurements was about 127 kJ/mol.
- Two types of ageing mechanisms as described by Ahagon were observed for thermo – oxidatively aged rubber. These include types I and III mechanisms, indicating crosslinking and scission respectively with low ageing temperature favouring the crosslinking mechanism, and high ageing temperatures favouring the scission mechanism.
- The Time temperature Superposition model for predicting functional life was validated for an ageing temperature of 50°C.

6.11 References

(1) Loo, C. T. *Polymer* **1974**, *15*, 357-365.

(2) Ivankovic, M.; Incarnato, L.; Kenny, J. M.; Nicolais, L. *Journal of applied polymer science.* **2003**, *90*, 3012.

(3) Bartenev, G. M.; Nikiforov, V. P. *Journal of Polymer Science : Polymer Chemistry Edition* **1975**, *13*, 289.

(4) Kumar, N. R.; Chandra, A. K.; Mukhopadhyuy, R. *J. Mater. Sci.* **1997**, *32*, 3717-3725.

(5) Hamed GR; Zhao J *Rubber Chemistry and Technology* **1999**, *72*, 721.

(6) Bell, C. L. M.; Stinson, D.; Thomas, A. G. *NR Technol* **1980**, *11*, 53-58.

(7) Yang, K. K.; Wang, Y. L.; Wang, Y. Z.; Wu, B.; Jin, Y. D.; Yang, B. *European Polymer Journal* **2003**, *39*, 1567-1574.

(8) Regnier, N.; Guibe, C. *Polymer Degrad Stab* **1997**, *55*, 165-172.

(9) Ono, K.; Kaeriyama, A.; Murakami, K. *Rubber Chem Technol* **1977**, *50*, 43-48.

(10) Baldwin, J. M.; Bauer, D. R.; Ellwood, K. R. *Rubber Chem Technol* **2005**, *78*, 336-353.

(11) Baldwin, J. M.; Bauer, D. R.; Ellwood, K. R. *Rubber Chem Technol* **2005**, *78*, 767.

(12) Straus, S.; Madorsky, S. L. *Rubber Chem Technol* **1957**, *30*, 93-111.

(13) Mott, P. H.; Roland, C. M. *Rubber Chem Technol* **2001**, *74;*, 79.

(14) Ngolemasango, E. F.; Bennett, M. Clarke, J. *J. Appl. Polym. Sci.* **2006**, *102*, 3732-3740.

(15) Gillen, K. T.; Celina, M.; Keenan, M. R. *Rubber Chem. Technol.* **2000**, *73*, 265-283.

(16) Gillen, K. T.; Celina, M.; Bernstein, R. *Polym Degrad Stab* **2003**, *82*, 25-35.

(17) Ahagon, A.; Kida, M.; Kaidou, H. *Rubber Chem Technol* **1990**, *63*, 683-697.

(18) Spanos, P. *Rubber World* **2003**, *229*, 22-27.

(19) Levenspiel, O. In *Chemical reaction engineering;* John Wiley and sons: U.S.A., 1999; pp 62-63.

(20) Gillen, K. T.; Bernstein, R.; Derzon, D. K. *Polym. Degrad. Stab.* **2005**, *87*, 57-67.

(21) Fan, R. L.; Zhang, Y.; Li, F.; Zhang, Y. X.; Sun, K.; Fan, Y. Z. *Polym. Test.* **2001**, *20*, 925-936.

(22) Fan, R.; Zhang, Y.; Huang, C.; Zhang, Y.; Fan, Y.; Sun, K. *J. Appl. Polym. Sci.* **2001**, *81*, 710-718.

(23) Bevilacqua E.M. In *Thermal and Oxidative Degradation of Natural Rubber and Allied Substances;* Robert T. Conley, Ed.; Thermal Stability of Polymers; Marcel Dekker: New York, 1970; Vol. 1, pp 189-222.

(24) Howard, J. *Rubb. Chem. Technol.* **1974**, *74*, 975-990.

(25) Kaidou, H.; Ahagon, A. *Rubber Chem Technol* **1990**, *63*, 698-712.

(26) Ramesan, M. T. *Reactive and Functional Polymers* **2004**, *59*, 267-274.

(27) Chaudhari, C. V.; Bhardwaj, Y. K.; Patil, N. D.; Dubey, K. A.; Kumar, V.; Sabharwal, S. *Radiation Physics and Chemistry* **2005**, *72*, 613-618.

(28) Menon, A. R. R.; Pillai, C. K. S.; Nando, G. B. *Polym. Degrad. Stab.* **1996**, *52*, 265-271.

CHAPTER 7

7 Effect of Ageing on Dynamic and Fracture Properties.

7.1 Introduction

Fracture in rubber, like all other materials, is initiated by imperfections inadvertently present or introduced in the body of the material or on its surface. Failure under dynamic service conditions usually occurs by the development of cracks. Their growth then leads to catastrophic failure by fatigue. The crack growth characteristics of rubber are the main factors determining its strength.[1, 2]

For engine mounts the fatigue process is also affected by temperature and ageing since they may experience as much as 90°C or even more during long drives and in certain tropical regions.[3] It has been stated that temperature has less effect on the crack growth of strain crystallising elastomers, especially over the range where crystallisation is effective, and that reduction in crack growth rates may be due to viscoelastic effects, and changes in fracture surface roughness.[4] In addition to the direct effect of temperature, engine mounts at long run may fail as a result of surface cracks caused by ageing which may progressively propagate through the rubber with time. The number and depth of these cracks will be related to the temperature history of the component.

7.2 Effect of Ageing on Dynamic Mechanical Properties

Both ageing and dynamic properties are very important in the design of automobile components such as hydraulic mounts. For the dynamic mechanical measurements, a multi – strain tests were carried out on both the unaged and aged rubber compounds. Samples were aged at 70°C for 24 hours to four weeks and at 90°C, for periods ranging from one week to four weeks. All the dynamic measurements were conducted at 30°C. Figures 7.1 to 7.6 show the variation of storage modulus, loss modulus and loss tangent, tanδ for the aged compounds. The general shape of the curves are similar for the unaged and aged compounds. The decrease in the storage modulus (G') with increasing strain amplitude and the appearance of a tan delta

maximum at around 2% to 5% (200μm – 500μm) is known as the Payne effect. As explained by Payne[5-7], at small amplitudes of oscillation, little structure is broken down, and the out of phase or viscous modulus G" is small. As strain increases, G" reaches a maximum and the maximum rate of structure breakdown occurs at approximately 2% strain amplitude. At large amplitudes, the structure is so extensively broken down that reformation of the structure is very much slower than the cycle time and G" is low again. (It was observed that with an amplitude increase, the loss modulus increases to a maximum at about 200μm to 500μm (~2% - 5% strain) depending on the ageing temperature. This was the same behaviour for the loss tangent (Figures 7.1 – 7.6).

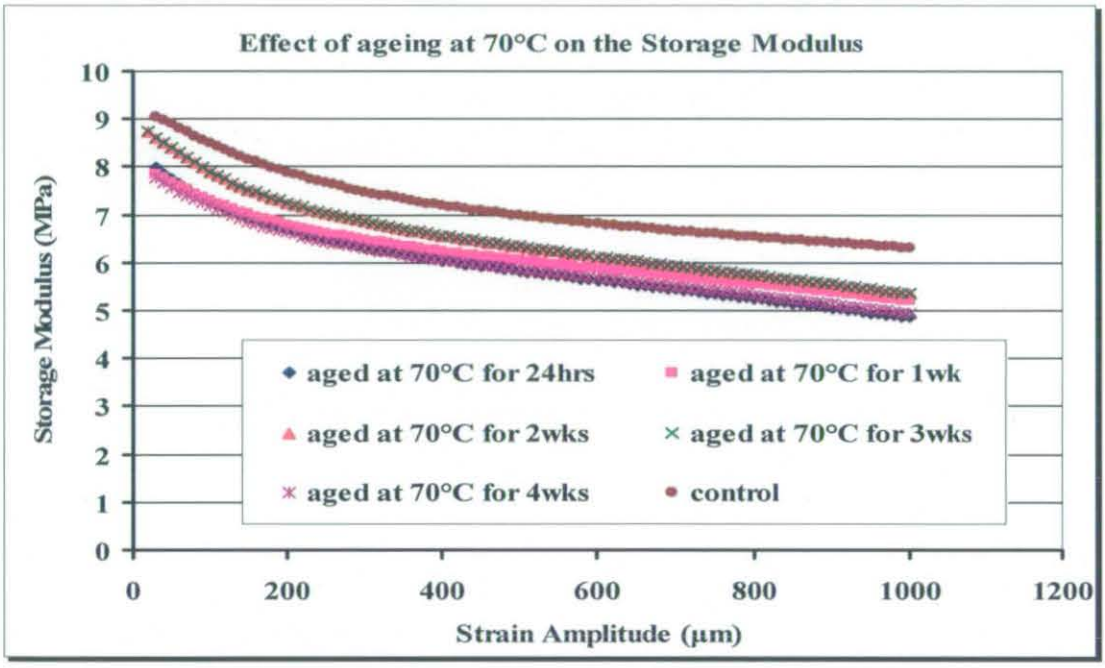

Figure 7.1: Effect of strain amplitude on the storage modulus of the natural rubber compound aged at 70°C

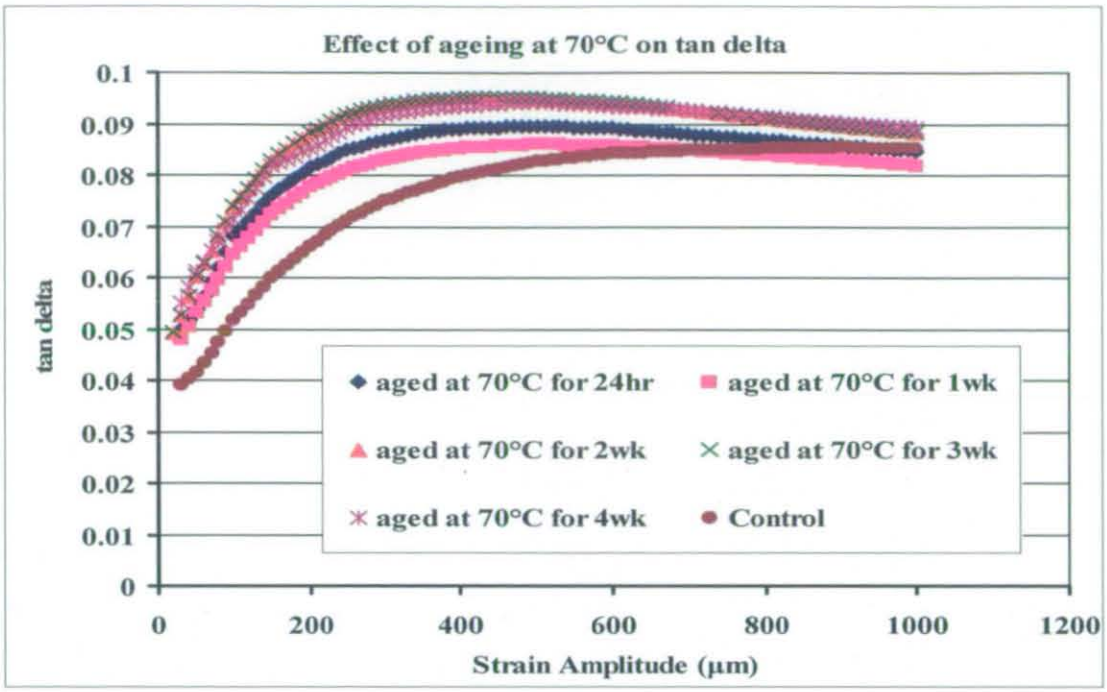

Figure 7.2: Effect of strain amplitude on the loss tangent of the natural rubber compound aged at 70°C

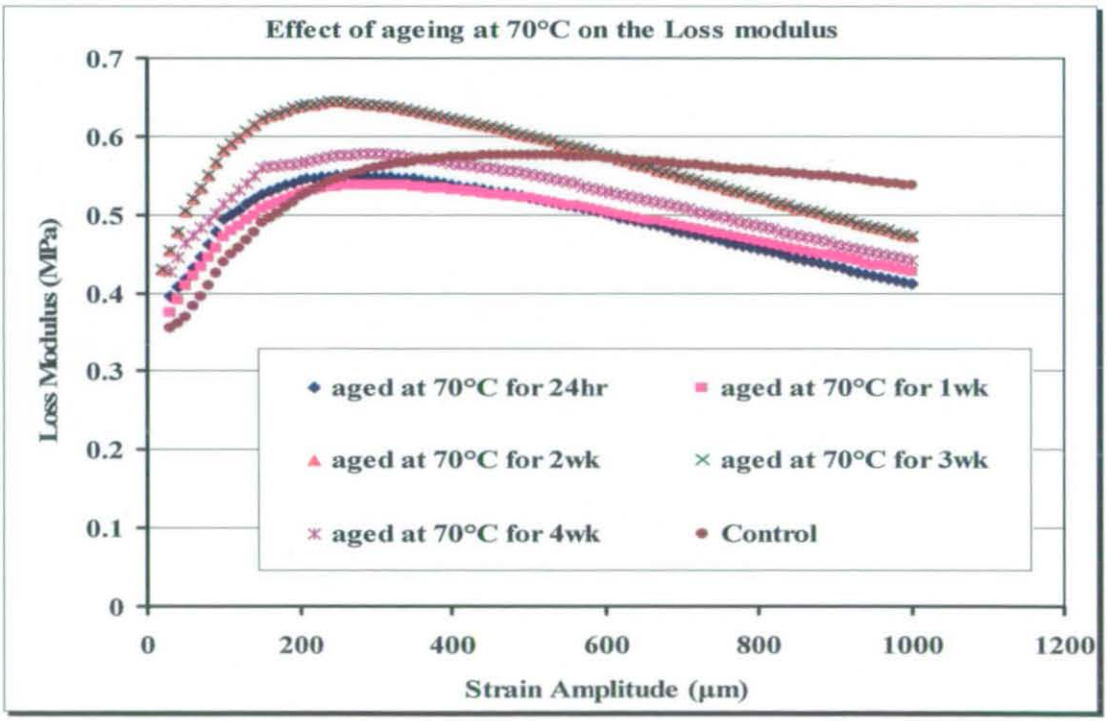

Figure 7.3: Effect of strain amplitude on the loss modulus of the natural rubber compound aged at 70°C

The loss modulus (G") increases up to a strain amplitude of about 500μm (5% strain) and then drops as the strain amplitude is increased further. The loss tangent which is the ratio of the loss modulus (viscous modulus) and the storage modulus (elastic

modulus) also increases with ageing temperature. This indicates that the elastic component of the rubber is lost in favour of the viscous component and all the energy dissipation processes. The observed decrease in the loss modulus and the tanδ may be attributed to the breakdown of weak interparticle bonds and the rupture of weak associations between rubber molecules and carbon black. The amplitude at which the maximum in tanδ occurs decreases with increase in ageing time and this is more pronounced for rubber aged at 90°C. The reason for this is probably the reduction in rubber molecular chain segment length caused by the crosslinking and scission reactions of ageing. Shorter chain segments have less extensibility and so the breakdown of rubber to filler bonds during the dynamic cycling will necessarily occur at a smaller strain.

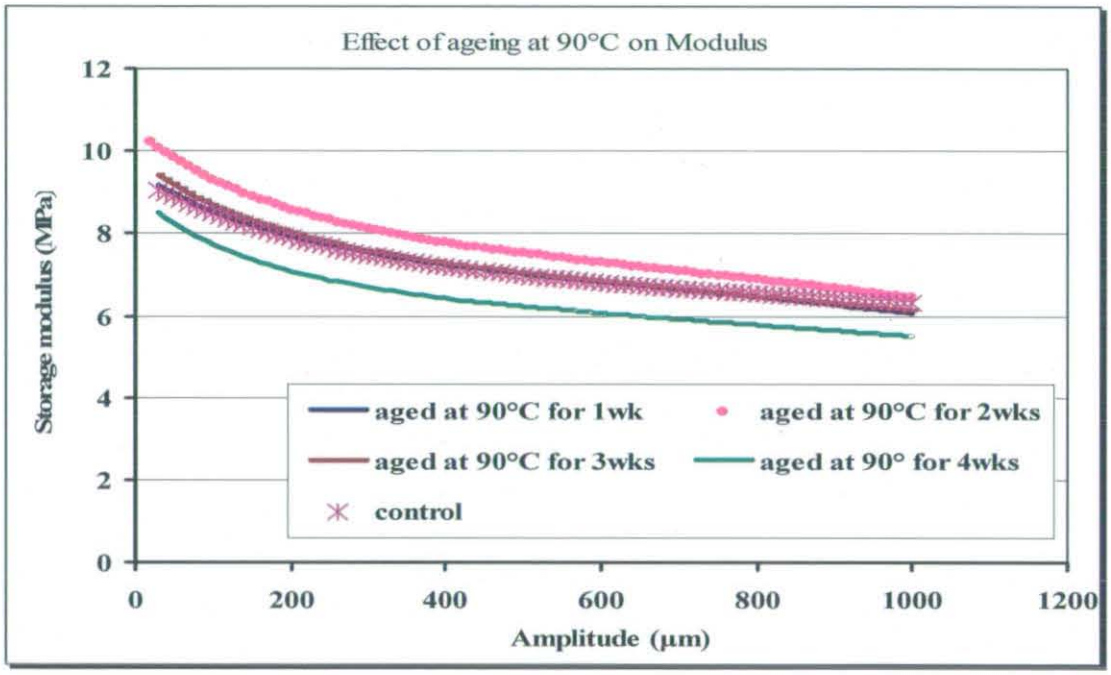

Figure 7.4: Effect of strain amplitude on the storage modulus of natural rubber compound aged at 90°C

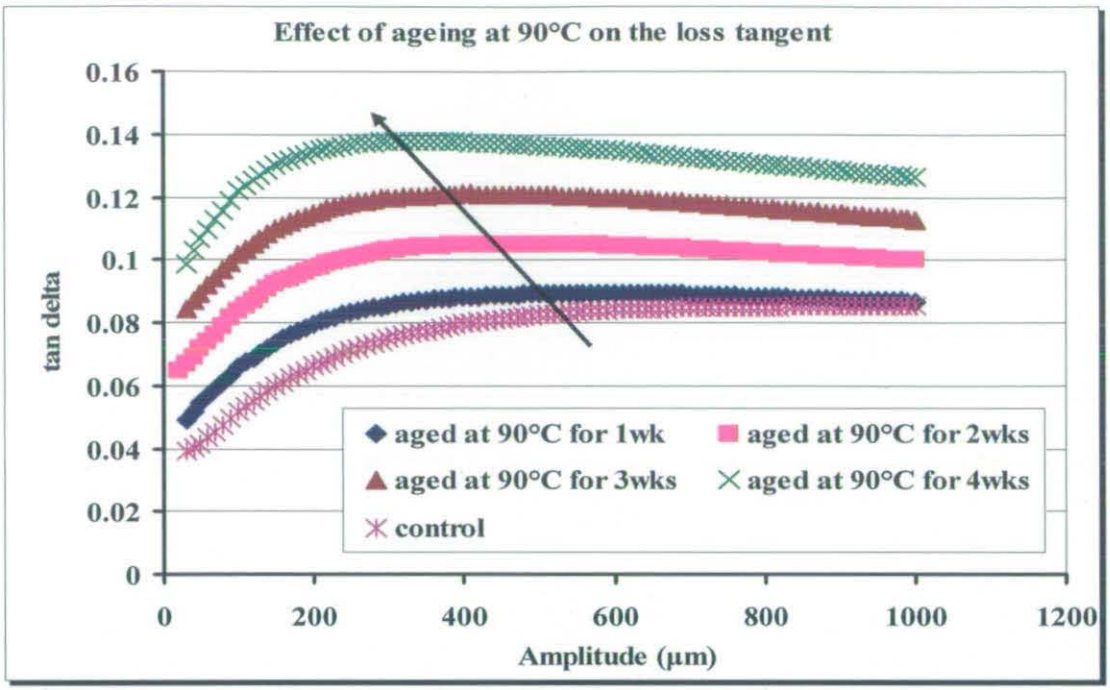

Figure 7.5: Effect of strain amplitude on the loss tangent of the natural rubber compound aged at 90°C

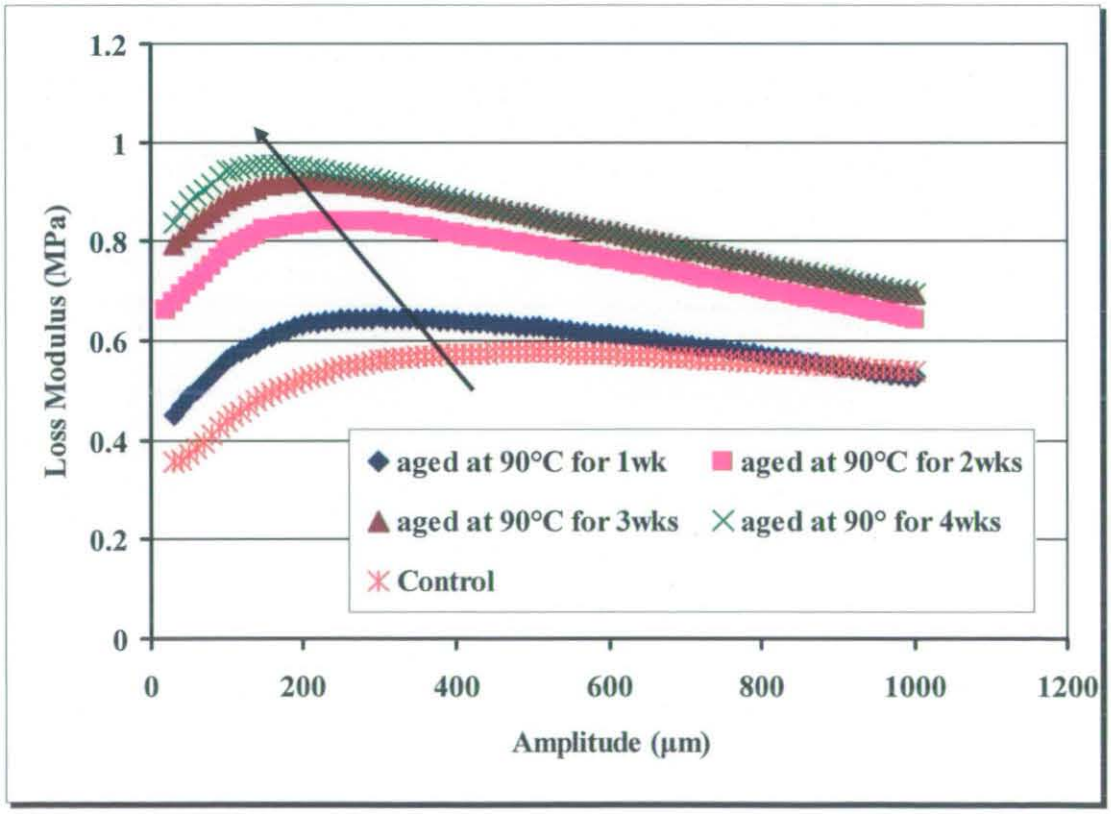

Figure 7.6: Effect of strain amplitude on the loss modulus of the natural rubber compound aged at 90°C

7.3 Effect of Temperature Variation on the Dynamic Mechanical Properties of the Aged Natural Rubber Compound

Dynamic mechanical measurements were carried out on the aged natural rubber samples, with a temperature sweep of –100°C to 120°C, and a strain amplitude of 256μm. Dynamic storage and loss modulus and tanδ results are shown in Figures 7.7 to 7.12

Figures 7.7 – 7.12, indicate that as the ageing time is increased for a particular temperature, the tanδ peak reduces in height slightly presumably due to increased crosslinking and chain scission that reduces chain segment length, resulting in a lowering of rubbery behaviour. Figures 7.10, 7.11 and 7.12 show that the Tg for rubber aged at 110°C (Tg = -40°C) is lower than that aged at 90°C (Tg = -35°C). Figures 7.10 and 7.11 also indicate a decrease in Tg with increased ageing time at 110°C. However, there is no change in Tg with ageing at the lower temperature of 90°C. It appears that only aging under the most severe conditions results in a decrease in Tg, probably due to the prominence of scission reactions.

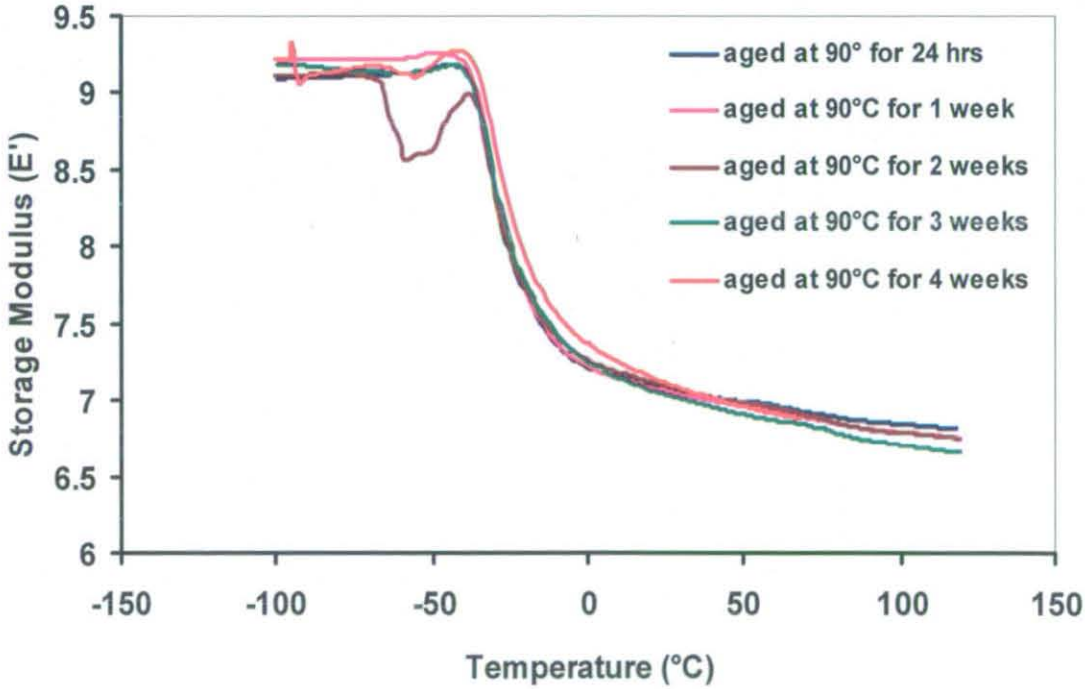

Figure 7.7: Effect of ageing at 90°C on the storage modulus

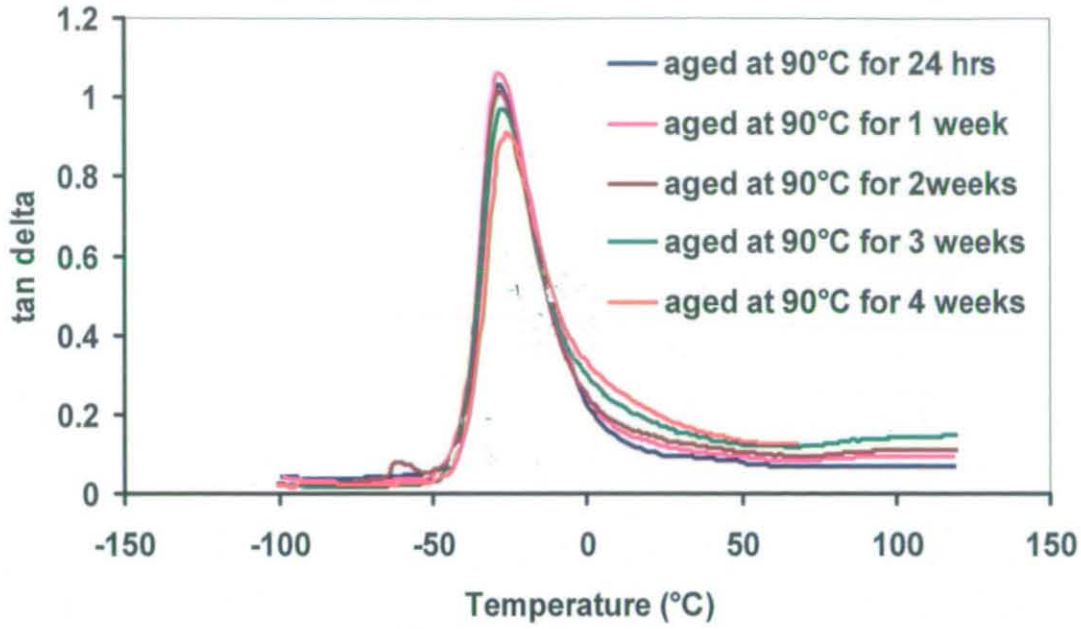

Figure 7.8: Effect of ageing at 90°C on the loss tangent

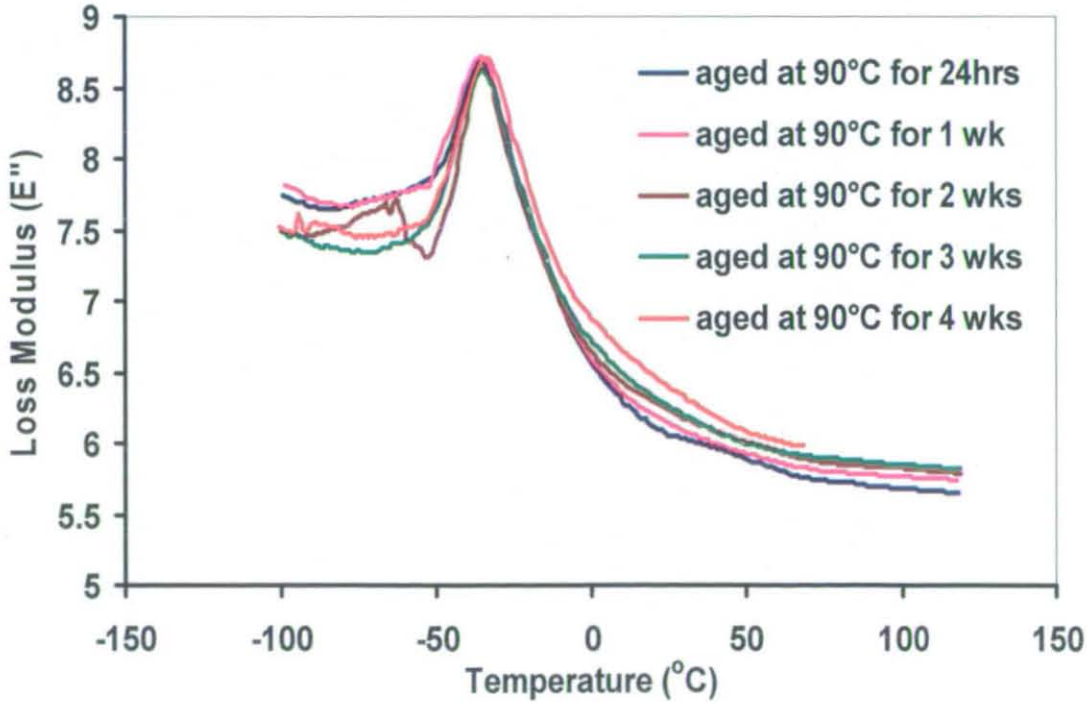

Figure 7.9: Effect of ageing at 90°C on the loss modulus

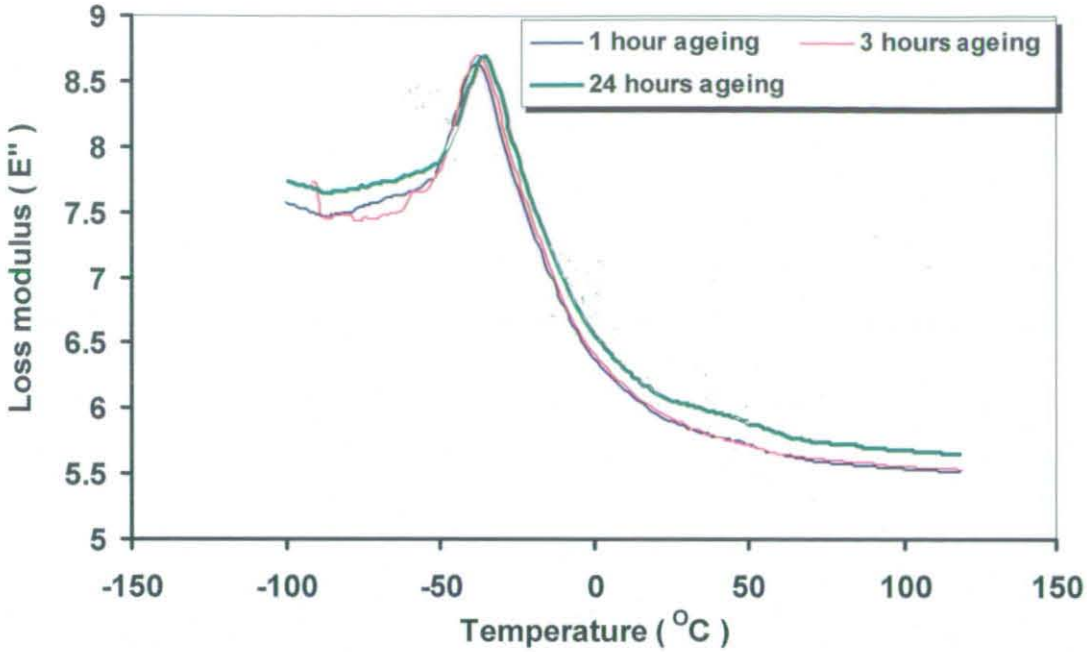

Figure 7.10: Effect of ageing at 110°C on the loss modulus

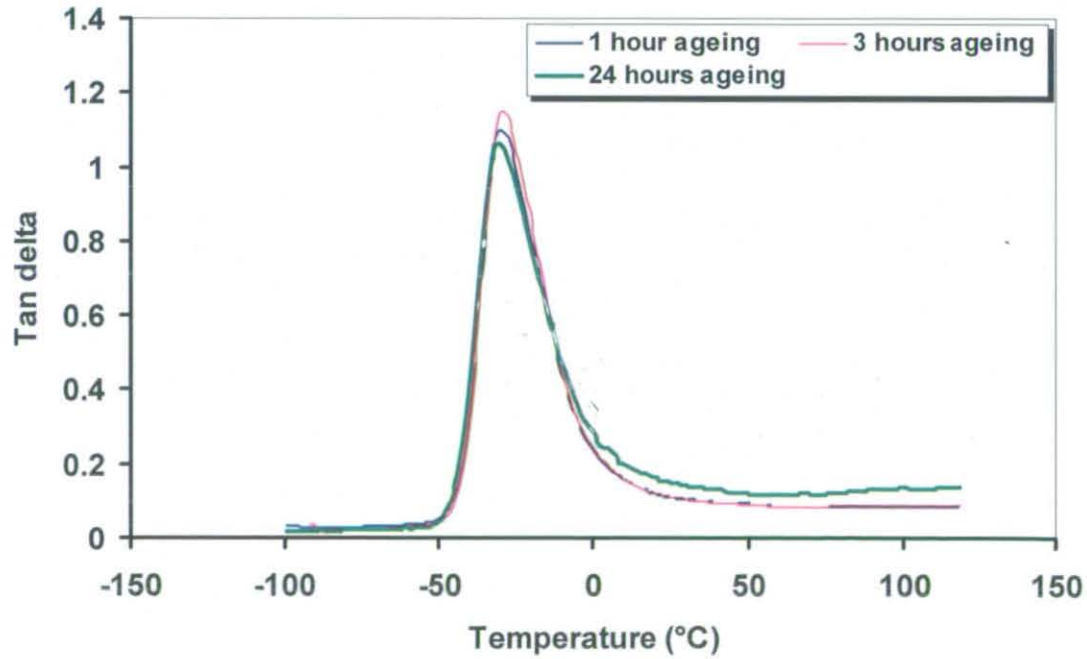

Figure 7.11: Effect of ageing at 110°C on the loss tangent

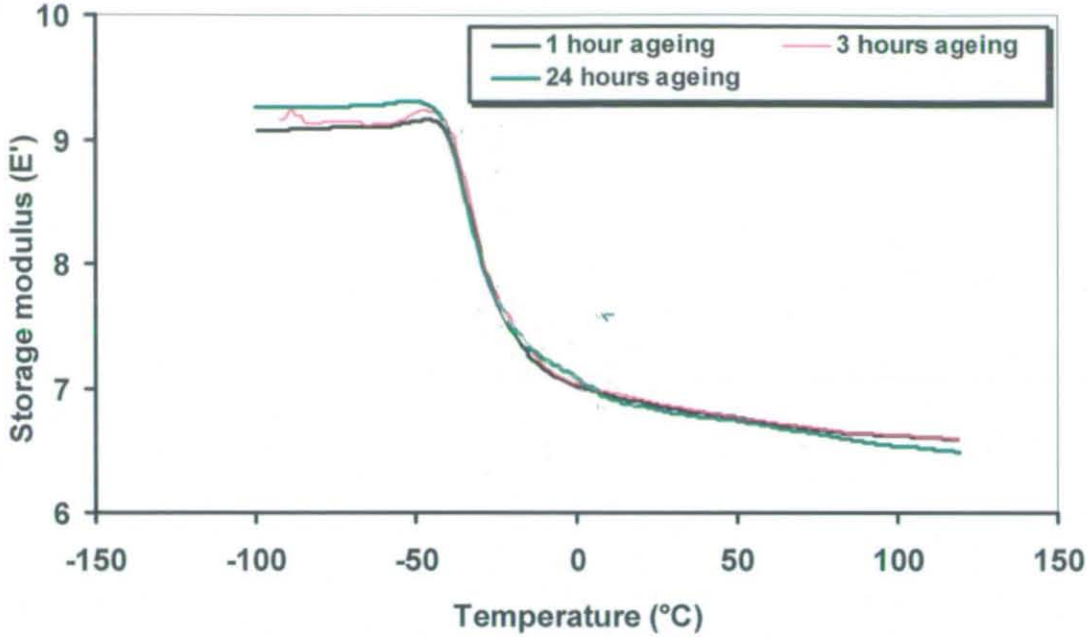

Figure 7.12: Effect of ageing at 110°C on the storage modulus

7.4 Effect of Ageing on Crack Growth

The effect of ageing on crack growth was investigated using static or single cycle tests (trouser tear test) and dynamic tests (fatigue testing using a single edged notch test).

7.4.1 Effect of Ageing on Tearing Energy

Figure 7.13 shows the tearing energy of the natural rubber engine mount compound aged at various temperatures. There is a general decrease in tearing energy with increase in ageing time. However, at the lower ageing temperatures of 70°C and 80°C there is a low, broad peak in tearing energy observed at relatively long ageing times; approximately 400 hours and 180 hours at 70°C and 80°C respectively. This maximum in the tear strength might be as a result of increase in energy dissipation which is associated with the types of crosslinks present in the rubber. At low ageing temperatures polysulphidic crosslinks are more likely to survive and these are better able to dissipate energy at the crack tip and so increase tearing energy. Higher temperature ageing may result in more monosulphidic crosslinks, resulting in a restriction of chain motions which reduces energy dissipation by hysteresis and so crack propagation is enhanced.[8, 9] Similar trends were observed for modulus data in

section 6.5, where high temperature ageing gave higher modulus at shorter ageing times as a result of formation of shorter monosulphidic networks. Ageing times where initial increases in modulus were observed also gave low tearing energies for these ageing times.

At high ageing temperatures, the stick – slip and or knotty tear is reduced and more continuous tear is observed. Strain –induced crystallisation at the tip of the crack has been advanced by Greensmith and Thomas as the reason why natural rubber does not tear continuously[10] .Therefore the reduction in knotty tear at higher ageing temperatures or longer ageing times is probably due to ageing affecting the molecular structure in such a way as to reduce its ability to strain crystallise.

Using the time temperature superposition approach described in section 6.4.3.2 with all data shifted to the reference temperature of 70°C, (Figure 7.14) the activation energy for the effect of ageing on tearing energy of the rubber, was determined to be about 135 kJ/mole.(Figure 7.15). Values of between 83 kJ/mole to 133 kJ/mole were obtained by Gent et. al.[11] on measurements of the tear strength of SBR and BR vulcanizates in their studies on the effect of ageing on strength of elastomers.[11] Another way of looking at the kinetics in terms of tearing energy is to consider the tear energy at particular percentages of the original value. Considering 50% or 60% of the original tearing energy of the unaged NR as a failure criterion (Table 7.1) and the corresponding life time (t_c) for the aged rubber compounds to attain this level of tear energy, then applying the Arrhenius equation for the time to attain this limit, we have:

$$t_c = \beta e^{-E_a/RT} \qquad [7.1]$$

Where t_c is the time to attain 50% or 60% of the damage level, β, a constant, *Ea* the activation energy and R is the universal gas constant. Using the logarithmic form of the equation, a plot of the log of the "life time", tc, against 1/T (Figure 7.16) was drawn

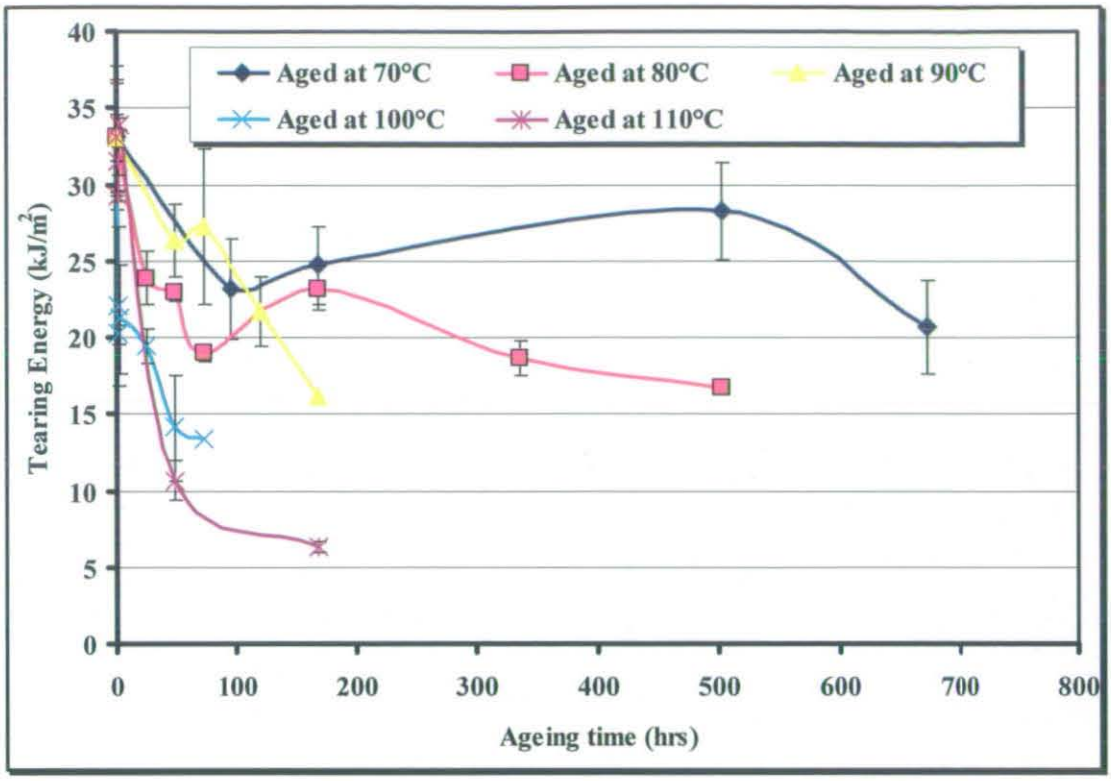

Figure 7.13: Effect of ageing on tearing energy of NR compound cured at 140°C.

It is worthwhile mentioning that an extrapolation was made at certain ageing temperatures such as 70°C in order to estimate the time at which the failure criterion was met.

Table 7.1: Critical life with respect to tearing energy for the aged natural rubber compound

		50% reduction in tearing energy		60% reduction in tearing energy	
Temperature (K)	1/T	tc	log tc	tc	log tc
343	0.002915	840	2.924279	720	2.857332
353	0.002833	504	2.702431	336	2.526339
363	0.002755	168	2.225309	244	2.38739
373	0.002681	48	1.681241	24	1.380211
383	0.002611	24	1.380211		

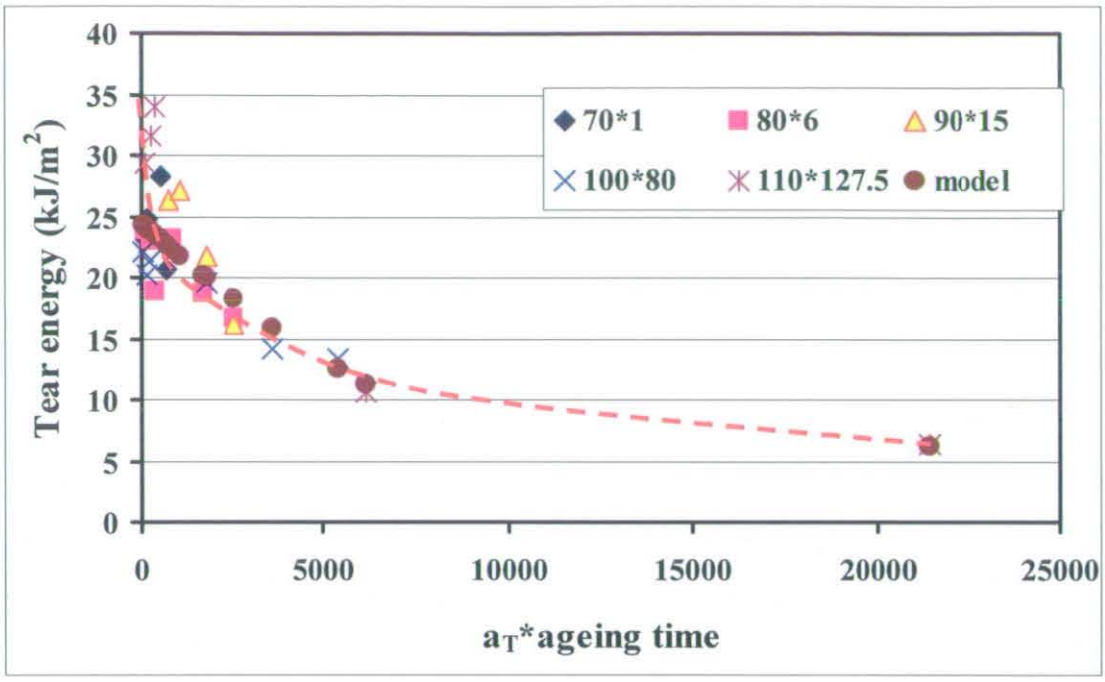

Figure 7.14: Ageing time /ageing temperature superposition plot of the fracture energy

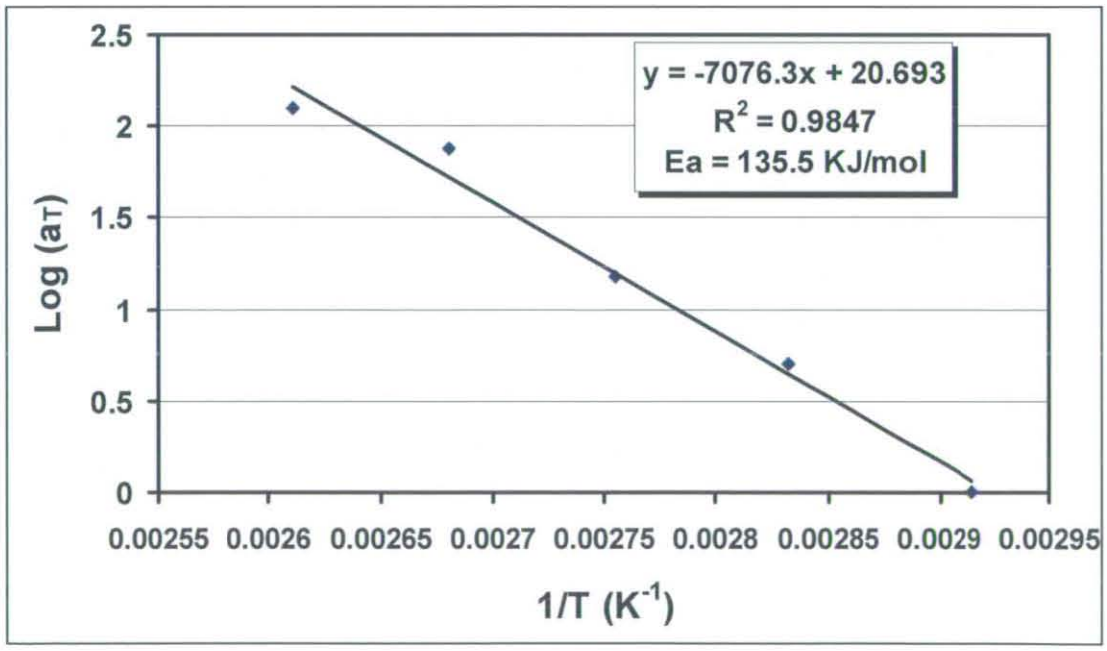

Figure 7.15: Arrhenius type plot of shift time with ageing temperature for tearing energy

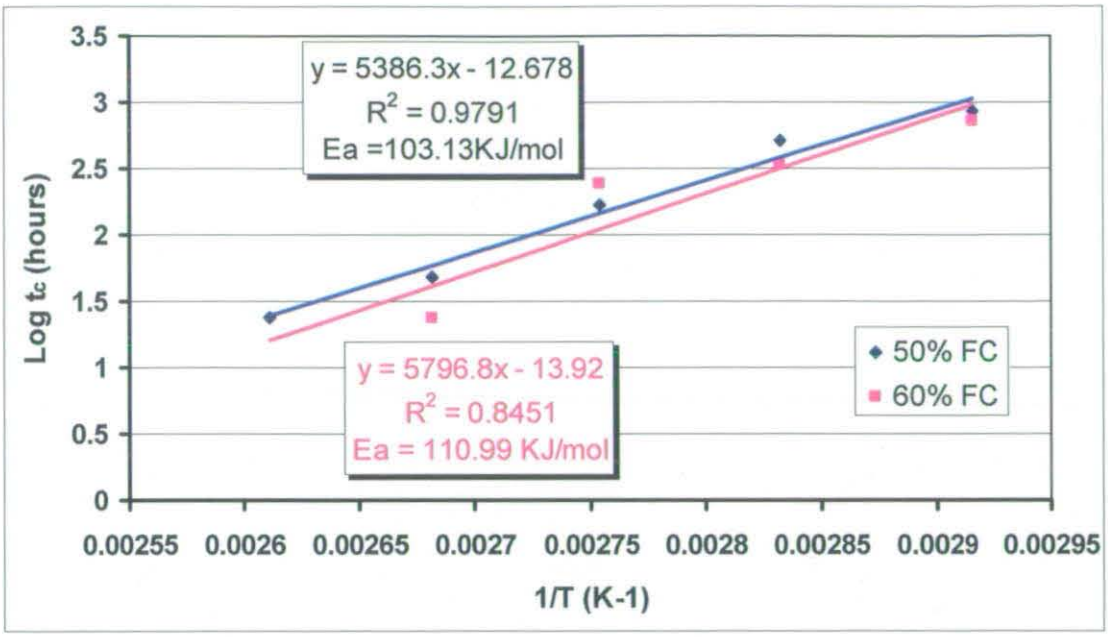

Figure 7.16: Arrhenius plots of the log of critical life

From these plots the activation energy needed to attain the required life time at 50% and 60% of the unaged tear energy was respectively about 103 kJ/mole and 111 kJ/mole. The difference in the value of the activation energy obtained between the time temperature superposition approach (135 kJ/mol) and the time to failure approach (110 kJ/mol) may be due to the way the data is handled. While the selected failure criterion deals with individual temperatures or single data points, the TTS approach makes use of all the available data to get a master curve. However, since the shapes of the curves are somewhat sinusoidal, a proper superposition cannot be obtained and as such results obtained through the TTS method are therefore approximations.

7.4.2 Effect of Ageing on Dynamic Crack Growth

The crack growth rate $\frac{dC}{dN}$ for the natural rubber aged at 100°C for 24 hours to 4 days is plotted as a function of the tear energy (fracture energy) t on a log – log scale (Figure 7.17). The rate of crack growth increased linearly with tearing energy. As discussed in Section 4.2.2, crack growth in rubbery materials generally follows the

power law relationship : $\frac{dC}{dN} = AT^{\alpha}$ taking logs on both sides gives

$$\log \frac{dC}{dN} = \log A + \alpha \log T \qquad [7.2]$$

where A and α are material constants.

Fatigue crack growth resistance was found to decrease with increase in ageing time for a given temperature. The reduction in the crack growth resistance may be due to loss in strength in the natural rubber compound aged at 100°C as has been explained in section 6.4.2. The apparent tear strength decreases with increase in ageing time for the samples aged at 100°C (Section 7.4.1). This ageing condition causes a massive decrease in the fatigue life to almost 30% of its original life (Section 7.4.3).

The values of the power index α, in the power law are not sensitive to ageing time, with values ranging from 2.20 – 2.44. These values agree with what is obtained in the literature for natural rubber which according to Lake et.al. was between 2 and 4.[13] As described by Shiyoung Kaang et.al.[14] in their studies comparing the fatigue resistance of NR and SBR, the low value observed for α in NR compounds indicated good crack growth resistance and was attributed to strain induced crystallisation at the crack tip of the NR. Although little difference was observed in the values of α obtained at different ageing times, the values of A decrease with ageing time. Though the values of alpha, α, are similar, the crack growth rate increases with ageing therefore it is reasonable to suggest that the threshold energy for the onset of mechanical crack growth (G_o) has decreased with ageing. It is likely that the decrease in threshold energy may be due to the increase in crosslink density with ageing time as observed in section 6.3.

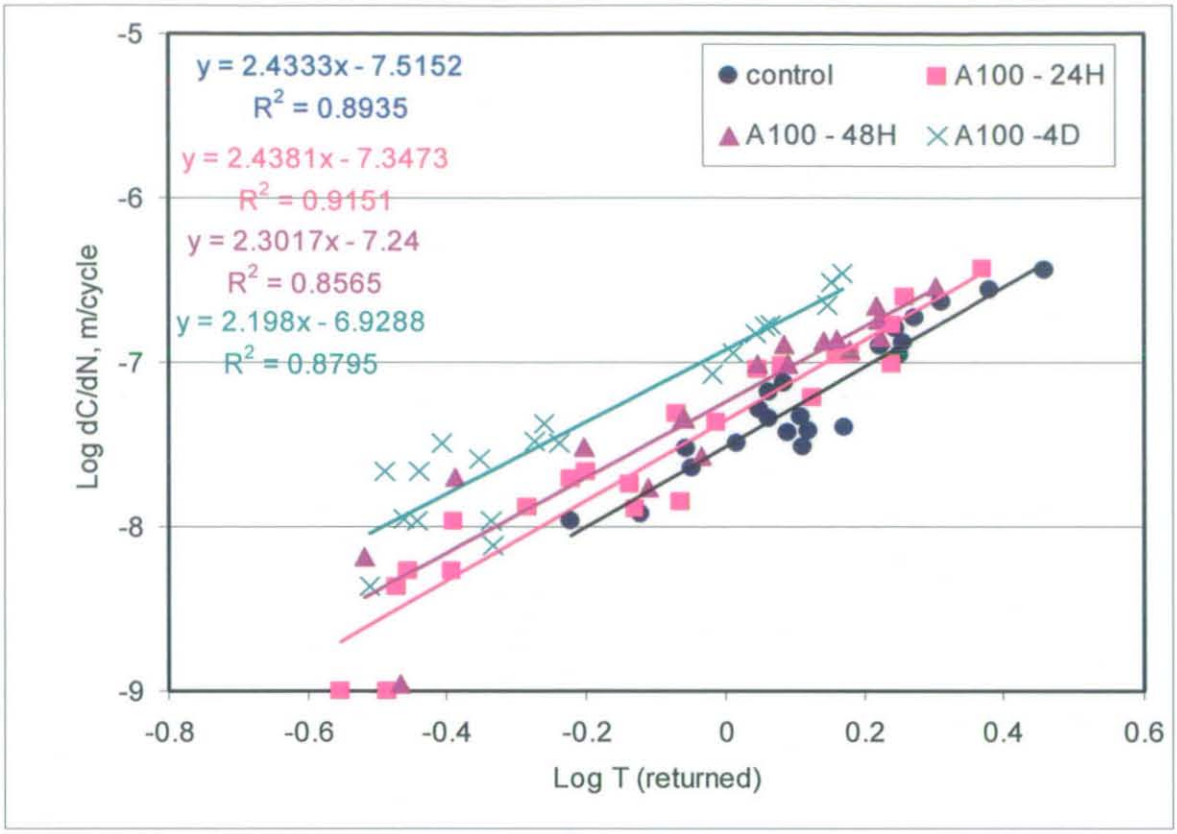

Figure 7.17: Effect of ageing time on crack growth resistance of a NR engine mount compound

7.4.3 Effect of Ageing on Fatigue Life

As ageing temperature and ageing time increases, the fatigue life decreases significantly (Figure 7.18). Several reasons may be advanced for the observed trend. It is well known that natural rubber strain crystallises, and that strain crystallisation inhibits crack growth. This effect is usually observed at low temperatures. The strain crystallisation is reduced as a result of oxidative ageing and once a crack is initiated, the fatigue crack growth rate significantly increases resulting in a decrease in the fatigue life[17].

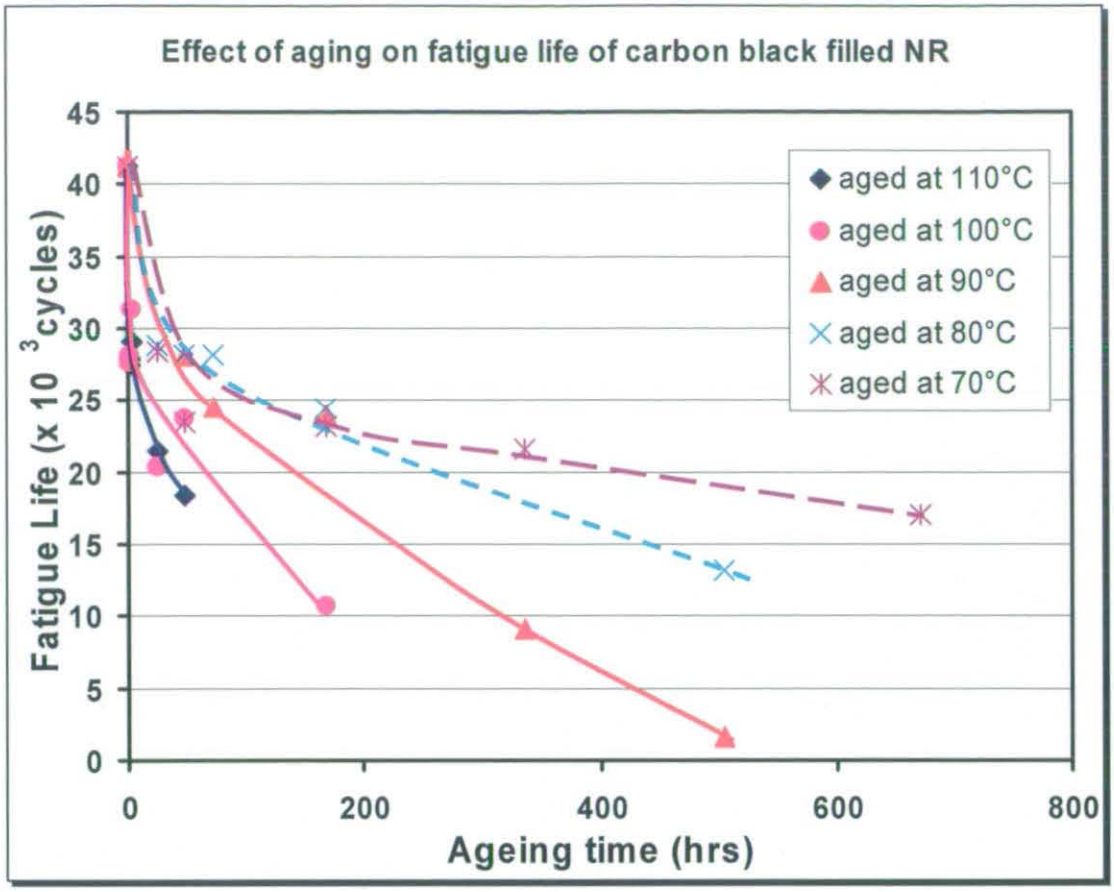

Figure 7.18: Fatigue life for aged natural rubber samples

Another reason for the decrease in fatigue life is that during ageing, antioxidants are consumed and oxygen diffuses into the rubber bringing about chain cleavage, but at higher temperatures, there is diffusion limited oxidation, resulting to a hard skin forming at the surface of the rubber which can easily crack during fatigue process. These cracks once initiated propagate easily resulting in failure of the compound. Mars and Fatemi[18] also found that ageing brought about a decrease in the fatigue life and attributed this to embrittlement of the rubber. Furthermore, the dominant types of crosslinks formed during ageing also affect the fatigue life. Polysulphidic crosslinks are said to be superior to monosulphidic crosslinks or carbon – carbon crosslinks. This is because the polysulphidic networks are long and highly mobile, and have the ability to break and subsequently reform. This leads to increased energy dissipation due to hysteresis and hence to crack tip blunting[18]. As ageing converts polysulphidic to monosulphidic crosslinks, this ability to reduce crack growth results in a loss of

fatigue life. Other crosslinking and chain scission reactions during ageing will also reduce fatigue life.

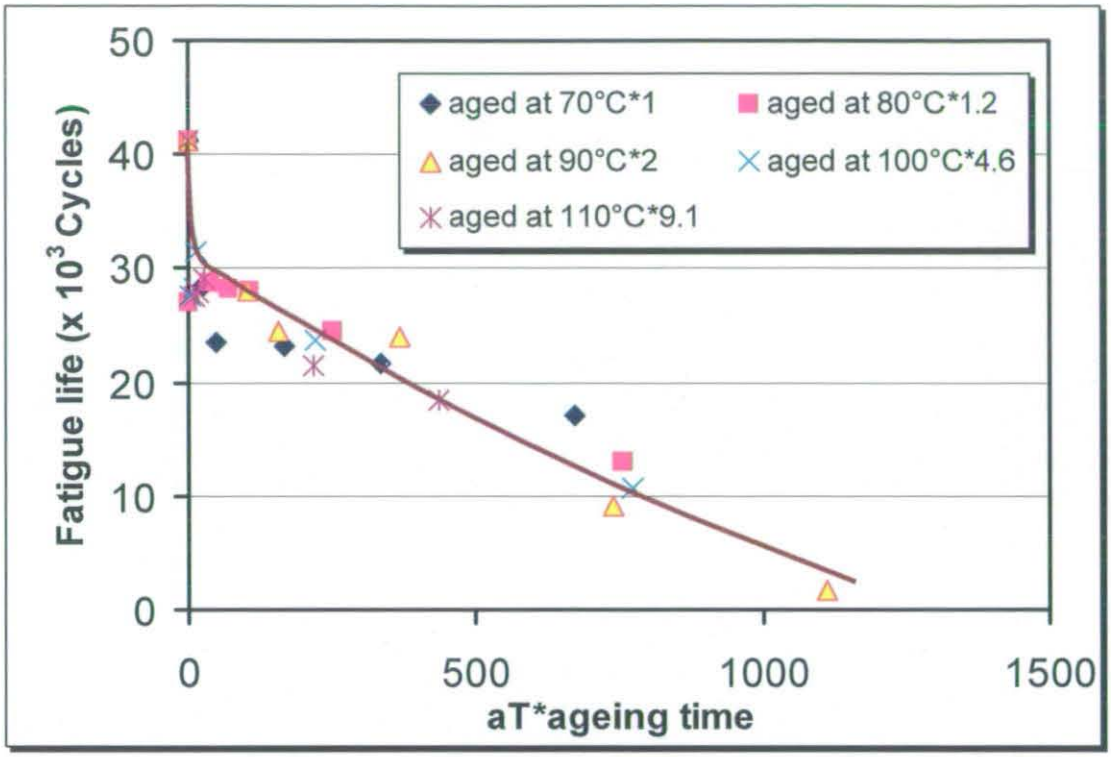

Figure 7.19: Time temperature superposition graph for fatigue measurements after static ageing

Using the time temperature superposition approach, to analyse data, (Figure 7.19), the activation energy of ageing as it affects fatigue life was calculated to be about 60 kJ/mol (Figure 7.20). This value of activation energy for the effect of ageing on fatigue is much lower than for the effect of ageing on tearing energy measured by the trouser tear method (135 kJ/mol) (section 7.4.1) or the tensile strength (93 kJ/mol) (section6.4.3.2).Inhomogeneity in crosslink density and chain lengths between crosslinks introduced during ageing potentially causes a large reduction in tensile strength, because chains are broken successively. In fatigue, the Mullins effect can to some extent equalise some of the inhomogeneities, hence, reducing some of the effect of ageing on crack propagation and so reducing the apparent activation energy of ageing.

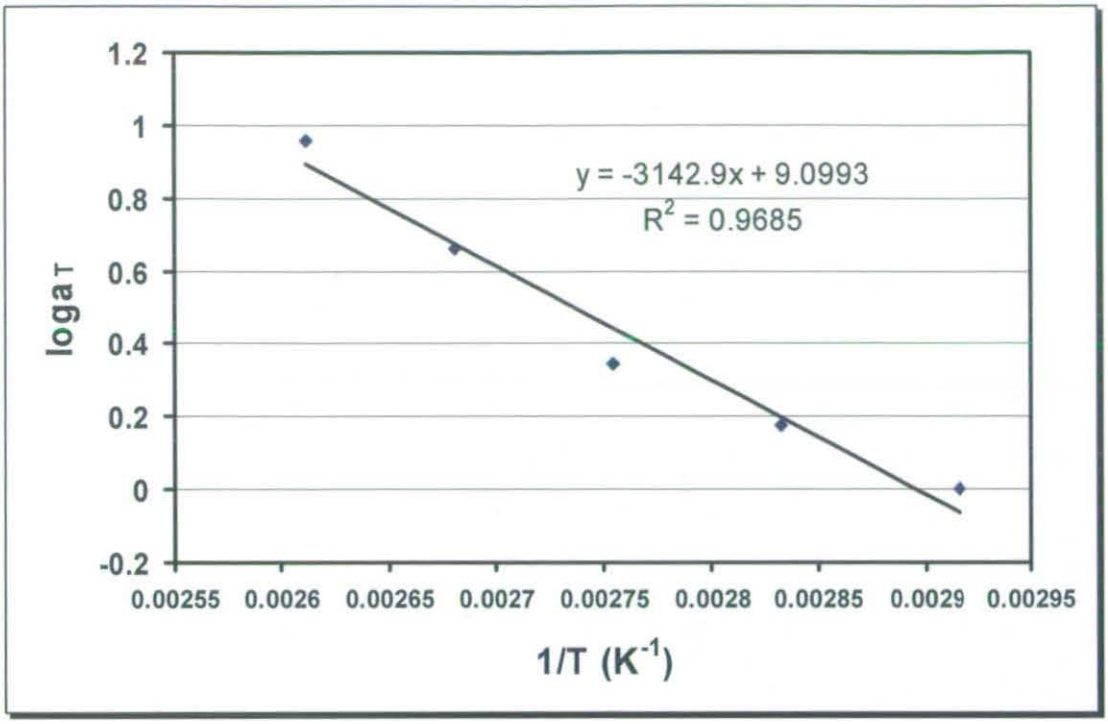

Figure 7.20: Arrhenius type plot for the shift factors against inverse absolute temperature

7.4.4 : Effect of Dynamic Ageing on Fatigue Life

Dynamic ageing was carried out as explained in section 5.8.1.1. The rubber was placed on a fatigue machine with a thermo - regulated hot air gun supplying the heating source. As can be observed, the fatigue life reduces with increase in temperature. (Figure 7.21) The deterioration in the fatigue life as explained by Cadwell et. al.[20] is two fold, firstly as a result of the vibration or oscillation of the sample at the elevated temperature during the cyclic fatigue and secondly, the deterioration due to heat ageing which would result from keeping the sample at the ageing temperature without vibration. From the results on statically aged rubber samples at 70°C that underwent fatigue at ambient temperature, it could be observed that it will take at least 48hrs (Figure 7.21) for the statically aged rubber to attain the same fatigue level as the dynamically aged rubber after 4.5hours at the same temperature. Therefore deformation during ageing accelerates the ageing effect. One

of the reasons for this could be that bonds broken by oxidation during mechanical fatigue are not able to reform, as deformation separates the broken ends.

It is possible that temperature rise due to hysteresis during fatigue contributes to thermo-oxifative ageing. For this reason, the temperature increase in the rubber due to heat build-up with fatigue cycles was monitored using a thermal imaging camera (Figure 7.22). Tests were carried out at 17°C, which was subtracted from the recorded temperature to obtain the temperature rise of the rubber samples. The temperature was recorded until a steady-state value was reached at when the amount of heat generated was equal to that dissipated from the sample. The plateau in temperature may also be affected by the Mullins effect, in which the decrease in stiffness of the rubber, due to stress softening of the rubber engine mount compound during the first few fatigue cycles will reduce the heat build-up in later cycles[21].

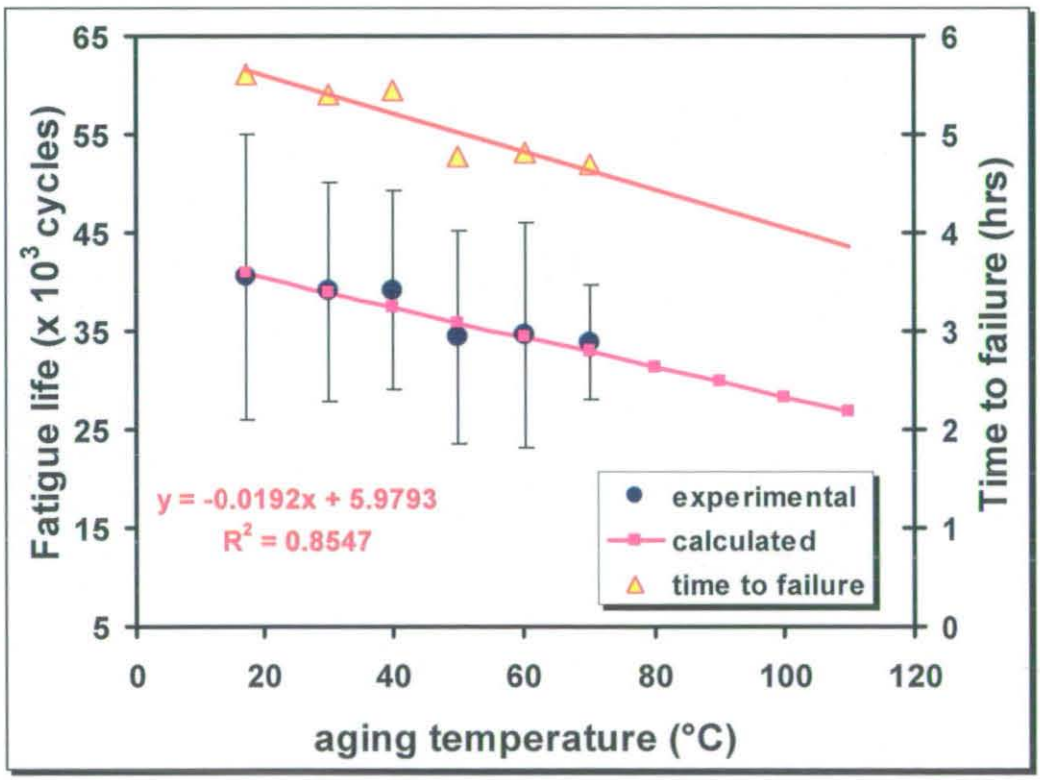

Figure 7.21: Effect of dynamic ageing on fatigue life of NR compound.

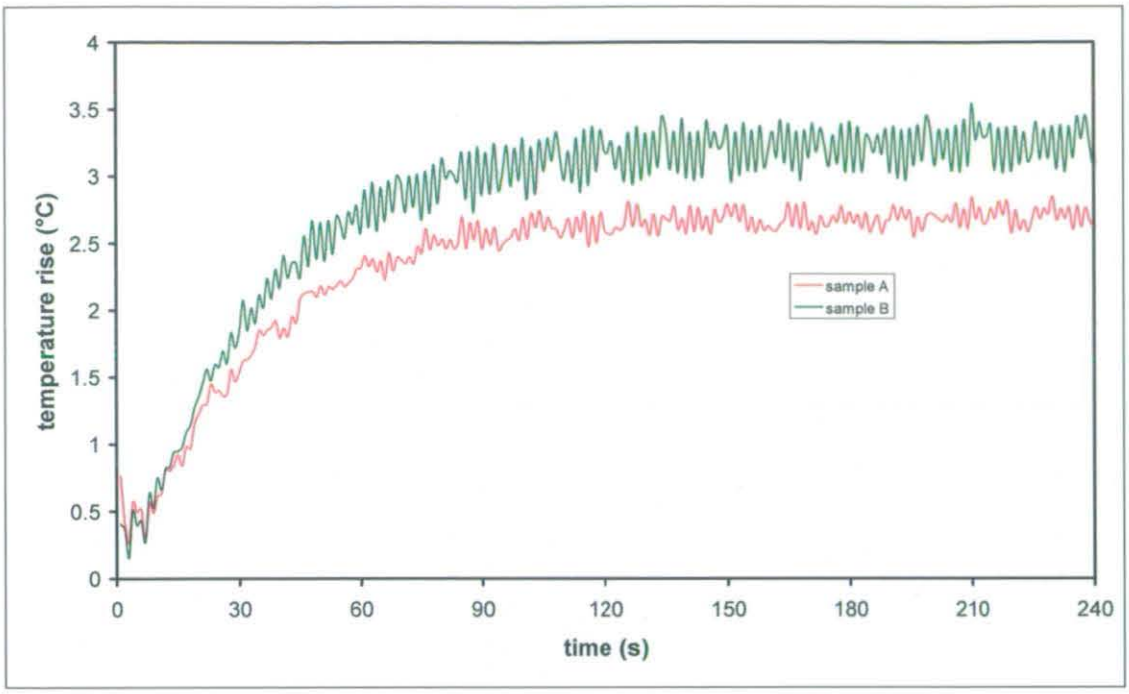

Figure 7.22: Temperature rise with time during fatigue of natural rubber samples (A and B) monitored by thermal imaging camera

The small temperature increase observed indicates that increased ageing due to higher temperatures in the rubber during dynamic ageing might not be responsible for the greater effect of ageing on fatigue life.

7.5 Conclusion:

This study revealed that, for a given tearing energy, the rate of crack growth for the filled engine mount compound aged at 100°C increases with increase in ageing time. This was probably as a result of loss in crystallinity and increased crosslinking density. For samples aged between 70°C and 110°C the fatigue life reduces with ageing time and the activation energy for ageing as it affects fatigue of the engine mount compound was found to be about 60 kJ/mol.

The tearing energy using the trouser tear approach was found to reduce with ageing time and temperature and the activation energy was found to be about 135 kJ/mol. Meanwhile if a 50% or 60% reduction in tearing energy compared to the original was considered as a failure criterion, the activation energy for tearing was about 103°C

and 111°C respectively. These activation energy values are in close agreement to that obtained by Gent et al[11]

7.6 References

(1) Gent, A. N. In Engineering with rubber, How to design rubber compounds; Hanser Verlag: Munich, 2001; pp 88.

(2) Gent, A. N.; Hindi, M. *Rubb. Chem. Technol.* **1990**, *63*, 123-134.

(3) Ellis, R. L. **2006**. Private Communication

(4) Lake, G. J. *Rubb. Chem. Technol.* **1995**, *68*, 435.

(5) Payne, A. R. *Rubb. Chem. Technol.* **1964**, *39*, 1190-1243.

(6) Payne, A. R. *Rubb. Chem. Technol.* **1963**, *36*, 432-442.

(7) Payne, A. R.; Whittaker, R. E. *Rubb. Chem. Technol.* **1971**, *44*, 440-478.

(8) HA Anh, T.; Vu – Khanh, T. *J. Mater. Sci.* **2005**, *40*, 5243-5248.

(9) Ismail, H.; Poh, B. T. *Eur. Polym. J.* **2000**, *36*, 2403-2408.

(10) Greensmith, H. W.; Thomas, A. G. *J. Polym. Sci.* **1955**, *18*, 189-200.

(11) Gent, A. N.; Liu, G. L.; Sueyasu, T. **1991**, *TR - 27*, 42.

(12) Chun, H.; Gent, A. N. *Rubb. Chem. Technol.* **1996**, *69*, 577-590.

(13) Lake, G. J.; Thomas, A. G. In Gent, A. N., Ed.; Engineering with Rubber, How to design rubber compounds; 2001; pp 100.

(14) Kaang, S.; Woong Jin, Y.; Huh, J.; Lee, W.; Bin Im, W. *Polym. Test.* **2006**, *25*, 347-352.

(15) Zhao J; Ghebremeskel G. N. *Rubber Chemistry and Technology* **2001**, *74*, 409.

(16) Kallrath, J.; Altstadt, V.; Schloder, J. P.; Bock, H. G. *Polym. Test.* **1999**, *18*, 11-35.

(17) Young, D. G. *Axel Physical testing services report* **July 2001**, *VI*, 1.

(18) Mars, W. V.; Fatemi, A. *Rubb. Chem. Technol.* **2004**, *77*, 391.

(19) Legorju – Jago, K.; Bathias, C. *International Journal of Fatigue* **2002**, *24*, 85-92.

(20) Cadwell, S. M.; Merrill, R. A.; Sloman, C. M.; Yost, F. L. *Rubb. Chem. Technol.* **1940**, *13*, 304-315.

(21) Kim, W. D.; Lee, H. J.; Kim, J. Y.; Koh, S. *International Journal of Fatigue* **2004**, *26*, 553-560.

CHAPTER 8: Effect of Nature of Flaws on Failure Properties

8 Introduction

The point of initiation of a fracture in rubber is usually at flaws, which are macroscopic or microscopic imperfections or inhomogeneities in the rubber. The flaws could be voids, cuts or notches introduced during moulding and/or curing of the rubber compounds. Others flaws include filler agglomerates and memory interfaces (weld lines). In order to assess the effect of various types of flaw on the failure properties of a natural rubber engine mount compound, different types of flaw were introduced into rubber specimens before, during or after curing. Tensile and fatigue measurements on the flawed samples were then made. The types of flaw examined were memory interfaces, carbon black agglomerates and pinholes. In addition, the kinetics associated with healing of a memory interface during moulding, was investigated.

8.1 Effect of Memory Interfaces on Failure Properties of an Engine Mount Compound

It is well established that weld lines in certain elastomers and other engineering materials are potential points of failure. [1, 2] Therefore, experiments were carried out to assess the effect of a weld line (memory interface) formed during processing on the properties of a natural rubber compound. In the current study the more general term "memory interface" is used to describe previously free-surfaces which have come together during processing. The memory interface might occur when two flow fronts come together during injection moulding. A memory interface would also occur in compression moulding where separate pieces of rubber are placed in a mould to produce a single component. The effects of the memory interfaces on tensile and fatigue properties are discussed in the following section in terms of the influence of cure temperature and proximity to scorch.

8.1.1 Effect of Memory Interface and Cure Temperature on Failure Properties

During curing of rubber components high temperatures are usually used to optimise yield, and to reduce cost of production, compromising to some extent the final properties of the product and therefore its service life. It is well known that cure time and temperature affect the bulk properties of rubber compounds. However, it is also possible that some cure conditions exacerbate the effect of memory interfaces on failure properties while other cure conditions ameliorate the effect. It is for this reason that the effect of cure temperature on the tensile properties of an engine mount compound, with and without memory interfaces, were investigated.

In the first set of experiments, sheets of rubber were pre-cured to well below its scorch level at a temperature of 120°C for 5 minutes (i.e. there was no crosslinking). Complete and partial cuts were made through the sheets to make the memory interfaces and then the sheets were cured completely at temperatures between 150 and 180°C. It can be observed in Figure 8.1 that all the samples cured at 150°C had a higher 300% modulus than those cured at 160°C and 180°C. This is because long cure times at high vulcanisation temperatures may cause a breakage of the backbone chains, resulting in a reduction in the stiffness and strength of the vulcanised rubber (section 6.4.2). The effect of cure temperature on stiffness was also seen in the cure curves. A marching curve was obtained when the rubber was cured at 150°C. At 160°C an equilibrium cure curve was obtained, while a reversion curve was obtained when the rubber was cured at 180°C.

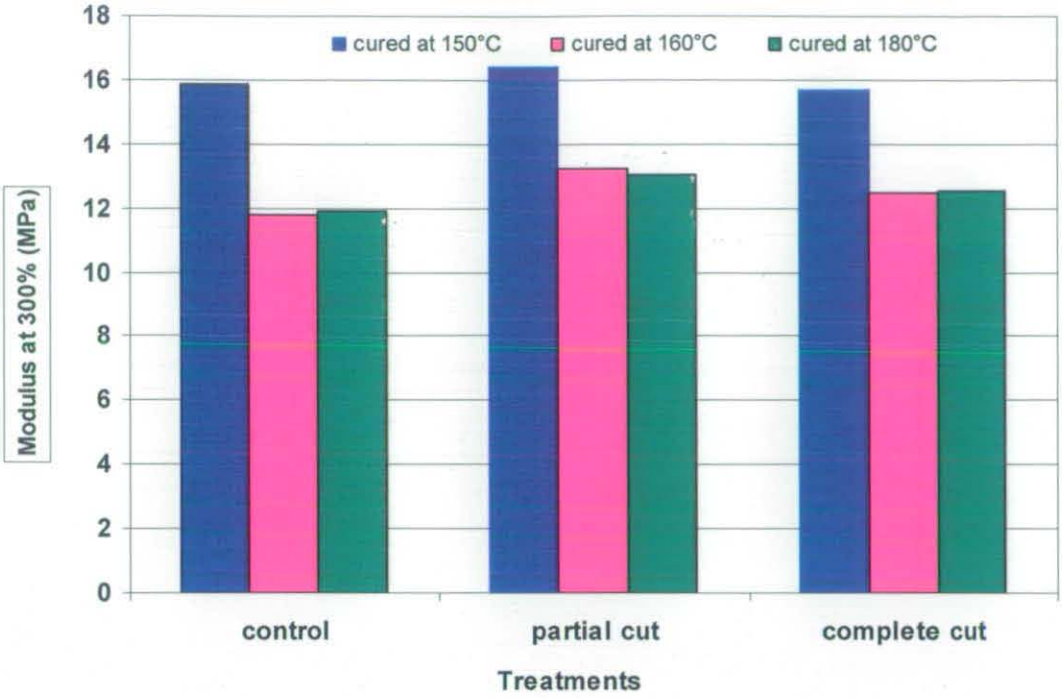

Figure 8.1: Effect of cure temperature and memory interfaces on the modulus of the NR compound

The partial and complete cutting of the samples before curing resulted in a very slight increase in modulus for all cure temperatures, but given the experimental variations, this increase was not significant. The tensile strength remains similar for all samples regardless of cure temperature or the presence of memory interfaces (Figure 8.2). The samples fractured at the region where the cut was introduced in most cases, suggesting an area of weakness at the memory interface. However, it is clear that the introduction of a cut certainly does not significantly reduce stiffness or strength. Stiffness is a bulk property and as such might not be expected to be affected by cutting. Strength, on the other hand, is expected to be affected by the cut, since the resulting memory interface would be likely to be a point of weakness. The results indicate that the cut natural rubber compound is able to "heal" itself, even when it has only a relatively short time available for healing before crosslinking begins (1 minute in the case of 180°C). Even though there is less time available for healing before scorch at 180°C, the higher cure temperature means that the mobility of the molecules is greater and so healing can be faster.

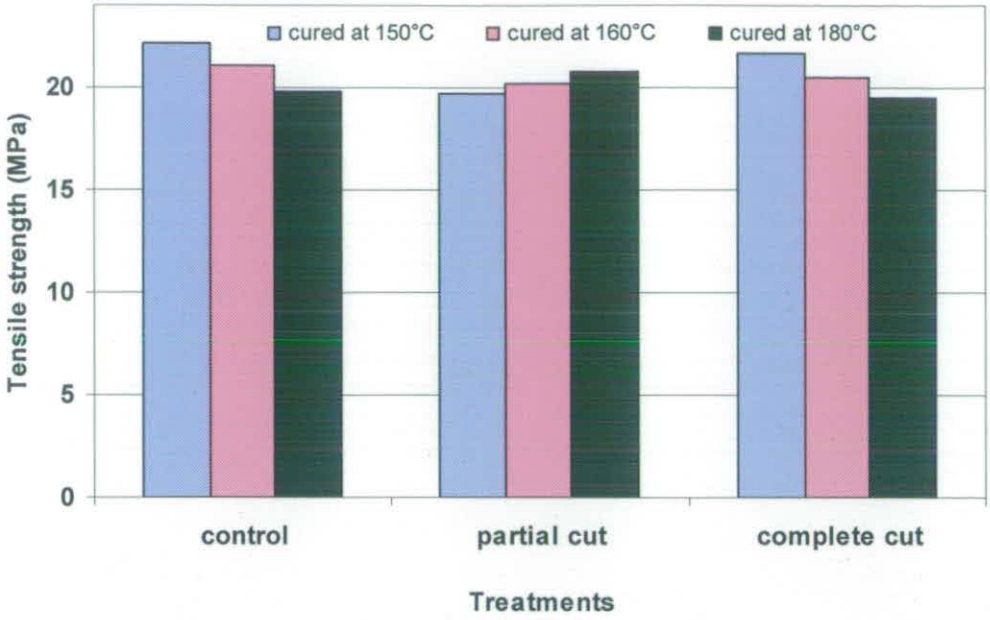

Figure 8.2: Effect of cure temperature and treatment on the tensile strength of a natural rubber compound

However, when the rubber is pre – cured for 3 min. at 140°C, a significant reduction in the tensile strength was observed (Figure 8.3). The result suggests that although the cut was introduced before scorch, there was not sufficient time left for effective healing to take place before scorch. Therefore, more detailed studies were carried out to determine the amount of time required for healing at different temperatures (see section 8.1.4).

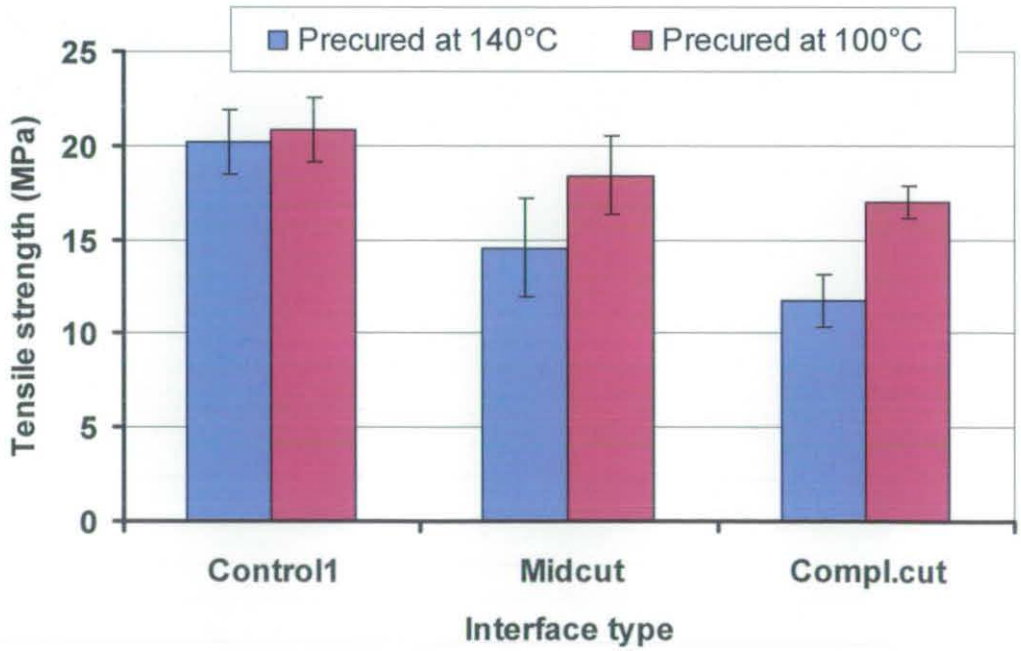

Figure 8.3: Effect of pre – curing at 140°C on memory interface

8.1.2 Fatigue Measurements

Fatigue measurements were carried out on the rubber compound where cuts had been introduced well below scorch, as in the first set of experiments described in the previous section. The results from the fatigue measurements operating at a frequency of 2Hz and a strain amplitude of 100% to zero strain are presented graphically in Figure 8.4. All tests were conducted at temperatures of between 17°C and 22°C. A clear trend in which there is a steady decrease in the fatigue cycles with the various treatments (control without cut > partial cut > complete cut) could be observed for rubbers cured at 150°C and 180°C. Results of the complete cut could not be presented because samples failed just after a complete cycle. The difference in fatigue cycles to failure between the control and cut samples is indicative of the fact that though self healing of the cut was apparent for tensile measurements, (see section 8.1.1), healing was not complete as far as fatigue failure was concerned. The results indicate that fatigue failure is more sensitive to the presence of memory interfaces than single cycle failure.

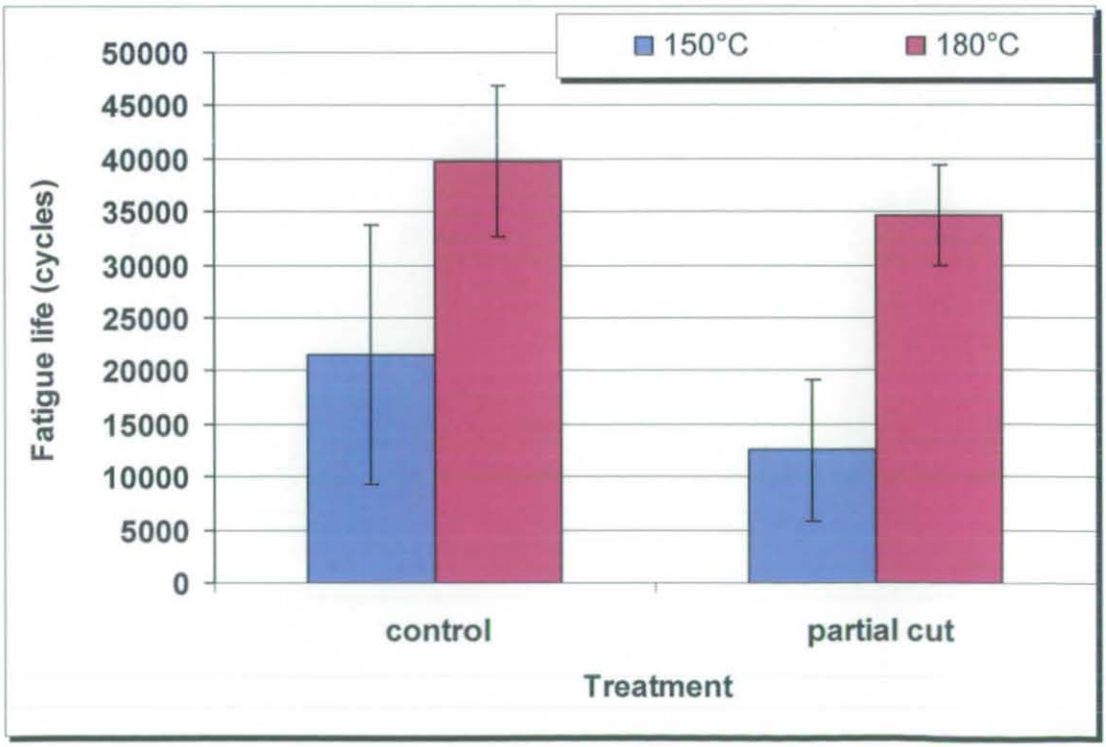

Figure 8.4: Effect of memory interface on the fatigue life of rubber compound.

Apart from the effect of memory interfaces, Figure 8.4 shows that the fatigue life is strongly affected by cure temperature. This is because the rubber cured at 180°C is less stiff than that cured at 150°C (see Fig. 8.4). A low curing temperature results in a higher modulus (section 6.5) and this in turn gives a greater stress or energy input per cycle and so is likely to result in lower fatigue life.

8.1.3 Effect of Pre-curing to Scorch on the Tensile Properties of a Memory Interface

Results from the previous section showed how readily the natural rubber compound was able to self – heal in the absence of scorch. In this section the effect of scorch on the ability of the compound to self – heal is investigated. The natural rubber compound was pre-cured to scorch (Mooney scorch time was used) at 120°C for 13 minutes, partial cuts and complete cuts were carefully made on the pre moulded sheets and cured completely at 150°C and 180°C. The results are compared with those pre - cured below scorch.

8.1.3.1 Effect of Pre-curing to Scorch on Modulus

The effect of pre-curing to scorch of the natural rubber compound on modulus is indicated in Figure 8.5. The modulus is lower for higher vulcanisation temperature as commented on section 8.1.1.

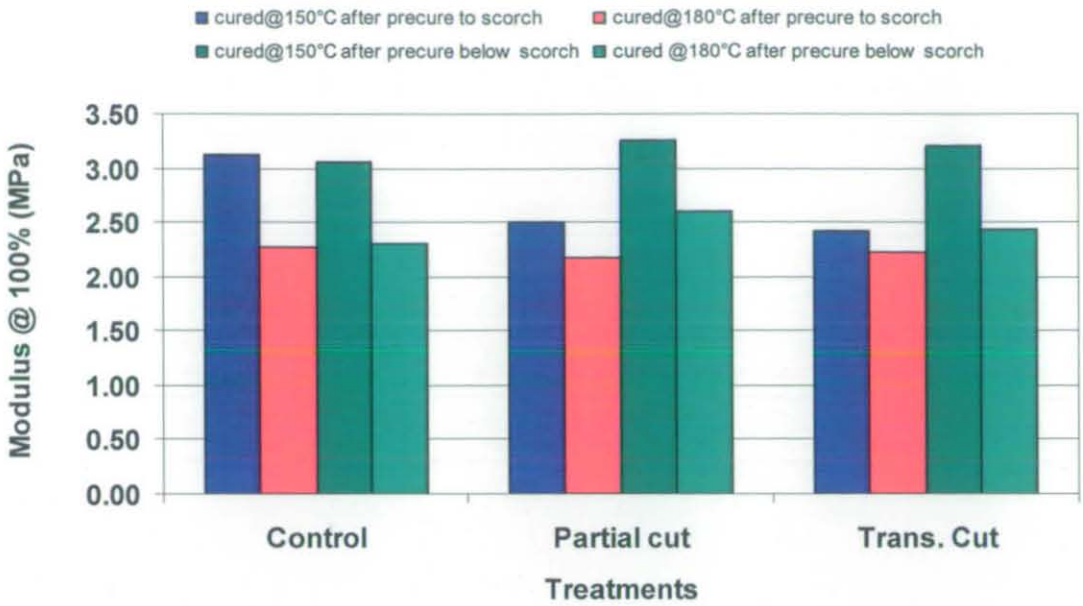

Figure 8.5: Effect of pre-curing to scorch on the Modulus of natural rubber compound

For the partially and completely cut samples pre-cured to scorch, before curing at 150°C, the modulus was found to be lower than for samples cured below scorch. This is because at scorch some crosslinks have been formed which are disrupted or broken upon introduction of a cut. Upon completion of the cure the interface would have fewer crosslinks and the lower level of crosslinking and entanglement across the interface would reduce the stiffness of this region and hence reduce overall modulus. Although the effect of cure temperature could clearly be observed, no significant difference in modulus was observed for samples pre-cured to scorch and then cured at 180°C. Surprisingly it seems that more healing of the memory interface occurred at the higher cure temperature.

Hamed and Zhao[4] explained that network disruption can result from hydrocarbon backbone chain scission and crosslink rupture; that simple crosslink rupture will lower network chain density without creating chain ends. For a tetrafunctional network, one disrupted crosslink will create two new network chains. On the other hand, backbone scission eliminates one network chain, creating two new, chain –end segments only attached to the network at one end. These segments are non – load bearing defects, expected to lower strength and stiffness, since the applied load is now distributed to the other chains in the network[4] .

8.1.3.2 Effect of Pre-curing to Scorch on the Tensile Strength and Elongation at Break of a Memory Interface

Figures 8.6 and 8.7 show that both tensile strength and elongation at break were significantly reduced when a cut was introduced in the compound pre - cured to scorch. The results indicate the importance of crosslinking in preventing the healing of the memory interface and the sensitivity of the process to the proximity of scorch.

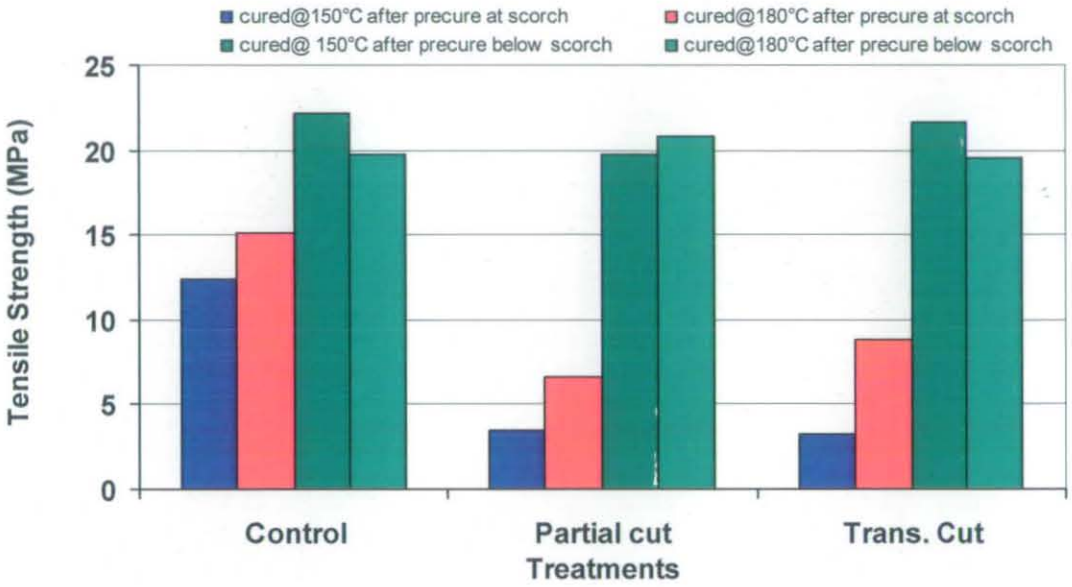

Figure 8.6: Effect of pre-curing to scorch on the tensile strength of natural rubber compound

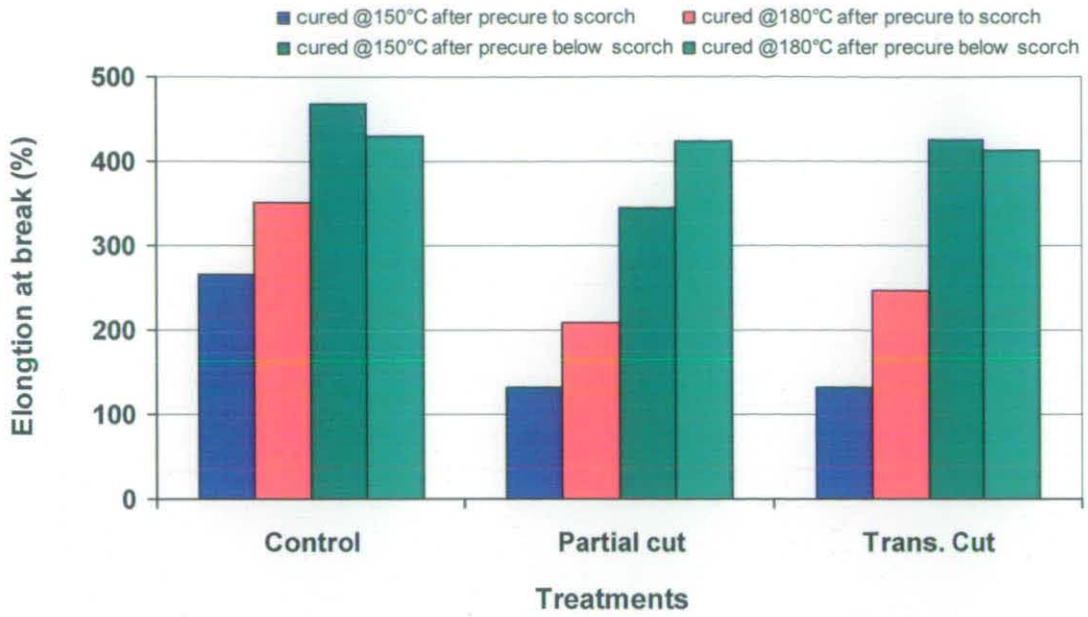

Figure 8.7: Effect of pre-curing to scorch on the elongation at break of natural rubber compound

8.1.4 Healing of Memory Interfaces During Curing

Interfaces can be introduced during calendering, compression moulding or injection moulding and the presence of these interfaces could be critical if healing in the rubber compound does not take place effectively during curing. The healing of memory interfaces during moulding of rubber is postulated as follows. When cut surfaces are placed together, or flow fronts come together, inter-diffusion and re-entanglement of molecular chains across the interface will occur by the normal Brownian movement of chain segments. The rate of re-entanglement is expected to increase with increase in temperature since the molecules will be more mobile at higher temperatures. However, if crosslinks have started to form before the healing process is complete, re-entanglement will be inhibited. The region which has not gained complete healing is likely to act as an area of weakness since the lack of entanglement means that any applied load will be carried on only a few chains and crosslinks. The concentration of stress is thus likely to result in initiation and easy propagation of a crack. Although the entanglement process will increase in rate with increase in temperature, crosslinking, being a chemical reaction, will also increase in rate with increasing temperature. Hence, healing can be both accelerated and inhibited by increasing temperatures.

Experiments were carried out to determine the effect of cure temperature on the healing time of a memory interface and to determine the kinetics associated with its healing. The interface was deliberately introduced, by cutting through the compound at various pre-curing times before it was fully cured (see Section 5.9.1). It is assumed that healing must occur before scorch is reached, since significant amounts of crosslinking will prevent further healing. The healing time of the material was defined as follows:

Healing time = the **difference between the scorch time and the greatest pre-cure time at which a cut introduced in the pre-moulded sheet, causes no significant change in tensile strength**.

In order to find the healing time, several samples had to be prepared with different times available for healing. This is illustrated in Figure 8.8, where tc is the pre-cure time at which the cut was introduced. Tensile tests were then carried out on these samples and the results were used to determine the healing time.

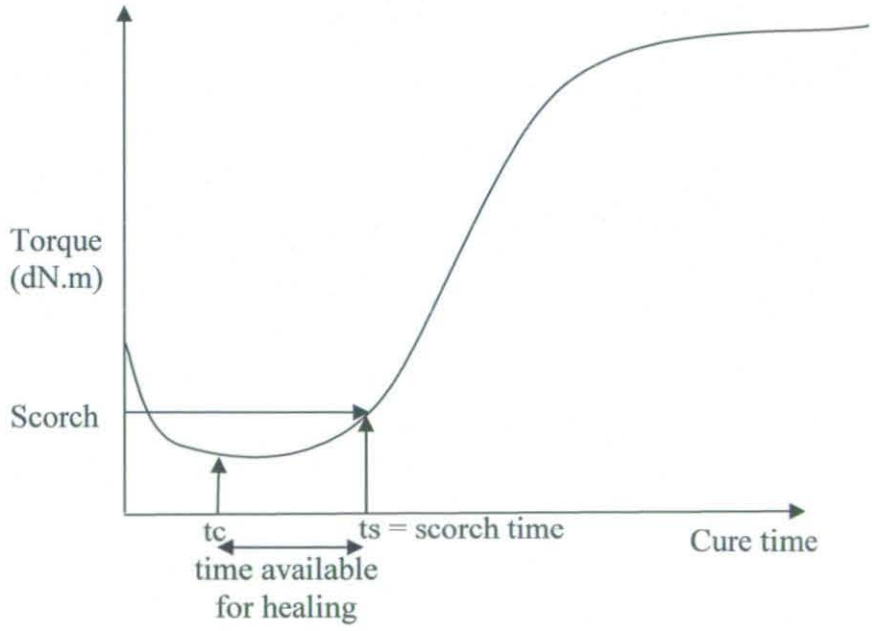

Figure 8.8: Cure curve showing the parameters used to determine the healing time of the natural rubber compound (tc is time at which cut is introduced)

Cure characteristics have a very important effect on healing time since the onset of crosslinking (scorch) or a rapid rate of crosslinking (cure rate index) will limit the amount of healing that can take place. The cure characteristics at different cure temperatures are shown in Table 8.1. Scorch times at different levels of torque rise (in dN.m) were measured to see whether it had an effect on the values of healing time determined. As expected, the scorch time decreases with increase in temperature. The cure rate index (CRI), which is a measure of the rate at which the cure reaction takes place, increases with increase in the cure temperature. Both these cure characteristics obey Arrhenius relationships, as shown in Figure 8.9. It is important to demonstrate that scorch time shows Arrhenius behaviour since healing time is partly derived from it. It was observed that the activation energy was not significantly affected by the torque rise levels at which scorch times were determined, though this did have an effect on the healing time as discussed in section 8.1.3.

Table 8.1: Effect of temperature on cure characteristics and healing time

	Cure characteristics					Healing time*		
Cure temp (°C)	ts_1 (min)	ts_2 (min)	ts_5 (min)	tc_{90} (min)	CRI (min^{-1})	ts_1 (min)	ts_2 (min)	ts_5 (min)
100	57.85	61.6	66	88.3	3.75	22.85	26.53	31
110	24.9	27.96	30.87	56.01	3.52	1.9	4.96	7.87
120	14.68	15.92	17	46.77	3.24	1.68	2.92	5
130	6.98	7.58	8.8	22.5	6.68	1.48	2.08	3.3
140	4.65	5.17	6.0	12.73	13.23	1.65	2.17	3
150	2.60	2.83	3.20	7.06	23.64	1.06	1.83	2.2
R^2	0.9951	0.9958	0.9964			0.6006	0.7597	0.8727
$E^{\spadesuit}_a$ (kJ/mol)	79.99	79.66	77.76			61	62	63

ts_1 = time taken for torque to increase by 1 unit from the minimum torque etc.

* Healing time considered using tensile strength measurements calculated using the different scorch levels,

♠Activation energy calculated over the entire temperature range

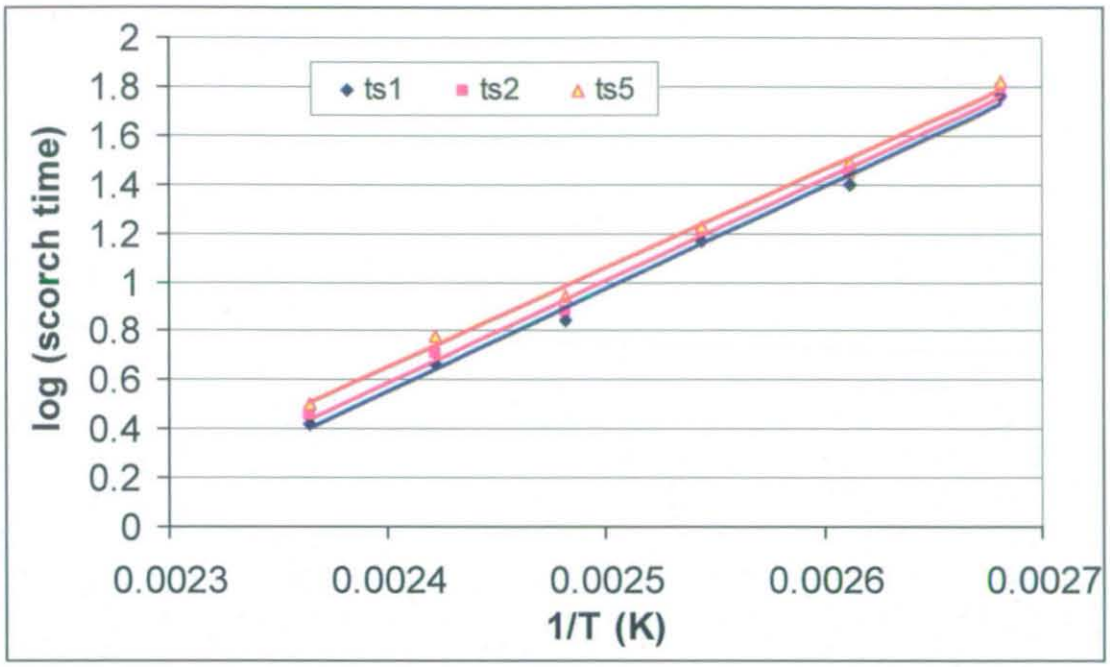

Figure 8.9 : Arrhenius relationship for scorch times

Tensile strength measurements and elongation at break data for the samples with memory interfaces are graphically presented in Figures 8.10 and 8.11. It can be observed that the tensile strength and elongation at break did not change significantly until the pre - moulding time at which the cut was introduced reached a critical value, after which the properties decreased sharply.

If we consider our definition of the healing time, we see that the healing time reduces with increase in the cure temperature.

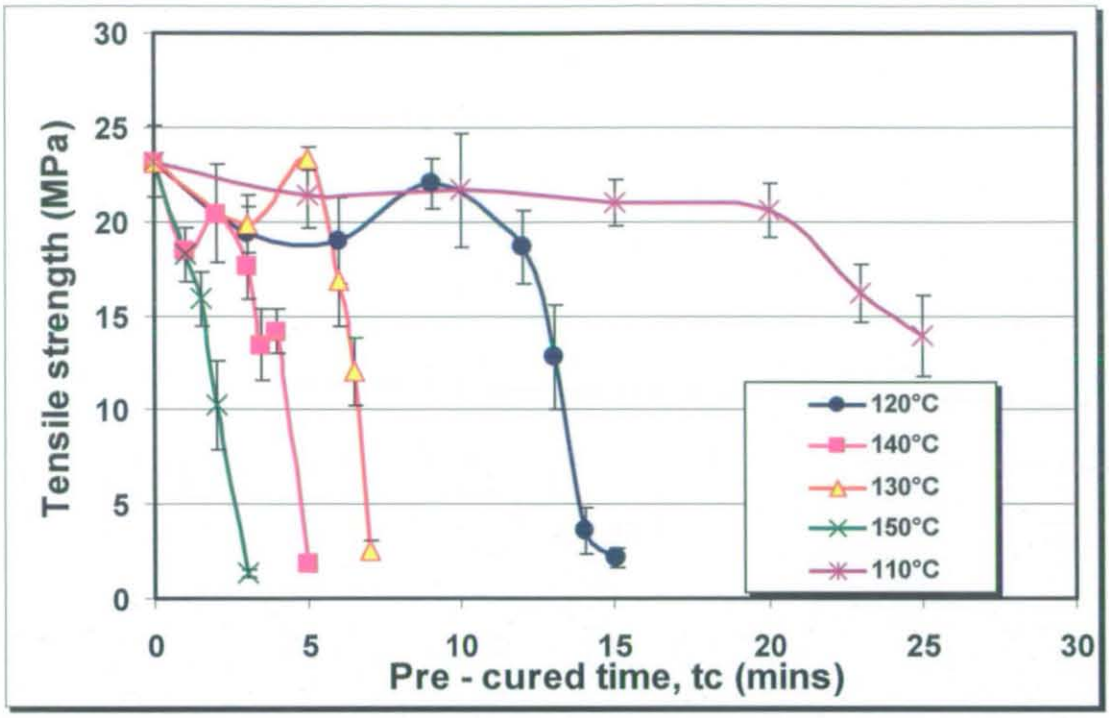

Figure 8.10: Effect of pre – cure time (tc) at different temperatures on the tensile strength of the NR sheet containing a memory interface

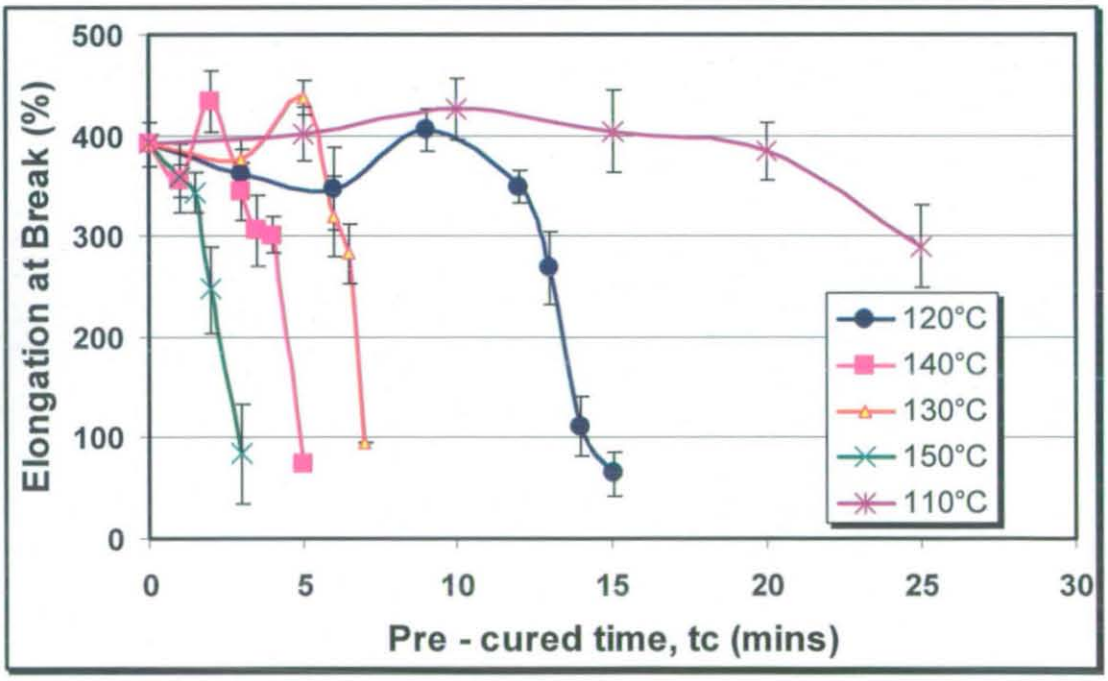

Figure 8.11: Effect of pre – cure time at different temperatures on the elongation at break of the NR sheet containing a memory interface

8.1.4.1 Kinetics of Healing

Tensile strength data were used to calculate the activation energy of healing of the memory interface. The critical time (t_{crit}) at which the introduction of a memory

interface had a significant effect on the tensile properties was taken as the tc value at which a 35% – 45 % reduction in the tensile strength was observed. The tcrit values were used to calculate the healing time (h_t) by subtracting tcrit from the scorch time. Now if we consider that the healing process follows an Arrhenius type relationship,

$$h_t = \alpha e^{\frac{-E}{RT}} \qquad [8.1]$$

Where,

h_t is the healing time,

α, a constant describing the healing rate,

Ea, the activation energy associated with healing,

R, the gas constant, and

T, the absolute temperature

Then

$$\log h_t = \log \alpha - \frac{E_a}{2.303RT} \qquad [8.2]$$

If the healing process obeys Arrhenius behaviour, a plot of log (h_t) against 1/T should give a straight line. Arrhenius plots for healing time calculated for different scorch levels are shown in Figure 8.12. The data from the higher temperatures follow a reasonably straight line, with the activation energy of healing calculated at about 31 kJ/mol considering the ts_2 for tensile strength data. The low activation energy is not surprising, since it is to do with the mobility of polymer segments and so might be expected to be similar to the activation energy of flow which for vulcanised natural rubber is about 22.2 kJ/mol for black filled and 24.3 kJ/mol for unfilled natural rubber[5] .However, the value for the lowest temperature, 100°C seems particularly far out from the line. It is not clear whether there is some sort of sudden change between 100 and 110°C, or whether the relationship is non-linear throughout the whole temperature range. A cause for a sudden change at a particular temperature could be something like a change in solubility of wax in the compound. Blooming of a wax to an interface could inhibit healing. Alternatively, if the change is over the whole temperature range then this suggests a gradual change in the mechanisms of healing with temperature. The cure reactions themselves clearly do follow Arrhenius behaviour (Figure 8.9)

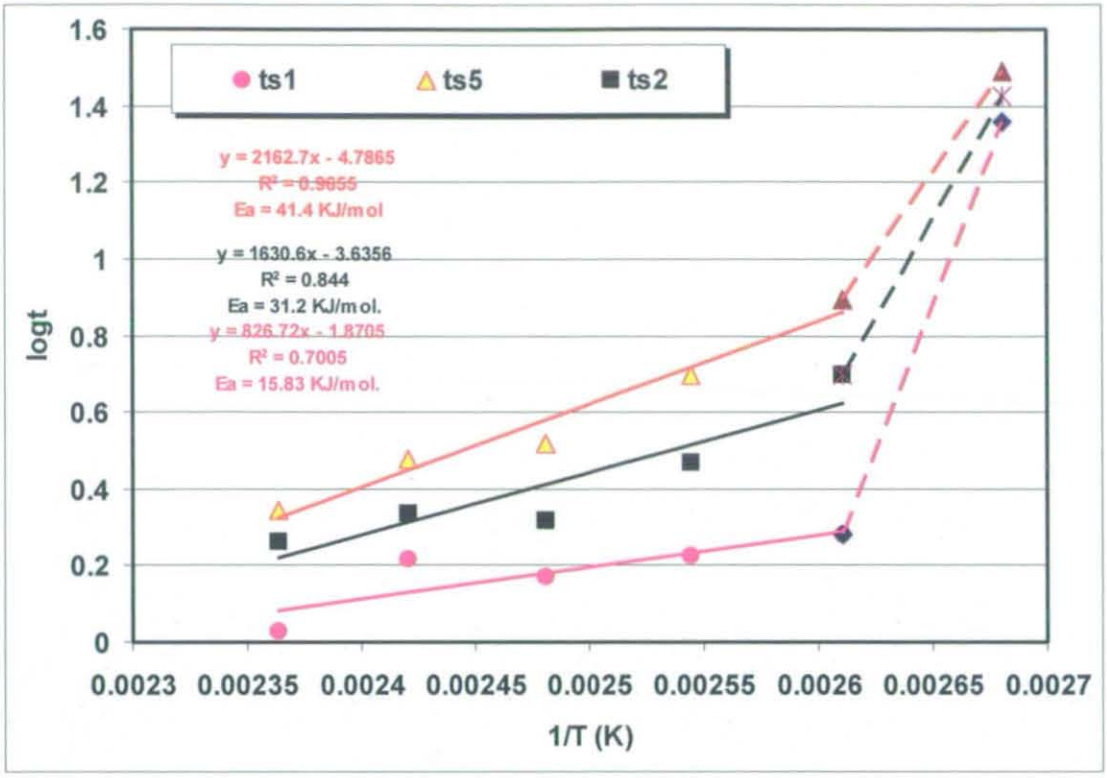

Figure 8.12: Effect of cure temperature on the Arrhenius relationship for healing

8.2 Effect of Particulate Contamination on Failure Properties

The effects of particulate contamination on the properties of a natural rubber compound are discussed in terms of their tensile and fatigue behaviour.

8.2.1 Tensile Properties

To assess the relative importance of poor dispersion in limiting strength properties, carbon black particulate filler was applied in a cut made in a pre-cured rubber sheet and also on the surface, across the centre of a pre-cured rubber sheet (see Section 5.10). The sheets were then cured at 140°C and tensile tested. Samples which had been cut, but without the carbon black added were tested as well, to allow for the effect of a memory interface.

The effects of particulate contamination on the tensile properties of the compound are presented in Figures 8.13, 8.14 and 8.15. The 100% modulus was not significantly affected by the presence of particulate contamination.

The tensile strength is seen to decrease when carbon black is applied through a partial cut in the rubber sample (Figure 8.14). The introduction of the cut caused a decrease

in the tensile strength, due to the memory interface effect. However, the carbon black had an additional strength-reducing effect. The presence of the carbon black particles along the cut length might further reduced the ability of the memory interface to heal. However, the carbon black agglomerates in the cuts acts are also likely to act as stress raisers.

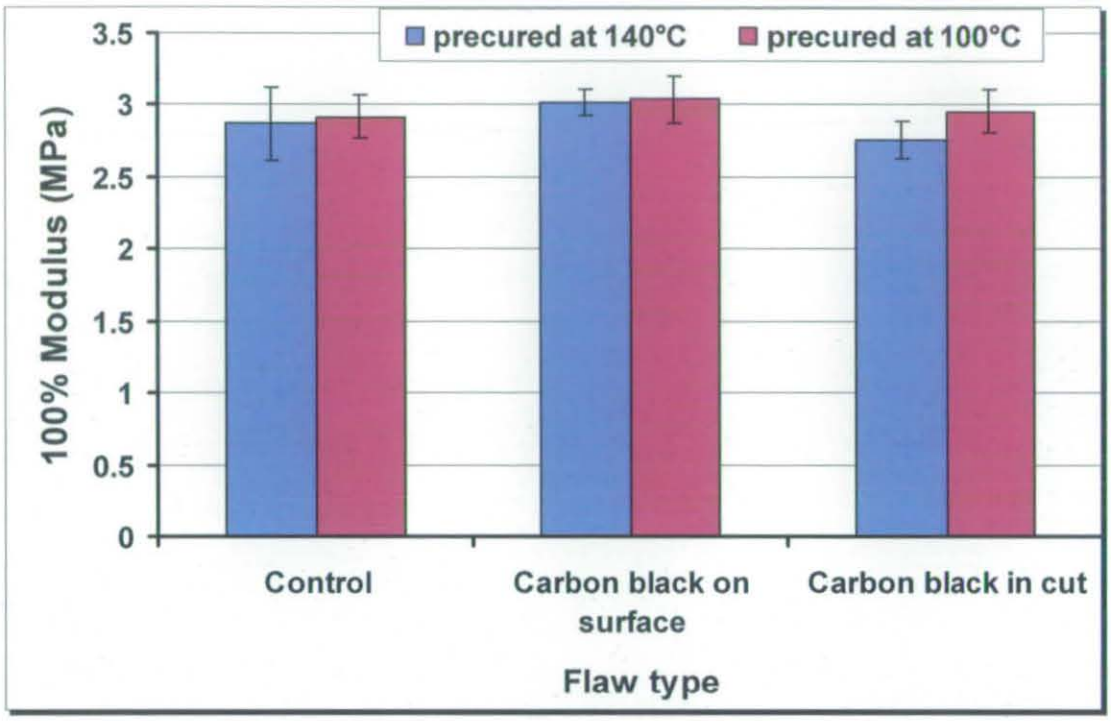

Figure 8.13: Effect of particulate contamination on the modulus of natural rubber compound (CBSappl – carbon black on surface application, CB cut – carbon black in cut)

It has been established that fillers play an important role in determining the strength of rubber compounds [4, 6, 7].Generally, tensile strength increases with increase in carbon black loading up to a certain level because of the reinforcement mechanisms, and then decreases at higher loading due to carbon black dispersion effects. As explained by Zhao and Ghebremeskel[6], at high loading, carbon black may agglomerate into large clusters which increase flaws that can easily crack and subsequently develop into catastrophic failure. Furthermore, Sharma et. al. .[8] explained that the drop in tensile strength experienced by filled composites with increased particulate loading is because the filler – filler interaction becomes more pronounced than the filler – matrix interaction. Also, the applied force cannot be transferred from the polymer matrix to rigid filler particles due to reduction in the effective cross – sectional area of the composites caused by filler particles[8].

In the current study the carbon black embedded in the rubber consists of large agglomerates, (Figure 8.17) which behave locally like highly filled compounds, causing the rubber to be very stiff and brittle and likely to fracture. The carbon black agglomerates once fractured, constitute cracks which can propagate resulting in failure of the compound (see Figure 8.16). Also, weak interfacial bonding between the rubber matrix and the applied carbon black particle may result to the reduction in both tensile strength and elongation at break.

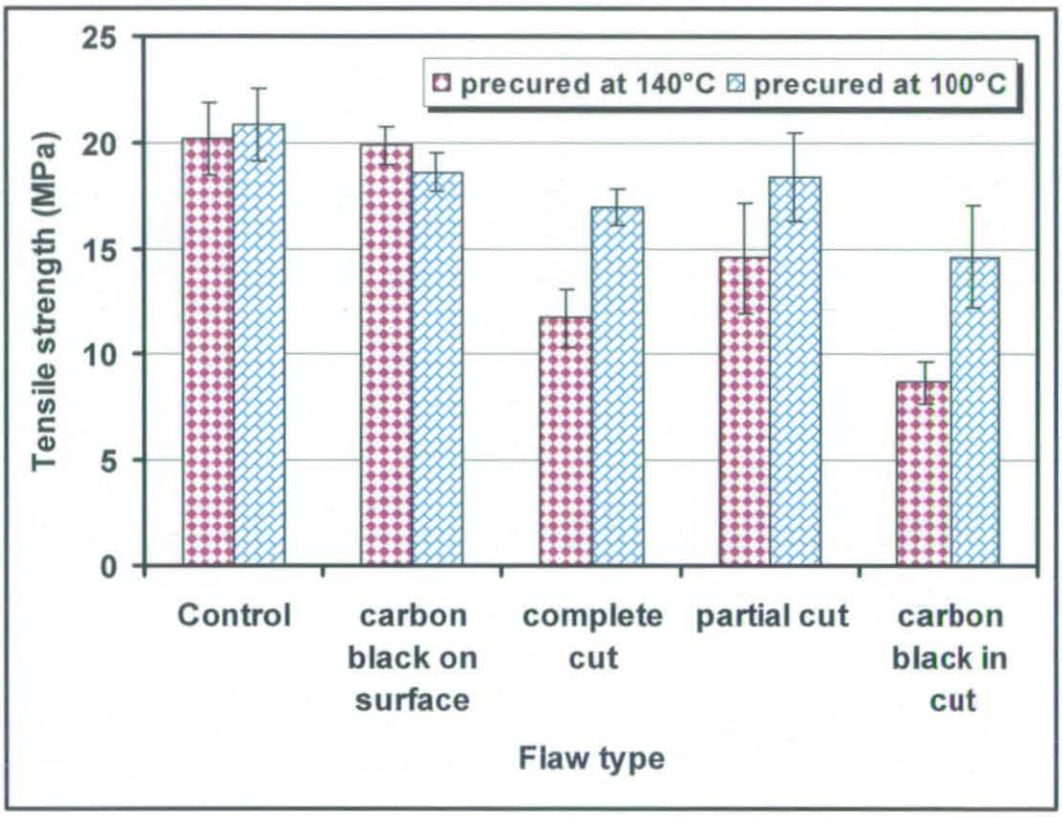

Figure 8.14: Effect of particulate application on the elongation at break of NR compound

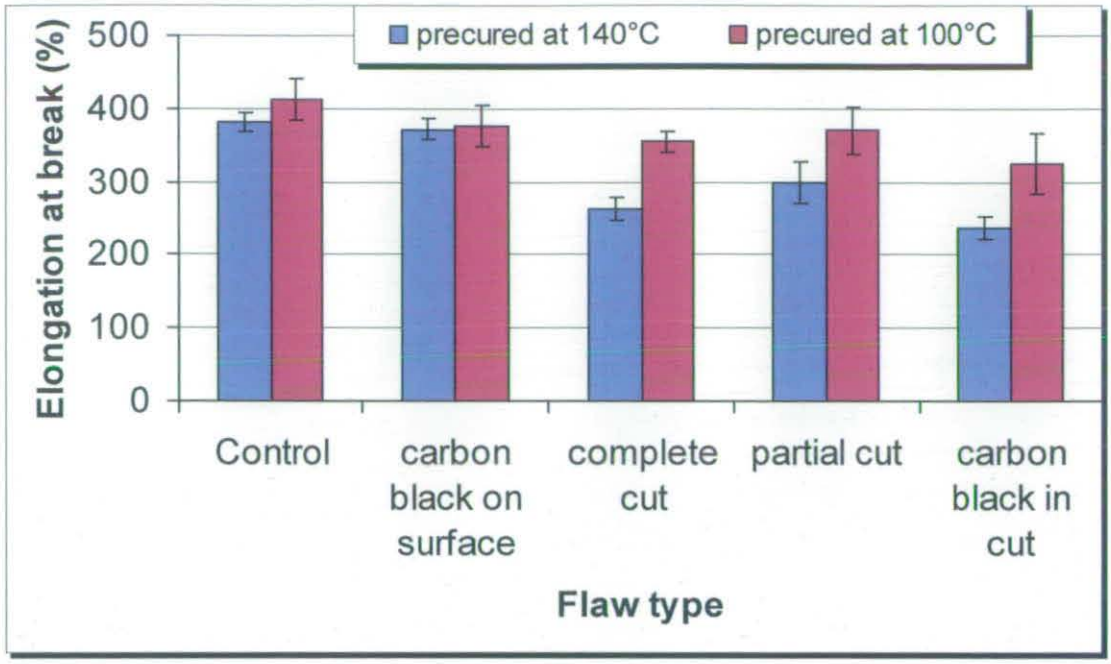

Figure 8.15: Effect of particulate contamination on the elongation at break of the natural rubber compound

Studies on effect of particulate fillers on fractured surfaces using scanning electron microscopy technique are presented in Figures 8.16 – 8.19.

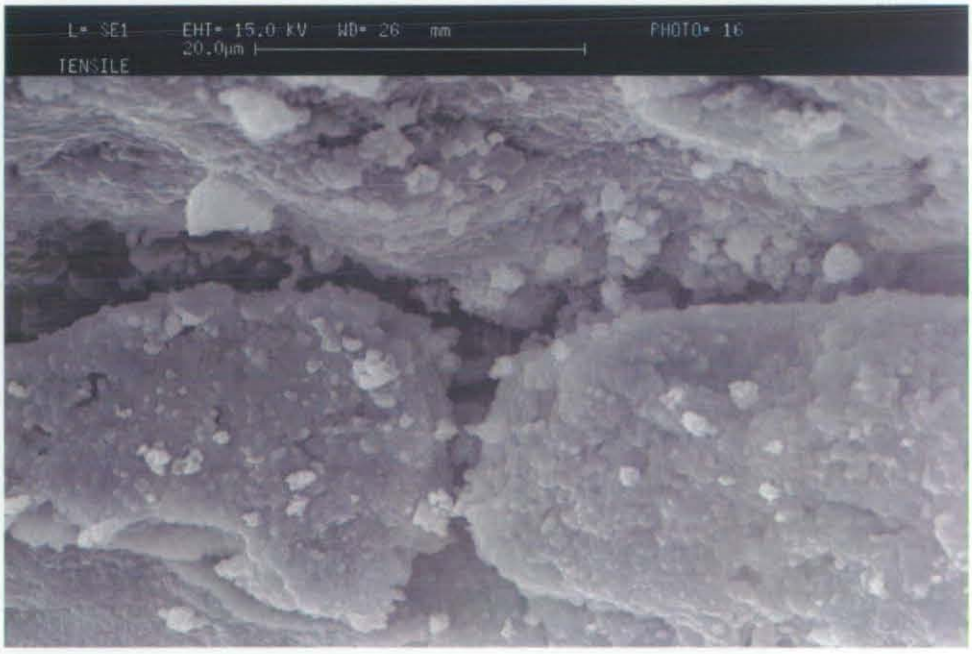

Figure 8.16: SEM micrograph of tensile fractured surface of cut with carbon black application *(Agglomerates may have acted as stoppers to the advancement of the crack which propagates perpendicularly to the applied force)*

From the SEM (Figures 8.16 – 8.19) it could be seen that agglomerates of carbon black applied at the surface penetrated the network matrix. It was expected that such points should act as stress raisers but this was not the case as both modulus and tensile strength were comparable to the control (Figure 8.13 and Figure8.14). In the surface application of carbon black the concentration of carbon black agglomerates is parallel to the direction of tension and any cracks in the carbon black rich layer will only be quite shallow, thus having relatively little effect on strength. However, when carbon black is applied in the cut the carbon black rich layer is perpendicular to the tensile direction and cracks will propagate to a substantial length in the sample, causing a significant reduction in strength (Figure 8.18).

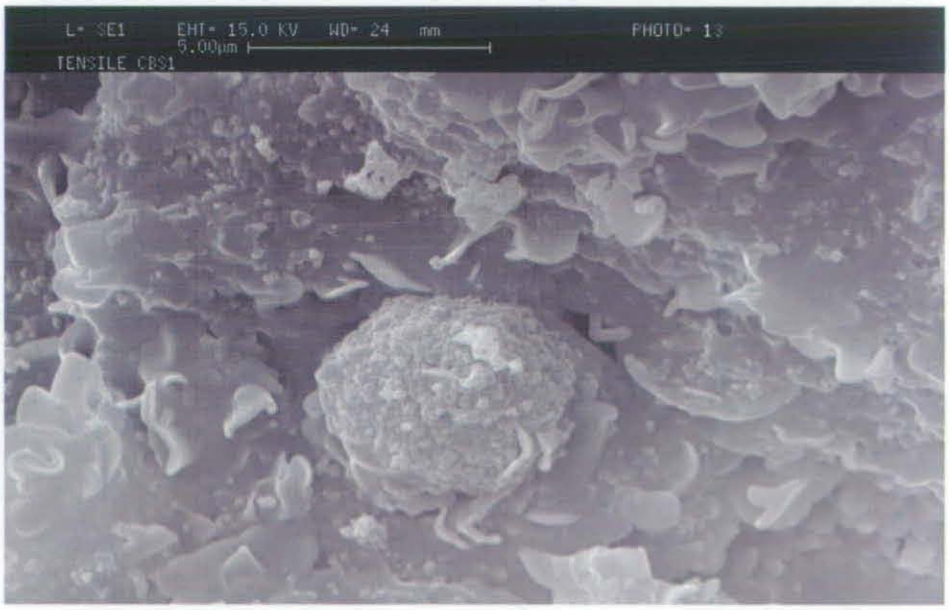

Figure 8.17: SEM micrograph showing carbon black agglomerate in the tensile fracture surface on sample with surface application of particulate. ***(carbon black agglomerate that penetrated the rubber could be seen)***

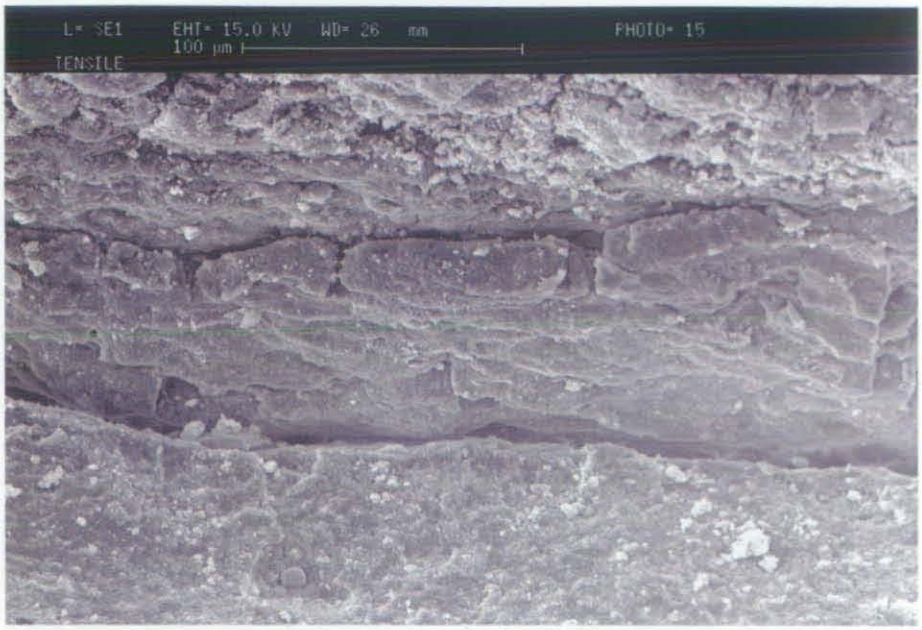

Figure 8.18: SEM micrograph of tensile fractured sample showing carbon black agglomerate embedded in cut

Figure 8.19: SEM micrograph showing carbon black agglomerates on surface of rubber

8.2.2 Fatigue Measurements

Fatigue measurements on samples with carbon black on surface or in the cut and cured at 150°C and 180°C, shows a significant difference in the fatigue life for the various treatments for natural rubber cured at 150°C and 180°C (Figure 8.20).

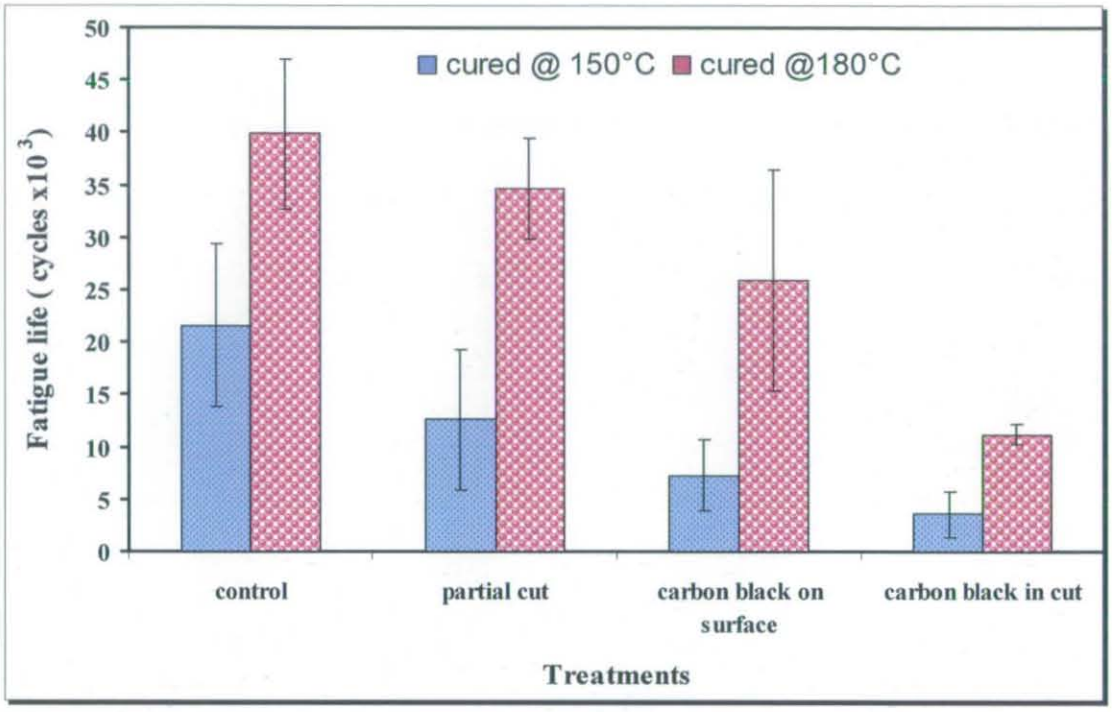

Figure 8.20: Effect of particulate filler application on the fatigue life of rubber compound.

The causes for reduction in fatigue failure will be the same as those causing reduction in tensile strength, as explained in the previous section. However, it is noted that surface application of carbon black significantly reduces fatigue life, though it had little effect on tensile strength. It seems that, as with the effect of memory interfaces reported in section 8.1.1, the fatigue life is more sensitive to the presence of flaws than tensile strength.

8.3 Effect of Pinhole Flaws on the Mechanical Properties of the Natural Rubber Compound

Almost all materials contain flaws to a certain extent but the way in which these materials respond to the presence of the flaw differs. The intrinsic flaws size is an

important parameter that should be taken into account when estimating strength and fatigue life of the rubber compound. The intrinsic flaws resulting from a manufacturing process distribute randomly in rubber, and the size of the intrinsic flaw depends on the type of filler (in this case carbon black type), crosslink density and dispersion of ingredients[3, 9] Bell and others reported that for unfilled natural rubber, the intrinsic flaw size is estimated to be about 0.025mm[10]

8.3.1 Tensile Properties

The effect of pinhole flaw sizes on the tensile properties of a natural rubber engine mount compound are shown in Figures 8.21 – 8.23

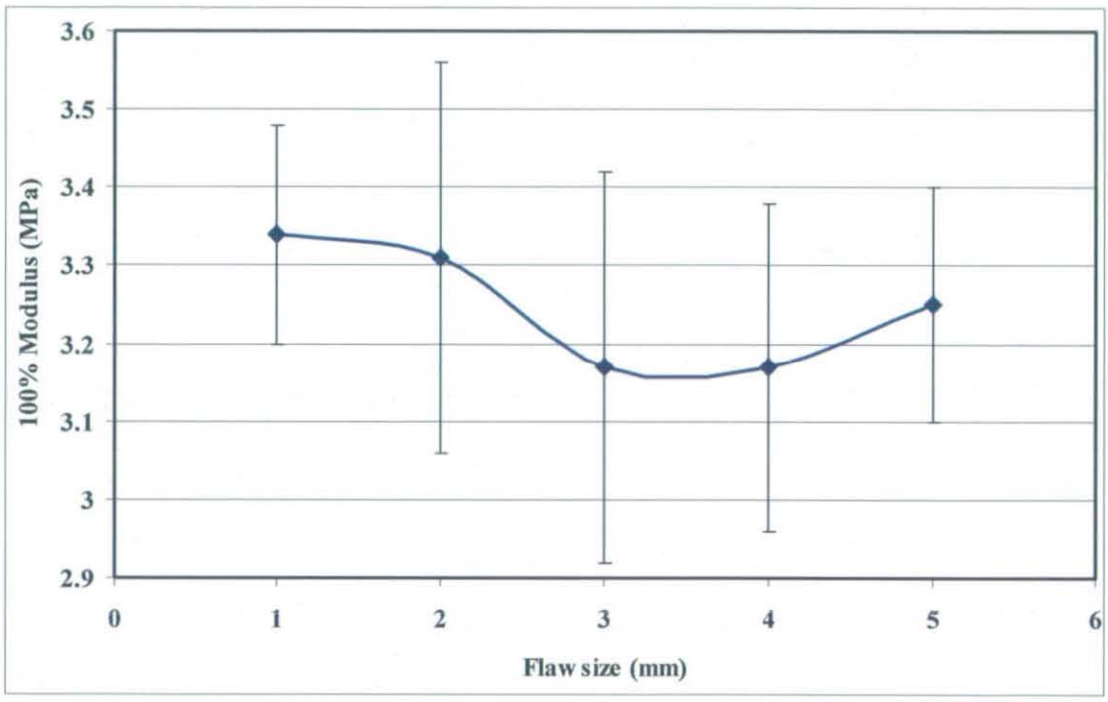

Figure 8.21: Effect of pinhole flaw size on Tensile Modulus

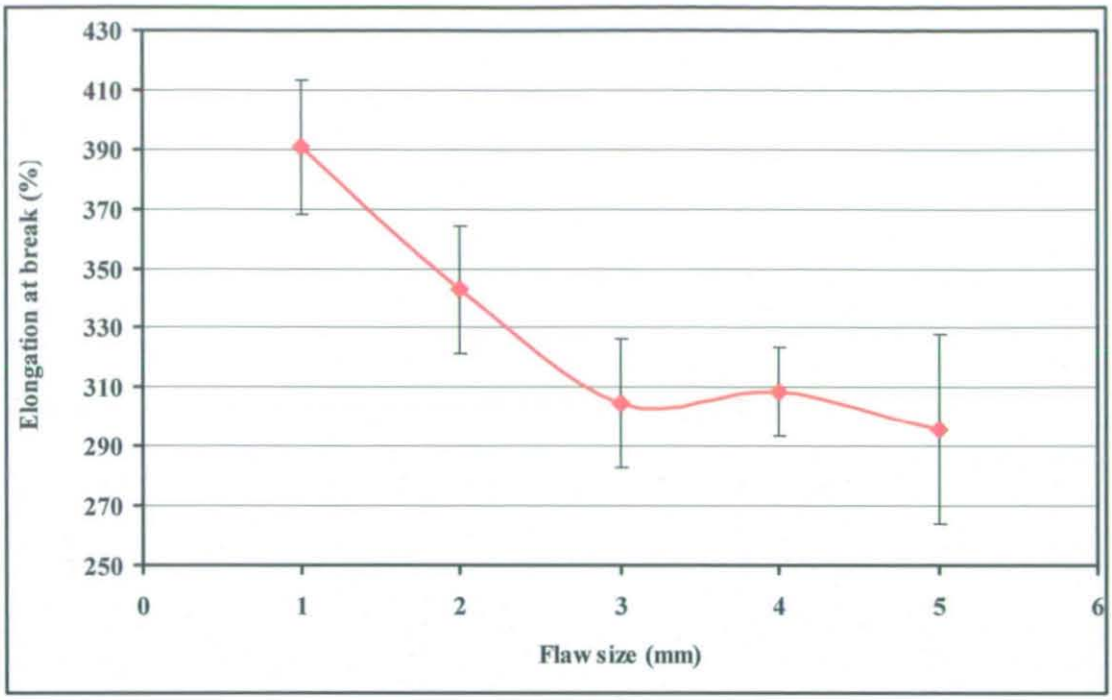

Figure 8.22: Effect of pinhole flaw size on Elongation at break

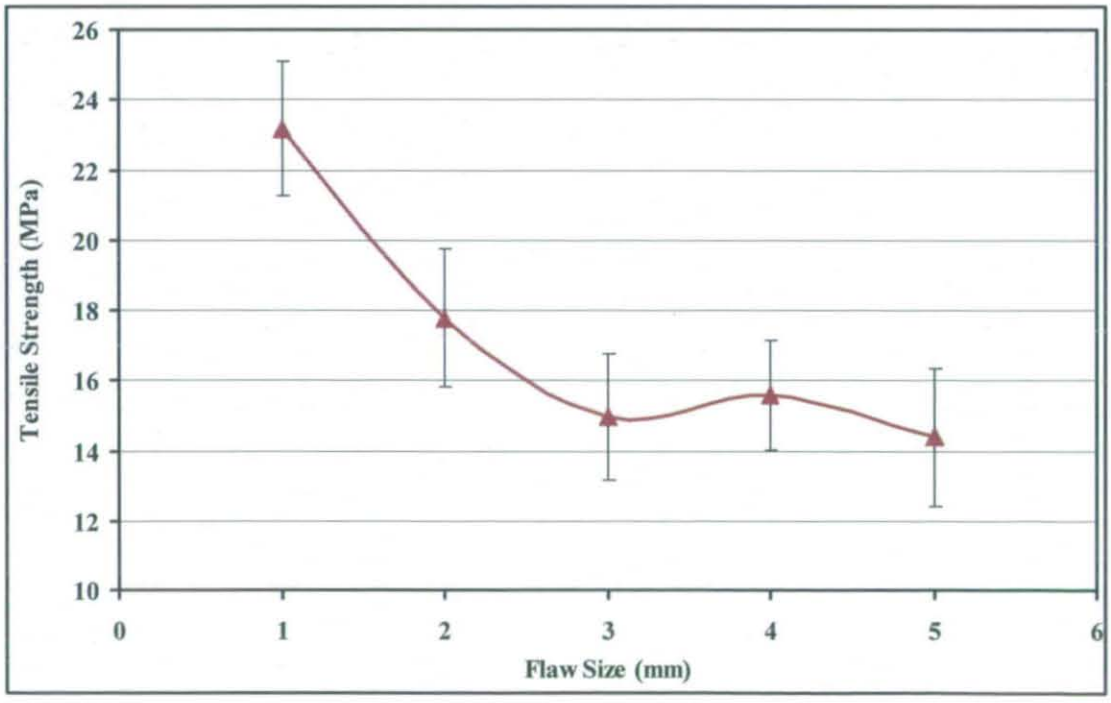

Figure 8.23: Effect of pinhole flaw size on Tensile strength

As expected, the tensile modulus is not significantly affected by pinhole flaw size (Figure 8.21). The elongation at break and tensile strength decreases with increase in the pinhole flaw size. These pinhole flaws are like surface defects or pre – existing cracks in certain materials which can propagate through the material causing it to fracture. Griffith[11] explained that for crack propagation to occur, the energy supplied at the crack tip should be equal to, or greater than the energy required for crack growth. With increase in the diameter of the pinhole flaw, more energy is supplied to the crack region resulting in the crack propagating faster.

To determine the intrinsic pin flaw size in the rubber, a plot of the log of the tensile strength against the log of the pin flaw size was carried out. The tensile strength of the sample without a pinhole flaw was considered to be the perfect compound. A line was drawn from this tensile strength value parallel to the pin flaw size axis (x – axis). The line linking the pin flaw points were extrapolated to meet the tensile strength of the compound without pinhole flaws (Figure 8.24). The intrinsic flaw size was estimated to be about 0.2 mm (200μm).

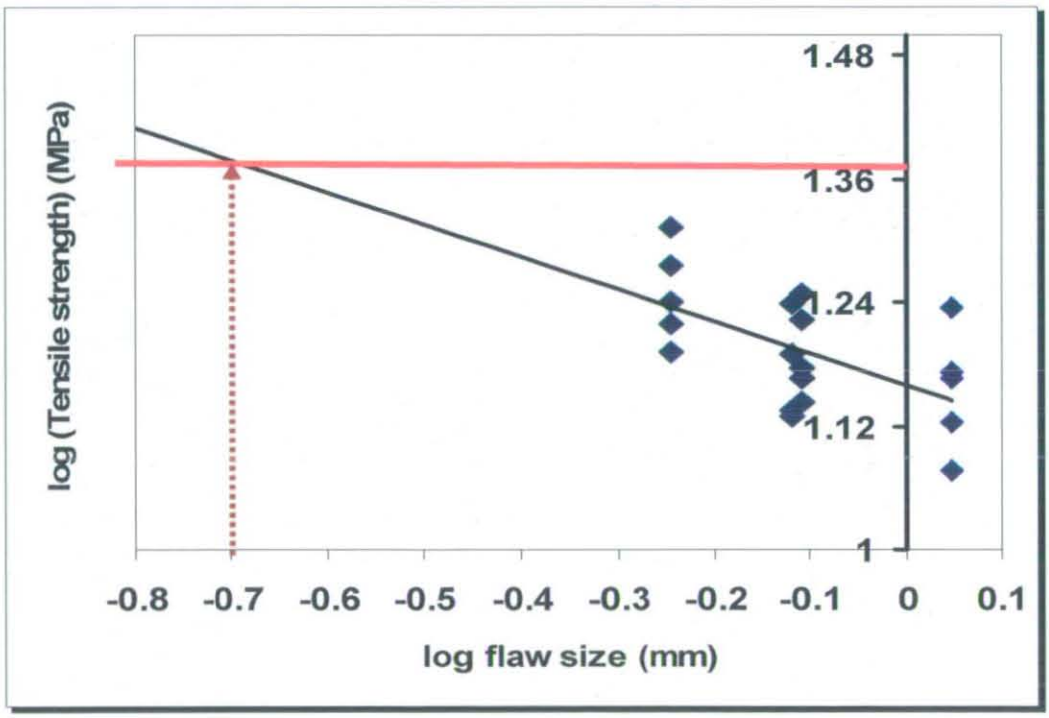

Figure 8.24: A log – log plot to estimate the intrinsic flaw size of the rubber compound

Another method that has been used to calculate the flaw size of a material is the stress – flaw constant. The stress flaw constant which is calculated by multiplying the tensile strength of each specimen by the square root of the diameter of the flaw causing the specimen to fail has been used to estimate the strength and intrinsic flaw

size of a material. The stress flaw constant is independent of the size of the specimen and so is representative of the material behaviour, that is, the stress flaw constant represents an inherent material property[3].

Using the equation 8.3, stress flaw constant can be calculated

$$\sigma\sqrt{d} = \kappa \qquad [8.3]$$

Where σ is the failure stress and d is the characteristic dimension of the flaw that caused failure, and κ, the stress flaw constant.

Table 8.2 shows how the stress flaw constant changes with flaw size and strength of the rubber compound

Table 8.2 : Flaw size, average tensile strength, stress - flaw constant and estimated tensile strength of rubber compound

Specimen flaw size	Average Tensile strength (MPa)	Stress flaw constant (MPa mm$^{1/2}$)	Estimated strength from κ
Control	21.18		
0.57	17.78	13.42	18.3
0.76	14.97	13.05	15.88
0.78	15.59	13.77	15.68
1.11	14.38	15.15	13.14
Average stress flaw constant		13.85	

Assuming the average value of the stress force constant is representative of the material, the tensile strength for each specimen can be estimated as shown in Table 8.2. The estimated strength agrees closely with the experimental values. The intrinsic flaw size of the control material was estimated using this approach to be about 0.357mm.

8.3.2 Fatigue Life

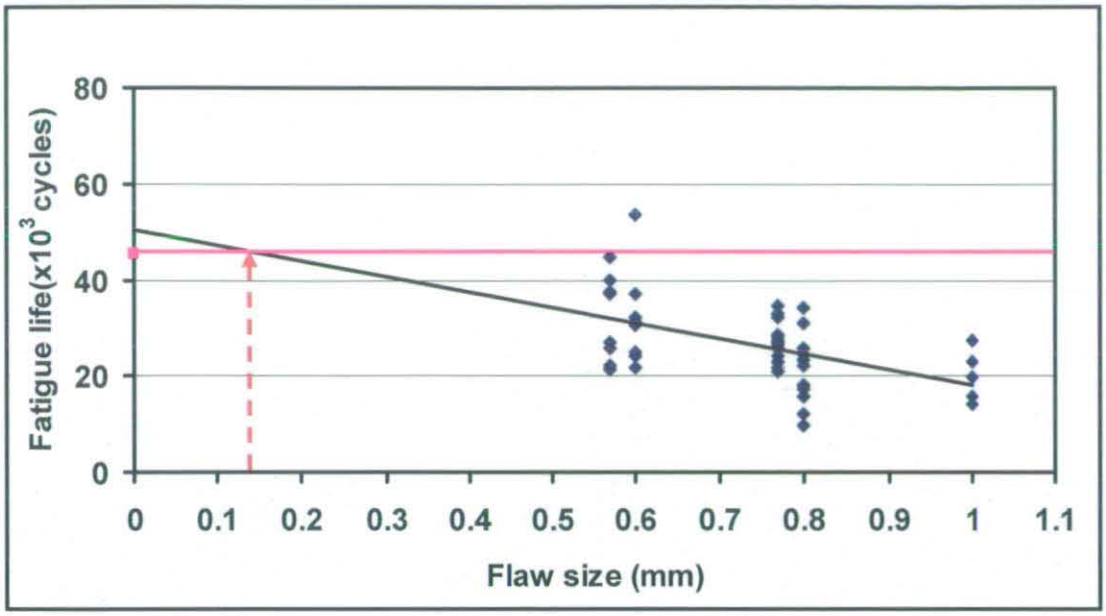

Figure 8.25: Effect of pinhole flaw on fatigue life

It was observed that the fatigue life reduces with increased pinhole flaw size (Figure 8.25). This is because once a flaw is present in the rubber and it is subjected to cyclic tension, the crack easily propagates through the rubber resulting in failure of the material. The crack propagates more quickly for samples with bigger flaw because more energy is available at the tip for crack propagation. The results are consistent with the intrinsic flaw size of 0.2 mm determined from the tensile results.

8.4 Conclusions

- The presence of cuts introduced below scorch and allowing sufficient time for healing, did not significantly affect the tensile properties of the rubber.
- The healing time of the rubber reduces with increase in temperature. The activation energy of healing was found to be about 31 kJ/mol, between 110°C and 150°C.
- Fatigue life is more sensitive to the presence of memory interfaces and particulate contamination than is tensile strength.

- Agglomerates of carbon black embedded in the rubber surface did not affect the tensile strength but caused a reduction in fatigue life.
- The presence of carbon black in cuts within the compound significantly reduced both tensile strength and fatigue life.
- The presence of pinholes in the cured compound significantly reduced both tensile and fatigue strength, the reduction increasing with increase in size
- The pinhole equivalent intrinsic flaw size of the compound was calculated to be about 200μm
- Using the stress – flaw constant, the pinhole equivalent of the intrinsic flaw size was estimated to be 360μm

This study has shown how imperfections introduced during processing can significantly affect failure properties of a rubber compound but also how it is capable of healing itself, given the right conditions.

8.5 References

(1) Philip, M.; Bolton, W. In *Technology of Engineering Materials;* Butterworth Heinemann: Oxford, 2002; , pp 387.

(2) Singh, R. *Sdhan : Academy proceedings in engineering sciences.* **2000**, *25*, 319-330.

(3) Odom, E. M.; Adams, D. F. *J. Mater. Sci.* **1992**, *27*, 1767-1771.

(4) Hamed GR; Zhao J *Rubber Chemistry and Technology* **1999**, *72*, 721.

(5) Lukomskaya, A. I. *Polymer Mechanics* **1967**, *3*, 511-516.

(6) Zhao J; Ghebremeskel GN *Rubber Chemistry and Technology* **2001**, *74*, 409.

(7) Milczewska, K.; Voekel, A.; Jeczalik, J. *Macromol. symp.* **2003**, *194*, 305-311.

(8) Sharma, N.; Chang, L. P.; Chu, Y. L.; Ismail, H.; Ishiaku, U. S.; Moh'd Ishak, Z. A. *Polymer Degradation and stability* **2001**, *71*, 381-393.

(9) Chou, H. W.; Huang, J. S.; Lin, S. T. *J. Appl. Polym. Sci.* **2007**, *103*, 1244-1251.

(10) Bell, C. L. M.; Stinson, D.; Thomas, A. G. *NR Technol* **1980**, *11*, 53-58.

(11) Griffith, A. A. *Phil. Trans. R. Soc.* **1920**, *221a*, 163.

CHAPTER 9: Conclusions and Recommendations

9.1 Conclusions

- Engine mounts are usually subjected to both static and dynamic ageing and this study showed that static and dynamic ageing affects the properties of the engine mount in different ways. Static ageing reduces the tensile strength while the modulus is increased. Rubber cured at 140°C generally had a higher activation energy of ageing in terms of its effect on tensile strength compared to rubber cured at 150°C. Dynamic ageing was evaluated in terms of fatigue. The fatigue life of the rubber reduced with increase in ageing time and ageing temperature. The activation energy of ageing in terms of the fatigue life was found to be lower than for tensile strength. Tear strength also reduces with ageing time. The properties of the engine mount compound were affected by the nature and type of flaw. While the tensile strength was not affected by a weld line introduced below scorch, the fatigue life greatly reduced with intensity of weld line introduction and flaw(from partial cut to full cut as well as size of the pinhole flaw). When a cut is present below scorch during moulding, the rubber could heal with the healing time reducing with increase in cure temperature.

9.1.1 Effect of Ageing on Mechanical Properties

- Thermal ageing results in a decrease in tensile strength and elongation at break and an increase in modulus with ageing time.
- Thermo –oxidative ageing of the natural engine mount compound resulted in a decrease in the tensile strength and elongation at break, and an increase in the modulus when the rubber was aged at temperatures of between 70°C and 110°C.
- The change in modulus with ageing was markedly affected by the cure temperature. The rubber that was cured at 140°C had an initial peak in modulus between 0 and 64 hours of ageing while this was absent for rubber cured at 150°C. This was attributed to maturation of crosslinks when rubber was cured at 140°C.

- Dynamic properties were also affected by ageing, with the loss modulus and loss tangent increasing to a maximum with increase in ageing time. However the strain amplitude at which this maximum occurred decreased from around 400μm to 200μm as the ageing time increases. This was as a result of an increase in stiffness with ageing time and temperature.

9.1.2 Activation Energy of Ageing

- The activation energy for the kinetics of ageing determined from tensile strength and elongation at break gave similar results. For example, for a cure temperature of 140°C and using the Time Temperature Superposition method, activation energies were about 93 kJ/mol and 98 kJ/mol for tensile strength and elongation at break data respectively.
- The activation energy of ageing determined from modulus results was 88 kJ/mol and 151 kJ/mol for rubber cured at 140°C and 150°C respectively. The Arrhenius plot for the activation energy calculation for rubber cured at 150°C passed through a minimum indicating the dangers of predicting service life by extrapolating to lower temperatures.
- The activation energy values determined by the critical life approach are similar for tensile strength and elongation at break and are in close agreement to that obtained by Gent et al [1]. The higher values from the TTS method are believed to be due to the fact that all the available data are used for the calculation while other methods are averaging the data.
- The activation energies of ageing were generally higher for rubber cured at 140°C compared to rubber cured at 150°C. For example, the activation energy for rubber cured at 140°C was about 109 kJ/mol compared to 88 kJ/mol. For the rubber cured at 150°C, when tensile strength measurements are considered using the rate law approach. It is thought the higher activation energy is because ageing of the compound at the lower cure temperature predominantly takes the form of maturation of the crosslinks and hence, a relatively greater energy input is required to bring about damage to the main network chains that result in a decrease in strength.

- The tensile strength after ageing for 13 weeks at 50°C was predicted to be 18.7 MPa, which was very close to the experimental value of 19.0(±2.25)MPa. It was predicted that the engine mount compound will take approximately 80 days for the tensile strength to reduce by fifty percent at a temperature of 70°C.

9.1.3 Mechanisms of Ageing

- Mechanisms of ageing were investigated using the Ahagon plot method. Two types of ageing mechanisms (type I and III) were predominant for thermo – oxidatively aged rubber compound. Type I ageing was characterised by crosslinking being the dominant event resulting in an increase in modulus and lowering of the elongation at break. Type I ageing was observed for low ageing temperatures (<90°C) and at early stages of ageing. Type III was characterised by both crosslinking and chain scission due to oxidation at high temperatures (>90°C) and at later stages of ageing.
- The slopes describing the Type I mechanism changed with cure temperature that is -0.71 for rubber cured at 140°C and -0.85 for rubber cured at 150°C indicating the effect of cure temperature on the mechanism of degradation. Crosslinking reactions being more predominant for the rubber cured at 140°C while scission of crosslinks must have accounted for the change in slope for rubber cured at 150°C.

9.1.4 Effect of Ageing on Failure Properties

- For a given tearing energy the rate of crack growth for the engine mount compound aged at 100°C increases with increase in ageing time. However, the slopes of the plots tearing energy versus fatigue life for rubber aged at 100°C did not change with ageing time. This is because the threshold tear energy had been exceeded.
- For samples aged between 70°C and 110°C the fatigue life reduces with ageing time and the activation energy for ageing determined from fatigue measurements was about 60 kJ/mol. which was lower than those calculated from tensile measurements, indicating that fatigue is more sensitive to ageing.
- The tearing energy using the trouser tear approach reduced with ageing time and temperature. The activation energy of ageing determined from tearing

energy was about 135 kJ/mol. (using the Time - Temperature superposition approach) and 103-111 kJ/mol (using the critical life approach).

9.1.5 Dynamic Ageing

- Dynamic ageing drastically reduces the fatigue life of the engine mount compound. The fatigue life reducing with increase in the dynamic ageing time.
- It took about 4 hours for the compound to fail when dynamically aged at temperature of 70°C compared to the statically aged rubber which took 48hours to fail when aged at 70°C. This is because bonds broken during oxidation by mechanical fatigue were not able to reform.

9.1.6 Effect of Flaws on Failure Properties

- The presence of cuts introduced below scorch and allowing sufficient time for healing, did not significantly affect the tensile properties of the rubber.
- The fatigue life of the rubber with weld lines, carbon black embedded in the surface and carbon black embedded in a cut were greatly reduced. Fatigue life was more sensitive to the presence of flaws than the tensile properties.
- The healing time of the rubber reduces with increase in temperature. The activation energy of healing was found to be about 31 kJ/mol, determined for rubber cured between 110 and 150°C.
- Carbon black agglomerates of about 100μm in diameter embedded in the surface of the rubber during processing did not significantly affect the tensile properties of the rubber compound; however, fatigue life was reduced.
- The presence of pinholes in the cured compound significantly reduced both tensile and fatigue strength, the reduction increasing with increase in size
- The pinhole equivalent intrinsic flaw size of the compound was calculated to be about 200μm.
- Using the stress – flaw constant method, the pinhole equivalent of the intrinsic flaw size was estimated to be 360μm

9.2 Recommendations for Further work

To fully predict the service life of the rubber compound in an engine mount, a suitable model which could encompass all the factors affecting service life could be developed. These factors should include the following:

- The effect of oils on static and dynamic properties of aged rubber engine mount compound.
- Effect of intermittent dynamic ageing on the service life of the engine mount compound.

In addition, to make the model more general, the effects of other components in an engine mount compound could be investigated :-

- Studies on the effect of other fillers such as silica on a natural rubber engine mount compound may be carried out in order to better understand the role of other fillers on ageing.
- The effect of blends of natural rubber and other polymers.
- The intrinsic flaw size of the rubber using different types and grades of fillers should be investigated, provided material of similar crosslink density is produced so as to avoid the effect of crosslink density on flaw size.
- Investigate the effect of pre – vulcanisation inhibitors on the healing time.

9.3 References

(1) Gent, A. N.; Liu, G. L.; Sueyasu, T. **1991**, *TR - 27*, 42.

APPENDIX I

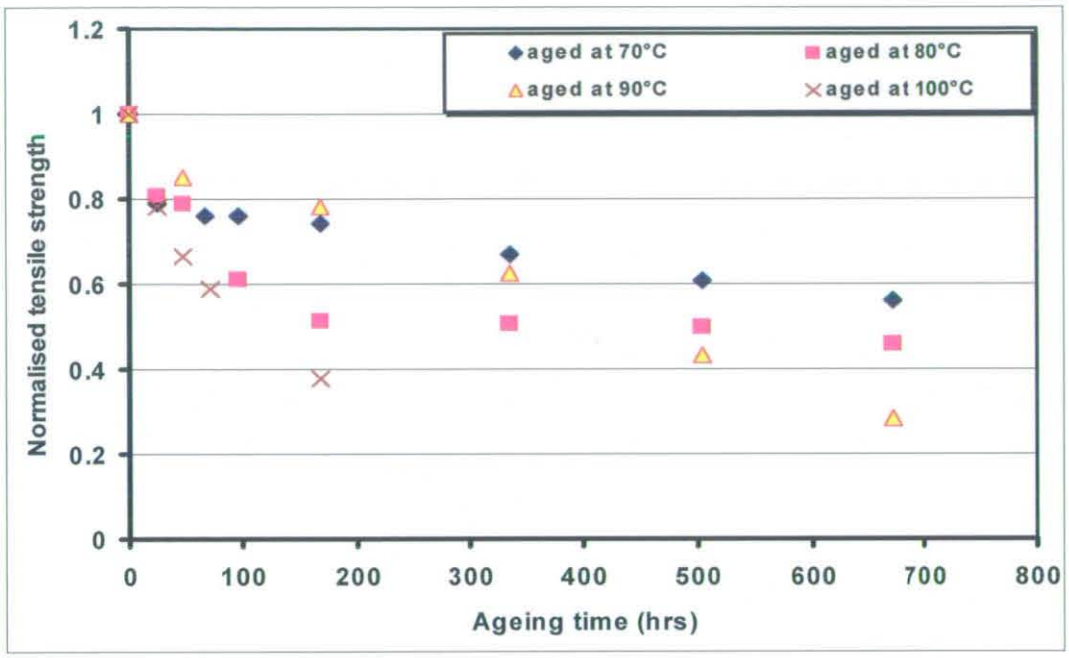

Figure A1.1: Normalised data to show the effect of thermal ageing on Tensile strength

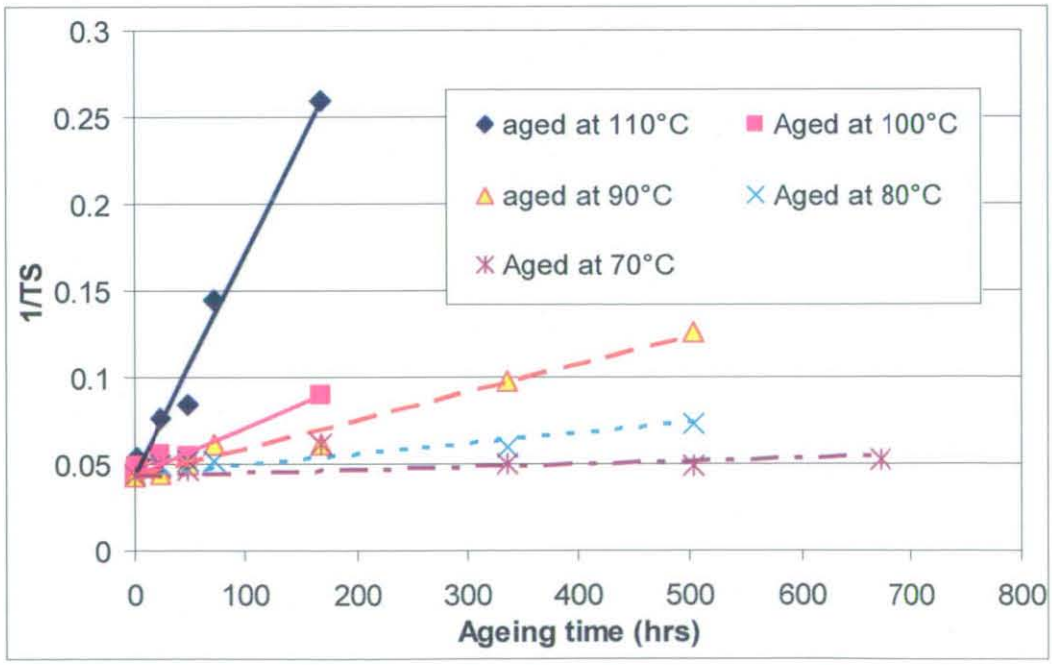

Figure A1.2: Second order plot for the effect of ageing on tensile strength of the natural rubber compound cured at 140°C

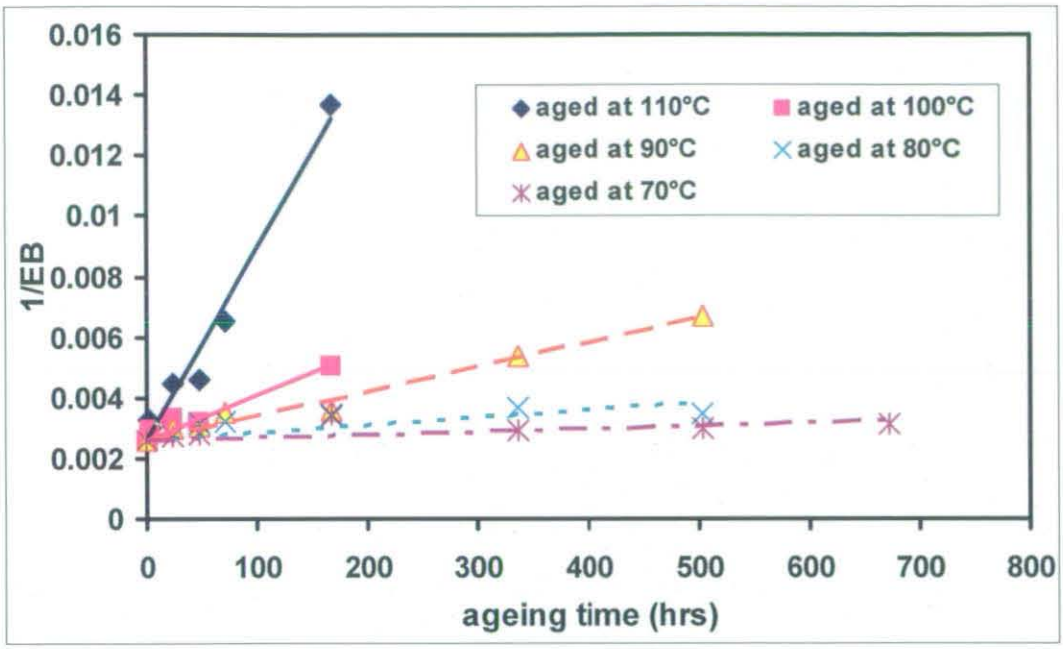

Figure A1.3: Second order plot for the effect of ageing on elongation at break of the natural rubber compound cured at 140°C

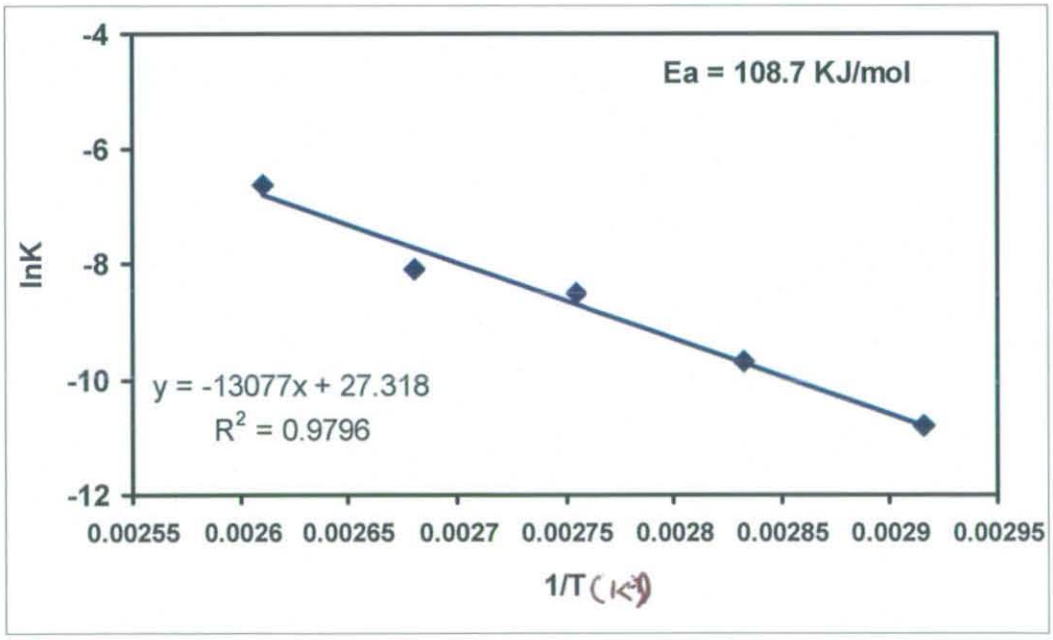

Figure A1.4: Arrhenius plot for the rate constants for ageing determined from the effect of ageing on tensile strength for rubber cured at 140°C

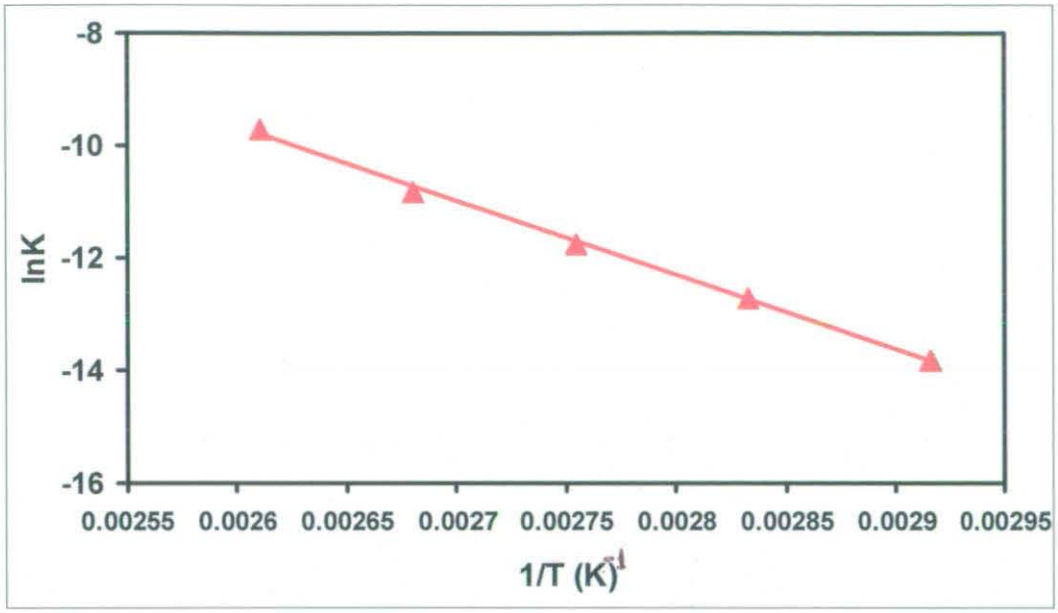

Figure A1.5: Arrhenius plot for the rate constants for ageing determined from the effect of ageing on Elongation at break for rubber cured at 140°C

APPENDIX II

Publications from this Thesis

1. Kinetics of the Effect of Ageing on Tensile Properties of a Natural Rubber Compound, *Journal of Applied Polymer Science*, **102**, 2006, 3732 – 3740.

2. Degradation and Life Prediction of a Natural Rubber Engine Mount Compound, Submitted to the *Journal of Applied Polymer Science*, 2007.

3. Kinetics of Thermo – oxidative Ageing of an engine Mount Compound, Proceedings of a Conference on Elastomers for Engineering: Future Trends, 23 November, 2006 at The Royal Overseas League, London UK, 78 – 83.

4. Effect of Method of Analysis on the Activation Energy of Thermo – oxidatively Aged Natural Rubber Vulcanizate – Manuscript

5. Kinetics Associated with the Healing of a Natural rubber Compound – Manuscript

6. Influence of the Nature and Type of Flaw on the Properties of a Natural Rubber Compound. Manuscript

7. Effect of ageing on the Dynamic and Fracture Properties of an engine Mount Compound.Manuscript

Kinetics of the Effect of Ageing on Tensile Properties of a Natural Rubber Compound

E. F. Ngolemasango,[1,2] M. Bennett,[3] Jane Clarke[1]

[1]*Institute of Polymer Technology and Materials Engineering, Loughborough University, Loughborough, Leicestershire, LE11 3TU, United Kingdom*
[2]*Department of Chemistry, Faculty of Science, University of Buea, Buea, Cameroon*
[3]*Avon Materials Development Centre, Brook Lane Industrial Estate, Westbury, Wiltshire, BA13 4EP, United Kingdom*

Received 18 January 2006; accepted 10 April 2006
DOI 10.1002/app.24634
Published online in Wiley InterScience (www.interscience.wiley.com).

ABSTRACT: Natural rubber (NR) undergoes chemical changes on heat and air ageing. These changes affect its physical properties and as such, affect the service life of the rubber compound. In this study, a vulcanized NR compound of a typical engine mount composition was subjected to thermo-oxidative ageing at temperatures from 70 to 110°C, to assess the effect on the tensile properties. The kinetics of degradation of the rubber compound, in terms of changes in these properties, was investigated. A fractional rate law was used to describe the kinetics of ageing in terms of its effect on modulus. Rates of ageing, in terms of effect on modulus, passed through a minimum at about 80°C, indicating the danger of trying to extrapolate in-service ageing behavior from high temperature ageing data. The activation energy of ageing in terms of its effect on modulus, determined for temperatures of 90–110°C, was 151 kJ mol^{-1}. A second order rate law was used to describe the kinetics of ageing in terms of its effect on tensile strength and elongation at break, with activation energies of 88.32 and 74.3 kJ mol^{-1}, respectively. According to Ahagon's (Ahagon et al., Rubber Chem Technol, 1990, 63, 683) classification of ageing mechanisms, Type I and Type III ageing mechanisms were predominant. © 2006 Wiley Periodicals, Inc. J Appl Polym Sci 102: 3732–3740, 2006

Key words: natural rubber; degradation; tensile properties; kinetics; activation energy

INTRODUCTION

The use of natural rubber (NR) components for under-hood applications requires them to withstand high temperatures with minimal deterioration. One such NR component used in under-hood applications is the engine mount. This component during its service life is subjected to various temperature conditions, amplitudes, and frequencies of vibration, which result in changes in the material's properties over time. These changes are usually traced to physical and chemical changes in the molecular structure, which may adversely affect the mechanical behavior of the engine mount and shorten its service life.[1,2]

Ageing of NR and other polymers, which can be thermal, photodegradative, or thermo-oxidative has been widely investigated.[3–10] Most of these studies employ destructive techniques such as the thermogravimetric methods at elevated temperatures, to determine the kinetics of degradation and so, predict the service life of the material. Such predictions are usually misleading in that they either overestimate the service life of the material or underestimate it.[11] Another method is the solution method, which is based on the changes in the average molecular weight of the material.[12] Because of the complexity of NR compounds, few studies of the degradation kinetics of NR vulcanizates have been undertaken using nondestructive methods, which mimic service conditions.[1,13,14]

Natural rubber [poly(*cis*-1,4-isoprene)] contains double bonds, which renders it particularly sensitive to oxidation in the presence of molecular oxygen.[15] The oxidation of NR, in the solid state, is complex, with two competitive processes; scission and crosslinking taking place almost simultaneously. These two mechanisms change the physical properties of the material. Chain scission will result in the loss of stiffness and elasticity, whereas crosslinking will result in increased stiffness and a consequent increase in brittleness. As a general rule, the more predominant effect of the oxidation process is chain scission. However, in the case of polybutadiene, for example, it has been shown that crosslinking overrides chain scission.[16] For poly(isoprene), whether a scission or crosslinking, mechanism predominates depends strongly on the quantity of oxygen that diffuses into the material.[17,18]

Using a nondestructive method, we attempt to derive the kinetics of thermo-oxidative ageing of a NR

Correspondence to: J. Clarke (j.Clarke@lboro.ac.uk).
Contract grant sponsors: Commonwealth Scholarship Commission in the United Kingdom and Avon Rubber p.l.c. (Materials Development Centre).

TABLE I
Formulation for the Natural Rubber Compound

Material	Composition (phr)
NRCV60	100
Carbon black (N772)	49
Zinc oxide	5
Stearic acid	2
Antiozonant wax	2
6PPD	1.5
TMQ	1
TBBS	0.7
TMTD	0.5
Sulfur	1.7

compound, by monitoring changes in physical properties over a range of time and temperature conditions.

EXPERIMENTAL

Materials

Natural rubber (SMRCV60) was supplied by the Tun Abdul Razak Research Centre, UK; carbon black (N772) was supplied by Columbian Chemicals, UK; tetramethylthiuram disulfide (TMTD), *N*-(1,3-dimethylbutyl)-*N'*-phenyl-*p*-phenylenediamine (6PPD), 2,2,4-trimethyl-1,2-dihydroquinoline (TMQ), *N-tert*-butyl-2-benzothiazolesulphenamide (TBBS) were supplied by FLEXSYS Belgium; antiozonant wax was supplied by Richard Baker Harrison Ltd., (UK). Sulfur, zinc oxide, and stearic acid were also used.

Compounding

The formulation used for the compound is given in Table I, representing a typical engine mount compound.

The NR compound was prepared in a water cooled Francis-Shaw K1 intermix having a volume of 5.5 L. A fill factor of 0.55 was used and the mixing was done at a speed of 40 rpm, with a circulating water temperature of 40°C. The rubber was first masticated in the internal mixer for 2 min together with the activators (zinc oxide and stearic acid), the antiozonant wax and the antioxidants (TMQ and 6PPD). Carbon black was then added and the compound was mixed for a further 4 min before introducing the accelerators (TMTD and TBBS) and the crosslinking agent (sulfur). The mixing was then carried out for a further 1 min before dumping. The compound was then sheeted out on a two-roll mill to a thickness of about 3.2 mm.

TABLE II
Cure Properties of the Fresh Compound

Maximum torque, M_H (dN/m)	87.72
Minimum torque, M_L (dN/m)	19.16
Scorch time, ts_2 (min)	2.62
Cure rate index, CRI	8.64
tc_{95} (min)	14.2

Cure parameters were determined using a Monsanto R100S Rheometer operating at a strain amplitude of 3° and at a temperature of 150°C. From the rheographs obtained, the scorch time, cure rate index, minimum and maximum torque were determined. Test samples were then compression molded to 95% cure at a temperature of 150°C for 15 min.

Accelerated thermo-oxidative ageing

Thermo-oxidative ageing was carried out in a circulating air environmental chamber at temperatures of 70, 80, 90, 100, and 110°C for times ranging from 1 to 4 weeks depending on the ageing temperature.

Tensile testing

Tensile properties were measured in accordance with the BS903-A2[19] on Type II dumbbell test pieces, which

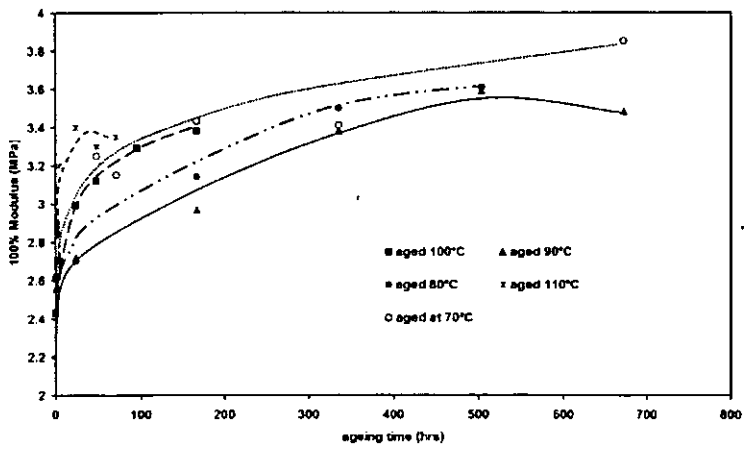

Figure 1 Effect of ageing temperature on 100% modulus.

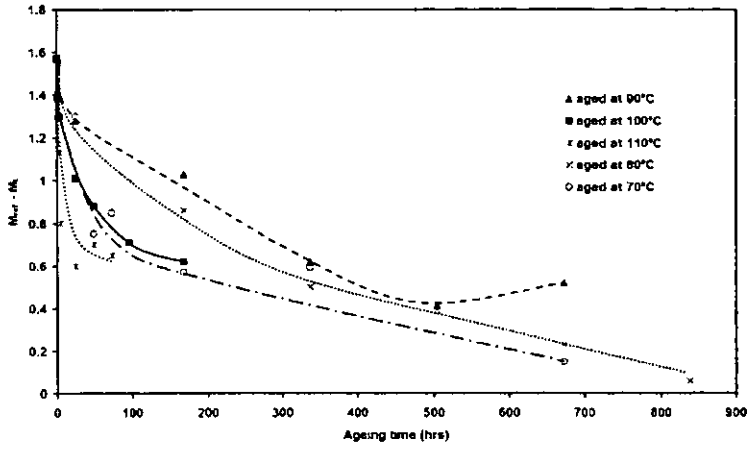

Figure 2 Relationship between ageing time and reduced modulus at the different ageing temperatures.

were die stamped from the 2 mm thick vulcanized sheets along the milling direction. A Hounsfield tensile testing machine was used, operating at a cross head speed of 500 mm/min, with a Hounsfield 500L laser control apparatus attached to measure the extension. The tensile strength, elongation at break, and modulus were acquired using QMAT-Dongle: 2003 computer software. A minimum of eight specimens were tested from each molded sheet.

RESULTS AND DISCUSSION

Various kinetic models have been employed to study the degradation of polymers.[20] Using the Kissinger, Ozawa, Van Krevellen, Horowitz–Metzger, Coats–Redfern, and MacCallum–Tanner methods, Regnier and Guibe[5] found that the activation energy for the multistage degradation of polyimide polymer was between 143 and 206 kJ mol^{-1}. It is worthwhile noting that all these methods apply high temperature weight loss thermal analysis techniques and not direct physical property measurements, as in our case.

The cure properties of the fresh compound are shown in Table II. The effect of ageing time and temperature on tensile modulus were qualitatively different from the effects on tensile strength and elongation at break. The two effects are discussed separately in the following two sections.

Modulus

The stress at 100% strain, referred to as the 100% modulus, (M_{100}) was used to follow the changes in stiffness of the compound during ageing. As the ageing time increased, the modulus (M_{100}) also increased until a point where it either leveled off, at the lower temperatures, or decreased at the higher ageing temperatures (Fig. 1). Ahagon et al.[1] and Baldwin et al.,[14] in their studies of accelerated ageing of tire compounds, also observed a modulus increase and subse-

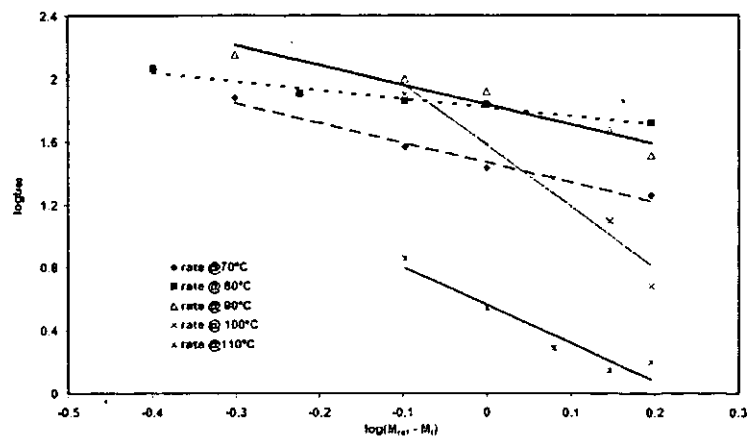

Figure 3 Fractional rate law plot for ageing reactions as they affect modulus.

TABLE III
Order and Rate Constants for Ageing of NR, in Terms of Effect on Modulus

Ageing temperature (°C)	n	k (10^{-3})	r^2	E_a (kJ mol^{-1})
70	2.26	8.1	0.9806	151.92
80	1.55	3.56	0.9601	
90	2.26	4.5	0.9316	
100	4.91	12.8	0.9571	
110	3.43	62.7	0.9214	

quent reduction, depending on the ageing mechanism. From 90 to 110°C, the rate of modulus increase decreases with increasing temperature, as would be expected. However, between 70 and 90°C the rate of modulus increase increases with decrease in temperature. Particularly striking is the fact that ageing at 70 and 100°C has a similar effect on modulus, at least up to 200 h. The apparently anomalous effect of ageing temperature on modulus is likely to be due to the complexity of the reactions taking place in the rubber. During ageing there are both crosslinking and scission reactions occurring at the same time, which have opposing effects on modulus. Since the crosslinking and scission reactions are likely to have different activation energies from each other, the relative contribution of each reaction to overall ageing is likely to vary with temperature.

The fractional life equation[21] shown below was used to describe the kinetics of degradation of the NR vulcanizate in terms the modulus (M_{100}).

$$t_F = \frac{(0.8)^{1-n} - 1}{k(n-1)} (M_{\text{ref}} - M_t)^{1-n} \quad (1)$$

where $M_{\text{ref}} - M_t$ is the reduced modulus; t_F is the time taken for the reduced modulus at time t to fall to 80% of its value; n is the order of the reaction; k is the rate constant.

Using this method, reduced modulus ($M_{\text{ref}} - M_t$) was plotted against ageing time t (Fig. 2) and values of t_F were determined. A value for the reference modulus M_{ref} of 4 MPa was chosen as the asymptotic value approached, at very long ageing times at low temperatures.

Taking logarithms on both sides of eq. (1), we have

$$\log t_F = \log \left(\frac{0.8^{1-n} - 1}{k(n-1)} \right) + (1-n) \log(M_{\text{ref}} - M_t) \quad (2)$$

From eq. (2), it can be seen that a plot of log t_F against log ($M_{\text{ref}} - M_t$) should give a straight line. Using this plot, the order of the reaction can be obtained from the slope and the rate constant from the intercept. Figure 3 shows the fractional rate law plots for the various ageing temperatures. It is notable that the slope and therefore, the order of the ageing reaction varies with ageing temperature. The orders of reaction and reaction rate constants were obtained from the plots and are shown in Table III. There is a general increase in order of reaction with increase in ageing temperature and this is perhaps a reflection of the increased complexity of the reactions affecting modulus at higher temperatures. The correlation coefficient r^2 from linear regression analysis was found to be in the range $0.9214 \leq r^2 \leq 0.9806$, supporting the validity of using this approach to describe the kinetics of ageing.

It is usual to make use of the Arrhenius relationship below, to obtain activation energies of reactions.

$$k = A\, e^{(-E_a/RT)} \quad (3)$$

where A is the pre-exponential constant; E_a, the activation energy; R, the gas constant; T, the absolute temperature; k, the rate constant at temperature T.

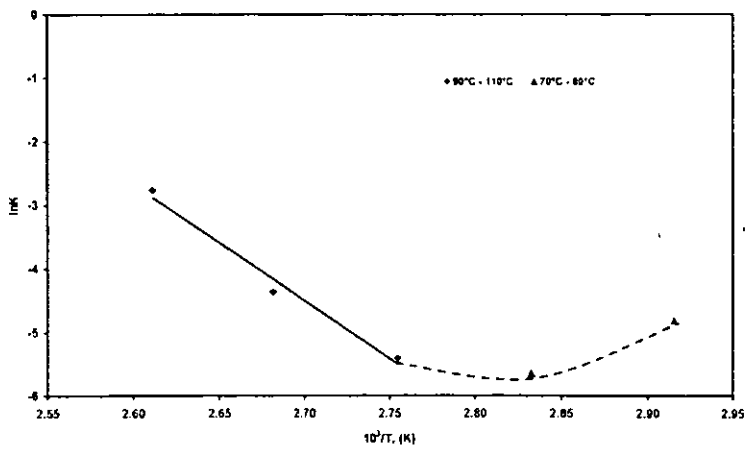

Figure 4 Arrhenius plot for ageing in terms of its effect on modulus.

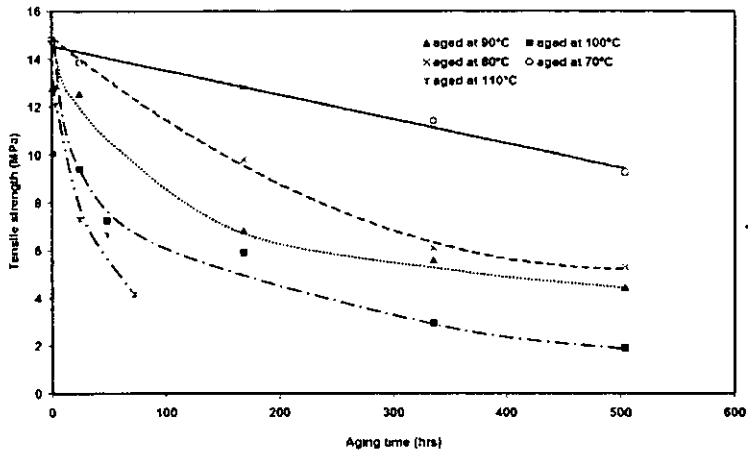

Figure 5 Effect of ageing temperature on tensile strength.

From eq. (3) one obtains

$$\ln k = \ln A - \frac{E_a}{RT} \tag{4}$$

Thus, when $\ln k$ is plotted against $1/T$ the slope of the resulting straight line can be used to give the activation energy.

Figure 4 shows an Arrhenius plot for the ageing reaction in terms of modulus. The points clearly do not lie on a straight line but lie on a curve that passes through a minimum. Using only the higher ageing temperature results (90–110°C), an activation energy of 151 kJ mol^{-1} can be obtained. However, if these high temperature data were extrapolated to lower temperatures, to predict the changes in modulus during the service life of the rubber material, then completely incorrect values would be obtained. The results illustrate the dangers of using accelerated ageing data to build predictive models. The curved shape of the Arrhenius plot indicates that there are two processes, which affect modulus in opposite ways and that each process has a different activation energy. It is known that ageing causes both crosslinking reactions, which result in an increase in modulus and scission reactions, which result in a decrease in modulus as has been explained elsewhere.[14,22] Both of these reactions will increase in rate with increase in temperature. However, the results indicate that the scission reactions have a higher activation energy than the crosslinking reactions. Hence, with decrease in temperature, the rate of scission reactions decrease more rapidly than the rate of crosslinking, giving the appearance, over a particular temperature range (70–80°C) that rate of crosslinking actually increases as temperature decreases. Extrapolating this effect to lower temperatures would suggest that the lower the temperature, the more rapid the increase in modulus would become. Clearly, this will not happen and so, at lower ageing temperatures it is expected that a negative slope for the Arrhenius plot would be

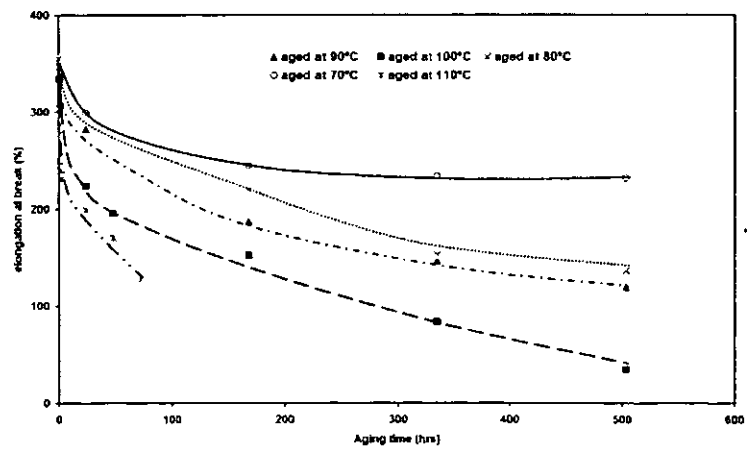

Figure 6 Effect of ageing temperature on elongation at break.

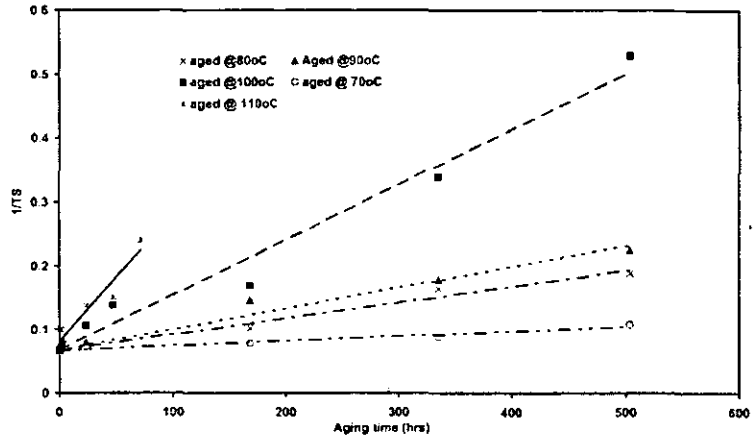

Figure 7 Second order rate plot of ageing in terms of its effect on tensile strength.

re-established. It is likely that the slope in the low temperature region will be lower than that in the high temperature region, corresponding to the lower activation energy required for crosslinking reactions.

Tensile strength and elongation at break

The tensile strength and elongation at break decreased with increase in ageing time (Figs. 5 and 6). The rate of decrease in these properties increased with increase in ageing temperature. The results are more straight forward than those for modulus, presumably because both crosslinking and scission reactions result in a decrease in strength. It is to be expected that scission reactions would cause a decrease in strength, because the tensile stress would be carried on fewer chains. Elongation at break would be expected to decrease with increase in ageing due to both crosslinking and scission reactions. However, crosslinking should not necessarily have a negative effect on tensile strength. For example, increasing the level of cure of a rubber compound can increase strength, until a maximum is reached, after which embrittlement can lead to a decrease in strength.

The effect of ageing on tensile strength and elongation at break was found to follow second order kinetics.

$$\frac{1}{\xi_t} = kt + \frac{1}{\xi_0} \tag{5}$$

where ξ_t is the property at time t of ageing and ξ_0 is the initial value before ageing.

A plot of $\frac{1}{\xi_t}$ versus t using eq. (5) gives straight lines (Figs. 7 and 8), for rubber aged at 70, 80, 90, 100, and 110°C. The significance of these plots are $0.878 \leq r^2 \leq 0.97673$ (Table IV), indicating a good correlation.

The rate constants, determined from the slopes of the lines, were then plotted on Arrhenius coordinates (Figs. 9 and 10). The activation energy was calculated to be about 88.32 kJ mol^{-1} for the tensile strength and

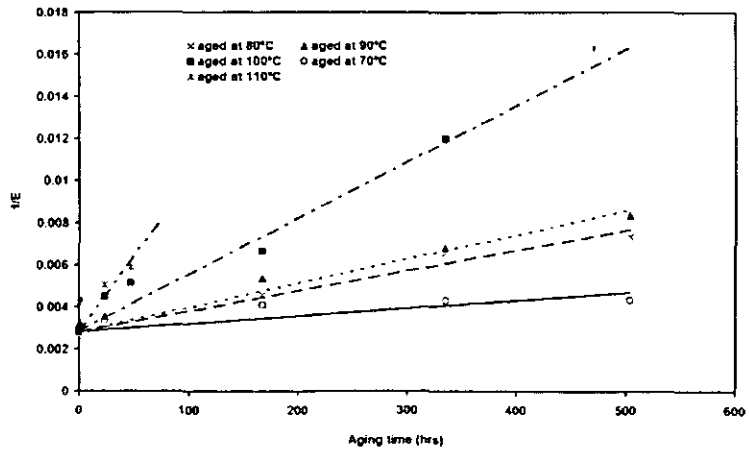

Figure 8 Second order rate plot of ageing in terms of its effect on elongation at break.

TABLE IV
Rate Constants for Ageing of NR, in Terms of Effect on Tensile Strength and Elongation at Break

Ageing temperature (K)	Tensile strength			Elongation at break		
	k	r^2	E_a (kJ mol^{-1})	k	r^2	E_a (kJ mol^{-1})
343	7.0×10^{-5}	0.9571	88.32	4.0×10^{-6}		74.3
353	3.0×10^{-4}	0.9749		1.0×10^{-5}	0.9712	
363	3.0×10^{-4}	0.9629		1.0×10^{-5}	0.9666	
373	9.0×10^{-4}	0.9767		3.0×10^{-5}	0.9544	
383	23×10^{-4}	0.8780		7.0×10^{-5}		

74.3 kJ mol^{-1} for the elongation at break. However, the activation energy calculated from modulus data at high temperatures (151 kJ mol^{-1}) is significantly greater than the values calculated from tensile strength and elongation at break data. This is probably because data from lower temperatures were included in the calculation using tensile strength data. At lower temperatures, crosslinking reactions predominate and so it is likely that their lower activation energy contributes more to the apparent overall activation energy of the ageing process. Other investigators found that the activation energy for the oxidation of sulfur-vulcanized NR was 102 kJ mol^{-1}.[23] For accelerated ageing of tires, Baldwin et al.[14] found that when the tire was inflated with air and a 50/50 blend of N_2/O_2, and aged at temperatures of between 40 and 70°C for one set of experiments and between 70 and 110°C for another, the wedge rubber had an activation energy of 107 kJ mol^{-1}. These two temperature ranges were selected to study the mechanism of degradation under these two conditions of air and a 50/50 blend of N_2/O_2.

Straus and Madorsky[24] studied the effect of various additives to NR with or without subsequent vulcanization on the degradation process during pyrolysis in a vacuum. They found that pyrolysis was completed at 390°C and carried all subsequent experiments at this pyrolysis temperature. The rates and activation energies of the thermal degradation in vacuum of vulcanized and unvulcanized NR was also studied.[24] They found the activation energy value for the thermal degradation of vulcanized NR to be between 234.42 and 272.09 kJ mol^{-1} for the different formulations. Using swelling measurements and peel strength and applying the same technique from their previous study,[14] Baldwin et.al.[22] found that the activation energy for skim rubber in the tested tires was 101 kJ mol^{-1} for the swelling ratio and 109 kJ mol^{-1} for the peel strength. Meanwhile Mott and Roland[25] found the activation energy for the ageing of NR in air and seawater at temperature ranges of 60–120°C in both cases, to be around 94 and 66 kJ mol^{-1}, respectively. The results obtained at low temperatures by these authors are close to what we obtained in our study (temperature range 70–110°C), for tensile strength and elongation at break. From our results and those reported in the literature, it appears that there is a general increase in activation energy of ageing with increase in ageing temperature. However, it is also clear that the activation energy is dependent on the compound composition, precise ageing conditions, and the method used to detect the extent of ageing.

Mechanism of thermo-oxidative ageing

The rate of thermo-oxidative degradation is affected by the rate of oxygen diffusion into the NR compound. It

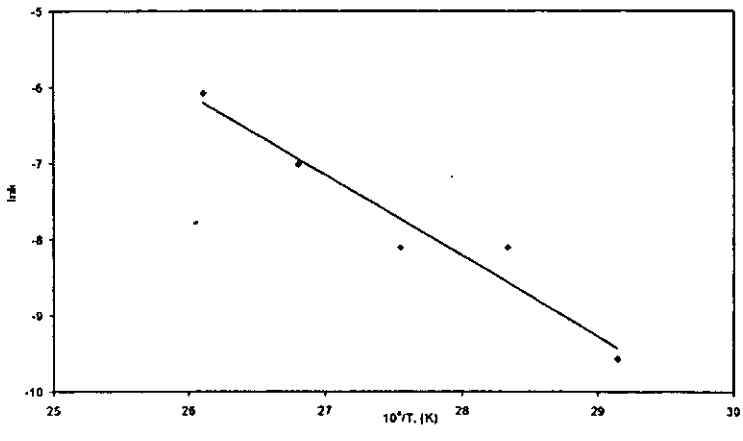

Figure 9 Arrhenius plot for ageing in terms of its effect on tensile strength.

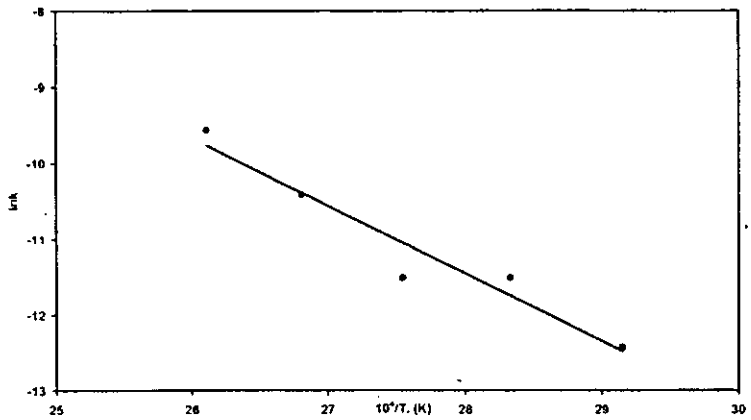

Figure 10 Arrhenius plot for ageing in terms of its effect on elongation at break.

has been postulated that if the temperature is relatively low, for an unprotected NR vulcanizate, diffusion occurs more quickly than oxidation and therefore there is oxidation throughout the product. However, as the temperature rises, the rate of oxidation increases much more than the rate of diffusion, so substantial oxidation occurs on the surface and an oxidized (hard skin) surface is formed.[26] For rubber containing antioxidants, the same effects are observed but the rate of diffusion of oxygen into the rubber is slowed down, because the antioxidant present in the rubber is being consumed at the surface. Surface oxidation that results in a brittle surface layer causes cracks to form on the surface of the rubber as it is being stretched. These cracks act as stress concentrators thereby reducing both the tensile strength and elongation at break. As ageing time is increased, more and more antioxidants are being consumed resulting in an increase in oxygen diffusion into the rubber and an increase in thickness of the oxidized layer accompanied by a further decrease in tensile strength. According to Bell et al.,[26] as ageing increases the thickness of the hard layer and hence, the size of the cracks increases. At a particular level of ageing the cracks become greater than the critical value for crack propagation, and test pieces tear rather than fracture, resulting in low tensile strengths. Upon tensile testing of rubber samples used in the current study, after ageing at 90°C for 72 h, cracks could be seen emanating from the surface in all directions (Fig. 11). The presence of cracks indicates that surface hardening has taken place and that oxidation is occurring more rapidly than oxygen diffusion.

According to Ahagon et al.[1] and Baldwin et al.,[14] three types of ageing mechanisms are observed in NR; Types I, II, and III. Type I ageing is characterized by crosslinking being the dominant event resulting in an increase in modulus and lowering of the elongation at break. In Type II ageing the modulus either changes a little or is reduced, and the factors involved in Type II ageing are main-chain modifications reducing the number of extensible units. Type III ageing is characterized by both crosslinking and chain scission due to oxidation at high temperatures. The Ahagon plot has also been used to describe the type of ageing process taking place in rubber tires.[1,14] According to Ahagon et al.[1,13] and Baldwin et al.,[14] aerobic ageing of rubber is characterized by a straight line when log of the elongation at break is plotted against log of the stress at 100% strain. Type I ageing is characterized by a slope of about −0.75. Type III high temperature aerobic ageing is characterized by an increase in the modulus (M_{100}) after ageing compared to the original, with the reduction in the elongation at break becoming larger with increasing ageing temperature. Type II anaerobic ageing of rubber gives data deviating from a straight line. It is worthwhile noting that the magnitude of the slope is a characteristic of the compound being studied.

From the Ahagon plot of data from the current study (Fig. 12), it was observed that ageing of the NR com-

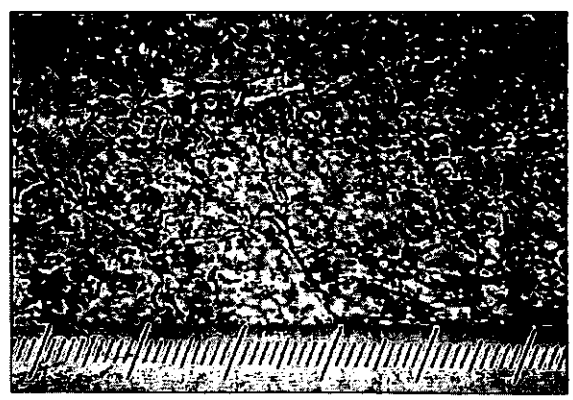

Figure 11 Light microscopic image showing crack surface of an aged rubber sample after tensile testing (each minor division is 10 μm).

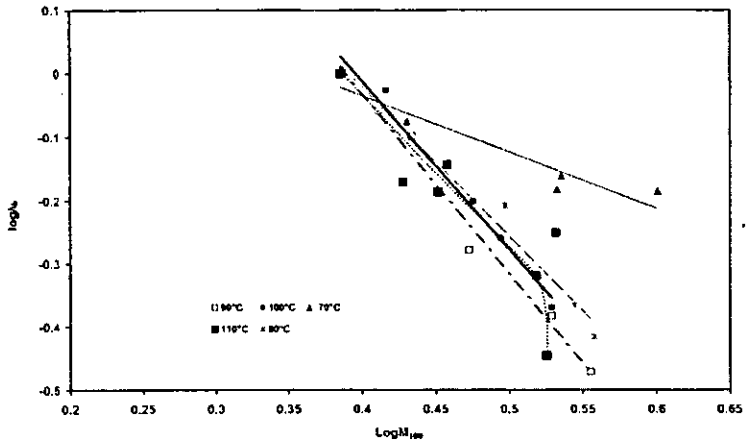

Figure 12 Ahagon plots for thermo-oxidative ageing.

pound at 70°C is Type I, with a slope of −0.89, and was dominated by crosslinking events, which resulted in a steady increase in the modulus and lowering of the elongation at break. At all the other temperatures Type III ageing was observed.

CONCLUSIONS

Ageing in air at temperatures between 70 and 110°C resulted in increases in 100% modulus. The fractional rate law describes the kinetics of degradation of the NR compound in terms of the modulus. Rates of ageing, in terms of effect on modulus, passed through a minimum at about 80°C. The minimum in the Arrhenius plot indicates the danger in trying to extrapolate in-service ageing behavior from high temperature ageing conditions. It is assumed that the phenomenon is due to the balance of chain scission and crosslinking reactions varying with ageing temperature. The activation energy of ageing in terms of its effect on modulus determined for temperatures of 90–110°C was 151 kJ mol^{-1}.

Ageing in terms of the effect on tensile strength and elongation at break were found to follow second order kinetics, with activation energies of 88.32 and 74.3 kJ mol^{-1}, respectively. Results are consistent with the chain scission reactions having a higher activation energy than the crosslinking reactions.

From Ahagon plots, two types of ageing mechanisms were identified, Type I for ageing at 70°C, being dominated by crosslinking and Type III for 80–110°C, being affected by both crosslinking and scission reactions.

The authors would like to thank the companies who have supplied free materials for the project; natural rubber from the Tun Abdul Razak Research Centre, UK, carbon black (N772) from Columbian Chemicals, UK, accelerators and curing agents from Flexsys, and antiozonant wax was supplied by Richard Baker Harrison Ltd.

References

1. Ahagon, A.; Kida, M.; Kaidou, H. Rubber Chem Technol 1990, 63, 683.
2. Nemeth, A.; Marosfalvi, J. Polym Degrad Stab 2001, 73, 245.
3. Scott, J. R. Rubber Chem Technol 1950, 23, 390.
4. Nair, S. J Rubber Res Inst Malaya 1969, 22, 135.
5. Regnier, N.; Guibe, C. Polym Degrad Stab 1997, 55, 165.
6. Maillo, C. M.; White, J. R. Plast Rubber Compos 1999, 28, 277.
7. Buzare, J. Y.; Silly, G.; Emery, J.; Boccaccio, G.; Rouault, E. Eur Polym J 2001, 37, 85.
8. South, J. T.; Scott, W. C.; Reifsnider, K. L. Rubber Chem Technol 2003, 76, 785.
9. He-Ping, Y.; Si-Dong, L.; Jie-Ping, Z.; Kui, X. Thermochim Acta 2004, 410, 119.
10. Saron, C.; Felisberti, M. I. Mater Sci Eng A 2004, 370, 293.
11. Ding, S.; Ling, M. T. K.; Khare, A.; Woo, L. ANTEC 1999, II, 2458.
12. Bonfils, F.; Flori, A.; Sainte Beuve, J. J Appl Polym Sci 1999, 74, 3078.
13. Kaidou, H.; Ahagon, A. Rubber Chem Technol 1990, 63, 698.
14. Baldwin, J. M.; Bauer, D. R.; Ellwood, K. R. Rubber Chem Technol 2005, 78, 336.
15. Bevilacqua, E. M.; English, E. S.; Gall, J. S.; Norling, P. M. J Appl Polym Sci 1964, 8, 1029.
16. Kuczkowski, J. A. Rubber World 1995, 212, 19.
17. Clough, R. L.; Gillen, K. T. Polym Degrad Stab 1992, 38, 47.
18. Bonfils, F.; Laigneau, J. C.; de Livonniere, H.; Sainte Beuve, J. Kautsch Gummi Kunstst 1999, 52, 32.
19. Physical testing of rubber. Method for Determination of Tensile Stress–Strain Properties, British Standard BS903-A2, Vol. A2; 1995.
20. Yang, K. K.; Wang, Y. L.; Wang, Y. Z.; Wu, B.; Jin, Y. D.; Yang, B. Eur Polym J 2003, 39, 1567.
21. Levenspiel, O. Chemical Reaction Engineering; Wiley: New York, 1999; pp 62, 63.
22. Baldwin, J. M.; Bauer, D. R.; Ellwood, K. R. Rubber Chem Technol 2005, 78, 767.
23. Ono, K.; Kaeriyama, A.; Murakami, K. Rubber Chem Technol 1977, 50, 43.
24. Straus, S.; Madorsky, S. L. Rubber Chem Technol 1957, 30, 93.
25. Mott, P. H.; Roland, C. M. Rubber Chem Technol 2001, 74, 79.
26. Bell, C. L. M.; Stinson, D.; Thomas, A. G. NR Technol 1980, 11, 53.

communications

Elastomers for Engineering: Future Trends

23 November 2006
1 Carlton House Terrace, London, UK

Published by
IOM Communications Ltd
1 Carlton House Terrace
London SW1Y 5DB
United Kingdom

Tel: +44 (0)20 7451 7300
Fax: +44 (0)20 7839 1702
www.iom3.org

IOM Communications Ltd is a wholly owned subsidiary of
The Institute of Materials, Minerals and Mining.
Registered Charity Number 1059475

Introduction

This is a conference organised by the Rubber in Engineering Committee of the Institute of Materials, Minerals and Mining

Progress in soft, highly extensible solid materials and their use is frequently the key step for innovation and success in components, devices and machines. Moreover, the principal application areas for devices and corresponding material requirements are changing rapidly. The conference will focus on emerging application areas, technical requirements, material developments and other technical solutions under the following themes.

Theme 1: ***Elastomers for the Future***

Theme 2: ***Fillers for the Future***

Theme 3: ***Life Prediction & Extension***

Theme 4: ***Products & Applications***

Contents

Theme 1: Elastomers for the Future 7

The Expected Evolution of Future Elastomers and their Compounds in the 21st Century 8
Claude Hepburn (Consultant, and Professor (Emeritus) University of Ulster, N Ireland, UK)

Smart Elastomers: Potential Applications, Approaches & Challenges 10
Vince Coveney (University of the West of England, Bristol, UK)

Novel Silicone-Based Materials for Medical Devices & Implants 12
Sean Gorman (Queen's University Belfast, UK)

A Novel Technology for Base Resistant Fluoroelastomers 16
Stefano Arrigoni (Solvay Solexis S.p.A., Italy) Steven Jagels (Solvay Solexis Inc., USA)

Temperature and Fluid Resistant Flexible Thermoplastics and Thermoplastic Elastomers Prepared using Rubber Crumb 23
Jane Clarke, K Chandio, D Nock (Loughborough University, UK)

Theme 2: Fillers for the Future 29

Carbon Nanotubes as Reinforcement in EPDM Compounds 30
Fabienne Barroso Bujans, M Arroyo, E San Juan, M A Lopez Manchado, E Riande (Instituto de Ciencia y Tecnología de Polímeros, CSIC, Spain) I Rodriguez-Ramos, M Perez-Cabero (Instituto de Catalisis y Petroleoquimica, CSIC, Spain)

Mechanical Behaviour of Elastomeric Model Nanocomposites 36
Giorgio Ramorino, F Bignotti, R De Santis, T Ricco (University of Brescia, Italy)

Enhanced Permeation Resistance of Elastomer Compounds with Glass Flake Particles 42
Chris A Stevens, D W Mason (NGF Europe Limited, UK)

Reinforcement of Natural Rubber with Organoclays 47
David Lowe (TARRC, Brickendonbury, UK & Queen Mary, University London, UK) A V Chapman, S Cook (TARRC, Brickendonbury, UK) J Busfield (Queen Mary, University London, UK)

Electrical Conductivity of Elastomer under Strain: Influence of Filler Type 53
Vineet Jha, J J C Busfield, A G Thomas (Queen Mary, University of London, UK) M Bennett (Avon Rubber, Westbury, UK)

Online Characterization of CB Dispersion and Distribution in Rubber Blends by use of the Method of the Online Conductance and TGA on Rubber Filler Gel 58
Le Hong Hai, S Ilisch, G R Kasaliwal, H J Radusch (Martin Luther University Halle-Wittenberg, Germany)

The Physical Behaviour of Elastomers Filled with Hollow Spherical Fillers 61
Robert Shorter, A G Thomas, J J C Busfield (Queen Mary, University of London, UK) J Smith (DSTL, UK)

A Micro Physically Motivated Hyper-Elasto-Visco-Plastic Model for Filled Elastomer 67
Julie Grandcoin[1], A Boukamel [1,2] ([1]Laboratoire de Mécanique et d'Acoustique de Marseille, France and [2]EGIM, Ecole Généraliste d'ingénieurs de Marseille, France)

Theme 3: Life Prediction & Extension

Trends in Finite Element Modelling and Life Prediction for Elastomeric Components 73
Peter Hanson, J Harris, S Mirza (MERL, Hitchin, UK) 74

Kinetics of Thermo - Oxidative Ageing of an Engine Mount Compound 78
Frederick Ngolemasango, J Clarke (Loughborough University, UK)

Lifetime Prediction and Qualification of Polymeric Components in Nuclear Utilities, the Pitfalls Associated with the Arrhenius Equation and Testing at High Dose Rates 84
John Dawson (Serco Group plc, UK)

Theme 4: Products & Applications

Polymer-Based Pressure Bags for Fatigue Tests on Turbofan Compressor Casings 90
Alan Muhr, Ian J Stephens (TARRC, UK) 91

Future Requirements for Elastomers in Aerospace Engineering 97
Dr Mike Taylor (Airbus)

The First Adhesive Free Plastic/Rubber System for Forming a Bond Between Polyamide 612 and EPDM 102
Frank Lorenz (Degussa AG, Germany)

Development of a Technology for Fabrication of an Artificial Worm for Minimally Invasive Surgery 106
Petra Meier, M Lang (Technical University Ilmenau, Germany)

Posters 112

Correlation of Compression Stress Relaxation and Compression Set of Epichlorohydrin Elastomers 113
Azizol Wahaba (Universiti Teknologi MARA, Malaysia)
A S Farid (Polymer Centre, London Metropolitan University, UK)
K D Arunashanthib (Richard Pieris Rubber Compounds Limited, Sri Lanka)

High Temperature Perfluoroelastomers 114
Giovanni Comino, Margherita Albano, Claudia Manzoni, Milena Stanga (Solvay Solexis S.p.A., Italy)

Temperature Requirements of Anti-Vibration Mounts used in Rail Powerpack Applications 120
Matt Easthope, Bill Mortel (Trelleborg Industrial AVS, UK)

Elastomers for the Future

KINETICS OF THERMO – OXIDATIVE AGEING OF AN ENGINE MOUNT COMPOUND

Frederick E. Ngolemasango* and Jane Clarke

Institute of Polymer Technology and Materials Engineering, Loughborough University, Loughborough, LE11 4TE,

email: e.f.ngolemasango@lboro.ac.uk, j.clarke@lboro.ac.uk

Introduction

Rubbery materials are usually subjected to physical and chemical property changes due to ageing, whether they are in service or during storage.[1-5] Because of considerable variation in conditions in terms of location and seasonal variations, it is very difficult to evaluate changes due to degradation in a natural rubber compound in absolute terms. In real service conditions, engine mounts are exposed to a combination of factors including oxygen, heat, various liquids, dynamic motions etc. Ageing therefore is a composite of all these factors.[6]

Engine mounts operate in very harsh conditions of temperature and vibration frequencies due to technological development in the design of cars. This has resulted in the reduction of the service life of this under hood component. In order to assess and predict the functional life of a natural rubber (NR) engine mount compound, the physical property changes were determined using accelerated ageing conditions. The rubber was aged at temperatures ranging from 70°C to 110°C at times of between one hour and five weeks. Static as well as dynamic measurements were used to characterise the ageing trends and mechanisms of the engine mount compound.

The elongation at break decreases with ageing time (figure 1). Stiffness of the compound showed an initial increase followed by a decrease and then increasing steadily with ageing time (Figure 2). This initial might be due to either postcuring which resulted in formation of more crosslinks, while the decrease might be as a result of scission of the weaker S –S bonds in the polysulphidic network. The further increase in modulus with ageing can be attributed to the formation of new networks. Dynamic ageing was carried out on a modified fatigue machine. The fatigue life decreased with increase in temperature and ageing time for the statically aged rubber (Figure 5a). Two types of ageing mechanism were predominant which include types I and III aerobic degradation mechanism as described by Ahagon [1]. (Figure 6) Type I ageing which is characterised by crosslinking being the dominant event resulting in an increase in modulus and lowering of the elongation at break, and Type III mechanism which is characterised by both crosslinking and chain scission due to oxidation at high temperatures, were predominant. Using the time – temperature superposition approach, ($a_T = \exp\frac{E_a}{R}\left(\frac{1}{T_{ref}} - \frac{1}{T}\right)$)[7-8], the activation of ageing of our natural rubber engine mount compound was found to be about 42.6 KJ/mol for elongation at break (Figures 3 and 4). The activation energy from fatigue measurements from the statically aged rubber was found to be 26.13 KJ/mol.(figure 5b) Taking a 50% reduction in elongation at break as a failure criterion, it was predicted that the engine mount compound would last approximately 140 times longer at 23°C compared to its lifetime at 70°C. (Table 1)

The rubber compound was aged for 13 weeks at 50°C to test the validity of the model. It was found that the tensile strength and elongation at break was predicted to be 18.73 MPa, and 327% which was very close to the experimental value of 19.04 (± 2.25SD) MPa, and 321 % (±33.8SD) respectively.

References

(1) Ahagon, A.; Kida, M.; Kaidou, H. *Rubber Chem Technol* **1990**, *63*, 683-697.

(2) Baldwin, J. M.; Bauer, D. R.; Ellwood, K. R. *Rubber Chem Technol* **2005**, *78*, 336-353.

(3) Baldwin, J. M.; Bauer, D. R.; Ellwood, K. R. *Rubber Chem Technol* **2005**, *78*, 767.

(4) Brown, R. P.; Butler, T.; Hawley, S. W. **2001**, 37-38.

(5) Ngolemasango, F.; Ehabe, E.; Ayrmard, C.; Sainte - Beuve, J.; Nkouonkam, B.; Gobina, S.; Bonfils, F. *Polym. Int.* **2003**, *52*, 1365-1369.

(6) Deng Huang, B.J. L.; Castro, J. M.; Ignatz – Hoover, F. *Polym. Degrad. Stab.* **2001**, *74*, 353-362.

(7) Gillen, K. T.; Celina, M.; Keenan, M. R. *Rubber Chem. Technol.* **2000**, *73*, 265-283.

(8) Gillen, K. T.; Bernstein, R.; Derzon, D. K. *Polym. Degrad. Stab.* **2005**, *87*, 57-67.

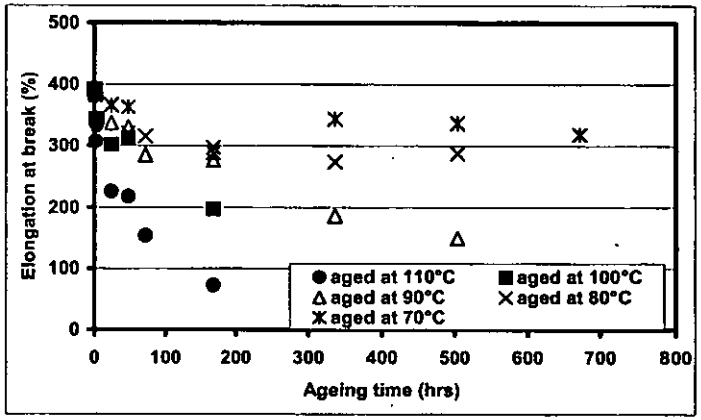

Figure 1: Effect of ageing on elongation at break

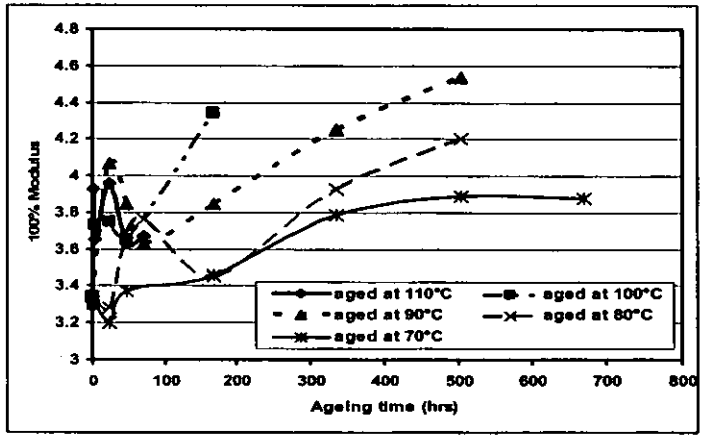

Figure 2: Effect of ageing on stress at 100% strain (100% modulus)

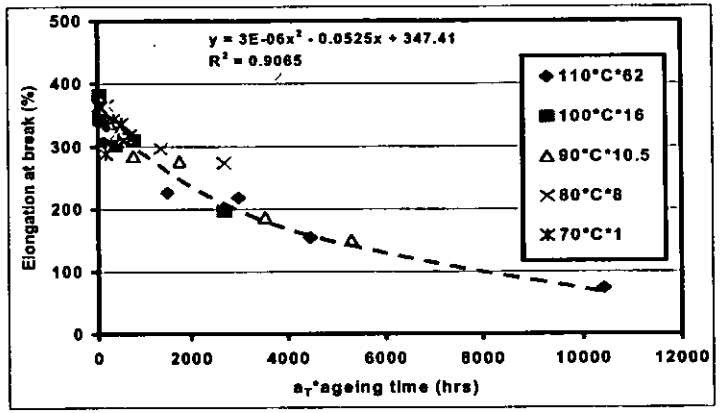

Figure 3: Time – temperature superposition plot for elongation at break for ageing of natural rubber at 70°C reference temperature

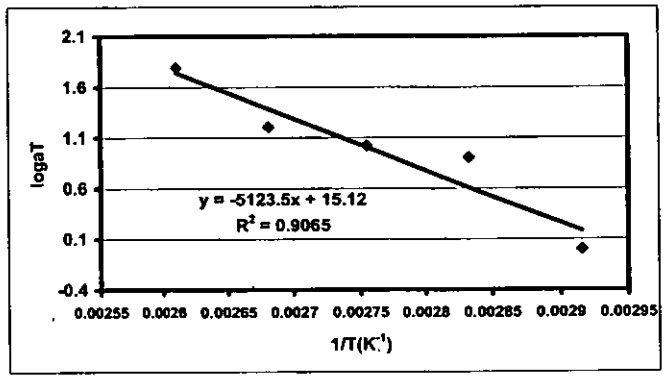

Figure 4: Arrhenius plot for log shifted time against inverse of absolute temperature for elongation at break

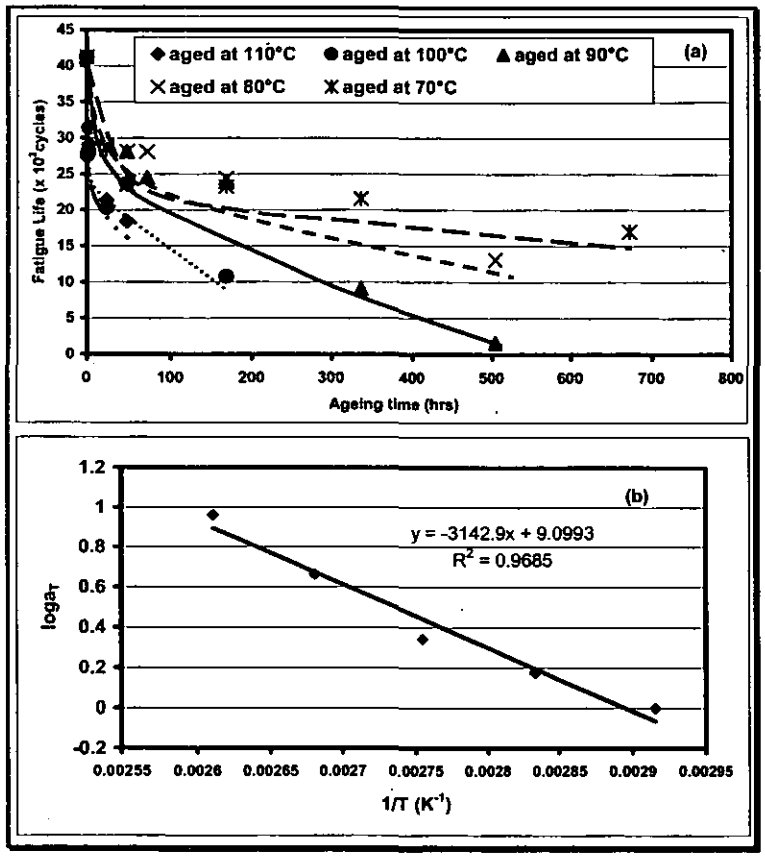

Figure 5: Effect of static ageing on (a) fatigue life and (b) kinetics of a natural rubber engine mount compound

Table I: Activation energies and service life prediction

Property	Ea (KJ/mol)	Prediction using TTS model	
		Experimental value at 50°C	Predicted value at 50°C
Tensile strength	40.4	19.04 (±2.3SD)	18.73
Elongation at break	42.6	321.04 (±33.8SD)	327.12
Modulus	(34.51) 87.84	4.17 ((±0.09 SD)	3.66

Service life Prediction in years(Failure criteria – 50% property reduction)

Property	Temperature			
	70°C	50°C	40°C	23°C
Elongation at break	~1	~ 6	~ 18	~ 154

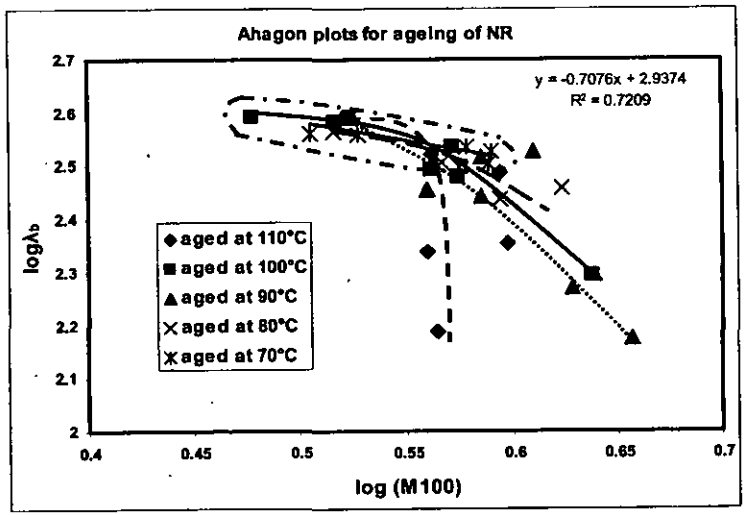

Figure 6: Ahagon plot for the ageing mechanisms of natural rubber compound